Provenance and Diagenesis of Middle Jurassic to Lower Cretaceous Clastic Sedimentary Systems in the SW Scotian Basin and the Fundy Basin

By

Dan-Cezar Dutuc

A Thesis Submitted to
Saint Mary's University, Halifax, Nova Scotia
in Partial Fulfillment of the Requirements for the
Degree of Masters of Science in Applied Science

November, 2015, Halifax, Nova Scotia

Approved: Dr. Georgia Pe-Piper

Approved: Dr. David J.W. Piper

Approved: Dr. Mark E. Deptuck

Approved: Dr. Cristian Suteanu

Approved: Dr. Brendan Murphy

Date: November 12, 2015

Abstract

Provenance and Diagenesis of Middle Jurassic to Lower Cretaceous Clastic Sedimentary Systems in the SW Scotian Basin and the Fundy Basin

By Dan-Cezar Dutuc

Mid Jurassic to Lower Cretaceous clastic deposits in the SW Scotian Basin are poorly known and understood. Detrital mineral chemistry was used to determine their provenance, whereas chemical composition of diagenetic minerals together with textures were used to determine paragenetic sequences. Mid Jurassic sediments indicate a Meguma terrane source, with local rivers and an influence from Labrador, with a river running along the Cobequid-Chedabucto fault zone depositing in the Fundy Basin. Late Jurassic sediments were sourced from the Meguma terrane. Lower Cretaceous sediments have similar sources as Mid Jurassic sediments, except that the Labrador river deposited in the central Scotian Basin. Diagenetic conditions in the SW Scotian Basin are slightly different from those in the Sable sub-basin. Coated grains formed in the sulfidic and ferruginous diagenetic zones. Eodiagenetic minerals imply fully marine conditions, as suggested by the high ratio of Ca^{2+} and Mg^{2+} to Fe^{2+}. Carbonates are the Ca^{2+} source for mesodiagenetic calcite.

November 12, 2015

Acknowledgements

First of all I would like to thank my supervisor Dr. Georgia Pe-Piper for offering me the chance to get a Masters degree, be professional and expand my knowledge related to sedimentary rocks. Thank you for being patient with me and for guiding me through the entire time of my thesis. At the same I would like to thank Dr. David Piper for the inspiration and the endless time spent trying to guide me on the right path whenever that was necessary. I know that sometimes things were hard with me and because of that I thank you both and appreciate all the help that I received. I will never forget that!

Thank you to both Dr. Mark Deptuck and Dr. Cristian Suteanu for accepting to be members of my committee and for providing feedback, thoughts and suggestions for improvement of this thesis.

Thank you to Dr. Brendan Murphy for accepting to be my external examiner.

Thank you to Dr. Yuanyuan Zhang from the Department of Geology at Saint Mary's University for being patient with me, answering my questions and providing possible suggestions for improvement of the thesis. She was like an extra member of my committee group who I could ask questions all the time.

Thank you to the Canada Nova-Scotia Offshore Petroleum Board and particularly to Nancy White for allowing me to obtain rock samples from conventional cores and cuttings samples necessary for this study.

Thank you to Owen Brown from the Sedimentology Lab at the Bedford Institution of Oceanography in Dartmouth for showing me the technique used for the separation of detrital heavy minerals from cutting samples.

Thank you to instructor Xiang Yang from the Department of Geology at Saint Mary's University for teaching how to use the Scanning Electron Microscope and different techniques necessary for both provenance and diagenesis work.

Thank you to Randolph Corney from the Department of Geology at Saint Mary's University for helping me with the preparation of samples necessary for the production of polished thin sections and whole rock geochemical analyses.

Thank you to instructor Dan MacDonald from the Department of Earth Sciences at Dalhousie University for teaching me how to use the Electron Microprobe as well as

the principles under which this apparatus works.

Thank you to all the grad students from the Grad Office (S402) at Saint Mary's University for the friendly and warm environment.

Thank you to my mom, Corina and my sister, Lori for encouraging me through all the difficult times and believing in me. I could have not done it without you two!!!

Thank you to my girlfriend, Gabrielle Picard who was the person close to me through all the good and bad moments since I started my thesis. She has been a motivation and an inspiration through all this time. I will never forget that!

Thank you to Saint Mary’s University for accepting me as a graduate student, for offering me the opportunity to come into interaction and learn from great Professors, for the scholarship, for the opportunity to be a Teaching Assistant and for the friendly environment and the amazing experience. I have learned a lot since I first started, I’ve become a better student and most important I’ve become a better man.

This project was funded by a Collaborate Research and Development (CRD) Grant from NSERC-Encana (administered through OERA) to G. Pe-Piper. Thank you very much for this funding that gave me this opportunity and made a dream come true!

TABLE OF CONTENTS

List of figures

List of tables

List of appendices

4-2: BSE images and EDS mineral analyses of sample B-93 5170 ……on CD

4-3: BSE images and EDS mineral analyses of sample B-93 5410 ……on CD

4-4: BSE images and EDS mineral analyses of sample B-93 5760 ……on CD

4-5: BSE images and EDS mineral analyses of sample B-93 5860 ……...on CD

4-6: BSE images and EDS mineral analyses of sample B-93 6210 ……on CD

4-7: BSE images and EDS mineral analyses of sample B-93 6340 ……on CD

4-8: BSE images and EDS mineral analyses of sample B-93 6540 ……on CD

4-9: BSE images and EDS mineral analyses of sample B-93 6750 ……on CD

5-1: BSE images and EDS mineral analyses of sample I-100 5990 ……...on CD

5-2: BSE images and EDS mineral analyses of sample I-100 7230 ……...on CD

5-3: BSE images and EDS mineral analyses of sample I-100 7840 ……...on CD

5-4: BSE images and EDS mineral analyses of sample I-100 8480 ……...on CD

5-5: BSE images and EDS mineral analyses of sample I-100 8810 ……...on CD

5-6: BSE images and EDS mineral analyses of sample I-100 11400 …….on CD

5-7: BSE images and EDS mineral analyses of sample I-100 12640 …….on CD

5-8: BSE images and EDS mineral analyses of sample I-100 13800 …….on CD

6: BSE images and EDS mineral analyses of sample G-29 3635 ……...on CD

7: BSE images and WDS analyses of detrital rutile from Mohawk B-93 ……...on CD

8: BSE images and WDS analyses of detrital rutile from Mohican I-100 ….....on CD

9-1: BSE images and EDS mineral analyses of sample I-100 2526.63 …….....on CD

9-2: BSE images and EDS mineral analyses of sample I-100 2529.62 …….....on CD

9-3: BSE images, EDS and WDS mineral analyses of sample I-100 2530.47…….on CD

9-4: BSE images and EDS mineral analyses of sample I-100 2538.84 …….....on CD

9-5: BSE images and EDS mineral analyses of sample I-100 3692.41 …….....on CD

9-6: BSE images and EDS mineral analyses of sample I-100 3964.6A …….....on CD

9-7: BSE images and EDS mineral analyses of sample I-100 4098.08 …….....on CD

10-1A: BSE images, EDS and WDS analyses of sample P-15 2563.67 …….on CD

10-1B: BSE images, SE images and EDS analyses of sample P-15 2563.67.....on CD

10-2: BSE images, EDS and WDS analyses of sample P-15 3306.03…….on CD

10-3: BSE images and EDS mineral analyses of sample P-15 3744.92 ……..on CD

10-4: BSE images and EDS mineral analyses of sample P-15 3750.94 …….....on CD

Chapter 1: Introduction

The Scotian Basin and the Fundy Basin, offshore eastern Canada, include Mesozoic–Cenozoic sandstones, shales and carbonates, up to 15 km thick. The first deposition started during the Triassic rifting of Panagea, when interbedded strata composed of evaporites, carbonates and poorly sorted clastic sediments (Wade and MacLean, 1990) became the dominant fill of half grabens originating along the eastern margin of the North American continent. These gave way to mixed carbonate and clastic depositional system in the Jurassic (Mohican and Iroquois formations in the Mid Jurassic and eventually Abenaki and Mic Mac formations in the Upper Jurassic) as North America drifted away from Africa (Schettino and Turco, 2009).

The depositional setting suddenly changed, in the Late Jurassic-Early Cretaceous, when sandy deltaic successions of the Missisauga and Logan Canyon formations were deposited on the Scotian Shelf (Pe-Piper and Piper, 2012). These deltas, which are several kilometres thick, are believed to have supplied turbidite sands into deep water reservoirs (Piper and Normak, 2009). These deltaic successions have been proved to host potential economic petroleum systems (Wade and MacLean, 1990). The Missisauga Formation is the major hydrocarbon-bearing unit offshore Nova Scotia (Cummings and Arnott, 2005).

Two hypotheses have been proposed in previous studies to be responsible for this sudden change in sediment supply: i) the development of a proto St. Lawrence River system, draining large areas of the outboard and more inboard Appalachian terranes and the Grenville Province, including the Labrador or ii) different tectonic evolution during Early Cretaceous compared to that of Early Triassic till Mid Jurassic, with rifting and

drifting of the Grand Banks from Iberia (Wade and MacLean, 1990) and that of Late Jurassic with rifting and drifting of Labrador from Greenland (Zhang et al., 2014).

The primary purpose of this thesis is to determine the provenance of clastic sediments deposited in the Shelburne sub-basin, located in the SW Scotian Basin, using their detrital heavy mineral composition. The composition of clastic sediments is a result of interplay between attributes of the plate tectonic setting and variables like provenance, weathering, relief, transportation and factors that operate during and after the sedimentation cycle (Bhatia, 1983). Tectonism has been advocated as the primary control on sedimentary composition (Bhatia, 1983).

On the other hand, the nature of distribution and dispersal of clastic sediments is mainly related to dynamic processes between the external (allogenic) and internal (autogenic) forces that govern the sediment deposition in clastic sedimentary systems (Somme et al., 2009). Locally sea level lowstands and hinterland tectonics are believed to have created conditions favouring increased supply of clastic sediments and the transfer to deep water (Bhatia, 1983). Even though in many basins sea level change is thought to be an important factor favouring transport of clastic sediments across carbonate platforms into deep water basins, the importance of tectonics is greater in many tectonically active basins. In such basins uplift mimics sea level lowstands and allows sediments to pass over platforms and to become deposited in basins (Mutti et al., 2003). Moreover, individual earthquakes may trigger sediment failure and transport to deep water during short periods of time (Goldfinger et al., 2007). However, the relative importance of short-term tectonic control on sedimentation in comparison to climate and eustasy remains poorly understood (Bourget et al., 2010). Although lots of research

has been done, which factors contributed most strongly to the drowning of the Jurassic carbonate platform are still poorly understood.

Detrital heavy minerals are important material for provenance because they are generally insensitive to chemical changes and modifications during transportation, deposition and after burial (Morton and Hallsworth, 1999). Rock slabs from conventional cores are representative of the entire rock; hence petrographic studies are intrinsically informative.

In order to obtain the best results regarding provenance we used a combination of detrital heavy and light mineral characteristics such as texture (ilmenite, rutile), morphology (zircon), inclusions (ilmenite, quartz, and feldspar), alteration (titania minerals) together with the mineralogical composition of lithic clasts.

The second purpose is to describe and understand the factors and processes that influenced these sediments, both chemically and morphologically, during transportation, deposition and after their burial for a better understanding of their diagenetic evolution. Diagenesis is the process of lithification-compaction of sedimentary rocks, at temperatures and pressures less than that required for the formation of metamorphic rocks. During diagenesis, sediments undergo physical, chemical and mineralogical changes before becoming a rock, having a huge impact on the sediment porosity and thus permeability.

Both the process of assessing potential sources and understanding of diagenetic processes that operate during and after deposition of clastic sediments are important to refine depositional models, understand tectonic evolution, and predict the distribution and presence of the hydrocarbon reservoirs. Moreover, understanding what factors

control the geochemistry, abundance and distribution of diagenetic minerals can be important in tracing the geochemical evolution of the primary or later stage pore waters during and after burial of sediments.

The Shelburne sub-basin was chosen for research because it is the least-studied part of the Scotian Basin compared to the central and eastern parts which are well known and studied.

This research aims to answer the following questions:

1) What are the magnitude, timing and dispersal of Mid Jurassic and Early Cretaceous sands in the Shelburne sub-basin?

2) What are the petrography, source and distribution of sandstones in the basin and how have these sandstones evolved diagenetically?

In addition, this thesis will test several existing ideas about the provenance and diagenesis of clastic sediments in the Shelburne sub-basin and surrounding areas. Do the clastic rocks on the southwestern shelf show a local supply from the Meguma terrane (as appears to be the case for the Naskapi N-30 well further east; Reynolds et al., 2009), or a more distant supply through the Fundy Basin (as suggested by Cretaceous deposits at Vinegar Hill in New Brunswick; Piper et al., 2007)? How are the factors that influenced sediments during and after burial together with changes that occurred in the chemical, structural and mineralogical composition of the detrital minerals, similar or different to those documented in the Sable sub-basin? How was the clay mineral evolution influenced by the increased carbonates in the western part of the margin?

To achieve the objectives proposed for this research, Mohawk B-93, Mohican I-

100, Moheida P-15 and Shelburne G-29 from the SW Scotian Basin and Chinampas O-37 from the Fundy Basin were studied. These wells were determined appropriate for this study because they have cutting samples from sandy intervals that comprise a diversity of detrital heavy minerals, useful for determination of provenance for clastic sediments. In addition, conventional cores are available for Moheida P-15 and Mohican I-100, which are useful for diagenesis work.

The detrital heavy minerals were separated from other minerals during the heavy mineral separation technique. Accurate identification and discrimination of distinctive detrital minerals species depends on the ability to separate provenance-sensitive features and avoid parameters that are influenced by other factors. The material obtained after heavy mineral separation was used for the production of polished thin sections that include detrital heavy minerals. In addition, conventional cores are useful for the sampling of rock slabs used for the production of polished thin sections. Both polished thin sections of rock slabs and detrital heavy minerals were analysed by the scanning electron microscope (SEM) and the electron microprobe (EMP). Detrital heavy minerals in polished thin sections of cuttings were analysed to determine the chemical composition. Polished thin sections of conventional cores were studied for chemical determination of both detrital and diagenetic minerals. In addition, back-scattered electron images were obtained in order to establish textural relationships and determine the paragenetic sequence of diagenetic minerals.

Chapter 2: General Geological Setting

2.1 Introduction

The Scotian Basin, located beneath the continental shelf and slope offshore Nova Scotia, Canada (Fig. 2.1), originated during the break up of Pangaea 200 million years ago, and is considered a passive-margin sedimentary basin (McIver, 1972; Wade and MacLean, 1990). It was initiated during the Late Triassic-Early Jurassic rifting and continued to develop as the North American plate drifted away from the African plate (Wade and McLean, 1990).

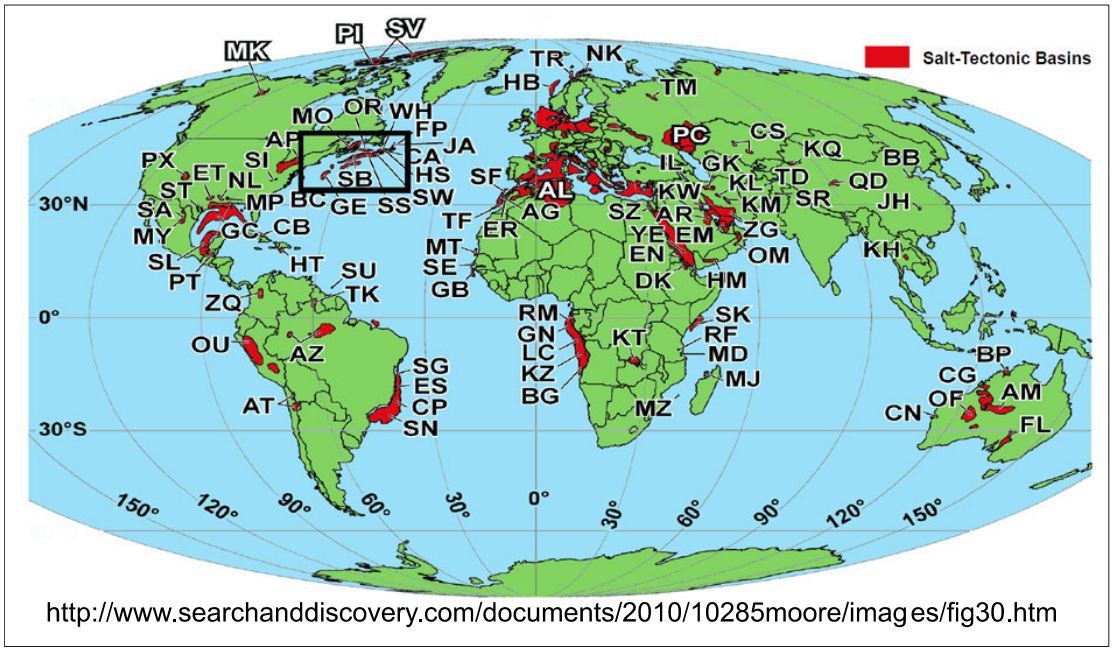

Figure 2.1: World map. The red color represents location of clastic sedimentary basins. The black square shows the location of the Scotian Basin, that extends over the margin of the eastern North American continent, beneath the continental shelf and slope offshore Nova Scotia.

The Scotian Basin is made up of several distinctive depocentres, from southwest to northeast named the Shelburne, Sable, Abenaki and Laurentian sub-basins (Wade and MacLean, 1990) (Fig. 2.2). Also underlying the Grand Banks, at the northeast end of the basin, is the South Whale Sub-basin. These depocentres were initiated during

Triassic rifting, but continued to develop through the Mesozoic and Cenozoic, with up to 17 km of strata preserved beneath some parts of the Scotian Shelf. To the northwest the Scotian Basin is bounded by the Appalachian orogen, whereas to the southeast is bounded by the Atlantic Ocean.

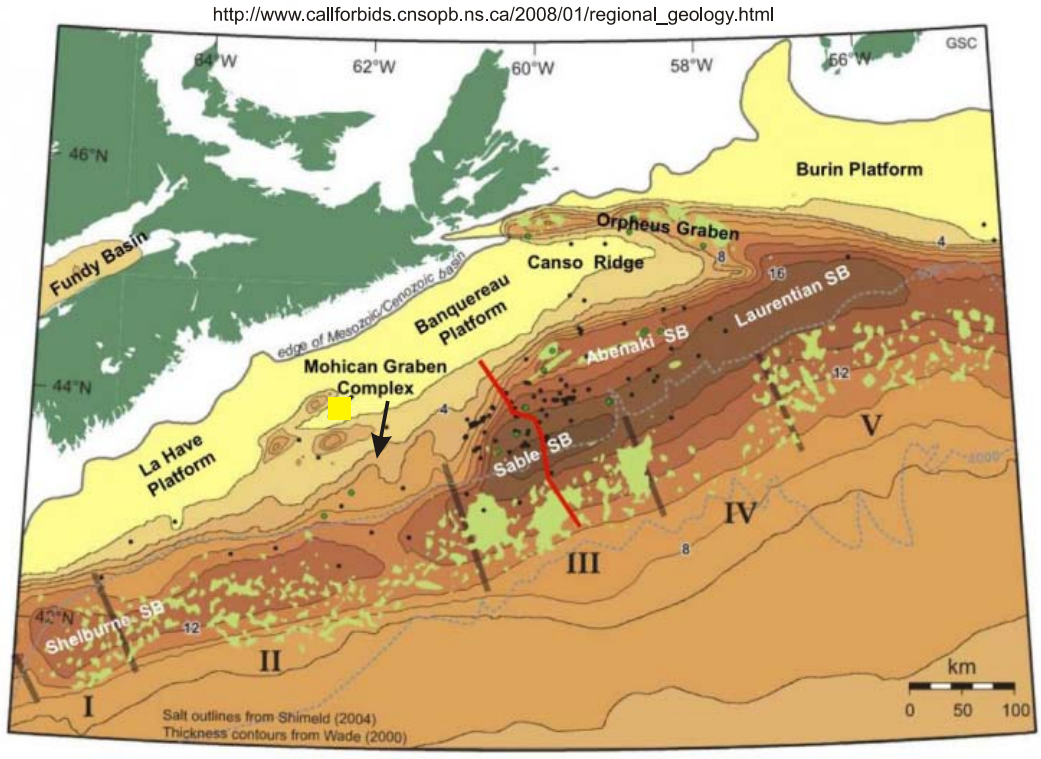

Figure 2.2: Major tectonic elements of the Scotian Basin showing depth to basement in kilometers and bathymetric contours in grey. The white labels from SW to NE represent the names of the four sub-basins that form the Scotian Basin. The four sub-basins are Shelburne, Sable, Abenaki and Laurentian. The pale green areas represent earliest Jurassic age Argo formation salt structures (Shimeld, 2004), with the Roman numerals indicating the salt basement regions as defined by Kidston et al. (2002) and Shimeld (2004). Thickness contours from Wade (2000).

The Appalachian orogen is divided into five terranes based on stratigraphic and structural contrasts between Cambrian-Ordovician and older rocks. From northwest to southeast, these terranes are the Humber, Dunnage, Gander, Avalon, and Meguma zones originally defined by Williams and Hatcher (1982). The Appalachian orogen has a parallel alignment to the length of the Scotian Basin, and thus the process of assessing potential sources for sediments in the Scotian Basin is challenging.

The Meguma terrane was deformed and assembled through the latest Neoproterozoic and Paleozoic and is the most outboard terrane of the Appalachian orogen, outcropping in southern Nova Scotia (Williams, 1995) and penetrated in wells on the Scotian Shelf (Pe-Piper and Jansa, 1999). Petrologically the Meguma terrane comprises a variety of metasedimentary, volcanic and plutonic rocks (van Staal, 2005). The terrane is made up mostly of a conformable succession of Neoproterozoic-Ordovician metamorphic strata up to 13 km thick, representing the Meguma Supergroup (White, 2010). In addition, the metamorphic rocks are intruded by Devonian granitoid plutons know from the literature as the Meguma Terrane granites (Clarke et al., 1997). Basement samples from offshore wells in the Scotian Basin, together with geophysical data, have shown that low grade metasedimentary rocks of the Meguma Supergroup comprise the basement underlying the Scotian Shelf (Pe-Piper and Jansa, 1999).

In Newfoundland, the Avalon terrane outcrops in the Avalon Peninsula and adjacent areas (Williams, 1995). Offshore it underlies all but the extreme southern Grand Banks of Newfoundland and Flemish Cap. In Nova Scotia the terrane is exposed in Cape Breton Island and in the inliers of the Antigonish Highlands and Cobequid Mountains (Williams, 1995). Petrologically, the Avalon terrane is composed of upper Precambrian sedimentary and volcanic rocks and overlying Cambrian-Ordovician shales and sandstones (Williams, 1995). In addition, the terrane is intruded by principally granitic plutons. Boundaries of the Avalon terrane with the Gander terrane in Newfoundland and New Brunswick are major faults (van Staal, 2005). In Nova Scotia the outboard boundary is the Cobequid-Chedabucto Fault Zone which separates

the Avalon terrane from the Meguma terrane (Keppie, 1983).

Both terranes have undergone several orogenic events. One of the most significant was the Acadian Orogeny during Mid Devonian causing regional deformation and dextral slip on the Cobequid-Chedabucto Fault Zone (Webb, 1969). This dextral motion continued through the Carboniferous (Murphy et al., 2011).

The Fundy Basin (Jansa and Wade, 1975; Brown, 1986; Brown and Grantham, 1992) occupies the boundary between the Avalon and the Meguma terranes (Wade et al., 1995). It is one of a series of half grabens, similar to Naskapi, Mohican and Orpheus grabens that formed along the eastern margin of North America during the Triassic-Jurassic rifting of Pangaea (Fig.2.3). The Fundy rift system formed during Early to Mid Triassic as a result of sinistral tensional reactivation of the older dextral Cobequid-Chedabucto Fault Zone transform fault system (Wade et al., 1995).

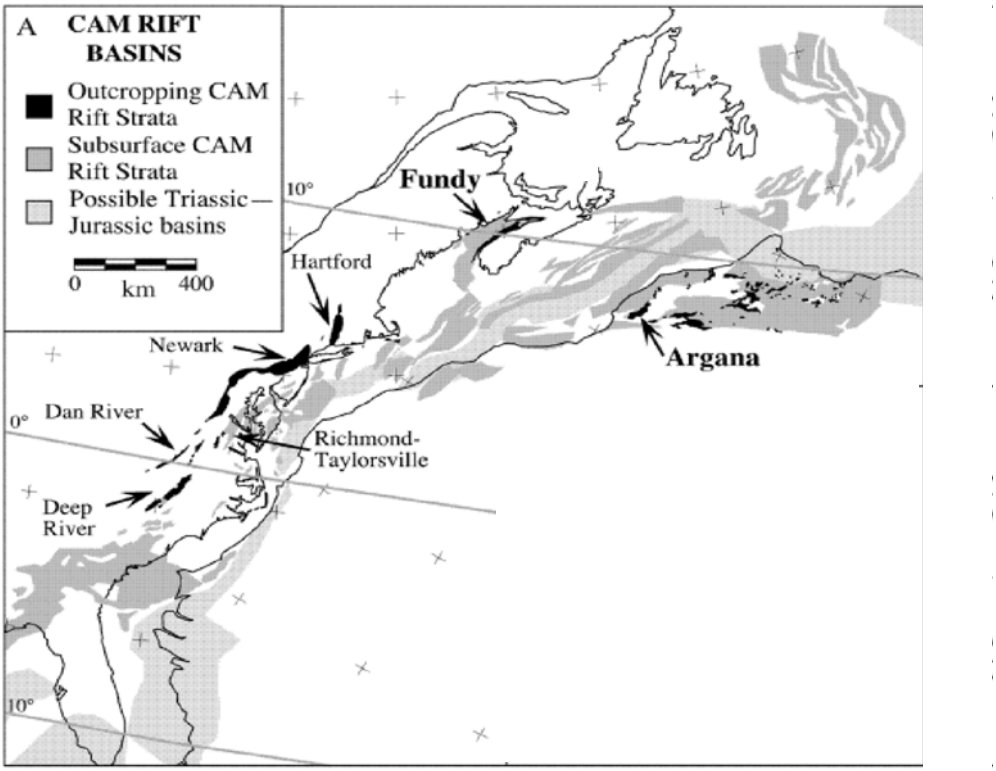

Figure 2.3: Position of the Fundy and other relevant basins during the Triassic-Jurassic rifting of Pangaea. Modified from Olsen et al. (2000).

2.2 Stratigraphy

Rift valleys that formed before the break up of Pangaea represent the first basins for Mesozoic clastic sediments (Given, 1977). The most recent lithostratigraphy, with biostratigraphy from Weston et al. (2012), is summarized in figure 2.4.

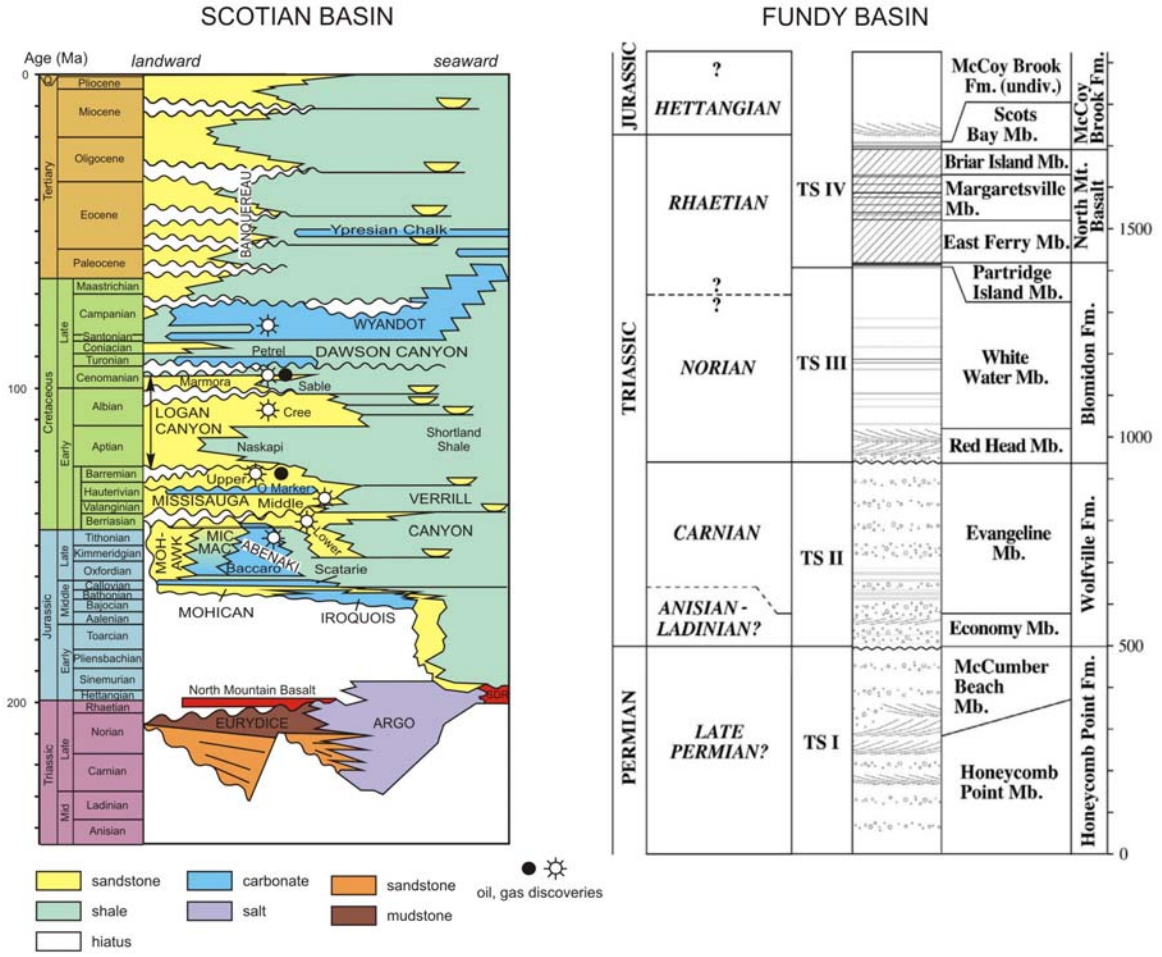

Figure 2.4: Lithostratigraphic columns of the Scotian Basin, modified from Weston et al. (2012) and the Fundy Basin, modified by Sues and Olsen (2015).

The earliest clastic sediments deposited in the Mesozoic rift basins off eastern Canada are known from the Wolfville Formation in the Fundy Basin and represent the initial phase of continental rift sedimentation (Wade et al., 1995). Red to brown, coarse to fine sandstone together with pebbly sandstone, conglomerate and minor shale represent the main deposits that compose the formation. The bottom of the formation is

no older than Early Carnian (Schlische and Olsen, 1990), with the top believed not to surpass Late Carnian (Olsen et al., 1989). In southern New Brunswick, four formations equivalent to the Wolfville Formation have been identified by Nadon and Middleton (1984), which are the Lepreau, Honeycomb Point, Quaco and Echo Cove formations.

Strata of the Blomidon Formation in the Fundy Basin are known from both Chinampas O-37 and Cape Spencer No. 1 offshore wells, characterized by Triassic fine grained clastic beds of red shale and siltstone. This Late Rhaetian to Early Hettangian formation (Holser et al., 1988; Fowell and Traverse, 1995) conformably overlies the Wolfville Formation sandstones.

The Late Triassic Wolfville Formation and the Late Triassic-Early Jurassic Blomidon Formation, exposed around and beneath the Fundy Basin, are lithologically similar and equivalent in age to the red-bed dominated Eurydice and evaporite dominated Argo formations deposited underneath the present Scotian Shelf and Grand Banks (Wade and MacLean, 1990).

The North Mountain Basalt is a succession of sub-aerial tholeiite flows (Puffer, 1992) extruded at about 201.4 Ma (Schoene et al., 2010), around the time of the Triassic-Jurassic transition. The tholeiite flows outcrop extensively in northwest Nova Scotia, along the SE margin of the Bay of Fundy, in the subsurface of the Fundy Basin and on the north and south part of the Grand Manan Island (Wade et al., 1995).

A basaltic unit similar to the North Mountain Basalt, named “Glooscap volcanics” occurs at Glooscap C-63 well above a bedded salt succession (Wade and MacLean, 1990) and is onlapped in turn by the clastics of the Mohican Formation. Although the basaltic unit is above the Argo Formation at Glooscap C-63 (Weston et al., 2012) and is

not radiometrically dated, it is in a similar stratigraphic position to the North Mountain Basalt and is geochemically similar to it (Pe-Piper et al. 1992).

The Scots Bay Formation tends to lie conformably above the North Mountain Basalt in the central part of the Fundy Basin, with minor onlap towards the basin margin (Wade and MacLean, 1990). On the northern margin of the Minas Basin the Scots Bay Formation has been replaced by the informally named McCoy Brook formation (Williams et al., 1985). Deposition of interbedded limestones, silty and cherty limestones, sandstones, siltstones and shales in the Scots Bay Formation was probably initiated in a small structural basin that quickly widened and included the southern part of the Fundy Basin (Wade et al., 1995). A variety of fossils indicate that the bottom of the formation is Early Jurassic (Olsen, 1981), probably Hettangian age (Barss et al., 1979). Due to erosion of almost 2000 m of strata from the top of the succession, the age of the strata at the top of formation cannot be assessed, but the youngest strata extend to at least the Pliensbachian (Wade et al., 1995). However, the upper age for the underlying strata of the North Mountain Basalt is dated as Early Hettangian (Wade et al., 1995).

The first sediments deposited in the tectonic sub-basins of the Scotian Basin, were Late Triassic–(?) Early Jurassic salt of the Eurydice and Argo formations. The lower part of the Mohican and Iroquois formations, represented by Mid Jurassic typical sabkha facies with shallow-water limestones and dolostones (Weston et al., 2012) are poorly constrained biostratigraphically, but are likely of Mid Jurassic age (Weston et al., 2012). The only biostratigraphic evidence for Early Jurassic taxa on the Scotian Shelf is known from a reworked specimen in South Griffin J-13 well.

The depositional setting in the Scotian Basin changed from marine conditions (upper Mohican Formation) and from typical carbonate sabkha facies (Iroquois Formation) to a period of widespread carbonate deposition corresponding to the Callovian to Tithonian Abenaki Formation (Weston et al., 2012). This Middle to Late Jurassic carbonate bank has been separated into several members: the Scatarie, Misaine, Baccaro and Artimon. The Scatarie Member, at the base of the Abenaki Formation, is a carbonate unit that overlies the top of the sandstone dominated Mohican Formation and the dolostone dominated Iroquois Formation (Weston et al., 2012). The Missaine Member overlies the Scatarie Member and in turn is overlain by the Baccoro Member. Seawards, the Misaine Member distally ie equivalent in age to the Upper Jurassic shales of the Verrill Canyon and Upper Jurassic proximal-deltaic clastics of the MicMac formations, whereas the Baccaro Member distally is equivalent to the MicMac Formation. Landward, both the Misaine and the Baccaro members are equivalent to the Mohawk Formation. The Artimon Member is of restricted distribution, present mostly in the central part of the basin.

In the central part of the Scotian Basin from Kimmeridgian to Tithonian, sandy deltaic facies of the lower member of Missisauga Formation (as defined by MacLean and Wade. 1993), partly coeval with the upper strata of the MicMac Formation, prograded across the carbonate shelf and graded laterally to the distal prodelta of the Verrill Canyon Formation (Cummings and Arnott, 2005). Along the southwestern shelf, however, carbonates equivalent in age to the Missisauga Formation continued to accumulate in areas far removed from clastic input (e.g. the Roseway unit in Mohawk B-93 well; Wade and MacLean, 1990). By Late Tithonian to Valanginian, and until

Hautervian clastic sediments representing the Middle Member of the Missisauga Formation, progressively extended across the Abenaki carbonate bank on the eastern part of the LaHave platform and passed into the distal prodelta corresponding to the Verrill Canyon Formation. The deposition of clastics of the Middle Member of the Missisauga Formation continued until a distinctive and widespread limestone unit, the informally named O-Marker, comprising multiple oolitic and bioclastic limestone beds with minor shale and sandstone, was deposited. The Upper Member extends up to the top of the Barremian and is represented by clastic sediments.

Aptian to Albian sediments on the Scotian margin are mostly encompassed by the Logan Canyon Formation, which can be several kilometers thick, particularly in the Sable sub-basin. The Logan Canyon Formation overlies more sandy rocks of the Missisauga Formation, and is composed of sandstones and shales, with some parts predominantly sandstone (the younger Marmora Member and the older Cree member), and some parts predominantly shale (the younger Sable Member and the older Naskapi Member). The sedimentary rocks typically grade into fine-grained prodelta shales and siltstones of the informal Shortland Shale (Jansa and Wade, 1975). The base of the Logan Canyon Formation is typically characterized by an age no older than intra-Aptian. Thin poorly preserved fluvial sedimentary rocks, known as the Chaswood Formation, are the equivalent of Missisauga and Logan Canyon formations onshore in southern New Brunswick and central-eastern Nova Scotia.

Clastic marine sediments of the Logan Canyon Formation are overlain by the Upper Cretaceous Dawson Canyon Formation with shale at the bottom, which in turn is overlain by the latest Cretaceous Wyandot Formation chalk, and latest Cretaceous and

Cenozoic mudstone and sandstone of the Banquereau Formation (McIver, 1972). On the Scotian margin only one member composed of thin limestone unit, the Petrel of probably Turonian age (Weston et al., 2012), was recognized from the Dawson Canyon Formation. The Banquereau Formation is separated from the underlying Wyandot Formation by a conformable boundary that generally ranges in age from Early Campanian up to at least Maastrichtian (Weston et al., 2012).

2.3 Plate tectonic and structural evolution

Pangaea was a supercontinent that existed during the Late Paleozoic and Early Mesozoic eras. It formed approximately 300 million years ago and then began to break apart after about 100 million years. The first break up of Pangaea into continental blocks started roughly in Mid Triassic (Fig. 2.5), and continued until Early Jurassic. During this period of time, Laurasia (Fig. 2.5) comprising North America, Europe and Asia and Gondwana (Fig. 2.5) comprising Africa and South America started to separate from central Pangaea (Schettino and Scotese, 2005). The second break up of Pangaea spanned the entire Cretaceous and resulted in segmentation of both Laurasia and Gondwana into other minor continental blocks.

Figure 2.5: The first break up of Pangaea into continental blocks, which started roughly in Mid Triassic, and continued until Early Jurassic. During this period of time, Laurasia comprising North America, Europe and Asia and Gondwana comprising Africa and South America started to separate from central Pangaea. The black square represents the location of Nova Scotia (figure modified after Faure and Mensing, 2010)

The process of fragmentation during the first break up can be described within an interval from the Late Ladinian (230 Ma) to the Tithonian (147.7 Ma) (Schettino and Turco, 2009). From the Late Ladinian (230 Ma) to the latest Rhaetian (200 Ma), the eastern margin of North America (Schlische et al., 2002), the northwest African margin (Davison, 2005) and the High, Saharan and Tunisian Atlas (Le Roy and Piqué, 2001; Ellouz et al., 2003) began to move apart from each other (Fig. 2.6). This process determined the formation of a separate Moroccan microplate at the boundary between Laurasia and Gondwana, from segmentation of the latter. From the latest Rhaetian (200 Ma) to the Late Pliensbachian (185 Ma), the first oceanic crust started forming and the Moroccan microplate continued to rift away from North America (Schettino and Turco, 2009). From the Late Pliensbachian (185 Ma) to Tithonian (147.7 Ma), plate motion started along complex fault systems between Morocco and Iberia, whereas a rift/drift transition occurred in the northern segment of the central Atlantic, between Morocco and the conjugate margin of Nova Scotia (Schettino and Turco, 2009), with implications for movement on the Cobequid-Chedabucto Fault Zone (CCFZ) (Fig. 2.6).

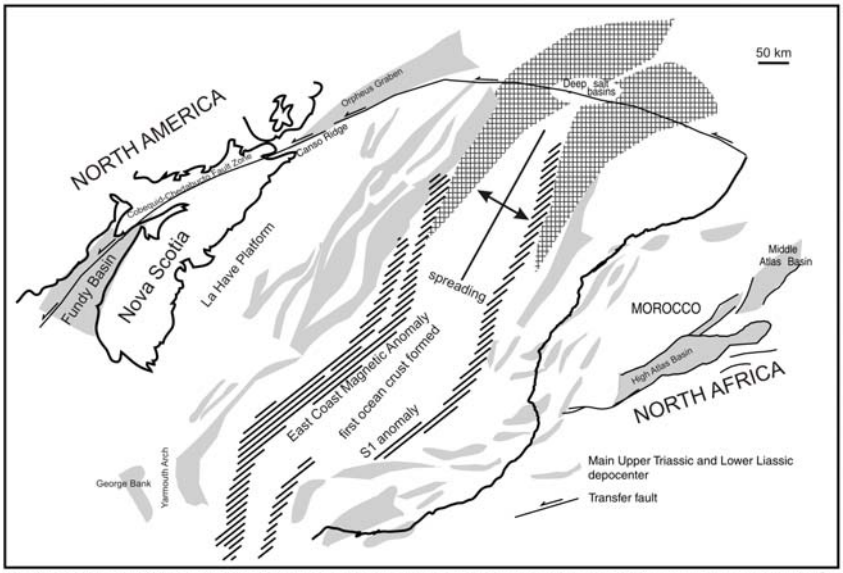

Fig. 2.6: Structural fragmentation of Pangaea showing the eastern margin of the North American continent and the northwest African margin moving apart from each other, as a rift/drift transition occurred in the northern segment of the central Atlantic, between Morocco and the conjugate margin of Nova Scotia. (figure modified after LeRoy and Pique, 2001).

Triassic extension resulted in several distinctive half grabens (e.g. the Fundy Basin) on the Laurentian margin, including generally northeast trending rift sub-basins, the Shelburne, the Sable, the Abenaki and the Laurentian, beneath the present day Scotian Shelf and Slope (Wade and MacLean, 1990). Within the same time period extensional pre-existing thrust faults and ramps formed during the Variscan and earlier orogenies (Manspeizer, 1988) were reactivated. The reactivation of these faults together with a sinistral strike slip motion of the CCFZ (Withjack et al., 1995) that was followed by several kilometers of dip-slip motion on the CCFZ (Pe-Piper and Piper, 2004) formed the Fundy Basin.

The Late Triassic–(?) Early Jurassic salt of the Eurydice and Argo formations in the Scotian Basin was probably deposited during drifting by progressive shallow water deposition in basins confined by basement geometry and/or synrift sedimentation (Albertz et al., 2010). During the Jurassic and the Cretaceous the Scotian Shelf started to subside as clastic sediments of the Mohican, Missisauga and Logan Canyon formations were deposited. The lithostatic pressure had a big impact on the tectonics which was dominated by expulsion of autochthonous salt creating accommodation on the present Scotian Shelf and emplacement of allochthonous salt bodies on the Scotian Slope (Albertz et al., 2010). Shimeld (2004) discriminated five distinctive salt tectonic zones along the strike of the Scotian Slope. Zones I and II are dominated by vertical structures, III and V by salt canopies and IV by a regional salt detachment overlain by an allochthonous synkinematic wedge of Jurassic sediments (Ings and Shimeld, 2006).

Deptuck (2011) separated the western Scotian margin (and Shimeld's 2004 zones I and II) into four proximal to distal postrift structural domains. The LaHave Platform

(LP) Province is the most landward of these and corresponds to a glaciated platform underpinned by thick continental crust broken in places by Triassic to Early Jurassic rift basins and intervening basement highs (Wade and MacLean, 1990). The boundary towards the sea is represented by a characteristic zone, known as hinge zone, across which basement depth increases abruptly (Deptuck, 2011).

The tectonic evolution that took place in the western part of the Scotian margin is characterized by folding and faulting of the bedded salt. This is clear evidence that the La Have Platform experienced both extension and localized inversion during rifting (Deptuck, 2011). In the Jurassic, the carbonate bank expanded over the platform by the time most of the grabens were filled and horsts were planed off. By the Cretaceous, the La Have Platform experienced low overall subsidence rates and was dominated by non-marine to outer neritic depositional environments for most of its history. An Early Eocene impact crater was penetrated by the Montagnais I-94 well (Jansa et al., 1989), located on the LaHave Platform. As a result, Cretaceous and Paleogene strata on the outer part of the outer La Have Platform were transported and deposited across a wide area, with a 65 km wide multi-tiered sub-circular failure scarp. The impact may have destroyed shelf-edge deltas above the carbonate platform that might otherwise have been preserved on the seaward parts of this low-accommodation shelf (Deptuck and Campbell, 2012).

The Slope Detachment (SD) Province is located seaward of the LP Province and an important margin hinge zone where basement depth increases abruptly and corresponds to the structural hinge zone that parallels the edge of the Upper Jurassic carbonate banks. This area is dominated by salt pillows and rollers, but except for the

mouth of the Mohican Graben, more prominent salt bodies are largely absent (Deptuck, 2011). Because of the steep morphology of the slope, Jurassic and Cretaceous sediments deposited in this area have experienced displacement with detachment above the weak primary salt layer (Deptuck, 2010a). The SD province topography has been created and modified through time by the presence of widespread canyoning as recorded on the deeply incised Late Jurassic, Cretaceous and Early Paleogene slope strata. The presence of canyons indicates that these might represent the path for clastic sediments to be transported from the LaHave Platform to deep water basins (Deptuck, 2011).

The SD Province passes down slope into the Diapir and Minibasin (DM) Province where expelled salt bodies are tallest and separate generally well-developed minibasins containing thick Jurassic and Cretaceous marine stratigraphic successions.

The seaward limit of the DM province is a major basement step that appears to define the seaward limit of the primary salt basin (Deptuck, 2011). The step is located within, and coincides closely with, the middle part of the East Coast Magnetic Anomaly (ECMA). The Outer ECMA Province of Deptuck (2011) is located outside the primary salt basin, in a region of minor salt overhangs that developed where the salt bodies were extruded up and out of the primary salt basin and now overlie the crust along the outer part of the ECMA.

2.4 Paleogeography

The first order control on geography and climate is latitude, via the effect on the angle of incidence of sunlight by the curvature of the Earth. Hence, the latitude at which a continent is located has the principal effect on climate, relative to other areas (Olsen and Et-Touhami, 2008).

Interpretations of paleomagnetic data available from the Newark Basin Coring Project (Kent et al., 1995; Kent and Olsen, 1999) together with techniques developed to overcome errors caused by sediment compaction (Tauxe and Kent, 2004; Kent and Tauxe, 2005), suggest that during the Late Triassic and earliest Jurassic the Fundy Basin was located about 20° N of the equator (Olsen and Et-Touhami, 2008). This means that the eastern North American sub-basins migrated from the humid tropics to the arid subtropics during the first deposition of synrift strata. Examples of such basins are the Fundy Basin which shows an overall upward trend to more arid environments in younger strata than in older strata, as would be expected with drift from the tropics to subtropics. The semiarid to arid climate of the rift valley is demonstrated by the presence in the Wolfville Formation of eolian sandstones, caliche paleosols, alluvial-fan conglomerates, and braided-river sandstones and by the abundant playa gypsiferous mudstones in the Blomidon red beds (Hubert and Hyde, 1982; Hubert and Mertz, 1980). The oxidized nature of the marginal facies in the Fundy Basin, together with their continental origin, large volumes of sediments and moderate sedimentation cycle suggest a generally hot and semiarid climate with periodic and/or seasonal heavy rainfall and subsequent high fluvial discharge (Wade et al., 1995), with such sources principally from the Meguma terrane (Li et al., 2012).

During deposition of the Eurydice red-beds in Late Triassic and Early Jurassic time, the climate in Nova Scotia was dominantly semiarid to arid, as evidenced by the evaporite features in many of the sandstones and sandy mudstones. The same climate continued at least until Early Jurassic when the salt of the Argo Formation and carbonates of the Iroquois Formation were deposited.

Until the end of Early Jurassic, the Scotian shelf is marked by an erosional hiatus sedimentation (Wade and MacLean, 1990) with influence from local developing rivers in the Meguma terrane. By the Middle Jurassic, carbonates of the Iroquois Formation and sediments of the Mohican Formation accumulated in rift-basins. The Middle Jurassic Mohican Formation was derived principally by rivers from the Meguma terrane (Li et al., 2012).

From Late Callovian and until the Late TIthonian the main depositional sediments in the central Scotian Basin were shelf carbonate rocks of the Abenaki Formation, typical of subtropical passive margin (Wade and MacLean, 1990). During the Jurassic, the Abenaki carbonate platform was situated below 30° N of the paleoequator, in a subtropical, easterly trade wind belt (Golonka et al., 1994; Scotese, 1997; Leinfelder et al., 2002). The dominance of carbonates during Late Jurassic in the Scotian Shelf is interpreted to result from opening of an ocean gateway for circumglobal equatorial flow (Berggren, 1982), increased rise in sea level and transgression of continental margin, as well as northward spread of warm water carbonate facies and associated regional aridity (Hallam, 1984b).

During the transition zone from Late Jurassic to Early Cretaceous, iron oolites were deposited in the southwestern Scotian Basin, specifically in Moheida P-15 and

Dauntless D-35 (Weston et al., 2012). The accumulation of oolitic ironstones suggests a subtropical to tropical environment (Hallam and Bradshaw, 1979). Westerly equatorial currents were diverted into high northern and southern latitudes by the configuration of Pangaea, resulting in warm climate at mid latitudes (van Houten, 1985).

During the Late Jurassic and Early Cretaceous, Nova Scotia and the Fundy Basin were located approximately 30º N of the equator (Irving et al., 1993), the Atlantic Ocean was approximately 1000 km wide (Ziegler, 1989), and the climate was warm and temperate (Rees et al., 2000).

According to previous researchers, two hypotheses are thought to have contributed to the change in rate of sand supply during Late Jurassic-Early Cretaceous. One is related to change in the geographic location of the North American continent due to northwest motion during the Late Jurassic and Early Cretaceous (Beck and Housen, 2003). This change thus resulted in the region moving from arid to more humid climate condition (Valdes et al., 1996) with development of a proto St. Lawrence River system draining large areas of the eastern Canadian Shield (Wade and MacLean 1990). The other hypothesis is related to the Early Cretaceous rifting and drifting of the Grand Banks of Newfoundland from Iberia (Wade and MacLean, 1990) with uplifting of the Avalon Terrane. Uplifting of the Avalon terrane was an important contributor for the supply of Late Jurassic and Early Cretaceous sediments in the SW part of the Scotian Basin. Recent provenance studies based on geochemical composition of Late Jurassic to Early Cretaceous sandstones and mudstones from core samples in the Scotian Basin suggest that abundance of coarse-grained clastic sediments was due to supply initiated by uplift and rifting (Labrador Rift) from Late

Kimmeridgian to Early Tithonian (Zhang et. al, 2014). Later on the absence of sandstones from the Aptian Naskapi Member in the Scotian Basin implies southwestwards diversion to the Fundy Basin of rivers that supplied sediments to the Scotian Basin, due to uplift of the Meguma Terrane and extrusion of basalts in the Aptian (Bowman et al., 2012) or high sea level as indicated from the presence of benthic forams in the Aptian which indicate marine inundation (Intra Aptian Maximum Flood Surface, Weston et al. (2012)).

2.5 Sources of diagnostic detrital minerals: generalities

Previous research, in the Scotian Basin and equivalent fluvial strata from the Lower Cretaceous Chaswood Formation onshore, suggests that sediments from Late Jurassic to Early Cretaceous have been transported from different areas of eastern Canada (Fig.2.7) by at least three rivers (Pe-Piper and Piper, 2012, Zhang et al., 2014), providing some constraints on minerals derived from specific sources.

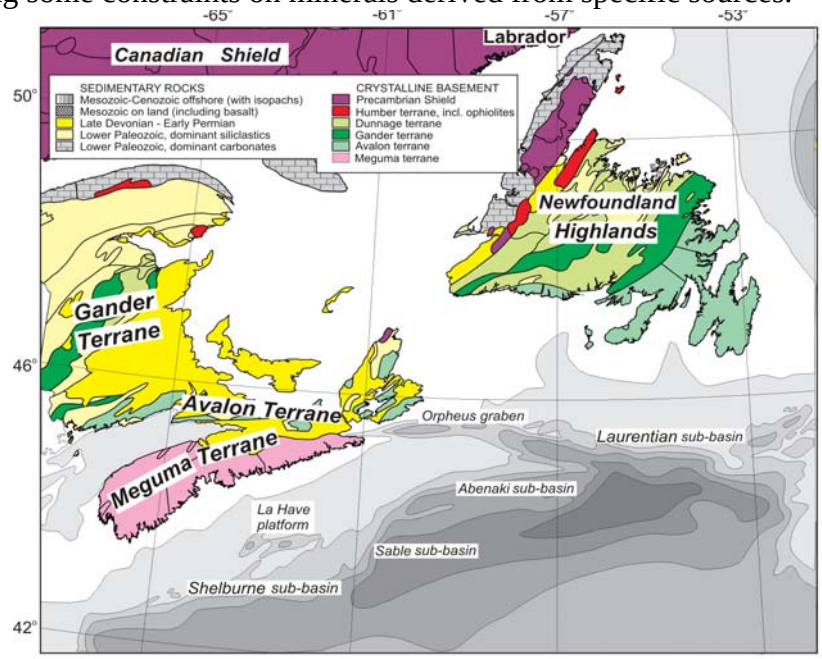

Fig.2.7: Regional geological map showing potential sources for mid Jurassic to early Cretaceous sediments deposited in the Scotian Basin. 2 km isopachs of offshore basins and principal rock types on land from Williams and Grant (1998). Map taken and modified from Pe-Piper et al. (2009).

2.5.1 Chaswood Formation

The Lower Cretaceous Chaswood Formation represents the equivalent fluvial strata for the deltaic Missisauga and Logan Canyon formations (Wade and MacLean, 1990), and has been identified in the central, northern and eastern part of Nova Scotia and the southern part of New Brunswick. Its occurrence in central Nova Scotia is limited in fault-bounded basins with outliers such as the Elmsvale Basin, Windsor and the West Indian Road Pit (Gobeil et al., 2006). In eastern Nova Scotia minor outliers are present at Brierly Brook and Diogenes Brook (Dickie, 1986; Stea et al., 1994; Pe-Piper et al., 2005c), whereas in northern Nova Scotia there is the Belmont outlier. The Chaswood Formation in southern New Brunswick is known only from the outlier at Vinegar Hill (Piper et al., 2007). The clastic sediments of the Chaswood Formation were derived from different sources (Fig.2.8) according to previous studies (Piper et al., 2007; 2008; Pe-Piper et al., 2005).

Heavy minerals in sandstones of the Chaswood Formation at Elmsvale Basin are mostly altered ilmenite. Staurolite, tourmaline, zircon, monazite, chromite and lithic clasts together with the light minerals muscovite and K-feldspar represent minor components that vary in abundance with increase in depth (Pe-Piper et al., 2004; Piper et al., 2008) (Fig.2.9). The most characteristic detrital heavy minerals present are zircon and monazite. Single-grain dating of monazite from sandstones in the Elmsvale Basin yielded Ordovician ages (463 to 498 Ma) (Pe-Piper and MacKay, 2006), which is an indicator of sediments sourced from northern New Brunswick. Most of the zircon is characterized as euhedral, an indicator of first-cycle detrital minerals from igneous sources. Few grains tend to be abraded suggesting a polycyclic origin. Lithic clasts

point toward a local supply from reworking of Ordovician to Late Paleozoic sandstones deposited in Nova Scotia with a minor influence from crystalline basement of the Avalon terrane (Piper et al., 2008).

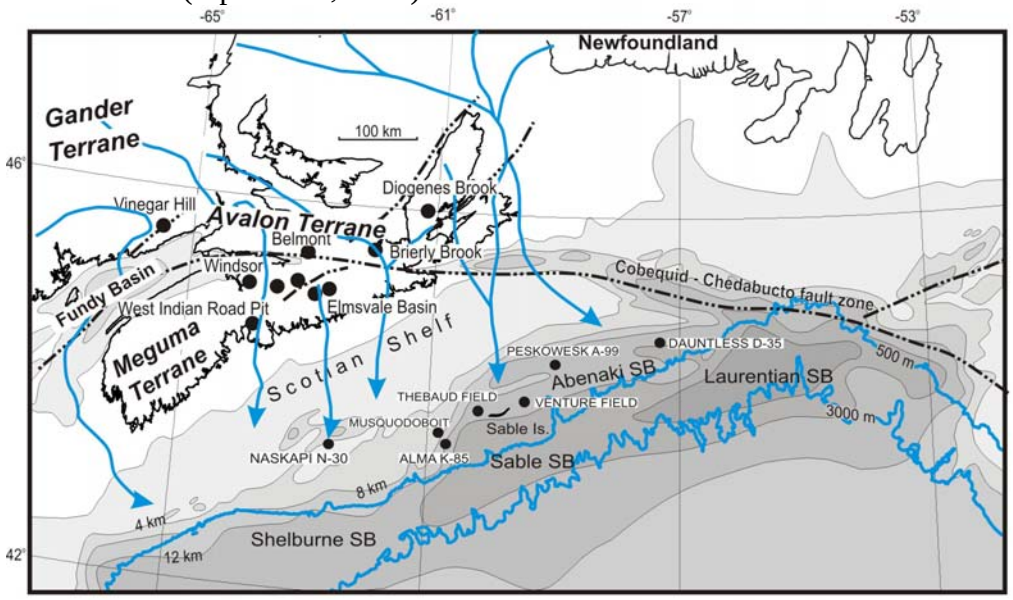

Fig.2.8: Schematic map showing potential rivers and sources for the Chaswood Formation on land (black dots) and late Jurassic-early Cretaceous sediments in the Scotian Basin. Potential rivers taken from Pe-Piper & Piper (2012) and Zhang et al. (2014). 2 km isopachs of offshore basins are from Williams and Grant (1998).

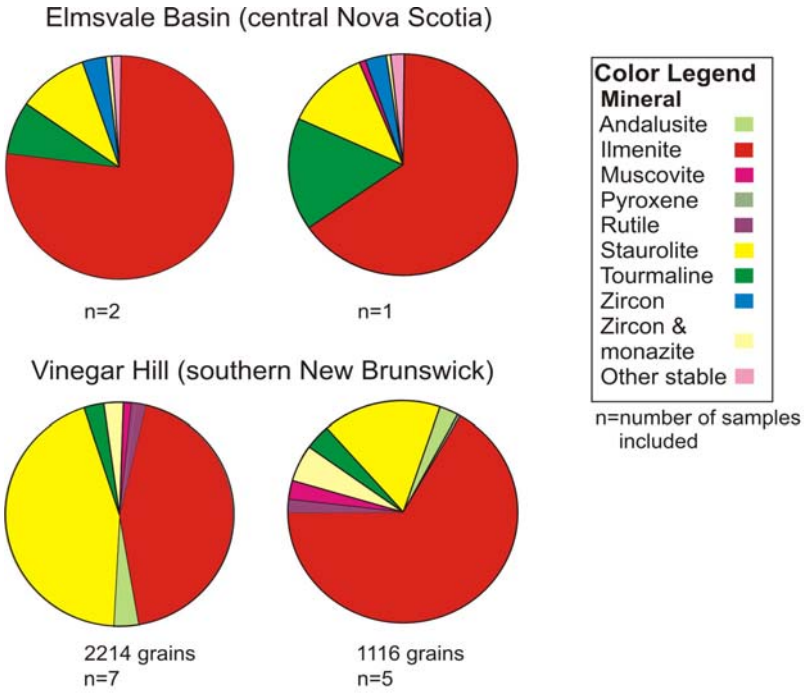

Fig.2.9: Pie chart diagrams showing modal abundance of detrital heavy minerals in outcrop samples at the Vinegar Hill and core samples from boreholes at the Elmvsale Basin. Data for the Vinegar Hill taken from Piper et al. (2007), whereas data for the Elmsvale Basin taken from Pe-Piper et al. (2004).

Detrital heavy minerals at Brierly Brook are composed principally of ilmenite, and in lesser amounts of staurolite and tourmaline, and varying amounts of zircon, monazite, and andalusite (Pe-Piper et al., 2005). Rarely we found detrital rutile, garnet, amphibole, clinopyroxene and orthopyroxene. Athough a light mineral, calcite is a significant, but variable component of the heavy mineral assemblage; dolomite, another light mineral is present as well. Most of the tourmaline chemistry indicates derivation from reworking of Carboniferous rocks originally derived from the Li-poor granite of the South Mountain Batholith (Piper et al., 2008). The remaining tourmaline has composition typical of metasedimentary rocks. Garnet (almandine) has similar chemical composition to garnet from the South Mountain Batholith, suggesting a first cycle source or may be of second-cycle origin derived from Carboniferous sedimentary rocks in Nova Scotia. The high proportion of staurolite at Brierly Brook may indicate supply predominantly from a Miramichi Highland source in New Brunswick, but also implies local derivation. Carbonate lithic clasts (dolomite and calcite) are most likely derived from the Windsor Group limestone.

The detrital heavy minerals present in the Lower Cretaceous Chaswood Formation at Vinegar Hill in southern New Brunswick were separated in two assemblages based on abundance (Fig.2.7): i) one with sub-equal presence of staurolite-ilmenite and less presence of orthopyroxene, clinopyroxene, tourmaline, andalusite, monazite/zircon and rutile and ii) one with abundant ilmenite, subordinate staurolite, equal amounts of monazite/zircon, andalusite and tourmaline. The high percentage of ilmenite and its alteration products in both assemblages at Vinegar Hill supports the idea that the sediments were derived possibly from two potential sources: i) directly from crystalline

rocks of the Avalon terrane enriched in ilmenite providing fresh ilmenite at Vinegar Hill which in turn altered as a result of diagenetic processes that operated during and after the burial of the sediments and ii) from reworking of older sandstones deposited in New Brunswick. Chemical composition of ilmenite with low values for Mn, when compared to those from northern Nova Scotia, suggests ilmenite is of igneous origin. Stable detrital heavy minerals like staurolite, andalusite, titanite and garnet appear to be sourced from rocks abundant in staurolite and andalusite. On the other hand tourmaline is both metamorphic and igneous, the latter likely to be derived from the Silurian granites outcropping in central New Brunswick (Piper et al., 2007). Unstable minerals such as actinolite and clinopyroxene are sourced from local sources in horsts (Piper et al., 2007). Ultra stable detrital minerals, such as zircon, indicative of polycyclic sources are almost absent (Piper et al., 2007). The Chaswood Formation in south New Brunswick has a local supply of lithic clasts from bedrock of the outboard Appalachians (Piper et al., 2007), with some diagnostic minerals reworked from Carboniferous sedimentary rocks. Based on the mineralogical composition and modal abundance of detrital minerals, the clastic deposits at Vinegar Hill were most likely derived from crystalline bedrock rather than through reworking of older sedimentary rocks. The aspect of sediments derived from crystalline rocks is also confirmed by monazite geochronology yielding Silurian age (Pe-Piper and MacKay, 2006) which suggest that the sediments were derived most likely from central New Brunswick (Piper et al., 2007). In addition, the lack of chromite, which is characteristic of the Humber terrane ophiolites and monazite with Ordovician age points that sediments at Vinegar Hill were not derived from more distant sources than central New Brunswick.

2.5.2 Horton Group

The Lower Carboniferous Horton Group is a first cycle sandstone-shale succession derived principally from the metasedimentary and granititc rocks of the Meguma terrane as inferred by chemistry of both detrital monazite and muscovite (Murphy and Hamilton, 2000). Other detrital heavy minerals identified are tourmaline, garnet, zircon and spinel/chromite. Tourmaline and zircon are abundant, whereas garnet and spinel/chromite are almost absent. In addition lithic clasts are present.

Four types of tourmaline were identified in samples from the Horton Group, which are type 1, type 2, type 3 and type 4; types 1 and 4 are abundant with minor types 3 and 2. Type 1 originates from granitoid rocks, type 2 from metapelites and calc-silicate rocks, type 3 may be derived from meta-ultramafic rocks, meta-carbonates or Cr-V-rich metasedimentary rocks, and type 4, is derived principally from metapelites and metapsammites (Henry and Guidotti, 1985; Kassoli-Fournaraki and Michailidis, 1984), although some may be derived from veins in granite (Clarke et al., 1989). The distribution of tourmaline varieties in the Horton Group sandstones is similar to those in the west Scotian basin, at Naskapi N-30 well where a major supply from the Meguma terrane is suggested (Tsikouras et al., 2011). The major supply with sediments from the Meguma terrane is also supported by the mineralogical composition of lithic clasts in the Horton Group together with ages of dated detrital zircons (Murphy and Hamilton, 2000; Pe-Piper and Piper, 2012).

Garnet from the Horton Group is typical of grossularite, which is abundant, followed by Mn-almandine, Ca- Mg-almandine and andradite, which are rare. Grossularite and Ca- Mg- almandine are found in the metagabbro and the anorthosites

of the Grenville Province. However, their abundance in the Great Village River in Nova Scotia, draining areas of the Avalon terrane, suggests that they are also derived from calc-silicate metasedimentary rocks (Tsikouras et al., 2011). Mn almandine is abundant in the Meguma Supergoup metasedimentary rocks and is perhaps characteristic of other metasedimentary rocks, for example in the Gander terrane (Tsikouras et al., 2011).

2.5.3 Sable and Abenaki sub-basins

Mineral assemblages in the Lower Cretaceous Upper Missisauga and Logan Canyon formations in Alma K-85 and Musquodoboit E-23 wells in the Sable sub-basin include mainly tourmaline, garnet (almandine with significant spessartine and gossular substitutions, spessartine), monazite, zircon, muscovite and spinel/chromite. Small amounts of accessory minerals like tremolite and Mg- Ca-rich clinopyroxene were also identified in Musquodoboit E-23. The Thebaud, Glenelg and Venture fields have characteristic spinel/chromite. Biotite is absent, probably as a result of dissolution with increase in depth (Pe-Piper et al., 2009).

Tourmaline and spinel/chromite are the most characteristic minerals identified. Specifically, tourmaline is of metamorphic origin, whereas MORB, IAT and boninitic spinel/chromite types are common mineral assemblage seen in all the wells from the Sable sub-basin. Relative constant zircon/chromite ratio indicates polycyclic sources (Tsikouras et al., 2011). Muscovite is predominantly of metamorphic origin with the exception of that at Alma K-85, which is predominantly igneous. Accessory minerals such as tremolite and/or Mg-, Ca-rich clinopyroxene at Musquodoboit E-23 appear to be derived from thermally metamorphosed impure carbonate rocks, similar to those of

the George River Group in Cape Breton Island, although a source on the inner shelf cannot be ruled out (Pe-Piper et al., 2009). Neither a contaminant origin from drilling mud can be completely excluded, since they have not been found in convemtional cores from the Scotian Basin.

In the Upper Jurassic Lower Missisauga Formation from Thebaud and Venture fields, tourmaline is predominantly type 4, followed by type 1 with minor type 3. The chemical composition of muscovite indicates metamorphic origin. Geochronology of detrital muscovite confirms a source for muscovite from metasedimentary rocks (Reynolds et al., 2009) that experienced resetting during the Alleghanian orogeny on the inner shelf (Reynolds et al., 2009). On the other hand, geochronology of detrital monazite and zircon (Pe-Piper and MacKay, 2006) indicate derivation of sediments from inboard terranes of the Appalachians and the Grenville province (Pe-Piper et al., 2009). Spinel/chromite of MORB, IAT and boninitic origin is present and is a mineral assemblage seen as well in the Lower Cretaceous formations of the Sable sub-basin with sources in the Paleozoic sandstones from western Newfoundland. The relatively high proportions of zircon and chromite/spinel in these sandstone indicates polycyclic sources (Tsikouras et al., 2011). However, recent studies on whole rock geochemistry of mudstones of the Cree member of the Logan Canyon Formation and Upper and Middle Missisauga formations at Alma K-85 have shown a Labrador crystalline source (Zhang et al., 2014). In addition, detrital monazite and zircon at Upper and Middle Missisauga formations, demonstrate important sources from the Appalachians and the Mesoproterozoic of Labrador (Zhang et al., 2014). Thus there is evidence for both, crystalline basement sources in the Appalachians and Labrador and polycyclic sources

probably mostly of Carboniferous age.

Lower Cretaceous formations (Middle and Upper member of Missisauga and Cree member of Logan Canyon) in Peskowesk A-99 and Dauntless D-35 in the Abenaki sub-basin comprise tourmaline, garnet, spinel/chromite, muscovite, biotite and lithic clasts. Tourmaline is not common, metamorphic clasts are common, garnet is present only in the Cree member of the Logan Canyon Formation and chromite/spinel is not as abundant as in the Sable sub-basin. Biotite is mostly of igneous origin. Dauntless D-35 contains an unusual high-Ca apatite (Pe-Piper et al., 2009). At Peskowesk A-99 the lithic clasts are principally of rhyolite-syenite-microgranite with different sources.

2.5.4 Naskapi N-30

The detrital mineral assemblage in Lower Cretaceous Missisauga Formation from Naskapi N-30 is: ilmenite, tourmaline, zircon, garnet, monazite, apatite, muscovite, plagioclase and biotite (Pe-Piper and Piper, 2007). Tourmaline resembles tourmaline of both metamorphic (metapelites/metapsammites) and igneous rocks (peraluminous granites) from the Meguma terrane. Garnet (spessartine with significant almandine substitution) is only of metamorphic origin and resembles garnet from the metasedimentary rocks of the Meguma terrane. Sub-equal abundances of metamorphic and igneous muscovite are present. Both geochronology and chemical mineralogy of muscovite point to a dominant supply from the South Mountain Batholith of the Meguma terrane (Pe-Piper et al., 2009). Geochronological ages for monazite (Reynolds et al., 2009) do not resemble the Ordovician monazite from the Chaswood Formation of central Nova Scotia, implying a lack of sediment supply to Naskapi N-30 from the

Chaswood Formation. Both, geochronology and chemical composition of muscovite and monazite point to a dominant sediment supply from the Meguma terrane. Particularly, monazites in the range of 300–340 Ma and Na-rich muscovite suggest derivation of some sediment from the inner shelf where there was Alleghanian resetting (Reynolds et al., 2009; Pe-Piper et al., 2009). Biotite is of metamorphic origin and resembles some biotites from the Chaswood Formation in central Nova Scotia. At Naskapi N-30 lithic clasts are almost exclusively polycrystalline quartz (Pe-Piper and Piper, 2007), presumably sourced from the metamorphic rocks of the Meguma terrane.

2.5.5 Polycyclic sources to Sable and Abenaki sub-basins

Polycyclic sources are important contributors for sediments in the central and eastern part of the Scotian Basin (Tsikouras et al., 2011). Previous work using whole rock geochemistry together with chemical composition, modal abundance, geochronology and relative abundance of different types of detrital mineral species have provide some information on crystalline sources and the relative influence of polycyclic sources.

Provenance studies in the central and eastern Scotian Basin suggest that at least four polycyclic sources have to be taken into consideration: i) reworking of Late Paleozoic/Carboniferous sandstones from Newfoundland (Tsikouras et al., 2011), ii) reworking of Carboniferous sandstones of the Horton Group in Nova Scotia, iii) reworking of Jurassic sandstones deposited in the proximal parts of the Scotian Basin and iv) erosion of sedimentary rocks in the Fundy Basin and New Brunswick (Piper et al., 2007).

The evidence of polycyclic sources is well preserved within clastic deposits from upper units in the Sable sub-basin. Specifically, Lower Cretaceous Formations at Alma K-85 are made up mostly by sediments transported by an ancestral Sable River with major sources in the Labrador and Newfoundland from reworking of Late Paleozoic/Carboniferous sandstones. Bulk geochemistry of rocks shows high Cr and Zr contents which are indicators of ultra-stable detrital minerals such as spinel/chromite and zircon (Morton and Hallsworth, 2007). In addition, modal abundance of detrital heavy minerals confirms the enrichment in zircon and spinel/chromite. The high abundance of spinel/chromite and zircon suggests concentration of these minerals through polycyclic reworking (Tsikouras et al., 2011). The influence of the Sable sub-basin with sediments through reworking of Late Paleozoic sandstones becomes more evident considering the low occurrence of the less stable ilmenite and its alteration products, suggesting involvement of more than one cycle of weathering and abrasion to concentrate high amounts of ultra-stable minerals (Pe-Piper et al, 2008). The varieties of spinel/chromite suggest that polycyclic spinel/chromite was ultimately derived principally from western Newfoundland, rather than central Newfoundland (Tsikouras et al., 2011). The higher presence of spinel/chromite and zircon to ilmenite and its alteration products in sediments from the central Scotian Basin can be considered indicator of polycyclic sources, but mineral abundance is further influenced by hydraulic sorting, dissolution with increase in depth (garnet) and other diagenetic processes. Tourmaline in the central Scotian Basin was predominantly derived from a major source in the Meguma terrane, possibly in part through polycyclic sources (Tsikouras et al., 2011). Garnet is abundant with varietal types of Ca-almandine and

Ca- Mg-almandine to be common suggesting a different ultimate source and probably polycyclic reworking (Tsikouras et al., 2011).

Chapter 3: Methodology

To fulfill the main objectives proposed for this study a number of steps were followed. The first step was the selection of wells suitable for diagenesis and provenance work. That was possible with the use of the BASIN database site, well history reports stored at CNSOPB and wireline log data from the Geological Survey of Canada. In this way the general assessment of data for the offshore wells, located in both the SW Scotian Basin and the Fundy Basin, was obtained.

Petroleum exploration programs that took place within the ’70s and mid ‘80s in the Fundy Basin and SW Scotian Basin resulted in a total of 12 offshore wells being drilled, including Mohawk B-93, Mohican I-100, Shelburne G-29 and Chinampas O-37; conventional cores, cutting samples and sidewall samples were obtained and stored for future studies (Table.3.1).

Table 3.1: Location and summary of SW Scotian Basin offshore wells

Well	Basin	Area /location	Latitude	Longitude	Total depth (m)	conventional cores	cuttings	sidewall cores
Acadia K-62	SW Scotian Basin	Scotian Slope	42.86222	61.91737	5287.4	-	✓	✓
Albatross B-13	SW Scotian Basin	Scotian Slope	42.70296	63.03662	4047.5	-	✓	✓
Bonnet B-23	SW Scotian Basin	LaHave Platform	42.38018	65.05052	4336	-	✓	✓
Chinampas O-37	Fundy Basin	Fundy Basin	44.94766	66.58963	3661.6	-	✓	✓
Glooscap C-63	SW Scotian Basin	Mohican Graben	43.20273	62.16576	4551.5	-	✓	✓
Mohawk B-93	SW Scotian Basin	LaHave Platform	42.70298	64.7314	2126	-	✓	✓
Moheida P-15	SW Scotian Basin	LaHave Platform	43.08231	62.27898	4297.7	3	✓	✓
Mohican I-100	SW Scotian Basin	LaHave Platform	42.99418	62.48092	4393.4	7	✓	✓
Naskapi N-30	SW Scotian Basin	LaHave Platform	43.49619	62.56684	2205.2	1	✓	✓
Oneida O-25	SW Scotian Basin	LaHave Platform	43.2493	61.5601	4109.9	-	✓	✓
Sambro I-29	SW Scotian Basin	LaHave Platform	43.64307	62.80473	3069.6	-	✓	✓
Shelburne G-29	SW Scotian Basin	Scotian Slope	42.6408	63.5593	4005	-	✓	✓

The well selection for this thesis was made based on the type of material available for study and sampling, e.g. whether conventional cores or only cutting samples are available; and on the lithologies that the available material represents. Wells that were previously studied and wells that do not have suitable lithologies available in form of conventional cores or in cuttings were excluded.

The second step comprises sample collection for the wells selected from both conventional cores and cuttings. Sample collection was based on studies of well history reports, washed cuttings and my own refinements for core samples. In the third step the samples obtained are used for the production of polished thin sections of both rock and cuttings and for whole rock geochemistry. In the final step the polished thin sections were analyzed first under the polarized microscope and secondly on both the Scanning Electron Microscope (SEM) and the Electron microprobe (EMP).

3.1. Sampling for detrital petrology, diagenesis and whole rock geochemistry

Of the 12 offshore wells, 11 originating in the SW Scotian Basin and 1 in the Fundy Basin, only 5 were selected for this study, Mohican I-100, Moheida P-15, Mohawk B-93, Shelburne G-29 and Chinampas O-37 (Fig.3.1). Of the 5 wells only 3 have conventional cores: Mohican I-100, Moheida P-15 and Naskapi N-30. Naskapi N-30 has been previously studied (Pe-Piper and Piper, 2007; Reynolds et al., 2009) and Moheida P-15 has only 3 short conventional cores, 3 m, 6 m and 14 m respectively in length. On the other hand, Mohican I-100 is represented by 7 cores corresponding to 54 m of recovered rock comprising lithologies with ages from Triassic (Eurydice Formation) to Early Cretaceous (Roseway Equivalent Formation).

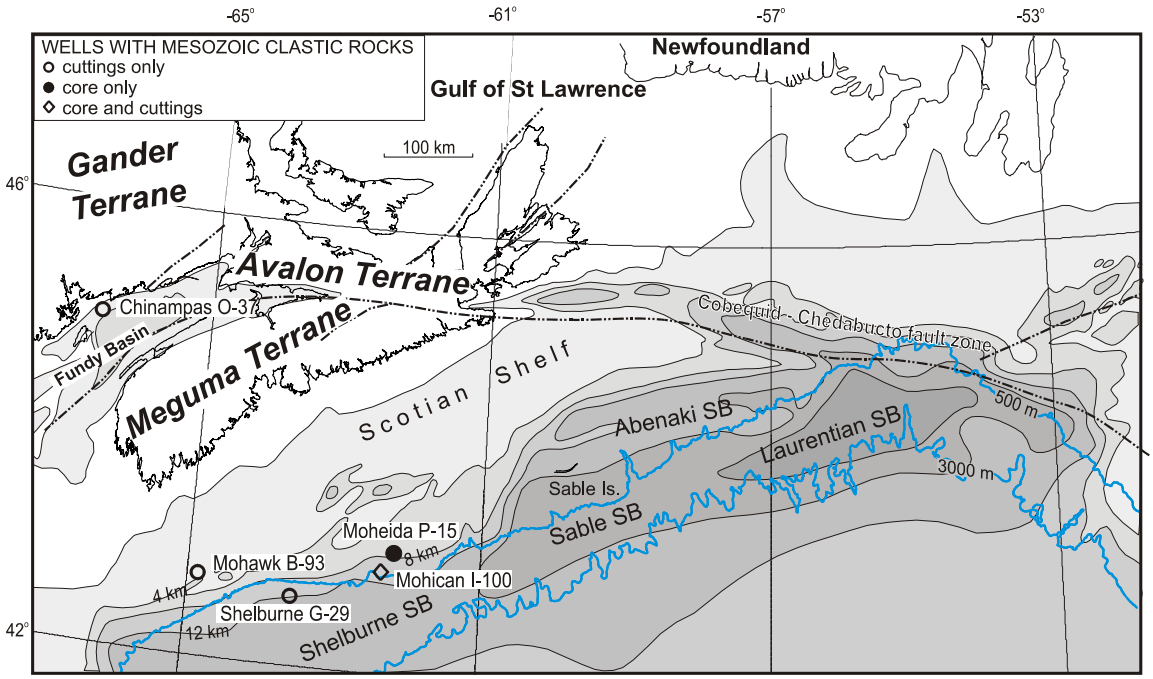

Figure 3.1: Regional geological map of Nova Scotia, New Brunswick, Fundy Basin and Scotian Basin showing location and material available for the wells selected in this study.

Stratigraphic columns for the wells selected were made based on cuttings lithology described in well history reports stored at Canada Nova Scotia Offshore Petroleum Board. Biostratigraphic markers for the formations identified and described are based on Weston et al. (2012) and the PFA, (2011). Digital data of natural gamma ray activity for each well was obtained from the Geological Survey of Canada (GSC) for the production of plots.

The purpose of making stratigraphic columns is to have a better understanding of the formations that are present in the SW Scotian Basin as well as their age and lithologies. With the information obtained from stratigraphy a correlation between wells is possible, which will show what conditions existed on the SW part of the Scotian shelf compared to the slope, as well as how do these formations change laterally. Correlation between wells was made using individual lithostratigraphy, biostratigraphy and gamma ray interpretation.

Lithologic descriptions of conventional cores from Mohican I-100 and Moheida P-15 wells (see appendices 1 and 2) were made at the Geoscience Research Centre of the Canada-Nova Scotia Offshore Petroleum Board, so that the depositional facies and possible diagenetic alteration of samples for provenance analysis were well understood. The lithologic description of conventional cores includes macroscopic identification of lithology and description of sedimentary structures. Such examples are grain size estimation with comparison chart and identification of distinctive types of rock interval. In addition, digital photos of conventional cores were obtained for the preparation of summary well plots that comprise lithologic and stratigraphic description of both sampled and non-sampled clastic intervals.

Slabs of rocks were cut from the back of conventional cores in Moheida P-15 and Mohican I-100, to be the most representative of the lithologies studied. The rock slabs were cut by the core lab technician. Conventional cores are preferred in this study because suitable samples can be collected for whole rock geochemical analysis and for making polished thin sections which are required for detrital petrology provenance and diagenesis work. Moreover, the use of conventional cores is important in understanding the overall stratigraphy of the SW Scotian Basin, from my own refinements as well as from already published work in the Scotian Basin. Polished thin sections are also important because they can be analyzed by polarized microscope, by SEM and/or by electron microprobe (EMP) depending on the purpose of the study.

The collection of offshore conventional cores is a very expensive and complicated process and at the same time lots of space is required for thousands of feet of rock to be stored. As a result, not all offshore wells are represented by conventional cores.

Offshore wells lacking conventional cores were studied using cutting samples for the extraction of detrital heavy minerals. The selection of intervals for cutting samples was made based on cutting lithologies (e.g. sand percentage), identified from washed cuttings and offshore well reports stored at CNSOPB. The preferred intervals for sampling of cuttings are those with high composition in sand. The presence of sand in cutting samples is important because it hosts diversity of detrital heavy minerals necessary in assessing potential sources for sediments. The cutting samples, with weight ~30 g, were washed and studied for detrital heavy minerals through the method known as heavy mineral separation that took place at the Sedimentology Laboratory at Bedford Institute of Oceanography (BIO) in Dartmouth.

All offshore wells are represented by cutting samples; however during this study from the total of 12 offshore wells, only 4 were selected for heavy mineral analyses which are Mohican I-100, Mohawk B-93 and Shelburne G-29 from the SW Scotian Basin and Chinampas O-37 from the Fundy Basin and only one, Mohican I-100 was selected for whole rock geochemical analyses. The remaining wells were excluded because they had conventional cores, e.g. Moheida P-15, because they were previously studied e.g. Naskapi N-30 or because the cuttings were mainly carbonates and can not be used in assessing potential sources for sediments e.g. Bonnet P-23, Acadia K-62, Albatross B-13.

A total of 55 representative samples, from conventional cores and cutting samples from Early Jurassic and Late Cretaceous strata (Fig.3.2) were obtained and used during this study. Of the 55 samples, 39 were obtained from conventional cores from Mohican I-100 and Moheida P-15 offshore wells, with 29 and 10 samples respectively. Of the 39

samples, 3 are shales and were used for X-ray diffraction analysis. The remaining samples are from cuttings.

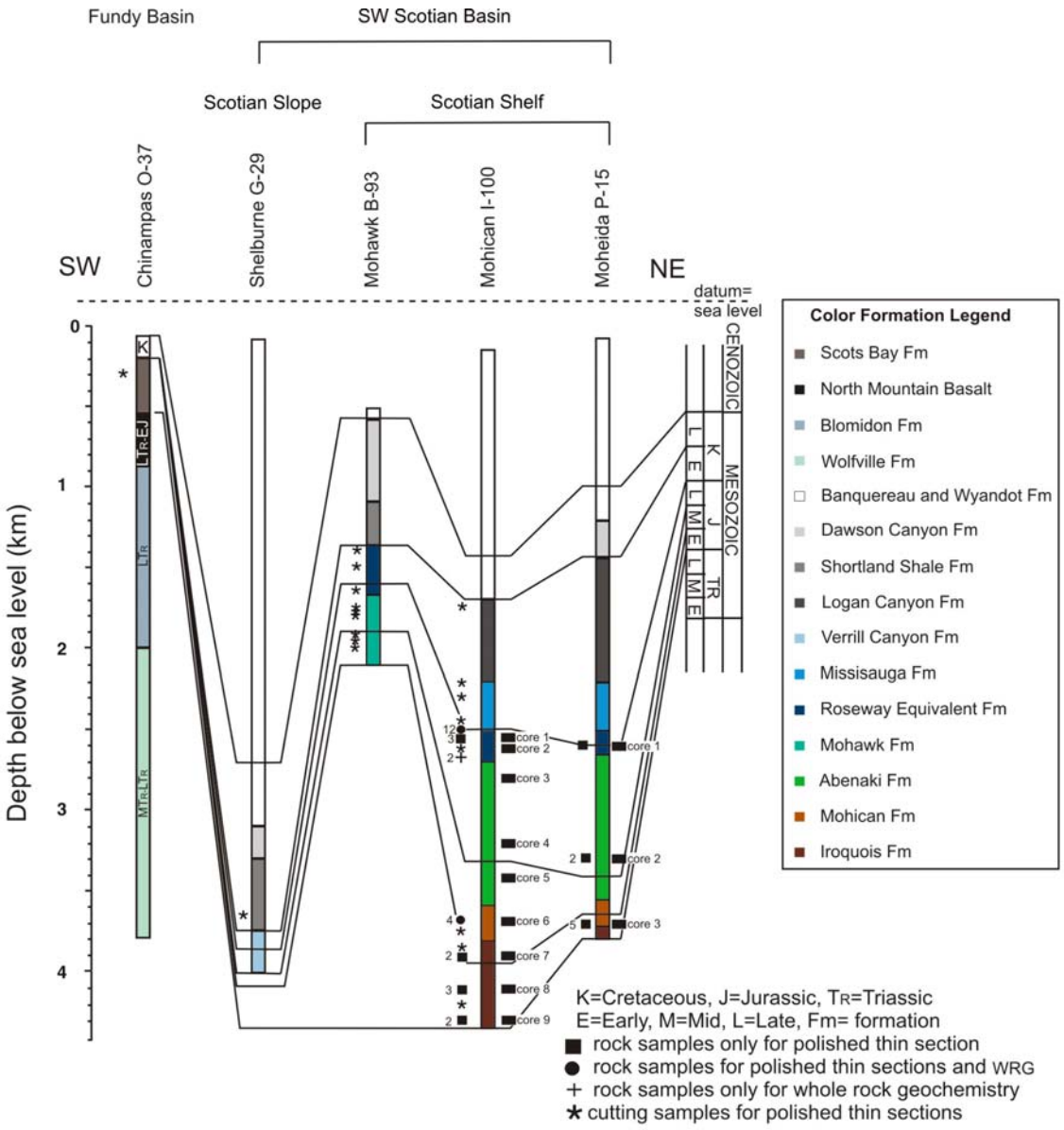

Figure 3.2: Schematic stratigraphic columns for the wells studied, showing stratigraphic location of anlysed samples (stratigraphic columns produced by author).

Note: the numbers in front of the symbols represent total number of samples collected. Symbols without numbers represent only one sample.

3.2 Preparation of polished thin sections (rock slabs from conventional cores)

A total of 28 rock slabs from conventional cores were collected from CNSOPB. Each sample was trimmed to the appropriate size required for the production of polished thin section using a Wizard saw thin section grinder with 4 inch diamond blade at the Thin Section Lab of the Geology Department of Saint Mary's University. In addition, the samples were washed with de-ionized water, to remove contaminants such as dust, mud and foreign sediments from the surface. Obtaining clean samples is a very important procedure during the process of producing polished thin sections, because impurities on the surface adversely affect the image quality of minerals analyzed by petrographic microscope, by SEM or by EMP and also alters the data obtained during chemical analyses. The trimmed slabs were shipped to Vancouver Petrographics Ltd, located in Vancouver, British Columbia, for vacuum impregnation with blue epoxy, grinding to a thickness of 30 μm and final polishing. From the 28 rock slabs only 26 polished thin sections (Table 3.2) were made as 2 of the rocks slabs were shale and polished thin sections could not be made. This representative set of polished thin sections was carbon coated and studied using a variety of analytical methods.

Table 3.2: Presentation of polished thin sections from conventional cores

Sample	Well	Depth (m)	Stratigraphic Unit	Age	Activity			Lithology
					Pm	SEM	EMP	
I-100 2526.53	Mohican I-100	2526.53	RE	EK-LJ	✓	✓		calc sst
I-100 2527.61	Mohican I-100	2527.61	RE	EK-LJ	✓			sandy, biocl lst
I-100 2529.62	Mohican I-100	2529.62	RE	EK-LJ	✓	✓		calc sst
I-100 2530.47	Mohican I-100	2530.47	RE	EK-LJ	✓	✓	✓	sandy, biocl lst
I-100 2530.60	Mohican I-100	2530.6	RE	EK-LJ	✓			sandy, biocl lst
I-100 2533.62	Mohican I-100	2533.62	RE	EK-LJ	✓			sandy, biocl lst
I-100 2537.08	Mohican I-100	2537.08	RE	EK-LJ	✓			sandy, biocl lst
I-100 2538.84	Mohican I-100	2538.84	RE	EK-LJ	✓	✓		calc sst
I-100 2541.6	Mohican I-100	2541.6	RE	EK-LJ	✓			biocl lst
I-100 3692.41	Mohican I-100	3692.41	MO	MJ	✓	✓		sst
I-100 3693.47	Mohican I-100	3693.47	MO	MJ	✓			sst
I-100 3964.6A	Mohican I-100	3964.6A	IR	MJ	✓	✓		sst
I-100 3964.6B	Mohican I-100	3964.6B	IR	MJ	✓			sst
I-100 4094.68	Mohican I-100	4094.68	IR	IJ	✓			sandy lst
I-100 4095.65	Mohican I-100	4095.65	IR	IJ	✓			sst
I-100 4098.08	Mohican I-100	4098.08	IR	IJ	✓	✓		calc sst
I-100 4331.05	Mohican I-100	4331.05	IR	IJ	✓			sst
I-100 4332.97	Mohican I-100	4332.97	IR	IJ	✓			sst
P-15 2563.67	Moheida P-15	2563.67	RE	EK	✓	✓	✓	oolitic ironstone
P-15 3306.03	Moheida P-15	3306.03	AB	LJ	✓	✓	✓	oolitic lst
P-15 3306.52	Moheida P-15	3306.52	AB	LJ	✓			oolitic lst
P-15 3744.92	Moheida P-15	3744.92	IR	MJ	✓	✓		sst
P-15 3745.8	Moheida P-15	3745.8	IR	MJ	✓			lst
P-15 3747.71B	Moheida P-15	3747.71	IR	MJ	✓			lst
P-15 3750.94	Moheida P-15	3750.94	IR	MJ	✓	✓		dlst
P-15 3758.61	Moheida P-15	3758.61	IR	MJ	✓			dlst

Note: RE=Roseway Equivalent, MO= Mohican, AB=Abenaki, IR=Iroquois
E=Early, M=Mid, L=Late, I-Indeterminate. K=Cretaceous, J=Jurassic, T=Triassic
Pm= Polarized microscope, sst=sandstone, lst=limestone, dlst=dolostone, calc=calcareous, biocl=bioclastic
SEM=Scanning Electron Microscope, EMP= Electron Microprobe

3.3 Preparation of geochemical samples

A total of 10 samples from conventional cores (Table 3.3) at Mohican I-100 contained sufficient material for geochemical analysis. The procedure of sample preparation is nearly identical to the procedure described in the preceding paragraph for production of polished thin sections. The clean rock samples were crushed using a shatterbox with an iron bowl. The rock powders were analyzed by Activation Labs, using their codes 4Lithore search and 4BI.

Table 3.3: Samples for whole rock geochemical analysis

Sample	Well	Depth (m)	Stratigraphic Unit	Age	Lithology
I-100 2527.61	Mohican I-100	2527.61	Roseway Equivalent	EK-LJ	sandy, biocl lst
I-100 2529.62	Mohican I-100	2529.62	Roseway Equivalent	EK-LJ	calc sst
I-100 2533.49	Mohican I-100	2533.49	Roseway Equivalent	EK-LJ	calc sst
I-100 2533.62	Mohican I-100	2533.62	Roseway Equivalent	EK-LJ	sandy, biocl lst
I-100 2537.08	Mohican I-100	2537.08	Roseway Equivalent	EK-LJ	sandy, biocl lst
I-100 2538.84	Mohican I-100	2538.84	Roseway Equivalent	EK-LJ	calc sst
I-100 2539.18	Mohican I-100	2539.18	Roseway Equivalent	EK-LJ	calc sst
I-100 2541.6	Mohican I-100	2541.6	Roseway Equivalent	EK-LJ	biocl lst
I-100 3692.41	Mohican I-100	3692.41	Mohican Formation	MJ	sst
I-100 3693.47	Mohican I-100	3693.47	Mohican Formation	MJ	sst

Note: E=Early, M=Mid, L=Late, K=Cretaceous, J=Jurassic
sst=sandstone, lst=limestone, calc=calcareous, biocl=bioclastic

3.4 Heavy mineral separation

Heavy mineral separates were studied from offshore wells. A total of 53 cutting samples from Mohawk B-93, Mohican I-100, Shelburne G-29 and Chinampas O-37 were collected at the CNSOPB. The purpose of heavy mineral separation is to use heavy minerals to produce polished thin sections which are finally chemically analyzed by SEM and/or by EMP. To produce polished thin sections there must be a desirable quantity of material comprising heavy minerals. Because of lack of material from individually distinctive sand intervals in most of the wells studied, mixing of adjacent samples was necessary. As a result from the 53 samples collected only 19 distinct polished thin sections were made (Table 3.4).

Table 3.4: Cutting samples used for polished thin sections

Sample	Well	Depth (m)	Stratigraphic Unit	Age	Activity	
					SEM	EMP
I-100 5990	Mohican I-100	1798.32	Logan Canyon Fm	EK-LJ	✓	
I-100 7230	Mohican I-100	2203.7	U Missisauga Fm	EK-LJ	✓	✓
I-100 7840	Mohican I-100	2389.63	M Missisauga Fm	EK-LJ	✓	
I-100 8480	Mohican I-100	2584.7	Roseway Equiv	EK-LJ	✓	
I-100 8810	Mohican I-100	2685.28	Roseway Equiv	EK-LJ	✓	
I-100 11400	Mohican I-100	3474.72	Abenaki Fm	MJ	✓	
I-100 12640	Mohican I-100	3852.67	Iroquois Fm	MJ	✓	
I-100 13800	Mohican I-100	4206.24	Iroquois Fm	IJ	✓	
B-93 4670	Mohawk B-93	1423.4	Roseway Equiv	EK	✓	
B-93 5170	Mohawk B-93	1577.33	Roseway Equiv	EK	✓	✓
B-93 5410	Mohawk B-93	1650.48	Roseway Equiv	EK	✓	✓
B-93 5760	Mohawk B-93	1743.45	Mohawk Fm	LJ	✓	
B-93 5860	Mohawk B-93	1787.64	Mohawk Fm	LJ	✓	
B-93 6210	Mohawk B-93	1892.8	Mohawk Fm	LJ	✓	
B-93 6340	Mohawk B-93	1932.43	Mohawk Fm	MJ	✓	✓
B-93 6540	Mohawk B-93	1993.41	Mohawk Fm	MJ	✓	
B-93 6750	Mohawk B-93	2058.92	Mohawk Fm	MJ	✓	
O-37 990	Chinampas O-37	301.75	Scots Bay Fm	EJ	✓	
G-29 3635	Shelburne G-29	3635	Shortland Shale Fm	EK	✓	

Note: E=Early, M=Mid, L=Late, K=Cretaceous, J=Jurassic

The maximum weight permissible for sampling was 30 g or 30 % of the starting sample weight stored in plastic bags, whichever was less. Even though there were samples for each of the sand intervals described in well history reports, some of the bags contained small amount of material (<30g), thus cutting samples could not be obtained. The majority of the samples, as a result of being stored in bags for almost more that 40 years since their collection, had a compact structure in form of aggregate. In order to decompose the aggregate set of sand particle into loose sediment, the samples were deposited into graduated glass beakers together with a liquid combination made of dishwasher liquid detergent and natural water. The samples were left for at least 3 days in the Geology Lab, located in the Department of Geology, Saint Mary's University, so that the mud, which was the main component of the cement, breaks up,

and released the individual clastic sediments. The purpose of adding dishwasher liquid detergent was not only to convert the samples from a compact structure into clastic sediment, but at the same time to get the samples as clean as possible.

After 3 days the cutting samples were washed with de-ionized water, sieved through a 53 μm sieve to separate the mud from the rest of the material, and finally put back in graduated glass beakers, water free this time.

The process of heavy mineral separation requires that the samples are completely dry and any form of water, liquid or vapor must be removed. To save time and speed up the process of sample drying, methanol was added. The samples were left with methanol in fresh air for 2 to 3 days from the time it was added.

Heavy mineral separation was carried out at the Sedimentology Laboratory at Bedford Institution of Oceanography (BIO) in Dartmouth. The process took about 10 working days. The cutting samples were first passed through a sieve with an opening of 250 μm so that rock fragments and mineral aggregate could be removed from the samples and the resulting material would consist as much possible in individual distinctive grains. In addition, the material comprising individual grains with diameter less than 250 μm was added in Fisherbrand 50 ml concentric base centrifuge plastic tubes along with sodium polytungstate, which has a density of 2.9 g/cm^3. Sodium polytungstate was used because it is non-toxic and it is more efficient compared to other heavy liquids. During this study heavy minerals were considered those with specific gravity >2.9 g/cm^3.

In turn the tubes were placed in a Thermo Fisher SorvalXR Floor model centrifuge that used 750 ml swinging buckets with inserts for 50 ml conical base

centrifuge tubes and rotated for 30 minutes. To separate the heavy minerals on the bottom of the tube from the light minerals on the surface of polytungstate liquid in the tubes, liquid nitrogen was used. The material from the bottom of the tube (S.G.>2.9 g/cm^3) was washed with de-ionized water to remove the additional sodium polytungstate. In addition, the samples were placed in an oven with a temperature of 60ºC for at least 3 days to remove any form of water. To produce polished thin sections there must be a desirable quantity of material comprising heavy minerals. Because of lack of material from individually distinctive sand intervals in most of the wells studied, mixing of adjacent samples was necessary. The final material obtained was used for polished thin sections, as described above.

3.5 Optical microscopy

The polished thin sections were studied first by a petrographic microscope, using polarized and reflected light, through which it was possible to identify and determine distinctive groups of minerals that make up the rock samples, as well as textures to distinguish detrital from diagenetic minerals (recrystallization, oxidation and alteration). The polarized microscope is useful equipment in identifying distinct mineral species within rock and cutting samples; to understand the petrography, textures, discriminate detrital minerals from diagenetic minerals and to describe special features where they can be identified.

The study was carried out in the Petrology-Mineralogy lab in the Department of Geology, Saint Mary's University using a Nikon Eclipse E400 POL polarized microscope. Images were obtained with a Pixel INK PL-A686C camera.

3.6 Scanning Electron Microscope (SEM)

All polished thin sections (rock slabs and cuttings) were analyzed by electron dispersion spectroscopy (EDS) using a LEO 1450 VP SME Scanning Electron Microscope with a maximum resolution of 3.5 nm at 30 kV equipped with an INCA X-max 80 mm^2 silicon-drift detector (SDD) with detection limit of > 0.1%, located at the Regional Analytical Centre at Saint Mary's University, Nova Scotia. To obtain high quality data during chemical analysis by energy dispersive spectroscopy (EDS), the polished thin sections were carbon coated at the Thin Section Lab of Department of Geology, Saint Mary's University. The SEM uses a conventional high vacuum with a cooling system of liquid nitrogen to -180ºC. A tungsten filament produces a focused beam of electrons which interacts with the atoms in the sample, generating signals that can be detected and contain information about the sample's chemistry, topography and other. A copper standard was used for the calibration of the SEM.

SEM analyses are important to determine the chemical composition of detrital heavy minerals and diagenetic minerals, something that can not be done with the polarized microscope, to describe textures accompanying these sedimentary rocks and to obtain back-scattered electron images of these textures and minerals for interpretation of their diagenetic evolution. Also, for determination of the chemical composition of distinctive minerals present within the lithic clasts, and hence possible rock sources, we used EDS chemical analyses. For texture we also used back-scattered electron images. All geochemical data were processed using MINPET software for Windows, whereas editing of maps and diagrams were made using Coreldraw version X3 software package for Windows.

3.7 Electron microprobe (EMP)

All wavelength-dispersive spectroscopy (WDS) geochemical analyses of detrital rutile were made using a JEOL-8200 electron microprobe with five wavelength spectrometers and a Noran 133 eV energy dispersion detector, located at the Regional Electron Microprobe Centre at Dalhousie University, in Halifax, Nova Scotia. The operating conditions were at 15 kV of accelerating voltage with a 20 nA beam current, a beam diameter of 1 micron and duration of analysis approximately 15 minutes. For rutile analyses the trace elements analyzed were Nb, Zr and V. Before measuring the intensities of the actual trace elements in detrital rutile from cutting samples, standards were used to avoid peak interference and for calibration of the apparatus. WDS detectors perform quantitative analyses compared to EDS which perform qualitative analyses. Although the electron microprobe works similarly to the SEM, it has the advantage of smaller electron beam and use of standards that are more similar to the actual samples, so quantitative mineral chemical analyses are possible and more accurate. All geochemical data were processed using MINPET software for Windows, whereas editing of maps and diagrams were made using Coreldraw version X3 software package for Windows.

3.8 Rock Classification

Classification of sedimentary rock types was determined by point counting. The point counting data was collected using a Nikon Eclipse E 400 Pol polarizing microscope equipped with a Coolpix digital camera, an automated stepping stage, and the Petrog software from Conwy Valley Systems. In order to have a larger data set that

will lead to better classification, a total of 600 different points were counted and analyzed. Of the 26 samples only 18 were selected for point counting (Table 3.5). The other 6 were 100% dolostone or limestone and hence not suitable for this purpose.

Table 3.5: Polished thin sections of conventional core selected for rock classification

Sample	Well	Depth (m)	Stratigraphic Unit	Age	Lithology
I-100 2526.53	Mohican I-100	2526.53	RE	EK-LJ	calc sst
I-100 2527.61	Mohican I-100	2527.61	RE	EK-LJ	sandy, biocl lst
I-100 2529.62	Mohican I-100	2529.62	RE	EK-LJ	calc sst
I-100 2530.47	Mohican I-100	2530.47	RE	EK-LJ	sandy, biocl lst
I-100 2530.60	Mohican I-100	2530.6	RE	EK-LJ	sandy, biocl lst
I-100 2533.62	Mohican I-100	2533.62	RE	EK-LJ	sandy, biocl lst
I-100 2537.08	Mohican I-100	2537.08	RE	EK-LJ	sandy, biocl lst
I-100 2538.84	Mohican I-100	2538.84	RE	EK-LJ	calc sst
I-100 3692.41	Mohican I-100	3692.41	MO	MJ	sst
I-100 3693.47	Mohican I-100	3693.47	MO	MJ	sst
I-100 3964.6A	Mohican I-100	3964.6A	IR	MJ	sst
I-100 3964.6B	Mohican I-100	3964.6B	IR	MJ	sst
I-100 4094.68	Mohican I-100	4094.68	IR	IJ	sandy lst
I-100 4095.65	Mohican I-100	4095.65	IR	IJ	sst
I-100 4098.08	Mohican I-100	4098.08	IR	IJ	calc sst
I-100 4331.05	Mohican I-100	4331.05	IR	IJ	sst
I-100 4332.97	Mohican I-100	4332.97	IR	IJ	sst
P-15 3744.92	Moheida P-15	3744.92	IR	MJ	sst

Note: RE=Roseway Equivalent, MO= Mohican, IR=Iroquois, E=Early, M=Mid, L=Late, K=Cretaceous, J=Jurassic, T=Triassic sst=sandstone, lst=limestone, calc=calcareous, biocl=bioclastic

The 18 samples were first described based on mineral composition under the polarizing microscope (Table 3.6). The minerals identified were divided into 8 groups: monocrystalline quartz, polycrystalline quartz, feldspars (includes both K-feldspar and plagioclase), unstable minerals (muscovite, chlorite, and biotite), resistant minerals (such as garnet, apatite, detrital TiO_2 minerals, and ilmenite) and lithic clasts (include igneous, metamorphic, and sedimentary rock fragments).

Table 3.6: Percentage of detrital grains for rock samples from the SW Scotian Basin

Well	Sample	Mono Qz %	Poly Qz %	Feldspar %	Unstable Minerals (bt, chl, ms) %	Resistant Minerals (zr, ilm, tur) %	Lithic clasts %	Total detrital grains %	Total dextral grains	Total Count
Mohican I-100	I-100 2526.53	89.1	5.0	2.0	2.6	1.3	0.0	50.3	302	600
	I-100 2527.61	100.0	0.0	0.0	0.0	0.0	0.0	7.7	46	600
	I-100 2529.62	96.0	2.0	0.3	0.6	0.6	0.6	58.8	353	600
	I-100 2530.47	87.4	1.0	1.0	10.7	0.0	0.0	17.2	103	600
	I-100 2530.60	93.9	0.0	6.1	0.0	0.0	0.0	11.0	66	600
	I-100 2533.62	94.4	1.9	3.7	0.0	0.0	0.0	9.0	54	600
	I-100 2537.08	96.7	0.0	0.0	1.6	1.6	0.0	10.2	61	600
	I-100 2538.84	92.1	0.0	3.6	4.3	0.0	0.0	23.3	140	600
	I-100 3692.41	70.1	0.0	7.8	0.0	13.1	9.0	55.8	335	600
	I-100 3693.47	87.3	1.4	8.5	0.0	2.8	0.0	35.3	212	600
	I-100 3964.6A	87.8	0.6	3.0	6.1	2.4	0.0	27.3	164	600
	I-100 3964.6B	88.3	0.0	7.8	1.6	1.6	0.8	21.3	128	600
	I-100 4094.68	91.3	0.0	4.3	0.0	4.3	0.0	3.8	23	600
	I-100 4095.65	98.0	0.0	2.0	0.0	0.0	0.0	16.8	101	600
	I-100 4098.08	91.8	0.0	7.6	0.0	0.6	0.0	28.5	171	600
	I-100 4331.05	95.8	0.0	3.6	0.0	0.7	0.0	51.0	306	600
	I-100 4332.97	94.9	0.0	5.1	0.0	0.0	0.0	32.7	196	600
Moheida P-15	P-15 3744.92	82.9	0.2	4.5	0.2	4.7	7.4	67.3	404	600

The numbers after I-100 and P-15 represent the depths from which the samples were collected
Lithic clasts include all lithic clasts (igneous, metamorphic, sedimentary) other than polycrystalline quartz

The samples then were classified using their mineralogical composition. For sandstone classification and paleotectonic environment, only quartz (monocrystalline and polycrystalline), feldspars, and lithic clasts were used. The data collected were plotted, using the software MinPet, into 3 ternary diagrams to determine rock classification and probable provenance type. The QFL sandstone classification diagram of Folk (1968) contains seven fields dependent upon variations in the percentages of each total quartz (Q) including both monocrystalline and polycrystalline, feldspar (F) including K-feldspar and plagioclase, and lithic clasts (L) including igneous, metamorphic and sedimentary rock fragments. These fields are arkose, lithic arkose, feldspathic litharenite, litharenite, subarkose, sublitharenite, and quartzarenite.

The paleotectonic environment of origin of sandstones can be determined by using two diagrams, the QFL and the QmFLt diagrams, developed by Dickinson et al. (1983).

These diagrams are divided into three main categories of provenance, which are continental block, magmatic arc, and recycled orogen. The QFL plot uses total quartz grains (Q), versus feldspar (F) and lithic clasts (L). The QmFLt plot, uses the same principal components as the QFL plot, regarding percentages of feldspar (F), with the only difference that polycrystalline quartz is included in the lithic clasts.

3.9 Contaminants

3.9.1 Cuttings

In petroleum exploration, drilling mud is used to aid the drilling of boreholes into the earth. The main functions of drilling muds include providing hydrostatic pressure to prevent formation fluids from entering into the well bore, keeping the drill bit cool and clean during drilling, carrying out drill cuttings, and suspending the drill cuttings while drilling is paused and when the drilling assembly is brought in and out of the hole. The drilling mud used for a particular job is selected to avoid formation damage and to limit corrosion. Water-based drilling mud most commonly consists of bentonite clay (gel) with additives such as barium sulfate (barite), calcium carbonate (chalk) or hematite.

Offshore wells during the 70’s and the 80’s in the Scotian Basin and the Fundy Basin were drilled by adding drilling mud as shown from well history reports stored at CNSOPB. As a result cuttings collected from offshore wells studied include contaminants from drilling mud by the time the cuttings were transported to the surface and collected.

The heavy mineral polished thin sections from the studied wells comprise a high amount of artificial contaminants (see appendices 3 to 6). The most common

contamintant identified is barite and PbO mineral, which are present in almost all the samples analyzed. In addition, hematite was found in great amount in sample I-100 7230 from Mohican I-100 well. Other contaminants in smaller amount are zincite, sphalerite and talc.

3.9.2 Polished thin sections

After the process in chapter 3.2.2 is accomplished the rock samples must be polished to achieve a desirable thinckness so that chemical analyses analyses and optical observations can be done. The desirebale thickness can be achieved by polishing the sample with water or other materials such as Sn powder.

Chemical analyses of polished thin section P-12 2563.67 in Moheida P-15 well has show high amount of cassiterite (see appendix 10-1B). Personal communication with the technician who produced the polished thin sections showed that a substance enriched in SnO_2 was used for polishing. As a result cassiterite is considered a contaminant.

4. Results

4.1 Stratigraphy

4.1.1 Lithostratigraphy and biostratigraphy

The lithostratigraphic correlation is presented in figure 4.1 based on lithologic picks from the PFA (2011). The oldest Jurassic strata in both Mohican I-100 and Moheida P-15 wells is represented by the Iroquois Formation, which comprises mostly dolomite with sand and shale interbedding. Although the lithologic composition of the Iroquois Formation in both wells seems to be similar, the formation expands over a bigger interval in Mohican I-100 (3787 m-4286 m) compared to Moheida P-15 (3728 m -4043 m).

The Iroquois Formation in both wells is in turn conformably overlain by the Mohican Formation. At Moheida P-15 the Mohican Formation has abundant sandy intervals, whereas at Mohican I-100 it is mostly shale and siltstone.

The Abenaki Formation was identified in both Mohican I-100 and Moheida P-15, above the Mohican Formation. The main lithology recognized is limestone of the Scatarie and Baccarro members. Shales and siltstone of the Misaine Member separate the two limestone members.

The Mohawk Formation was identified only at the bottom of Mohawk B-93 well. The formation comprises mostly coarse and fine sandstone. It is overlain in the Mohawk well by the Roseway Formation, made up of limestone with coarse and fine sandy intervals. The Roseway Formation passes vertically on the continental shelf into the shales and sands of the Missisauga Formation (see Mohican I-100 and Moheida P-15) and on the slope passes upwards into the shales of the Verrill Canyon Formation

(see Shelburne G-29). Small sandy-limestone intervals presumably equivalent to the sandy intervals of the Roseway Formation have been recognized at the bottom of Missisauga Formation in both Mohican I-100 and Moheida P-15 and attributed to the Roseway Equivalent Formation in these wells. The shaly-sandy Logan Canyon Formation occurs above the Missisauga Formation and is lithologically equivalent to the shaly Shortland Shale Formation at Mohawk B-93 and Shelburne G-29.

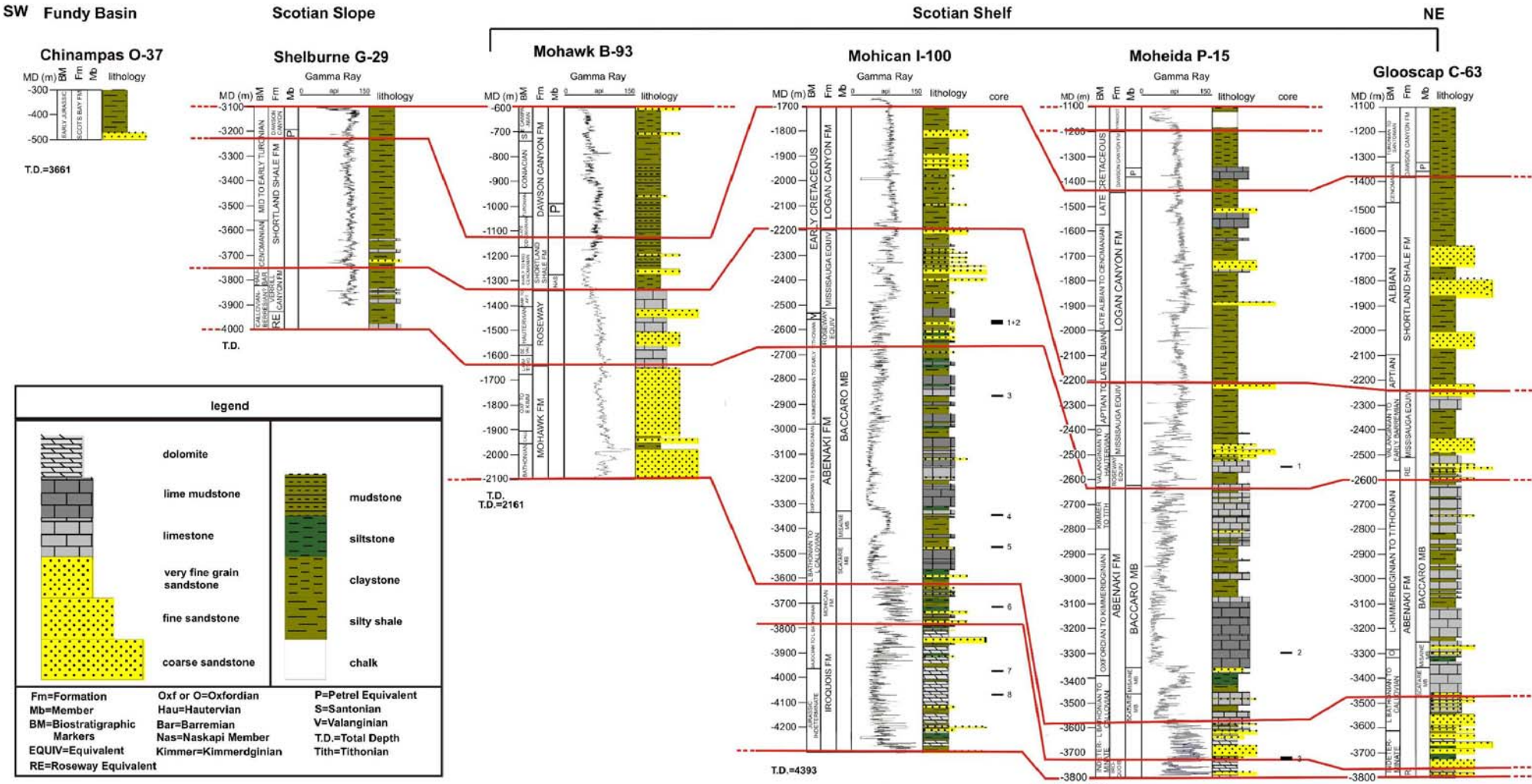

Figure 4.1: Lithostratigraphic correlation of wells studied. Lithology is based on cuttings with data taken from well reports stored at CNSOPB.

The data obtained after lithologic descriptions of conventional cores were made, were used for the production of summary core plots (Fig.4.2). Conventional core number 9 in Mohican I-100 well comprises reddish siltstones of the Late Triassic? Eurydice Formation. Conventional cores 8 and 7 in Mohican I-100 and conventional core 3 in Moheida P-15 comprise mostly dolostone with limestone interbedding of the Jurassic Iroquois Formation. An Exception is a small sandy interval in Moheida P-15. Different types of limestone of the Upper Jurassic Abenaki Formation, with some shale and mudstone interbedding were identified in cores 5, 4 and 3 in Mohican I-100. Rocks from the same formation were identified in core 2 in Moheida P-15. Cores 2 and 1 in Mohican I-100 and core 1 in Moheida P-15 comprise very fine and fine sandstone with mudstone-shale interbbedding of the Roseway Equivalent Formation.

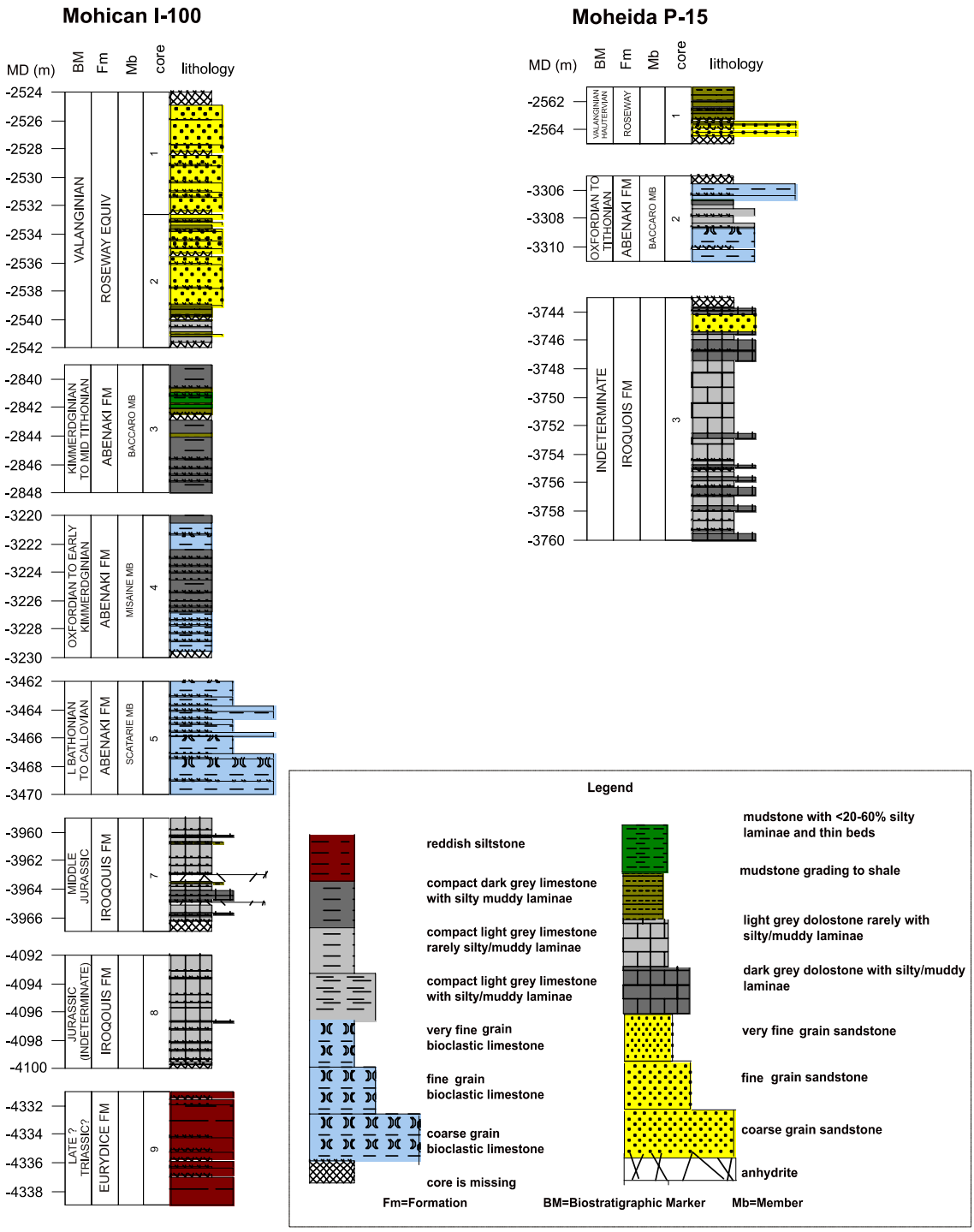

Figure 4.2: Summary plots of conventional cores from Mohican I-100 and Moheida P-15, showing lithostratigraphy and biostratigraphy.

The biostratigraphic correlation is presented in figure 4.3 based on the PFA (2011) and Weston et al. (2012). The biostratigraphic correlation indicates that the major lithostratigraphic units are not diachronous. It demonstrates that the Mohawk Formation is age equivalent of the Abenaki and Mohican formations.

The indeterminate Jurassic together with Bajocian to Bathonian are characterized mostly by the Iroquois and Mohican formations. The Late Bathonian to Callovian represents the upper section of the Mohican Formation and the Scatarie and Misaine members and the lower section of the Mohawk Formation. The Baccaro member is of Oxfordian to Tithonian age, as is the upper section of the Mohawk Formation and almost the entire section of Verrill Canyon Formation. Early Cretaceous deposits are very thick (~1.2 km) in the NE part of the study area, comprising the Roseway Equivalent (200 m), the Missisauga (300 m) and the Logan Canyon-Shortlan Shale Formation (800 m), to thin (~300) m in the SW part, comprising the Roseway Formation (250 m) on the shelf and the upper section of the Verrill Formation on the slope (50 m).

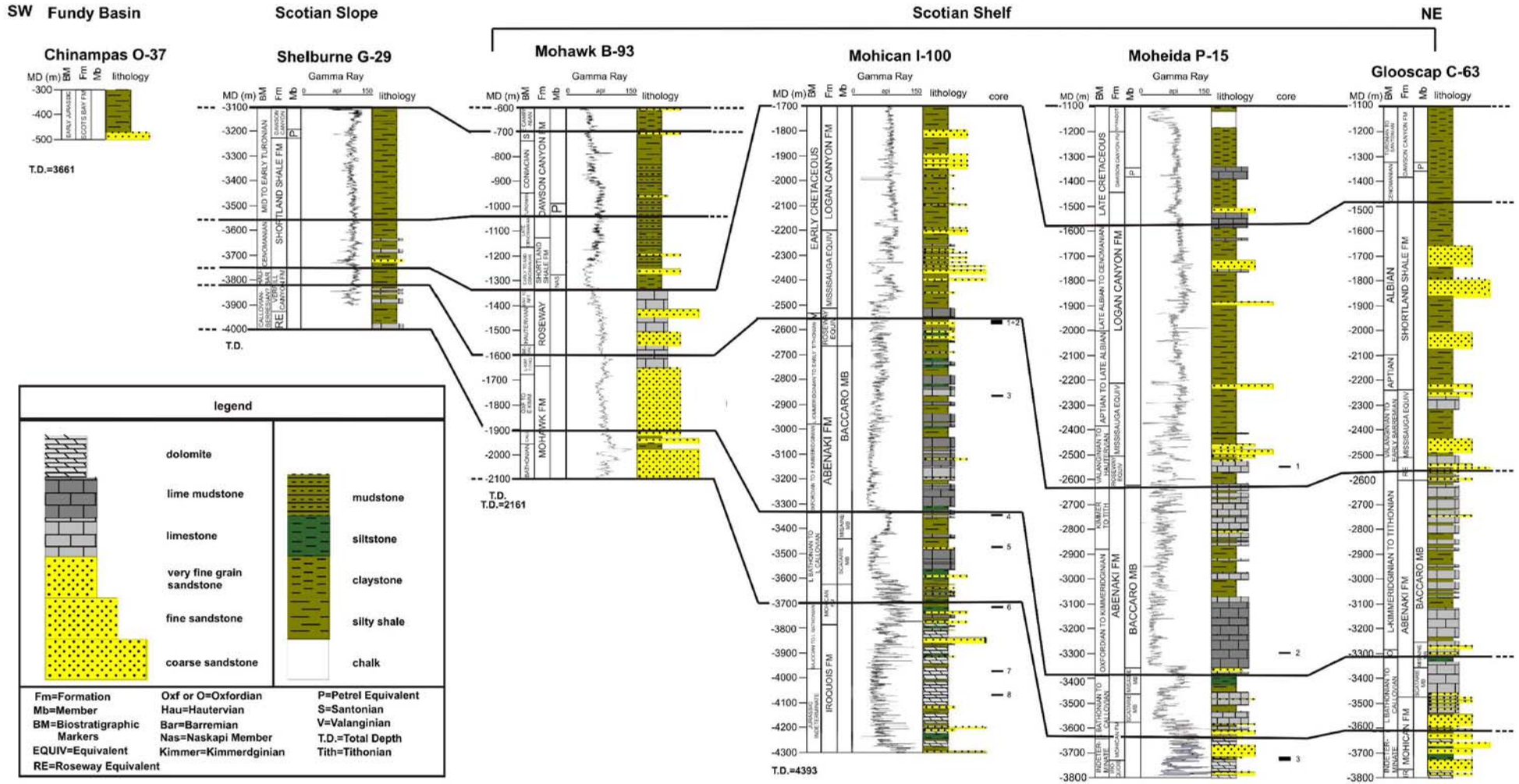

Figure 4.3: Biostratigraphic correlation of wells studied. Lithology is based on cuttings with data taken from well reports stored at CNSOPB, biostratigraphy based on Weston et al. 2012 and PFA.

4.1.2 Key correlation surfaces and uncertainties in well correlation

The objective of this sub-chapter is to to interpret and correlate strata with same age in the SW Scotian Basin. The correlation will help us understand lateral changes of lithology and determine depositional environments, episodic events (e.g. maximum flooding surfaces, unconformities) and transport of sediments from the shelf to the slope and further to deep water basins.

Of the five wells selected for study, only Mohican I-100, Moheida P-15, Mohawk B-93 and Shelburne G-29 are used for correlation. Chinampas O-37 is excluded because it is located in the Fundy Basin. Additional wells used are Bonnet P-23 and Glooscap C-63. Bonnet P-23 is used because it is similar in age to Mohawk B-93 and is located at the boundary between the shelf and the slope of the Scotian Basin. The correlation between the Mohawk B-93 and the Bonnet P-23 wells will help us understand if the coarse sands of the Mohawk Formation were deposited at Bonnet P-23 and if, under certain circumstances such as low sea level, tectonic uplift affected the outer shelf. Glooscap C-63 is used because it is lithologically similar to Mohican I-100 and Moheida P-15 and because it is located at the boundary between the SW and the central part of the basin. This will help us understand how the strata in the SW Scotian Basin change towards the central part of the basin and if there are significant differences in the river systems depositing sediments in these parts of the basin.The correlation of wells studied from the SW Scotian Basin is shown in figure 4.4 based on the PFA (2011) and Weston et al. (2012) and the present lithologies with similar ages are presented in chapter 4.1.1.

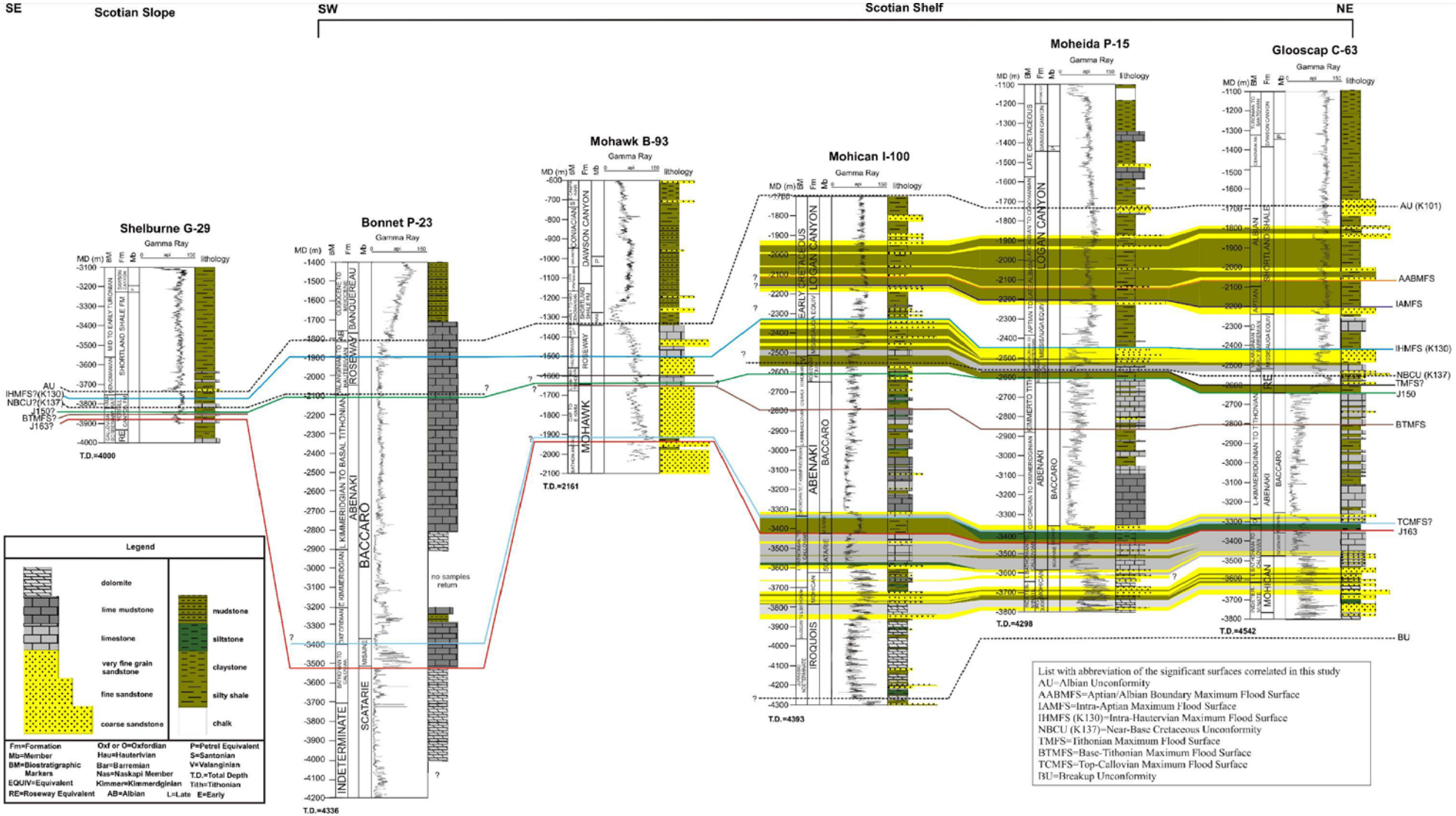

Fig.4.4: Correlation of Mesozoic strata identified in wells in the SW Scotian Basin. Location of significant surfaces in this study was taken from Wade and MacLean (1993), PFA (2011) and Weston et al. (2012).

4.1.2.1 J163 seismic marker

The J163 seismic marker was identified in Glooscap C-63 well at around 3350 m depth, where it corresponds to the top of the limestone Scatarie Member of Callovian age (Weston et al., 2012), characterized by low gamma ray spike. The seismic marker can be easily identified and followed in both Mohican I-100 and Moheida P-15 wells at the top of the same member having similar age and gamma ray spike as in Glooscap C-63. In Mohawk B-93 well the J163 seismic marker was identified at the boundary between a thin coarse sand interval and a shaly interval of Callovian age (Ascoli, 1988), characterized by a small gamma ray spike. I did not choose the gamma ray spike of Bathonian age within the Mohawk Formation because, as noted by Weston et al. (2012), the J163 seismic marker in Glooscap C-63 is close to the top of Misaine Member, which is of Callovian age. Further to the west, the seismic marker corresponds to top of the dolomite Scatarie Member in Bonnet P-23 well. Towards the slope, at Shelburne G-29 the J163 seismic marker is difficult to identify as the main lithology is shale with minor limestone intervals, thus the gamma ray seem similar through the entire well. However, at 3900 m a small gamma ray spike representing the top of a small limestone interval probably of Callovian age was recognized and interpreted as the J163 seismic marker.

4.1.2.2 Top Callovian Maximum Flooding Surface (TCMFS)

A maximum flooding surface was recognized at the Glooscap C-63, Moheida P-15 and Mohican I-100 wells below the top of the Misaine Member, having a high gamma ray spike. The surface is of Late Callovian age and represents the top of a shaly

interval just above the J163 surface. The TCMFS was recognized at the Mohawk B-93 well at the top of a thin shaly interval of Callovian age (Ascoli, 1988). In Bonnet P-23 the Callovian is mostly represented by low gamma ray as the main lithology is limestone. We recognized a small gamma ray spike of Late Callovian age close to the top of the limestone Misaine Member and tentatively interpreted it as the TCMFS in this well.

4.1.2.3 Base Tithonian Maximum Flooding Surface (BTMFS)

A Base-Tithonian MFS has been interpreted within the Baccaro Member in the Glooscap C-63, Mohican I-100 and Moheida P-15 wells (Weston et al., 2012). The surface represents the bottom of a limestone interval at Glooscap C-63 and Moheida P-15 and the bottom of a shaly-sandy-silty interval in Mohican I-100 well. In Mohawk B-93 the Tithonian is characterized mostly by limestone with small sandy interval at the top of the Mohawk Formation, thus to identify the key correlation surface is difficult but arguable. I recognized a small gamma ray peak at almost 1650 m that was considered to be the BTMFS. In Bonnet P-23 the surface could not be recognized because the Tithonian is represented entirely by limestone, thus the gamma ray is similar. In addition, some Tithonian strata have been removed by erosion (Weston et al., 2012).

4.1.2.4 J150 seismic marker

We recognized the J150 seismic marker in Glooscap C-63 and Moheida P-15 near the top of Baccaro member of Abenaki Formation. The seismic marker is characterized

by a small peak in the gamma ray, as the Baccaro member is made mostly of limestone and just above it lies the Roseway Equivalent Formation made up of sandstone, limestone and shales. In Mohican I-100 the location of this seismic marker is arguable because the top of the Baccaro member is composed mostly of shales with minor limestone and siltstone intervals, thus the gamma ray shows similar spikes making it difficult to recognize which spike characterizes the J150 seismic marker. However, we have drawn a key correlation line at around 2600 m in the Roseway Equivalent Formation, below the Upper Jurassic-Lower Cretaceous boundary, with low gamma ray spike that is considered to mark the J150 seismic marker. At Mohawk B-93 the J150 seismic marker was recognized within a limestone interval of the Roseway Equivalent Formation, just above the BTMFS, characterized by a low gamma ray spike. Due to the removal of Late Tithonian strata at Bonnet P-23, the J150 seismic marker was not recognized.

4.1.2.5 Tithonian Maximum Flooding Surface (TMFS)

The Tithonian maximum flooding surface occurs around the Late Tithonian in Glooscap C-63 and Moheida P-15, just above the J150 surface. The TMFS in these wells corresponds to the top of a thin shaly interval within the Roseway Equivalent Formation. At Mohican I-100 and Bonnet P-23 the TMFS could not be recognized as the surface was eroded beneath the Near Base Cretaceous Unconformity (NBCU). In Mohawk B-93 it is hard to recognize the TMFS because the Tithonian consists entirely of limestones of the Roseway Equivalent Formation and the gamma ray shows only low spikes. However, we attribute a low spike at the top of a limestone interval within the

Roseway Equivelant at the Late Tithonian to Early Berriasian boundary to the TMFS. The surface was drawn based on the fact that it is close to the bottom of the Roseway Equivalent Formation and has same age (Late Tithonian) as in the Glooscap C-63 and Moheida P-15 wells.

4.1.2.6 Near Base Cretaceous Unconformity (NBCU)

This surface can be easily followed in almost all of the wells studied looking at the biostratigraphy as there are gaps in age between Late Jurassic and Early Cretaceous (Weston et al., 2012). Mohawk B-93 is the only well where such a surface could not be recognized as the biostratigraphy seems to be continuous.

4.1.2.7 Intra Hautervian Maximum Flooding Surface (IHMFS) (K130)

The IHMFS it is recognized in the Glooscap C-63, Moheida P-15 and Mohican I-100 wells at the top of a thick sandy interval within the Missiauga Formation. The surface is of Hautervian age and it is characterized by a low gamma ray spike that corresponds to limestone. In Mohawk B-93 we recognized the surface above a thick sandy interval within the Roseway Equivalent, to correspond to a low gamma ray spike. In Bonnet P-23 according to Weston et al. (2012), the IHMFS was recognized at around 1900 m in the Roseway Equivalent Formation.

4.1.2.8 Intra Aptian Maximum Flooding Surface (IHMFS)

The Intra Aptian maximum flooding surface is present in Glooscap C-63, Moheida P-15 and Mohican I-100 wells at the top of a thin sandy interval at the

boundary between the Missisauga and Logan Canyon formations. In Mohawk B-93 well the surface was attributed to a small gamma ray spike within a thin limestone close to the top of the Roseway Equivalent. In Bonnet P-23 the surface was not recognized due to removal of Aptian strata.

4.1.2.9 Aptian Albian Boundary Maximum Flooding Surface (AABMFS)

The Aptian Albian boundary maximum flooding surface (AABMFS) was recognized at the top of a shaly interval within the Logan Canyon Formation in Moheida P-15 and Mohican I-100 and within Shortland Shale Formation in Glooscap C-63. The surface could not be recognized in Mohawk B-93 and Bonnet P-23 as from biostratigraphy it seems that Aptian and Albian strata have been removed by erosion.

4.1.2.10 Albian Unconformity (AU)

The Albian unconformity can be recognized in the Glooscap C-63, Moheida P-15 and Mohican I-100 around 1700 m and in Mohawk B-93 at around 1300 m from the gap in the biostratigraphy (Weston et al., 2012). In Bonnet P-23 the Albian unconformity was not specifically recognized, but Aptian strata are lacking.

4.2 Petrography

4.2.1 Modal composition-Sandstone classification

All sandstone samples have above 75% quartz (Fig. 4.5). The sandstones from Roseway Equivalent Formation are predominantly classified as quartzarenite, 7 samples from the total of 8, with one exception that has modal composition similar to

that of sublitharenite. On the other hand the samples from Mohican Formation have different modal composition compared to those from Roseway Equivalent Formation: one sample is subarkose and another sample is sublitharenite. The only sandstone sample from the Iroquois Formation at Moheida P-15 is classified as sublitharenite whereas the sandstones from the same formation at Mohican I-100 are mostly quartzarenites (5 from total of 7) with two subarkose samples.

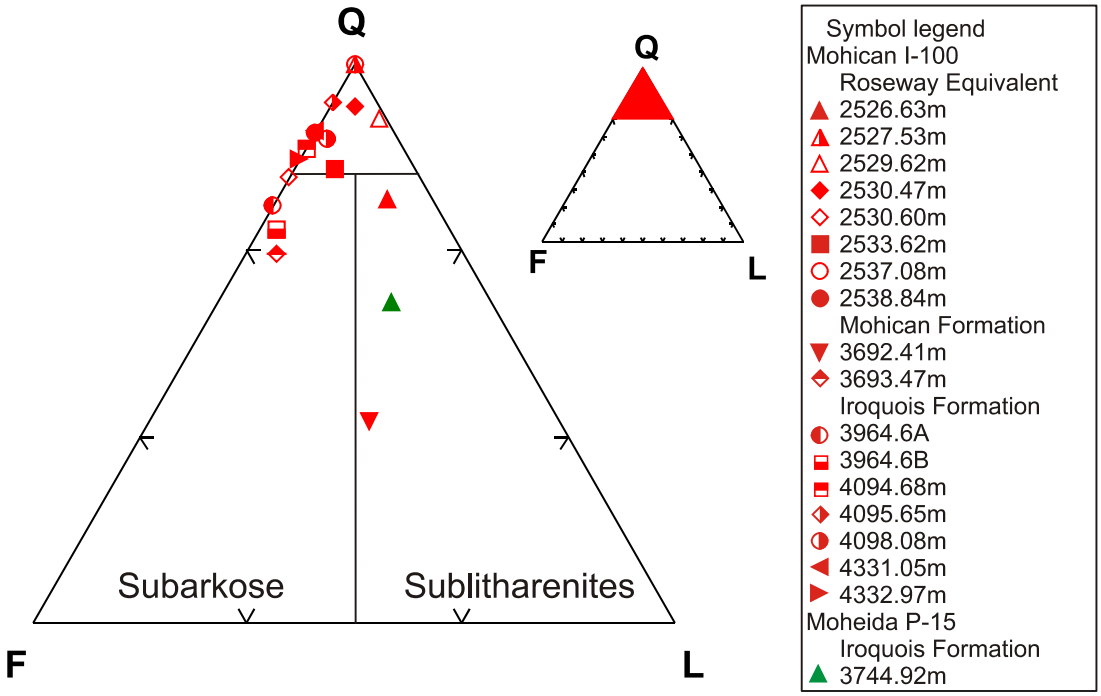

Figure 4.5: QFL plot showing composition of all sandstones studied, using nomenclature and fields from Folk (1968).

4.2.2 Modal composition-Paleotectonic classification

Based on both the QFL and the Q_mFL_t diagrams (Figs. 4.6, 4.7), almost all sandstones from Roseway Equivalent, Mohican and Iroqois formations at Mohican I-100 and Moheida P-15 tend to plot in the field that represents continental block and specifically in the craton interior subdivision. Exceptions are two sandstones one from Mohican Formation at Mohican I-100 and one from Iroquois Formation at Moheida P-

15 that plot only just in the recycled orogen field in both diagrams.

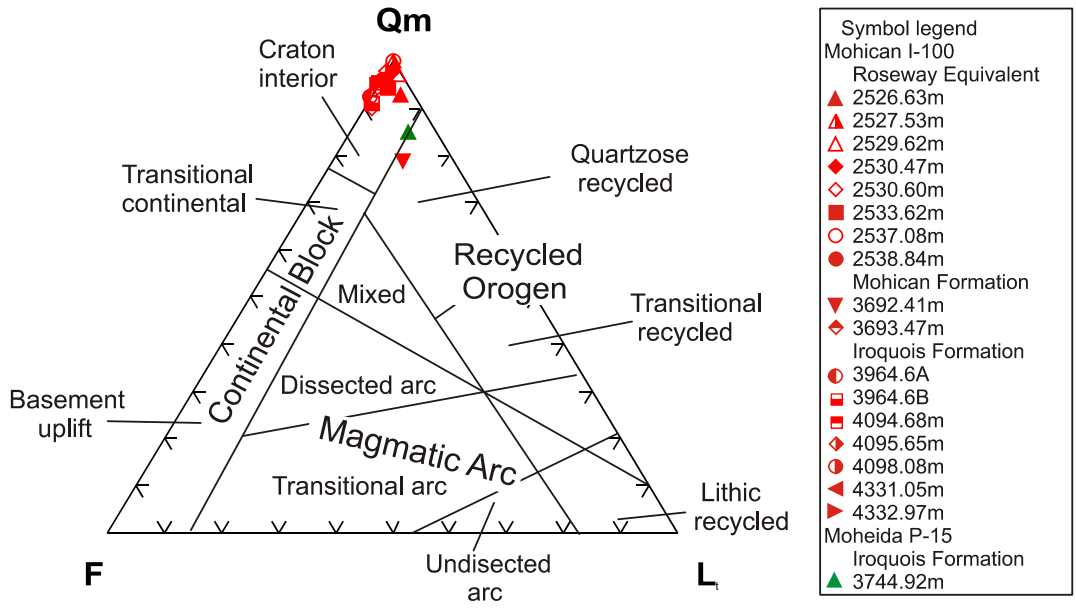

Figure 4.6: Q_mFL_t (Q_m=monocrystalline quartz, F= K-feldspar and plagioclase and L_t=lithic clasts plus polycrystalline quartz) plot for framework modes using paleotectonic fields from Dickinson et al. (1983).

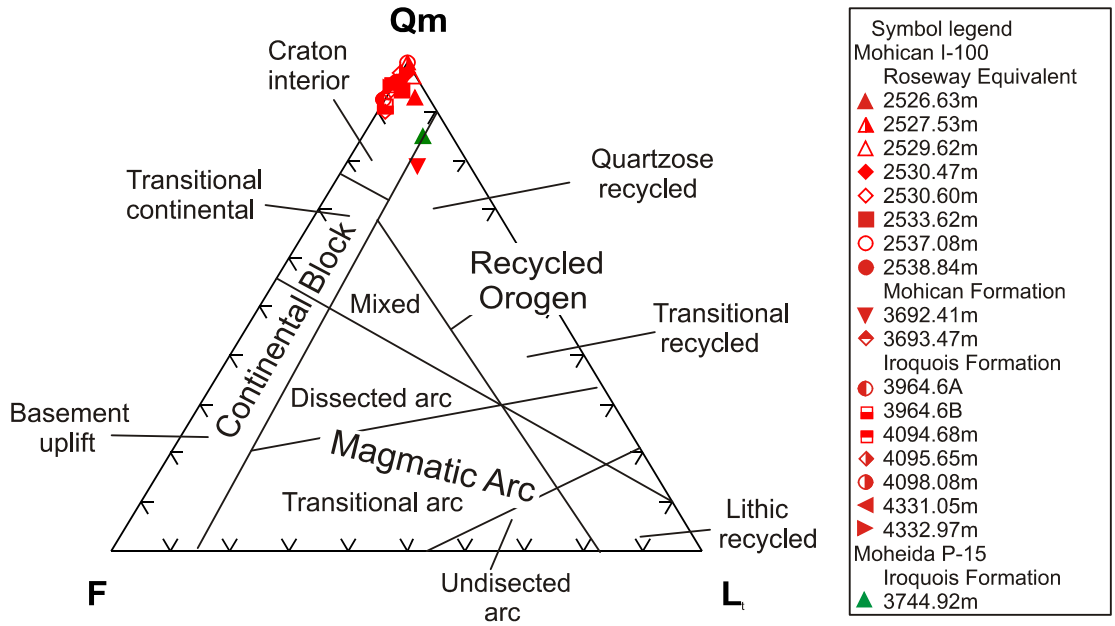

Figure 4.7: Q_mFL_t (Q_m=monocrystalline quartz, F= K-feldspar and plagioclase and L_t=lithic clasts plus polycrystalline quartz) plot for framework modes using paleotectonic fields from Dickinson et al. (1983).

4.2.3 Petrographic textures

To describe and understand the composition of clastic rocks in the SW Scotian Basin rock samples were collected from representative sandy intervals in conventional cores of Middle Jurassic to Lower Cretaceous formations (Roseway Equivalent, Abenaki, Mohican, and Iroquois) at Mohican I-100 and Moheida P-15. From the total of 26 available polished thin sections, 11 were chosen for petrographic work (Table 4.1). The remaining samples were not selected because they were either entirely dolostones or limestones or because some of the samples had the same characteristic features, such as mineral composition (detrital and diagenetic) and textures.

Table. 4.1: Presentation of rock samples

Well	Sample	Depth (m)	Formation	Age	Rock name
Mohican I-100	I-100 2526.53	2526.53	Roseway Equivalent	Lower Cretaceous	carbonate-cement sst
	I-100 2529.62	2529.62	Roseway Equivalent	Lower Cretaceous	carbonate-cement sst
	I-100 2530.47	2530.47	Roseway Equivalent	Lower Cretaceous	sandy, bioclastic lmst
	I-100 2538.84	2538.84	Roseway Equivalent	Lower Cretaceous	carbonate-cement sst
	I-100 3692.41	3692.41	Mohican	Middle Jurassic	sulphate-cement sst
	I-100 3964.6A	3964.6	Iroquois	Middle Jurassic	sulphate-cement sst
	I-100 4098.08	4098.08	Iroquois	Middle Jurassic	sandy, bioclastic lmst
Moheida P-15	P-15 2563.67	2563.67	Roseway/Equivalent	Lower Cretaceous	oolitic ironstone
	P-15 3306.03	3306.03	Abenaki	Upper Jurassic	oolitic limestone
	P-15 3744.92	3744.92	Iroquois	Middle Jurassic	sulphate-cement sst
	P-15 3750.94	3750.94	Iroquois	Middle Jurassic	dolostone

The 11 rock samples were discriminated into six groups considering macroscopic and microscopic observations. The general petrographic characteristics of these groups are as follows:

1. carbonate-cement sandstone (framework grains>80% of the total rock sample, 20% carbonate cement)

2. sulphate-cement sandstone (framework grains>80% of the total rock, 20% sulphate cement)

3. sandy-bioclastic limestone (framework grains<50% of the total rock, and 50% carbonate cement)

4. oolitic ironstone ($FeCO_3$ ooids>60%, ~40% carbonate rich cement)

5. oolitic limestone ($CaCO_3$ ooids>80%, ~20% carbonate cement)

6. dolostone (dolomite 100%)

In this study we consider peloids framework grains that are made up of micritic components such as calcite, pyrite and quartz with no internal structure or nucleus and no restriction on the size or origin of the grain (McKee and Gutschick, 1969).

In general coated grains are considered concentric layered grains that may have irregular accretion and may involve minerals other than CaCO3 minerals (Fluegel, 2004). The coated grains seen in this study are spheroidal framework grains made up of a series of concentric layers around a nucleus; their layers are made up of mostly siderite, kaolinite and chlorite with calcite between the layers; their nucleus can be a bioclast, a quartz grain or any other small fragment and

Ooids in this study are regular spherical grains made up of concentric growth of calcite.

The framework grains identified in these lithologies include monocrystalline and polycrystalline quartz, biotite, muscovite, chlorite, feldspar (albite, K-feldspar, perthite), F-apatite, lithic clasts, opaque minerals (ilmenite, spinel), bioclasts, ooids, coated grains, peloids, light-colored minerals (zircon) and dark colored minerals (tourmaline, rutile). The carbonate cement includes calcite (Mg-rich, Mg-Fe- rich, Fe-rich), siderite, ankerite and dolomite and the sulfate-cement includes only anhydrite.

Illite occurs as an alteration product of muscovite and feldspar in some low grade

metamorphic rocks as well as in weathering and hydrothermal environments. Illite is also common in sediments, soils, and argillaceous sedimentary rocks as diagenetic mineral. Because illite has similar composition as muscovite, very often it is difficult to discriminate them. For discrimination of illite from muscovite in this study we used three criteria: i) chemical composition, ii) crystal size and iii) texture. For the purpose of this study grains that have Al_2O_3 >=25% and SiO_2 ~45% (43 to 47%) are considered muscovite, whereas grains that have Al_2O_3 <25% and SiO_2 >47% are considered illite. Grains that are less than 20μm in size are considered illite whereas all other grains with size >20μm are considered muscovite. If the grains are present as inclusion in other detrital mineral (e.g. quartz, ilmenite) or as framework grains we consider them detrital, thus they are most likely to be muscovite. On the contrary if the grains are fibrous or fill primary porosity between framework grains and/or secondary porosity in both detrital and/or diagenetic grains and cement, we consider them diagenetic, and thus they are most likely to be illite. Although the previous criteria are important in discrimination between muscovite an illite there are still some constraints that need to be discussed. One of the issues is that muscovite tends to alter into sericite and hydromuscovite, and thus illite may be of detrital origin. As a result the chemical composition is not reliable in this case, because the Al_2O_3 and SiO_2 contents of the muscovite have been severely altered. Another issue is that during transportation some detrital minerals may not retain their primary grain size and thus only a very small fragment of the primary grain is deposited and preserved. As a result some detrital muscovite grains might have crystal size <20μm. In conclusion, in order to have a better discrimination between illite and muscovite all three criteria must be taking into

consideration and not each one individually.

The modal composition of the studied samples was determined by point counting (600 grains per sample) and use of the QFL discrimination diagram for sandstone classification (Folk, 1968).

Chemical composition of diagenetic minerals in association with textural relationship between the various diagenetic minerals was taken in consideration to establish the conditions under which the clastic sediments were influenced by diagenesis. The relative ages of diagenetic minerals identified have been established using their textural relationships in back-scattered electron images (BSE).

4.2.3.1 Mohican I-100 well

Summary petrographic description of Lower Cretaceous Roseway Equivalent sandstones and oolitic limestone

Sample I-100 2526.53 (Roseway Equivalent Formation, 2526.53 m) fine grained carbonate-cement sandstone (appendix 9-1)

Description

Based on the QFL discrimination diagram for sandstone classification, the modal composition of this sample is that of sublitharenite (Fig.4.5). The framework grains in this sample tend to come in direct contact with each other, suggesting compaction prior to lithification. The sample is characterized as poorly sorted.

The majority of the framework grains are quartz followed by perthite and lithic clasts, with sporadic zircon, chlorite, rutile, spinel and bioclasts (Fig.4.8). Minor zircon, rutile, spinel and perthite tend to have sub-rounded crystal grains (Figs.4.8 A, B, C, H).

Detrital quartz shows variations in grain size from <20μm to > than 20 μm, is corroded and has dissolution voids (Fig.4.8 B). In one perthite grain the albite lamellae alter into calcite and chlorite (Fig.4.8 C). Lithic clasts identified are made up of albite and muscovite (Fig.4.8 E). Muscovite is absent as a framework grain and appears only as inclusion in detrital quartz (Figs.4.8 F). Detrital chlorite is plastically deformed, thus creating a pseudomatrix (Fig.4.8 F). Bioclasts are made up entirely of Mg-calcite (Fig.4.8 E) or Mg-calcite and Fe-calcite (Fig.4.8 F).

c.q.=corroded quartz c-c=concavo-convex contact qz og= quartz overgrowth cal= pure calcite

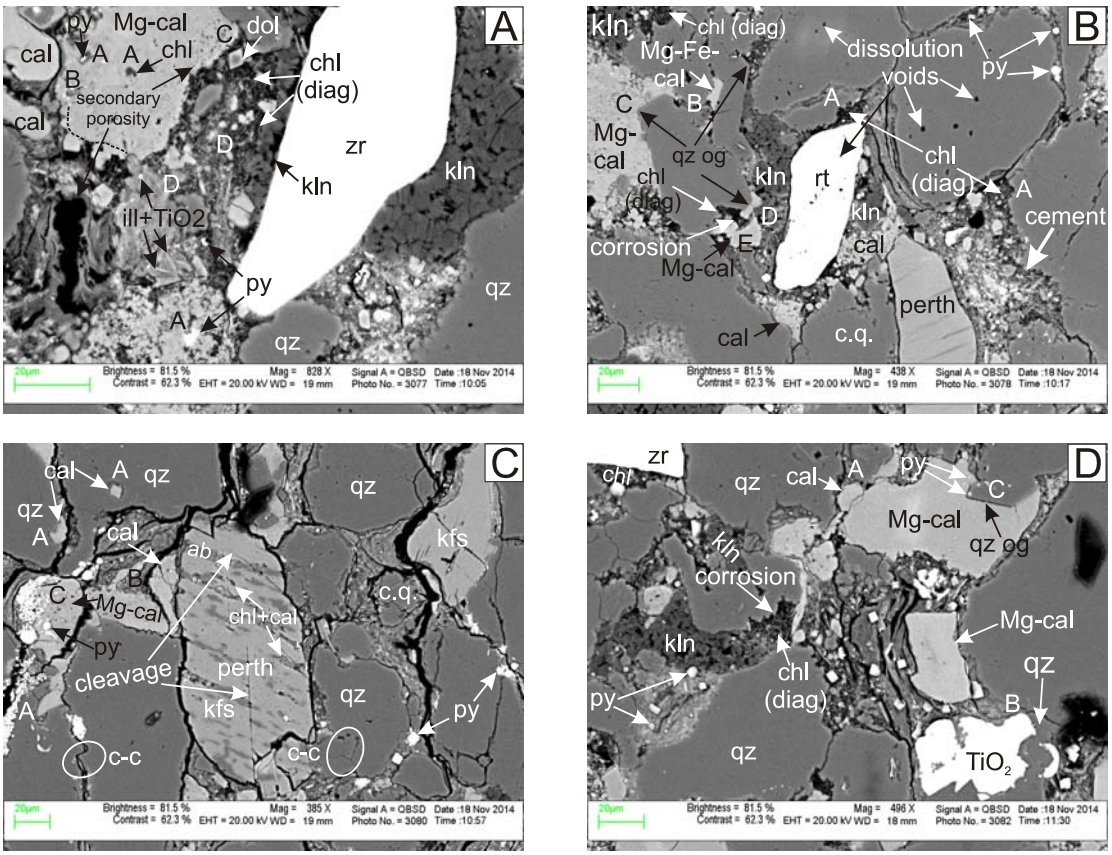

Figure 4.8: Representative back-scattered electron images of sample I-100 2526.53 from Mohican I-100 well. A) Diagenetic fibrous chlorite and pyrite fill secondary porosity in Mg-calcite (position A). Calcite invades Mg-calcite (position B). Dolomite rhombohedrons show replacive texture against diagenetic chlorite in the matrix (position C). Illite and some TiO_2 mineral are part of the cement (position D). Kaolinite seems to be later than diagenetic chlorite as it fils space between detrital zircon and diagenetic chlorite (position E). B) Detrital quartz is corroded (c.q), contains dissolution voids and shows variation in grain size. Diagenetic chlorite is fibrous and fills embayments in detrital quartz (position A) and in Mg-calcite (position E). Quartz overgrowths form around detrital quartz and often seems to be cross-cut by Mg-Fe-calcite (position B). Quartz overgrowths invade Mg-calcite (position C). Kaolinite fills embayment in Mg-calcite (positon D). C) Calcite fills secondary porosity and embayments in detrital quartz (position A) and the spave between Mg-calcite and detrital quartz (position B). One quartz grain has undergone dissolution leading to the penetration of one grain by another, thus creating concavo-convex contacts (c-c). The albite lamellae in perthite grains alter into chlorite and calcite. Secondary porosity in Mg-calcite is filled by framboidal pyrite (position C). D) Calcite engulfs Mg-calcite (position A). Detrital quartz is corroded (c.q.). Diagenetic TiO_2 minerals show replacive texture against detrital quartz grains (position B). Quartz overgrowths form around detrital quartz and invade Mg-calcite (position C).

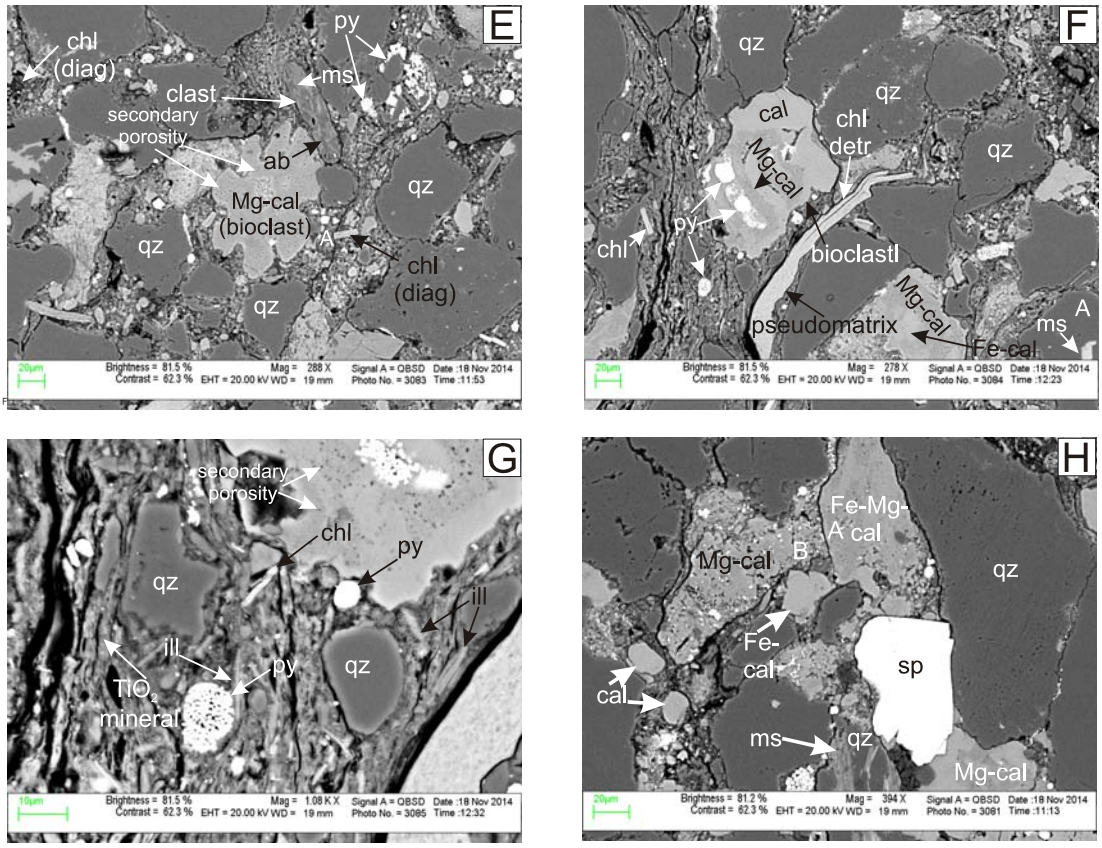

Figure 4.8: Representative back-scattered electron images of sample I-100 2526.53 from Mohican I-100 well. E) One lithic clast is made up of albite and muscovite. One bioclast, probably an echinoid spine, has been fossilized through entire replacement of the organic material by Mg-calcite, followed by dissolution with creation of secondary porosity. Diagenetic chlorite cross-cuts secondary fractures (position A). F) Muscovite is present as inclusion in detrital quartz (position A). One bioclast, probably a gasteropod is made up of Mg-calcite and calcite. The Mg-calcite shows secondary porosity and calcite is partly replaced by pyrite. Detrital chlorite is plastically deformed, thus creating pseudomatrix. G) Diagenetic chlorite and illite together with TiO_2 mineral are part of the cement. Framboidal pyrite fills secondary porosity in the matrix. H) Muscovite appears as inclusion in detrital quartz. Fe-Mg-calcite seems to cross-cut Mg-calcite (position A). Fe-calcite has straight crystal outlines and tends to invade Mg-calcite.

Sample I-100 2529.62 (Roseway Equivalent Formation, 2529.62 m) fine grained carbonate-cement sandstone (appendix 9-2)

Description

This sample is a quartzarenite based on the QFL discrimination diagram for sandstone classification (Fig.4.5). The framework grains in this sample tend to come in direct contact with each other, suggesting compaction. The sample is poorly sorted with low primary porosity.

The majority of the framework grains are quartz followed by perthite and lithic clasts, with sporadic tourmaline, chlorite, rutile, spinel, K-feldspar and F-apatite. Tourmaline, rutile, perthite, lithic clasts and F-apatite have subhedral crystal outlines (Figs.4.9 A, B, C, D). Detrital quartz is corroded and contains dissolution voids (Figs.4.9 C, E). Perthite exhibits brittle fracturing (Fig.4.9 B). Muscovite is present as inclusion in detrital quartz (Fig.4.9 D). Some lithic clasts are made up of quartz, chlorite and muscovite and some other of quartz and muscovite (Fig.4.9 D).Some detrital chlorite is plastically deformed, thus creating pseudomatrix (Fig.4.9 E) and some other have quartz inclusions and are partly replaced along the cleavage planes by unknown diagenetic mineral (Fig.4.9 B).

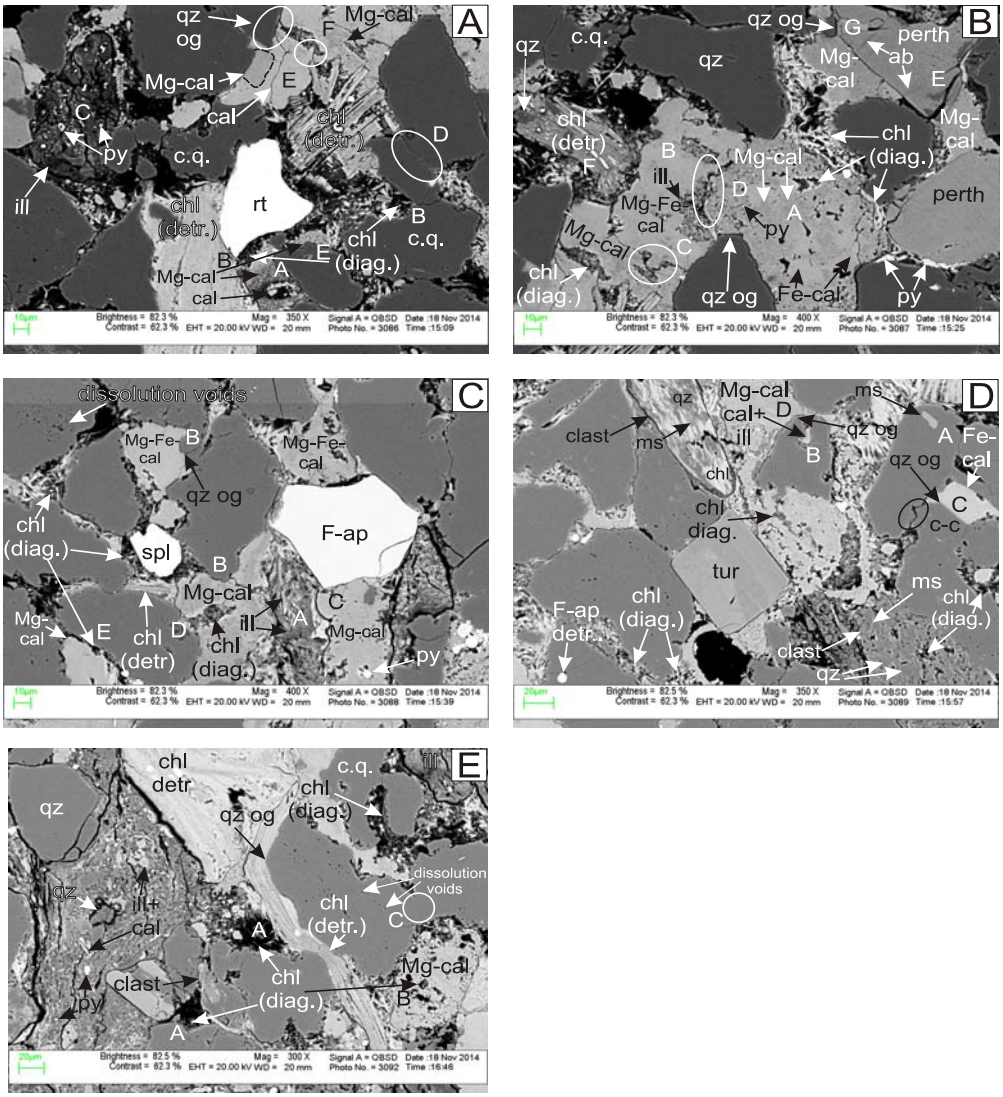

Figure 4.9: Representative back-scattered electron images of sample I-100 2529.62 from Mohican I-100 well. A) Calcite fills secondary porosity (position A, F) and engulfs (position E) Mg-calcite. Diagenetic divergent fibrous chlorite fills embayment in corroded quartz (c.q.) (position B) and Mg-calcite and occupies intragranular space between framework grains. Compact illite shows characteristic secondary fractures that are often filled by framboidal pyrite (position C). Crystal boundaries between detrital quartz grains are hard to distinguish in places where the cement is SiO_2 (position D). Quartz overgrowths tend to invade Mg-calcite (position E). B) There seems to be two generations of Mg-Fe-calcite: one that has high secondary porosity which is filled by diagenetic chlorite (position A) and one that is partly replaced by illite (position B). Mg-Fe-calcite (position B) seems to invade Mg-calcite (position C) and engulf Mg-Fe-calcite (positions A) in position D. One perthite has suffered brittle fracturing (position E). Detrital chlorite has quartz inclusions and is partly replaced along the cleavage planes by unknown diagenetic mineral (white color) (position F). Quartz overgrowths form around detrital quartz grains and seem to invade Mg-calcite (position G). C) Detrital quartz is corroded (c.q.) and contains dissolution voids. Illite is part of the cement in form of fibres (position A). Quartz overgrowths form around detrital quartz and invade Mg-Fe-calcite and Mg-calcite (position B). Mg-calcite invaded illite (position C). Diagenetic chlorite fills secondary porosity in Mg-calcite (position D) and fills open space between Mg-Fe-calcite and detrital quartz (position E). D) Rarely, at the contact between quartz grains, one grain has undergone solution leading to the penetration of one grain by another, thus creating concavo-convex contact. Some lithic clasts are made up of quartz, chlorite and muscovite and some other of quartz and muscovite. Muscovite is present as inclusion in detrital quartz (position A). Calcite and illite fill secondary porosity in detrital quartz (position B). Rarely quartz overgrowth forms around detrital quartz and invaded Mg-calcite (position C) and Fe-calcite (position D). Detrital quartz is corroded (c.q.) and contains dissolution voids. Diagenetic divergent fibrous chlorite fills embayment in corroded quartz (position A) and calcite (position B) and/or occupies intragranular space between framework grains. Detrital chlorite is plastically deformed, thus creating pseudomatrix. Crystal boundaries between detrital quartz grains are hard to distinguish in places where the cement is SiO_2, position C. Late fractures and secondary porosity lack diagenetic minerals, they are barren.

Sample I-100 2530.47 (Roseway Equivalent Formation, 2530.47 m) oolitic bioclastic limestone (appendix 9-3)

Description

The majority of the framework grains in this sample are peloids and bioclasts, with rare coated grains and detrital quartz. Rarely muscovite is present (Fig.4.10 A). The sample is poorly sorted. In general, the peloids have irregular shape and are made up principally of mixture of micritic Mg-Fe-calcite, Mg-calcite, quartz and pyrite (Figs.4.10 A, B, C, D). Moreover, the peloids do not have any internal structure (e.g. concentric layers) and lack nucleus. Coated grains have concentric layers of micritic material composed of calcite, chlorite and pyrite (Figs.4.10 C, D) in some cases with a nucleus of peloid. Euhedral to subhedral detrital quartz varies in grain size. One bioclast, probably foraminifera, consists of calcite and Mg-calcite (Fig.4.10 B). Okwese et al. (2012) discriminated four types of coated grains, type A, B, C and D at both Peskowesk A-99 in the Abenaki sub-basin and Thebaud C-74 in the Sable sub-basin. In this sample only type C was identified characteristically consisting of Fe- and Mg-calcite together with pyrite.

qz og= quartz overgrowth

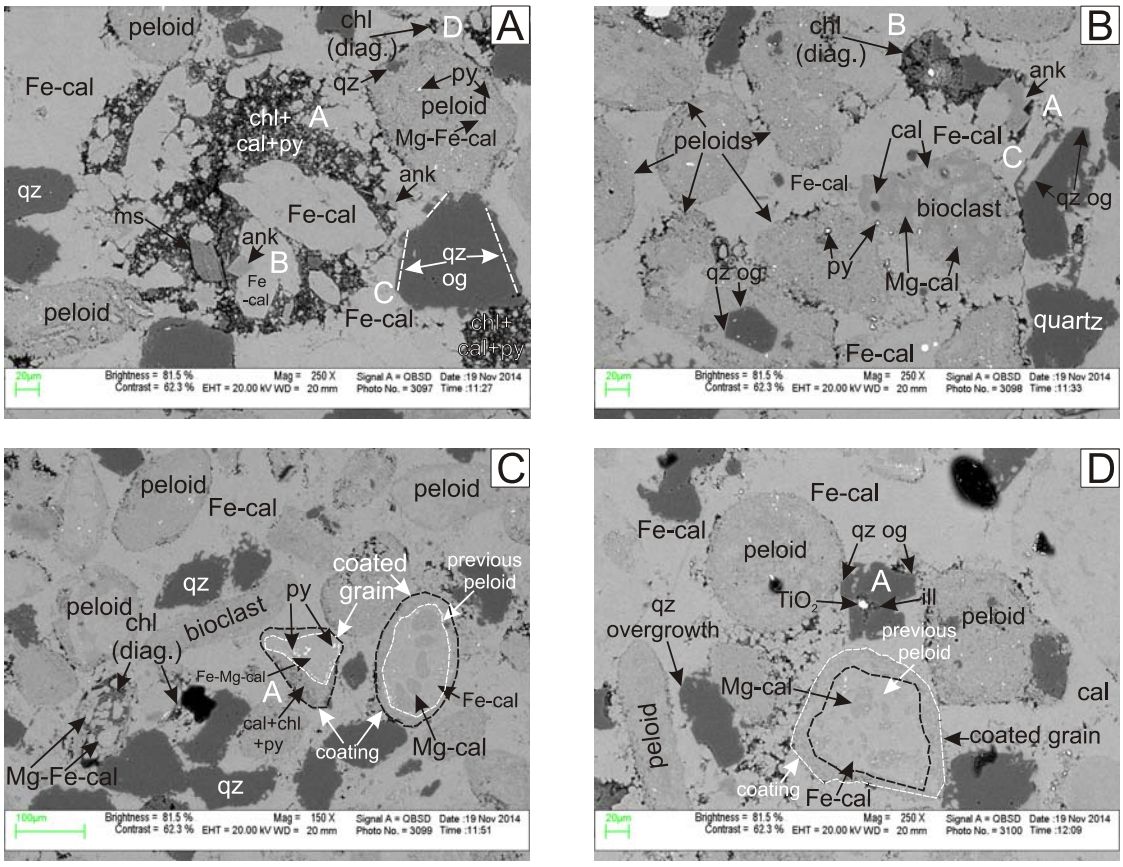

Figure 4.10: Representative back-scattered images of sample I-100 2530.47 (m) from Mohican I-100 well. A) Rare muscovite is present. The peloids are made up of micritic material composed of Mg-Fe-calcite, pyrite, quartz, chlorite and others. The cements is mostly Fe-calcite however in places the cement is a mixture between calcite, chlorite and pyrite (position A). Rarely ankerite can be part of the cement and it seems to replace Fe-calcite (position B). Quartz overgrowths form around detrital quartz and seem to invade Fe-calcite cement (position C). Rarely diagenetic chlorite fills secondary porosity in the cement (position D). B) One bioclast probably from foraminifera is entirely replaced by calcite and Mg-calcite. Ankerite engulfs Fe-calcite, thus is later (position A). Rarely diagenetic chlorite fills secondary porosity in the cement (position B).Quartz overgrowths form around detrital quartz and invade Fe-calcite cement (poisition C). C) Coated grains are previous peloids which are coated by micritic Fe-Mg-calcite, chlorite and pyrite (position A). D) Illite and diagenetic TiO_2 mineral fill secondary porosity in detrital quartz (position A).

Sample I-100 2538.84 (Roseway Equivalent Formation, 2538.84 m) fine grained carbonate-cement sandstone (appendix 9-4)

Description

Based on the QFL discrimination diagram for sandstone classification, the modal composition of this sample is that of quartzarenite (Fig.4.5). The sample can be characterized as poorly sorted. The sediment is loosely-packed, suggesting that cementation occurred before significant compaction took place.

The majority of the framework grains are quartz followed by sporadic chlorite, K-feldspar, muscovite, lithic clasts and F-apatite. Anhedral detrital quartz has suffered brittle and conchoidal fracturing and is corroded (Fig.4.11 A). In addition, dissolution voids are present in most of the quartz grains. One detrital chlorite is plastically deformed, thus creating pseudomatrix and has suffered brittle fracturing (Fig.4.11 A). Another detrital chlorite exhibits only brittle fracturing (Fig.4.11 B). F-Apatite is corroded and shows replacive texture against detrital quartz and cement (Fig.4.11 A). K-feldspar also shows brittle fracturing (Fig.4.11 B). Muscovite is plastically deformed in places, thus creating pseudomatrix (Fig.4.11 C). Lithic clasts are made up of ilmenite, muscovite and chlorite (Fig.4.11 C).

c.q.=corroded quartz qz og= quartz overgrowth

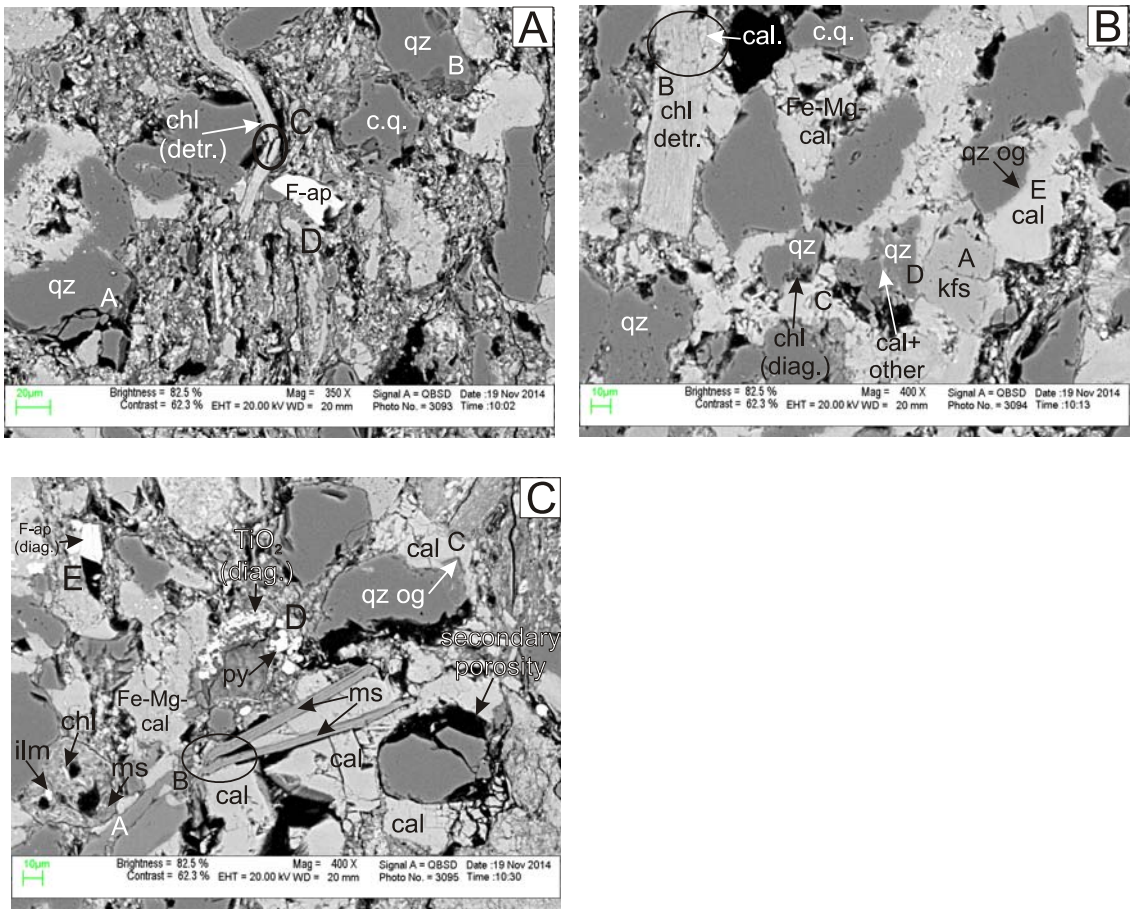

Figure 4.11: Representative back-scattered images of sample I-100 2538.84 (m) from Mohican I-100 well. A) Detrital quartz in corroded (c.q.), shows brittle (position A) and conchoidal (position B) fracturing. One detrital chlorite is plastically deformed, thus creating pseudomatrix, is partly replaced by calcite and exhibits brittle fracturing (position C). Muscovite is almost entirely replaced by calcite. Detrital F-apatite shows replacive texture against detrital quartz grains and the cement and is corroded (position D). B) K-feldspar shows brittle fracturing (position A). One detrital chlorite exhibits brittle fracturing and is partly replaced by calcite along its cleavage planes (position B). Calcite together with other diagenetic minerals seem to fill secondary porosity (position C) and embayment (position D) in detrital quartz. Quartz forms around detrital quartz grains and tends to invade calcite (position E). C) One lithic clast is made up of ilmenite, muscovite and chlorite (position A). Muscovite is plastically deformed in places, thus creating pseudomatrix (position B). Quartz overgrowth forms around detrital quartz grains and tends to invade calcite (position C). TiO_2 mineral and pyrite show replacive texture against the carbonate cement (position D). Secondary porosity in calcite is rarely filled with F-apatite (position E).

Summary petrographic description of Middle Jurassic Mohican sandstone

Sample I-100 3692.41 (Mohican Formation, 3692.41 m) coarse grained sulphate-cement sandstone (appendix 9-5)

Description

The sample is a poorly sorted sublitharenite (Fig.4.5). The majority of detrital grains identified in this sample are quartz, followed by abundant ilmenite and lithic clasts with sporadic K-feldspar, plagioclase, muscovite, chlorite, rutile, tourmaline and zircon. Based on potential protolith the lithic clasts in this sample are discriminated in two groups: i) metamorphic lithic clasts and ii) igneous lithic clasts. The metamorphic lithic clasts comprise a variety of detrital minerals such as quartz, muscovite, chlorite and ilmenite (Fig. 4.12 B) or muscovite, quartz and ilmenite (Fig.4.12 F). The igneous lithic clasts comprise detrital minerals such as quartz, muscovite and feldspar (Fig.4.12 F). Often muscovite and ilmenite are inclusions in detrital quartz grains (Fig.4.12 C). Muscovite is also seen as inclusion in albite grains (Fig.4.12 C). Detrital albite is subhedral to anhedral and shows dissolution voids (Fig.4.12 C). K-feldspar can be both altered and fresh. Fresh K-feldspar is subhedral to euhedral with characteristic fractures such as euhedral crystal outlines and dissolution voids (Fig.4.12 G). Altered K-feldspar together with detrital quartz are components of clasts that are hosted in the matrix (Fig.4.12 G). Ilmenite can be both fresh (Figs.4.12 A, D, E) and altered (Fig.4.12 F) mostly with characteristic quartz and muscovite inclusions. The matrix in this sample is composed of silt size detrital minerals such as quartz, chlorite and muscovite (Fig.4.12 E).

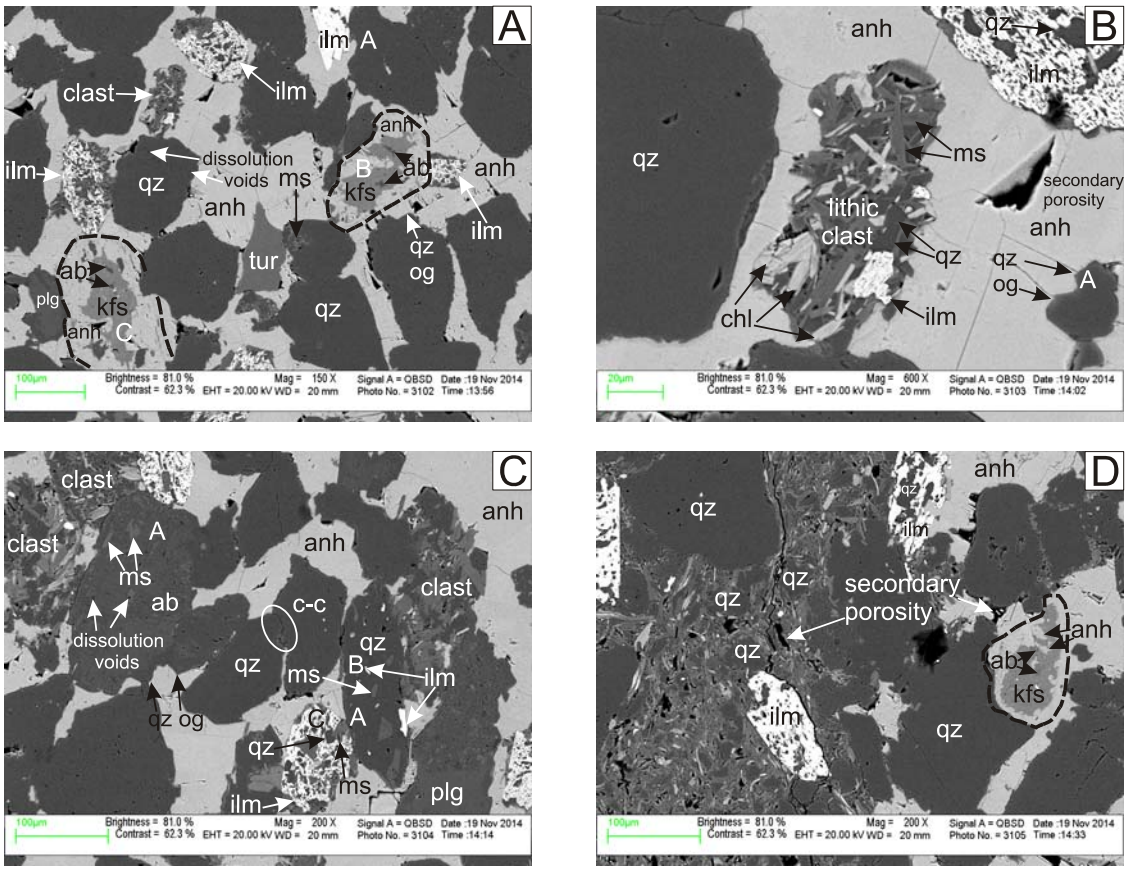

Figure 4.12: Representative back-scattered electron images of sample I-100 3692.41 from Mohican I-100 well. A) Ilmenite tends to be fresh (position A). Anhydrite cement (anh) fills primary porosity. Dertrital K-feldspar (kfs) is partly replaced by diagenetic albite (positions B, C). Remobilized anhydrite (light grey color) partly replaces albitized K-feldspar (position B, C). B) Lithic clasts derived from metamorphic rocks are made up of quartz, muscovite, chlorite and ilmenite. Quartz overgrowths form around detrital quartz and invade anhydrite cement (position A). C) At the contact between quartz grains, one quartz grain has undergone dissolution leading to the penetration of one grain by another, thus creating concavo-convex contacts (c-c). Muscovite is present as inclusion in quartz, albite and ilmenite grains (position A). Ilmenite is present as inclusion in detrital quartz (position B) and detrital quartz is present as inclusions in detrital ilmenite (position C). Detrital albite is subhedral to anhedral and shows dissolution voids. D) Albitized K-feldspar is partly replaced by remobilized anhydrite. Ilmenite seems to be fresh.

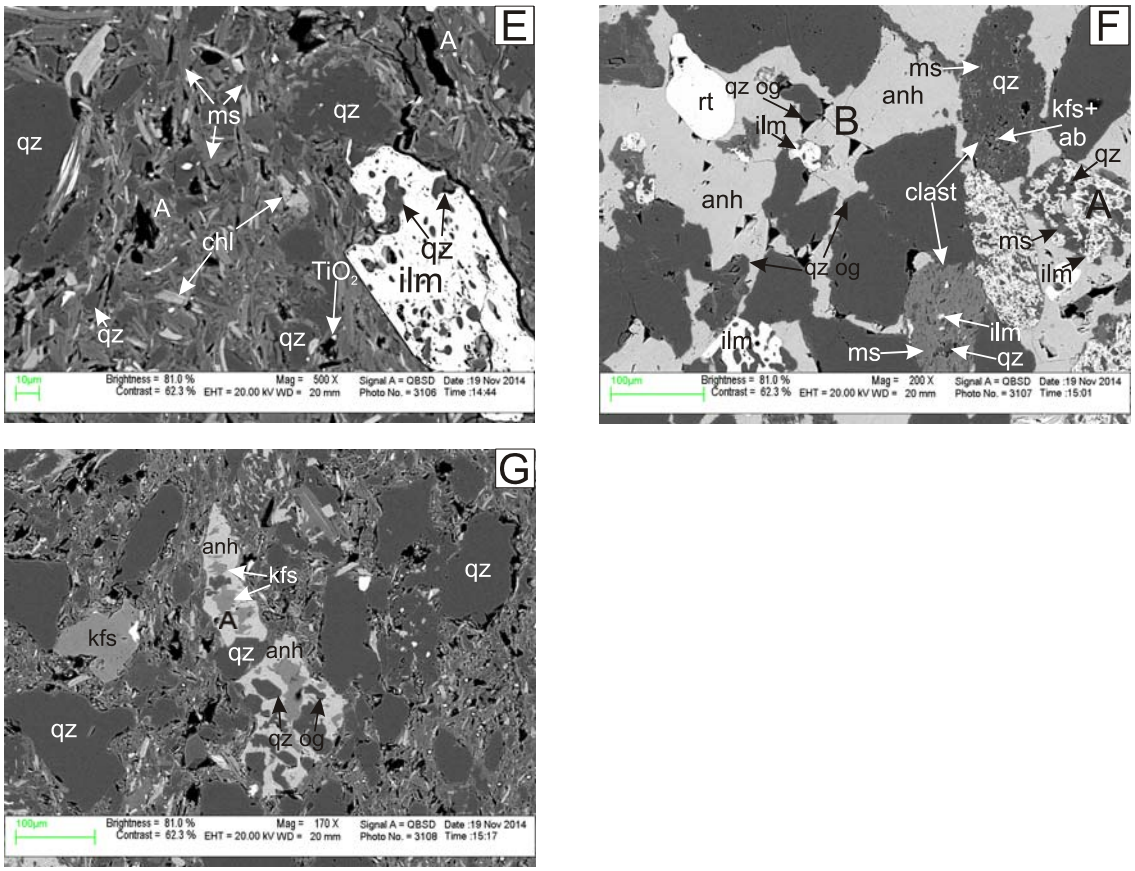

Figure 4.12: Representative back-scattered electron images of sample I-100 3692.41 from Mohican I-100 well. E) Fresh ilmenite with characteristic quartz inclusions. The matrix is made up of silt size muscovite, detrial quartz and detrital chlorite. Secondary porosity in the matrix lacks diagenetic minerals (position A). F) Altered ilmenite shows characteristic quartz and muscovite inclusions (position A). One lithic clast derived from metamorphic rock is made up of muscovite, quartz and ilmenite and another lithic clasts derived from igneous rocks is made up of quartz, muscovite and feldspar. quartz overgrowths fill secondary porosity in anhydrite cement (position B). G) Fresh K-feldspar is subhedral to euhedral. Albitized K-feldspar, party replaced by anhydrite can also be, together with detrital quartz, component of clasts that are hosted in the matrix (position A).

Summary petrographic description for Middle Jurassic Iroquois sandstone and limestone

Sample I-100 3964.6A (Iroquois Formation, 3964.6m) fine grained sulphate-cement sandstone (appendix 9-6)

Description

This sample is a poorly sorted subarkose (Fig.4.5). The sediment is packed, suggesting that compaction took place before cementation. Often, at the contact between quartz grains, one grain has undergone dissolution leading to the penetration of one grain by another, thus creating concavo-convex contacts (c-c) (Fig.4.13 B).

The main detrital components of this sample are quartz, followed by sporadic K-feldspar, albite, biotite, muscovite and chlorite. Detrital quartz has illite inclusions that probably occur as an alteration product of muscovite (Fig.4.13 A). K-feldspar can be fresh with anhedral to subhedral crystal shape or altered with dissolution voids and partly replaced by anhydrite (Figs.4.13 A, B). Biotite is plastically deformed, thus creating pseudomatrix (Fig.4.13 A). Albite shows dissolution voids (Fig.4.13 C). Some biotite and muscovite grains alter to chlorite (Fig.4.13 C). The matrix in this sample is composd of silt size detrital minerals such as quartz, albite, micas and chlorite (Fig.4.13 A). Muscovite is present as inclusions in detrital quartz (Fig.4.13 B).

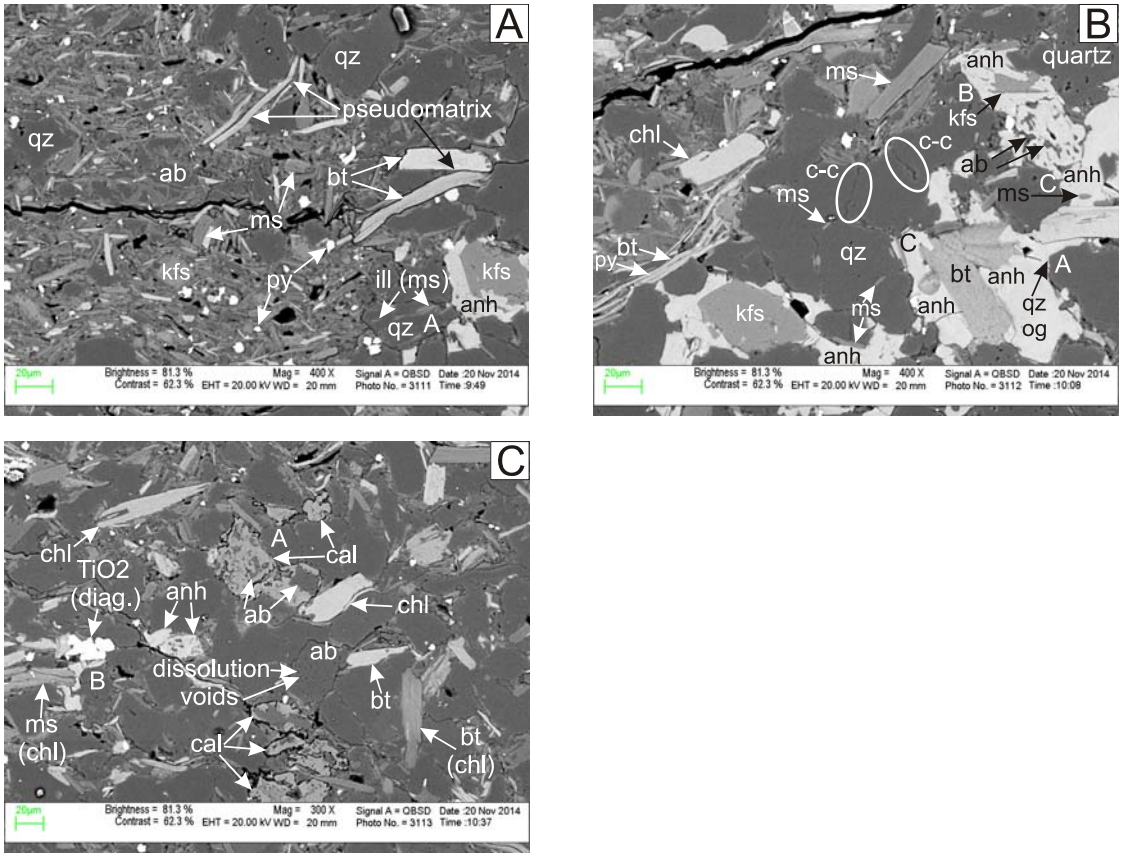

Figure 4.13: Representative back-scattered electron images of sample I-100 3964.6A from Mohican I-100 well. A) K-feldspar shows dissolution voids, has anhedral to subhedral crystal shape and is partly replaced with anhydrite. Detrital quartz has illite inclusions, that probably occur as an alteration product of muscovite (position A). Pyrite is diagenetic and shows displacive texture against the matrix (position B). Biotite and other minerals are platically deformed, thus creating pseudomatrix. The matrix is composed of silt size detrital minerals such as quartz, albite, muscovite, biotite and chlorite. B) Quartz overgrowths form around detrital quartz and tend to invade anhydrite cement (position A). Anhydrite partly replaces K-feldspar (position B) and engulfs biotite and muscovite (position C). Detrital quartz has muscovite inclusions (position D). Often, at the contact between quartz grains, one grain has undergone dissolution leading to the penetration of one grain by another, thus creating concavo-convex contacts. One biotite grain is partly replaced along the cleavage planes by pyrite (position E). C) Albite is either partly replaced with calcite (position A) or shows dissolution voids. TiO_2 mineral is diagenetic and shows replacive texture against the derital quartz (position B). Some biotite and muscovite grains alter to chlorite.

Sample I-100 4098.08 (Iroquois Formation, 4098.08m) sandy limestone (appendix 9-7)

Description

Based on the QFL discrimination diagram for sandstone classification, the modal composition of this sample is that of quartzarenite (Fig.4.5). The sample is poorly sorted. Chemically, a small variety of detrital minerals are identified in this sample: quartz, K-feldspar, muscovite and albite (Fig.4.14). Quartz is abundant with minor K-feldspar and albite. Muscovite appears as inclusions in detrital quartz as well as framework grains. K-feldspar is fresh with sub-rounded crystal outlines which are replaced by calcite.

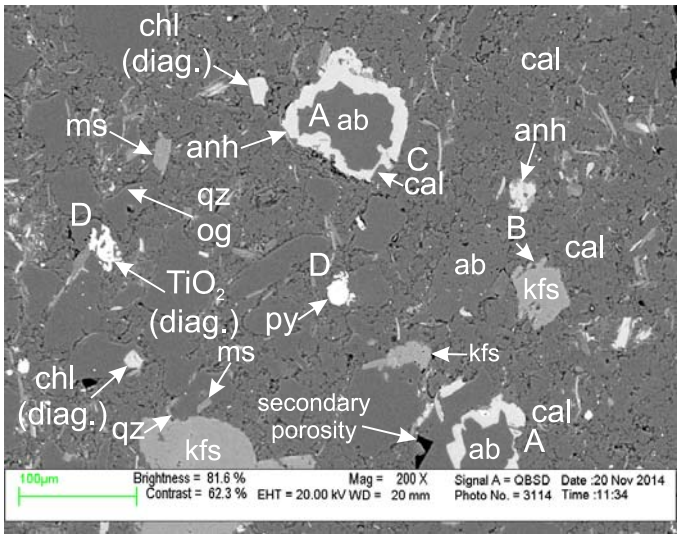

Figure 4.14: Representative back-scattered electron images of sample I-100 4098.08 from Mohican I-100 well. Detrital minerals in this figure are K-feldspar, albite , quartz and muscovite. Albite grains are partly replaced by anhydrite (position A), whereas K-feldspar shows rim replacement by calcite (position B). Muscovite appears as inclusions in detrital quartz as well as framerwork grains. Micritic calcite is the main cement that replaced anhydrite cement (position C). Rare quartz overgrowth forms around detrital quartz grains. Pyrite and TiO_2 appear to nucleate on cement and framework grains boundaries, and often they are replacing pre-extisting detrital minerals (position D).

4.2.3.2 Moheida P-15

Summary description of Lower Cretaceous Roseway Equivalent oolitic ironstone

Sample P-15 2563.67 (Roseway Equivalent Formation, 2563.67 m) oolitic ironstone (appendix 10-1A)

Description

This sample is composed mostly of coated grains that have spherical to oval shape with narrow concentric bands (Figs.4.15 A, D) comprising various proportions of siderite, kaolinite and other minerals (Fig.4.15 A). Although cassiterite is a main component of the coated grains it is considered contaminant from thin section polishing and as a result it has not been taken into consideration. Often massive calcite is trapped between concentric layers (Fig.4.15 A). Most of the coated grains lack nucleus. When present the nucleus is made up mostly of Fe-calcite aggregates with small amounts of siderite (Figs.4.15 A, D). Quartz is the only detrital mineral identified having fine grain size (Fig. 4.15 B). Rarely, bioclasts present are totally replaced by Mg-Fe-calcite (Fig. 4.15 A).

e=early and l=late

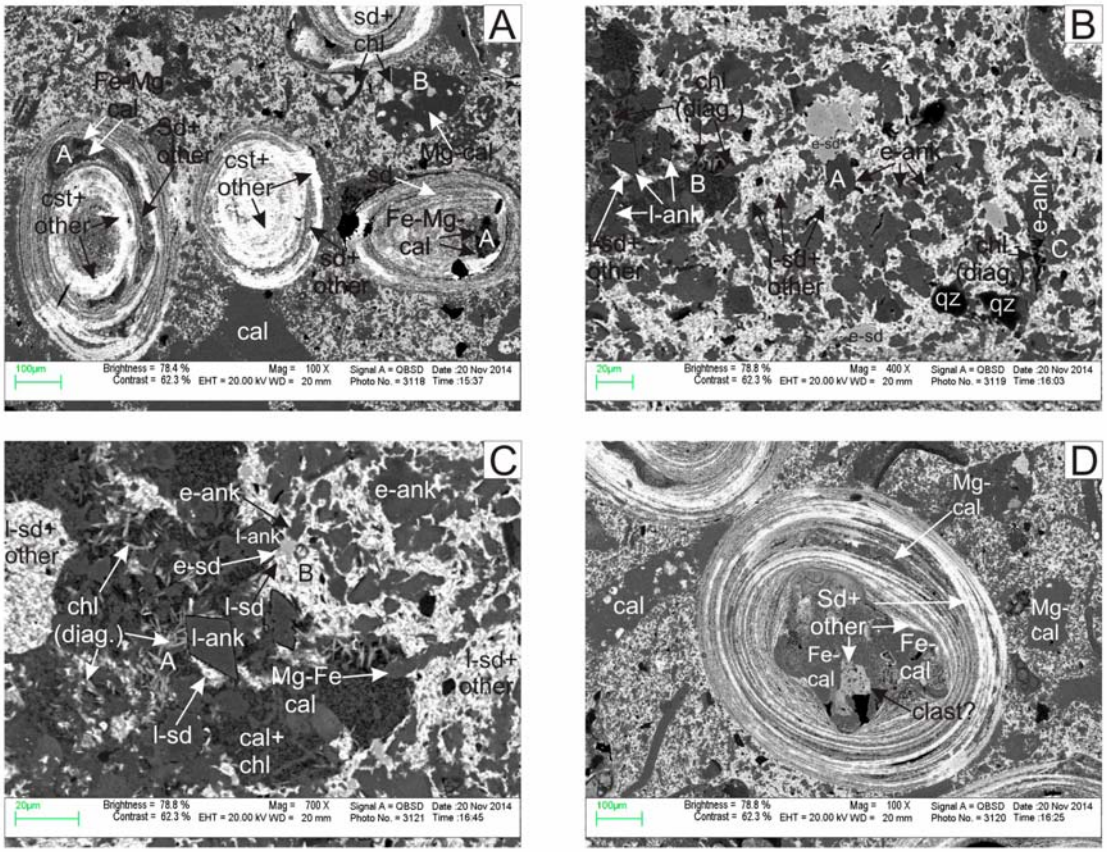

Figure 4.15: Representative back-scattered electron images of sample P-15 2563.67 from Moheida P-15 A) Framework grains are oolites with narrow concentric bands. The chemical composition of the coated grains is a mixture of siderite, kaolinite and other minerals. Often massive Fe-Mg-cal is trapped between concentric layers (position A). Although cassiterite (cst) is abundant it does nor represent a detrital nor a diagenetic mineral but instead is a contaminant. The coated grains lack nucleus and have spherical to oval shape. One bioclast is replaced by Mg-calcite and siderite with chlorite (position B). B) Quartz is the only detrital mineral identified having fine grain size. The cement is mixture of ankerite, siderite and chlorite. Late siderite engulfs early siderite. Early ankerite predates early and late siderite (position A). Late ankerite (position B) postdates early ankerite, both early and late siderite and chlorite. Chlorite fills secondary porosity in the cement (position C). C) Enlarged image to show the main components of the cement. Diagenetic minerals are ankerite, chlorite, apatite, calcite and siderite. Late ankerite (position A) tends to cross-cut both early and late siderite and diagenetic chlorite. Mg-Fe-calcite is partly replaced by late siderite. Late siderite surrounds early siderite and early ankerite (position B). D) Oval to spherical coated grain with narrow concentric bands and nucleus. The nucleus is made up of Fe-calcite aggregates with small amounts of siderite and other diagenetic minerals .

Summary petrographic description for Upper Jurassic Abenaki oolitic limestone

Sample P-15 3306.03 (Abenaki Formation, 3306.03 m) oolitic limestone (appendix 10-2)

Description

Peloids and ooids are the framework grains in this sample (Fig.4.16 A). All framework grains are made up mostly of a micritic mixture of Mg-calcite, calcite and pyrite. The peloids have irregular shape and size, do not have internal structure such as concentric bands and lack a nucleus (Fig. 4.16 A). The ooids have spherical shape and generally show internal structure of concentric bands and a nucleus of detrital albite or quartz (Fig.4.16 A). Rarely, at the contact between framework grains, one grain has undergone dissolution leading to the penetration of one grain by another (Fig.4.16 A).

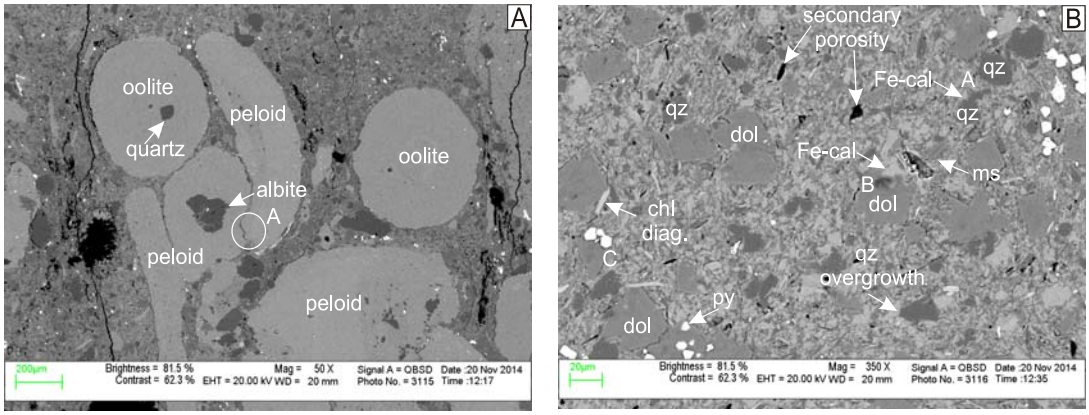

Figure 4.16: Representative back-scattered electron images of sample P-15 3306.03 from Moheida P-15 well. A) Peloids and oolites are framework grains in this figure. All framework grains are made up by micritic mixture of Mg-calcite, calcite, pyrite and other. Often, detrital albite and detrital quartz represent the nucleus for some of the oolites and or are components of the framework grains. Rarely, at the contact between coated grains, one grain has undergone dissolution leading to the penetration of one grain by another (position A). Secondary porosity in the cement lacks diagenetic minerals. The peloids have irregular shape and no internal structure. The oolites have a spherical shape and often tend to show internal structure such as nucleus and some concentric bands. B) This figure shows the main components of the cement that supports the framework grains in figure 4.15 (A) as well as their textural relationship. The supporting material is a mixture of silt seize dolomite, diagenetic chlorite, pyrite, muscovite, calcite, Fe-calcite and detrital quartz. Quartz overgrowths form around detrital quartz. Fe-calcite and calcite are the main cement replacing both detrital quartz (position A) and dolomite (position B). Pyrite is diagenetic and shows replacive texture against dolomite and cement (position C). .

Summary petrographic description for Middle Jurassic Iroquois sandstone and dolostone

Sample P-15 3744.92 (Iroquois Formation, 3744.92 m) fine grained sulphate-cement sandstone (appendix 10-3)

Description

Based on the QFL discrimination diagram for sandstone classification, the modal composition of this sample is that of sublitharenite (Fig.4.5). The sample is poorly sorted with low primary porosity that is filled with diagenetic minerals (Fig.4.17). The sediment is packed, thus the framework grains in this sample tend to come in direct contact with each other suggesting that compaction took place before cementation. Often, at the contact between quartz grains, one grain has undergone dissolution leading to the penetration of one grain by another, thus creating concavo-convex contacts (c-c) (Fig.4.17).

The majority of the framework grains are quartz followed by sporadic muscovite, chlorite, biotite and lithic clasts. Detrital quartz is highly corroded and commonly contains muscovite inclusions and/or illite inclusions that probably occur as an alteration product of muscovite (Fig.4.17 A). The lithic clasts are of metamorphic origin, show foliation, and are made up of quartz, chlorite, ilmenite and muscovite (Fig. 4.17 B).

c.q.=corroded quartz

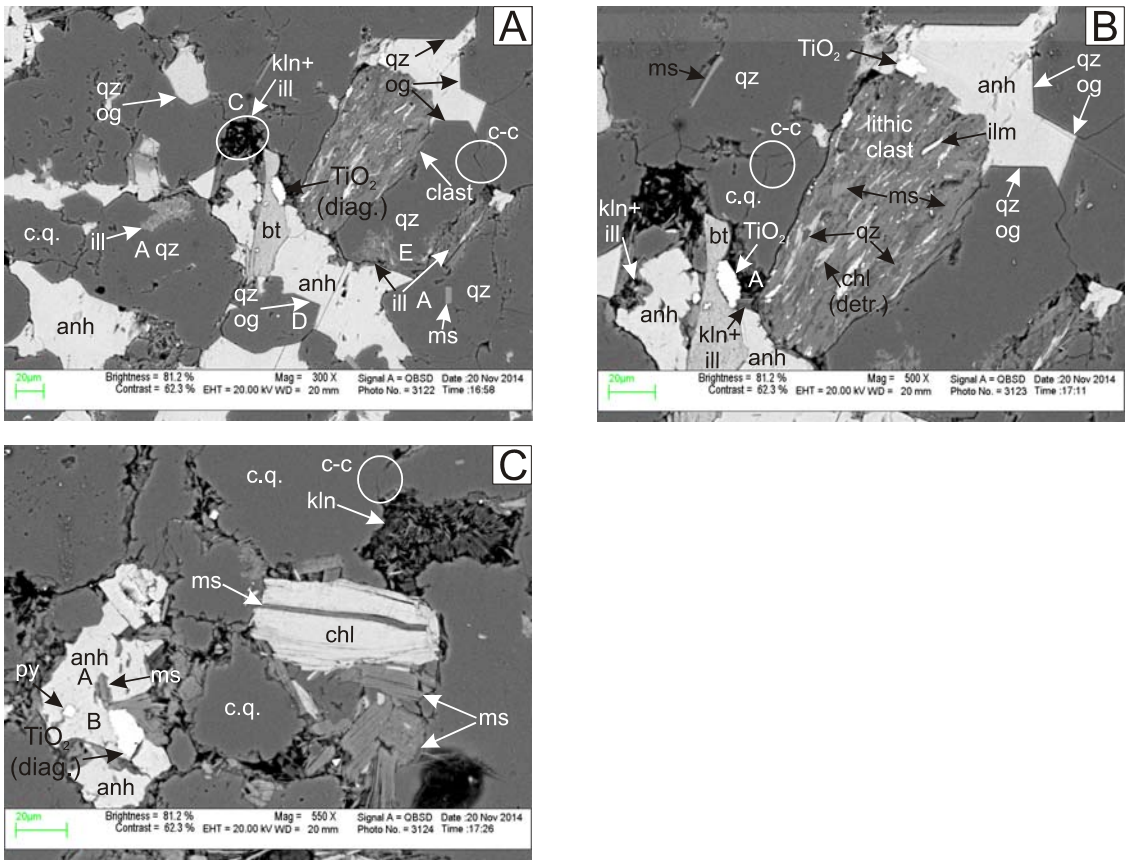

Figure 4.17: Representative back-scattered electron images of sample P-15 3744.92 from Moheida P-15 well. A) Detrital quartz is highly corroded and often contains muscovite inclusions and/or illite inclusions that probably occur as an alteration product of muscovite (position A). Anhydrite engulfs biotite (position B). In places, illite forms in the space between detrital quartz and anhydrite cement. Kaolinite and illite fill embayments in detrital quartz (position C). Quartz overgrowths for around detrital quartz and invade anhydrite cement (position D). Illite forms in the space between anhydrite cement and detrital quartz (position E). B) One lithic clast identified shows foliation, is derived from metamorphic rocks and are made up of quartz, chlorite, ilmenite and muscovite. TiO_2 mineral shows replacive texture against biotite (position A). Kaolinite and illite fill embayment in anhydrite cement (position B). Kaolinite and illite tend to be replaced by the TiO_2 mineral (position A). C) Anhydrite fills primary porosity and engulfs muscovite (position A). Framboidal pyrite shows replacive texture against anhydrite and TiO_2 mineral show replacive texture against anhydrite (position B). Both TiO_2 mineral and pyrite seem to cross-cut all the other minerals.

Sample P-15 3750.94 (Iroquois Formation, 3750.94 m) dolostone (appendix 10-4)

Description

The entire sample is made up of euhedral dolomite grains (Fig.4.18).

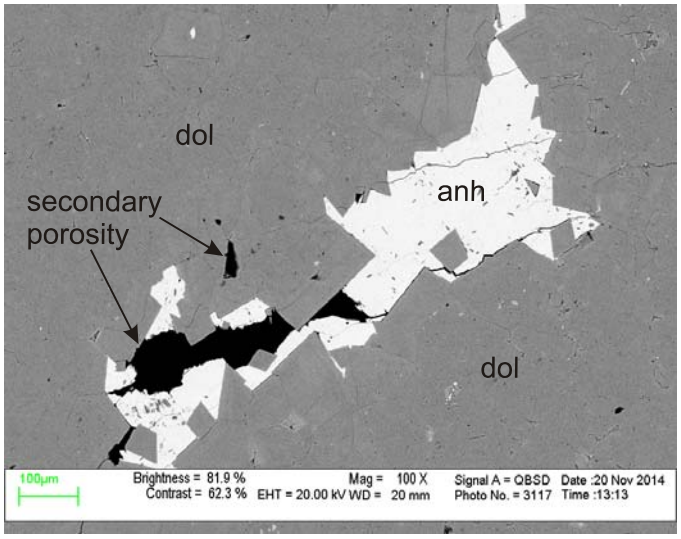

Figure 4.18: Representative back-scattered electron images of sample P-15 3750.94 from Moheida P-15 well. The entire sample is made up by dolomite, thus the rock is dolostone. Secondary porosity in the rock is partly filled with anhydrite.

4.3 Provenance

4.3.1 Modal composition for detrital heavy minerals assemblage from wells studied

The data presented for provenance in this section were obtained after analytical methods described in chapters 3.2.6, 3.2.7 and 3.2.8 were applied on polished thin sections of the heavy mineral separates. Mineral analyses from both the SEM and the EMP, together with back-scattered electron images were used for the discrimination between detrital heavy, detrital light and diagenetic minerals.

The modal composition of detrital heavy minerals identified in one sample is expressed as percentages of distinct individual detrital heavy minerals in that sample. The percentage of each distinct mineral is presented as the number of grains of that mineral divided by the total number of detrital mineral grains in the sample.

Although heavy mineral analyses have been successfully used in assessing potential sources for sediments (e.g. Pe-Piper et al., 2009) there are some constraints regarding this method: i) identification and counting of detrital heavy minerals in back-scattered electron images requires lots of skill as minerals with distinct chemical composition might show similar contrast and brightness (e.g. zircon and spinel, both have white color and high contrast) or some grains might be altered, thus as a result it is difficult to identify what mineral it is; ii) mineral mounts are made in general from individual grains but in some cases aggregates containing more than one mineral might be present, thus it is hard to determine the chemical composition of individual mineral in the aggregate; iii) the heavy mineral mount in made up grains with size >53 μm and <250 μm, thus if a mineral has grains outside this size range, it will not be identified.

4.3.1.1 Chinampas O-37 and Shelburne G-29

The data obtained for these two wells regarding their modal composition is presented in supplementary table 4.3 (see back of the Thesis). One sample from the Scots Bay Formation at Chinampas O-37 and one sample from the Shortland Shale at Shelburne G-29 were studied from a heavy mineral perspective. The weight percentage of the heavy fraction separates from the Scots Bay Formation in Chinampas O-37 was 10.82%, whereas the same weight percentage from the Shortland Shale Formation in Shelburne G-29 was 4.83%. The grain mounts of the heavy fraction in both wells included 92% to 98% light and diagenetic minerals.

The dominant detrital heavy mineral at Chinampas O-37 is magnetite (96.7%), followed by rare amphibole, apatite, garnet (spessartine with almandine substitution, pyrope), ilmenite and tourmaline (0.3%) (Fig.4.18). At Shelburne G-29 the dominant detrital heavy mineral is ilmenite (65.4%), followed by tourmaline and apatite, with equal zircon and chromium spinel and rare aluminium spinel (1.3%).

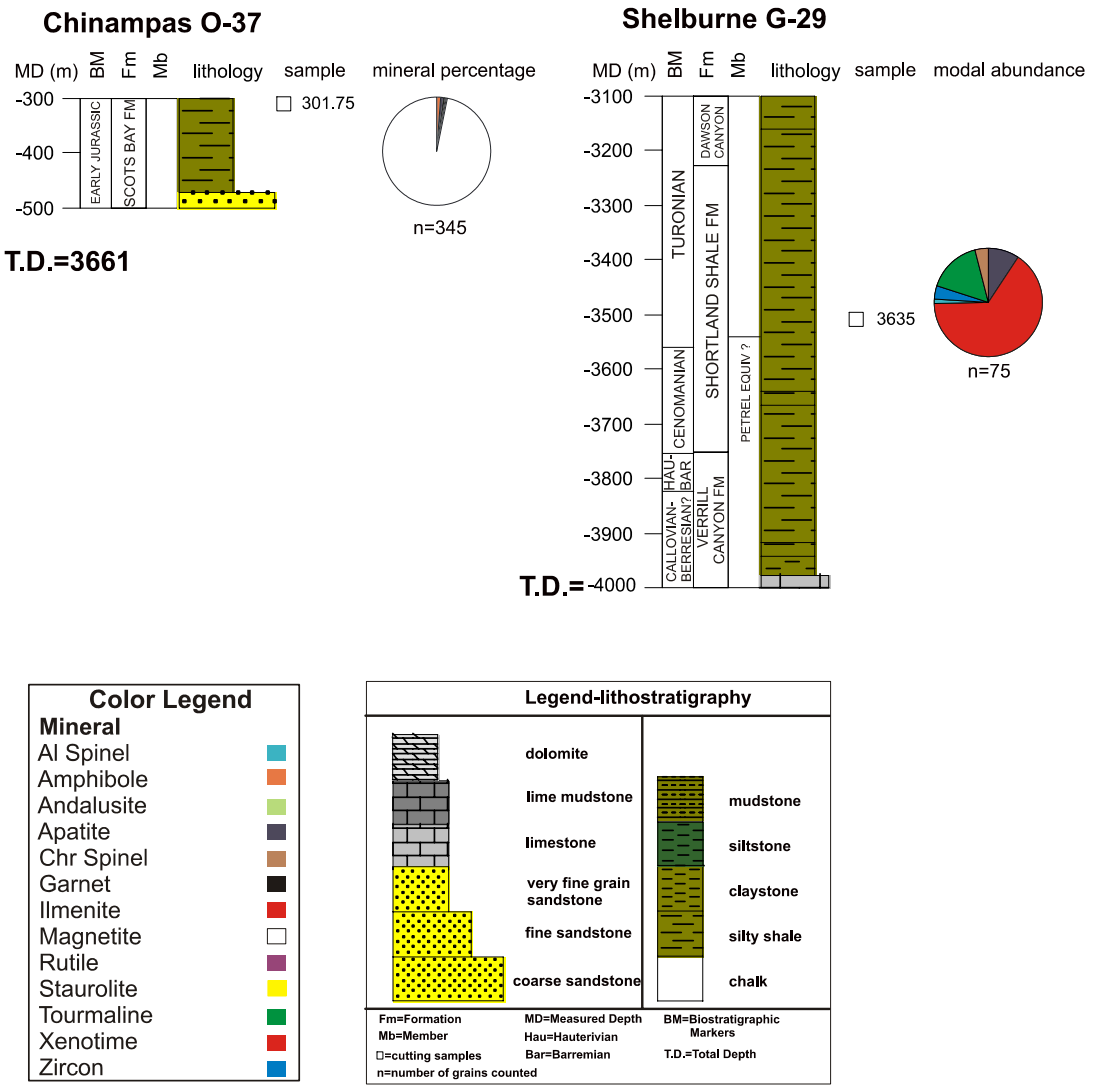

Figure 4.19: Stratigraphic columns of Chinampas O-37 and Shelburne G-29 showing location of cutting samples as well as modal abundance of detrital heavy minerals in each of the samples obtained.

4.3.1.2 Mohawk B-93

The data obtained for Mohawk B-93 well is presented in table 4.4 (see back of the Thesis). A total of 9 samples, 3 from Lower Cretaceous Roseway Equivalent Formation and 6 from Upper Jurassic-Middle Jurassic Mohawk Formation were obtained for detrital heavy minerals. The weight percentage of the heavy fraction separates in the

studied well ranged from 1.71% in sample B-93 6210 (1892.8 m) to 16.28% in sample B-93 4670 (1423.4 m).

Ilmenite is the dominant detrital heavy mineral in almost all samples from this well (Fig.20) with weight percentage ranging from 59.9% in sample B-93 6540 (1993.41 m) to 85.5 % in sample B-93 5410 (1650.48 m). In sample B-93 4670 (1423.4m) ilmenite has the minor weight percentage, around 23%. Tourmaline is the second most abundant detrital mineral in most of the samples with weight percentage that ranges from 19.4% at B-93 6210 (1892.8 m) to 5.9% in B-93 6340 (1932.43 m), except for 2 samples, B-93 5410 (1650.48 m) and B-93 5860 (1787.64 m) where it is the third most abundant and one, B-93 4670 (1432.4 m) where it is the fourth most abundant. Sample B-93 4670 has the highest percentage in zircon ~46.7% followed by samples B-93 5410 with 15% and sample B-93 6750 (2058.92 m) with 4%. Garnet percentage ranges from 1.7% in sample B-93 5410 to 13.9% in sample B-93 6450. Staurolite is present in samples B-93 5760 (1743.45 m) with 5.5% and in B-93 5860 (1787.64 m) with 6.9%. Other detrital heavy minerals like magnetite, apatite, monazite, rutile and xenotime are almost absent. Apatite is present in most samples; however its percentage ranges from 0.3% in sample B-93 5410 to 14.35% in sample B-93 4670. Magnetite is present in only 2 samples, B-93 4670 and B-93 5170, with weight percentage ranging from 9.5% to 1% respectively. Rutile was identified in 3 samples, B-93 5170 (2%), B-93 5410 (1%) and B-93 6340 (0.7%). Monazite, xenotime and aluminium spinel were identified in different single samples: B-93 6210 has 1.1% monazite, B-93 5410 has 0.3% xenotime and B-93 6340 0.4% aluminium spinel.

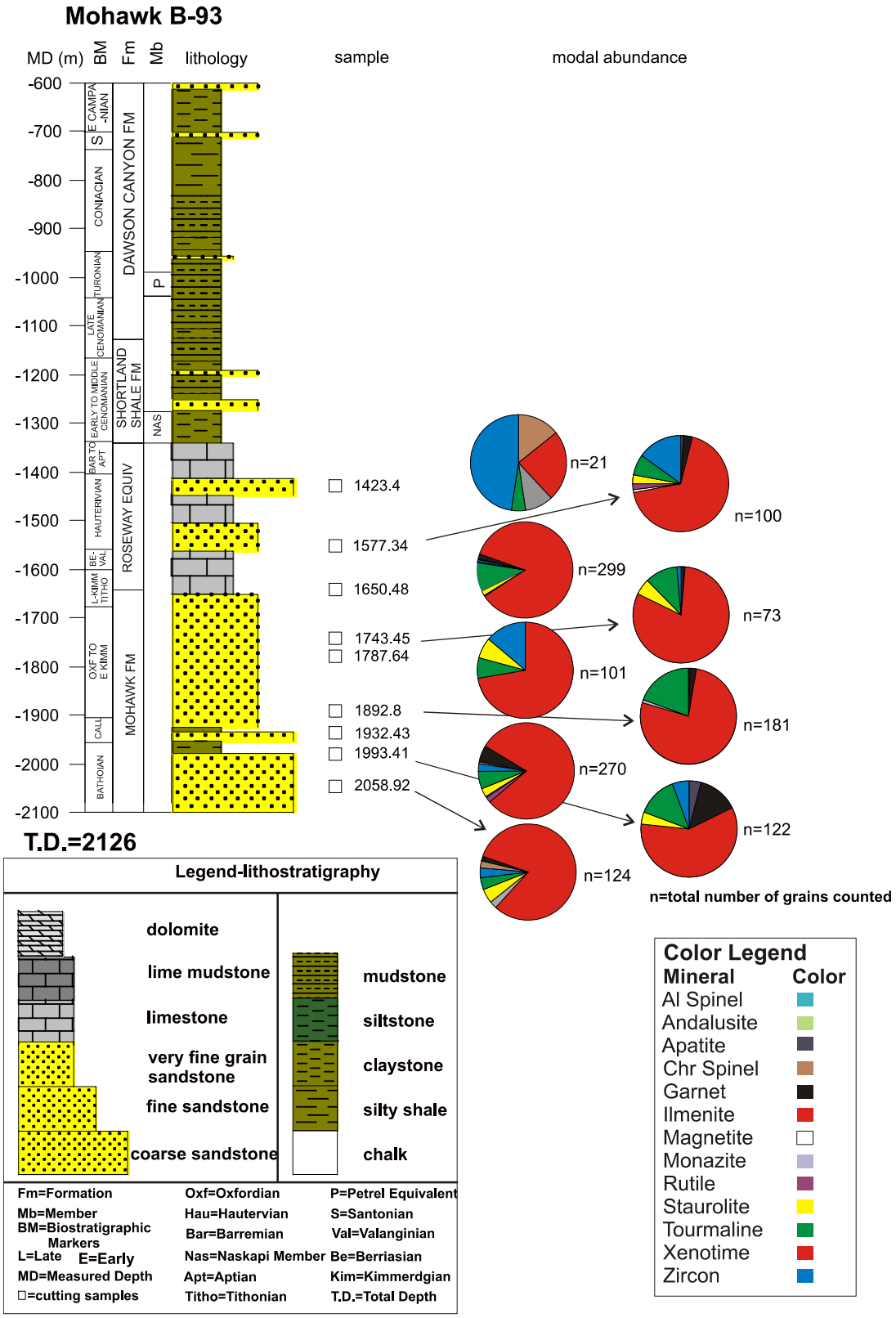

Figure 4.20: Stratigraphic column of Mohawk B-93 showing location of cutting samples and modal abundance of detrital heavy minerals in each sample.

4.3.1.3 Mohican I-100

The data obtained for Mohican I-100 well is presented in table 4.5 (see back of the Thesis). Three samples from Lower Cretaceous strata (1 from Logan Canyon, 1 from Upper Missisauga and 1 from middle Missisauga), 2 from Lower Cretaceous-Upper Jurassic strata (both from Roseway Equivalent Formation), 1 from Upper Jurassic strata (Abenaki Formation) and 2 from Middle Jurassic strata (both from Iroquois Formation) were studied for detrital heavy minerals. Ilmenite is the most abundant detrital heavy mineral in all the samples from this well (Fig.4.21) with weight percentage that ranges from 42.1 % at I-100 7840 (2389.63 m) to 81% at I-100 13800 (4026.24 m). Tourmaline is the second most abundant detrital heavy mineral in most of the samples with percentage that ranges from 6.9% in sample I-100 7230 (2203.7 m) to 21.7% in sample I-100 11400 (3474.72 m). Garnet pergentage ranges from 0.9% in samples I-100 8480 (2584.7 m) to 16.4% in sample I-100 12640 (3852.67 m). Sample I-100 7230 has the highest percentage in zircon ~12.1% whereas sample I-100 8480 has the lowest percentage in zircon ~3.5%. Other detrital heavy minerals like andalusite, apatite, monazite, rutile, aluminium spinel, chromium spinel and staurolite are almost absent. Andalusite is present only in two samples, I-100 5990 and I-100 13800 with 2.9% and 0.4% respectively. Apatite percentage ranges from 0.4% in sample I-100 13800 to 4.1% in sample I-100 11400. Monazite is present in two samples I-100 11400 (2.7%) and I-100 12640 (0.8%). Rutile was identified only in one sample I-100 7230 making up 5%. Spinel makes about 2.6% of the total in sample I-100 7230. Staurolite ranges from 0.9% in sample I-100 7230 to 8.8% in sample I-100 5990.

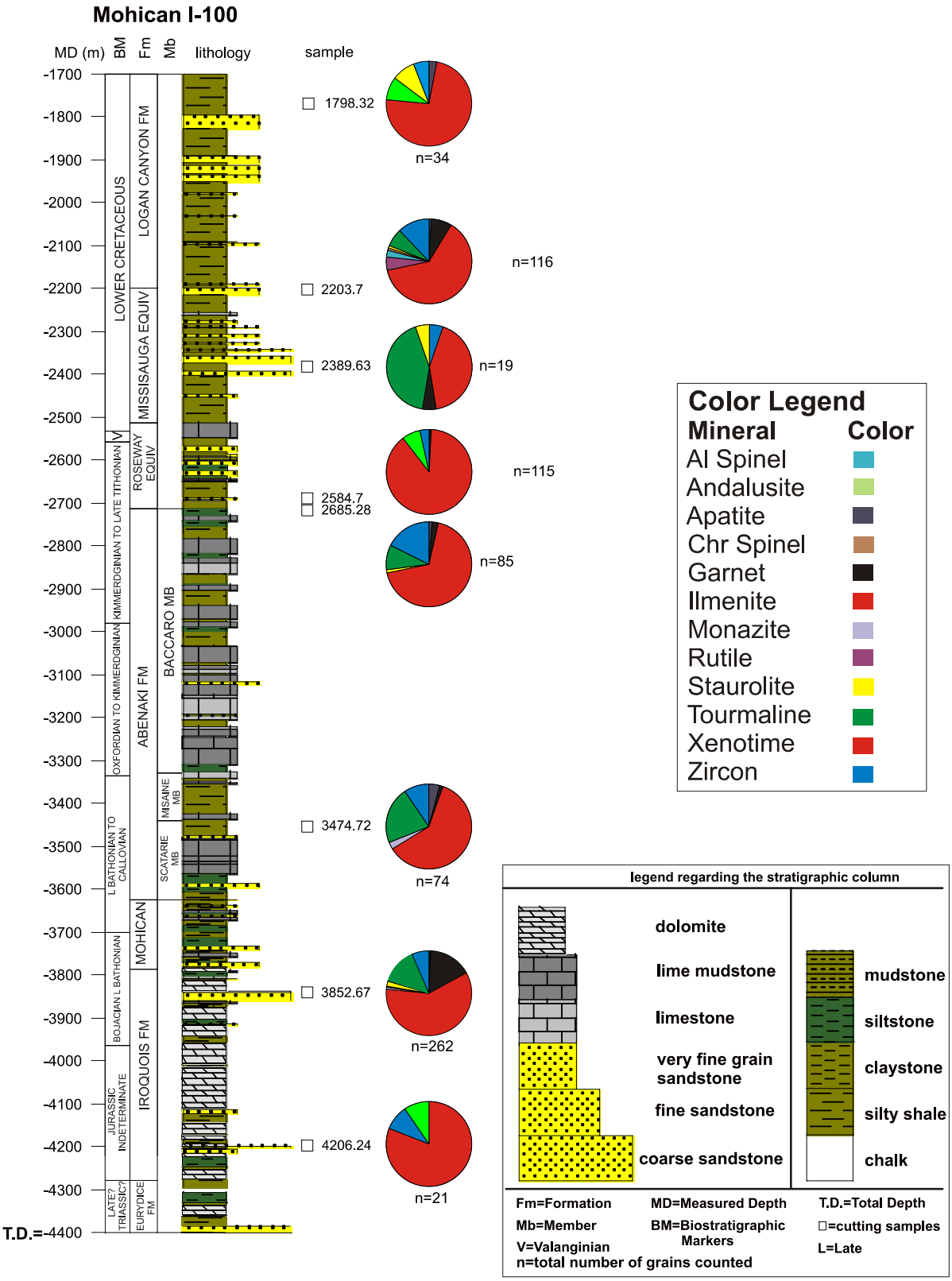

Figure 4.21: Stratigraphic column of Mohican I-100 showing location of cutting samples and modal abundance of detrital heavy minerals in each sample.

4.3.2 Chemical composition of detrital minerals (appendices 3 to 8)

Previous work regarding the sources for the Jurassic to Cretaceous clastic sediments in the central and eastern Scotian Basin was done using chemistry of common detrital heavy minerals such as tourmaline, garnet, spinel/chromite (Pe-Piper et al., 2009, Tsikouras et al., 2011), zircon (Piper et al., 2007) and rutile (Ledger, 2013). Light detrital minerals, such as feldspar, muscovite, biotite and chlorite, can also be diagnostic of rock sources and thus they have also been taken into consideration. Provenance in general was interpreted on the basis of several techniques, including geochemistry of detrital heavy minerals and modal abundance of heavy minerals (Pe-Piper et al., 2009), whole rock geochemical analysis (Pe-Piper et al., 2008, Zhang et al., 2014), morphology of detrital heavy minerals (Piper et al., 2007; Ledger, 2013), geochronology of detrital minerals (Pe-Piper and MacKay, 2006; Reynolds et al., 2009) and hot cathodoluminescence of detrital quartz (Sawatzky and Pe-Piper, 2013).

In this study we chose the geochemistry of detrital heavy minerals identified in polished thin sections of both cuttings and core samples as the primary technique, because detrital heavy minerals usually do not alter and can be transported far from the source and deposited in sedimentary basins.

4.3.2.1 High stability group detrital minerals

4.3.2.1.1 Tourmaline

Tourmaline is a common detrital mineral in the Mesozoic formations of the Scotian Basin and has been widely used as an indicator in assessing potential sources for sediments that form these formations (Li et al., 2012). Based on chemical variation,

tourmaline has been classified in terms of different type of sources, 10 in total, by Henry and Guidotti (1985) and Kassoli-Fournaraki and Michailidis (1994) (Fig. 4.22). A new discrimination of tourmaline, also based on its chemical variation, was introduced by Pe-Piper et al. (2009), which included only four types with four distinctive fields. The four distinctive fields projected for tourmaline discrimination are a result of a combination of fields proposed by Henry and Guidotti (1985) and Kassoli-Fournaraki and Michailidis (1994), with natural clusters in chemical composition of tourmaline analysed from Lower Cretaceous sandstones originating in the Scotian Basin (Pe-Piper et al., 2009). Chemically, type 1 suggests a granitic rock source, type 2 a metapelitic and calc-silicate rock source, type 3 a meta-ultramafic rock source and type 4 a metapelitic/metapsammitic rock source. Considering tourmaline discrimination introduced by Pe-Piper et al. (2009), only 3 from the total 4 types of tourmaline have been identified within Mesozoic sediments (Mid Jurassic to Early Cretaceous) deposited in the SW Scotian Basin: type 1, type 3 and type 4.

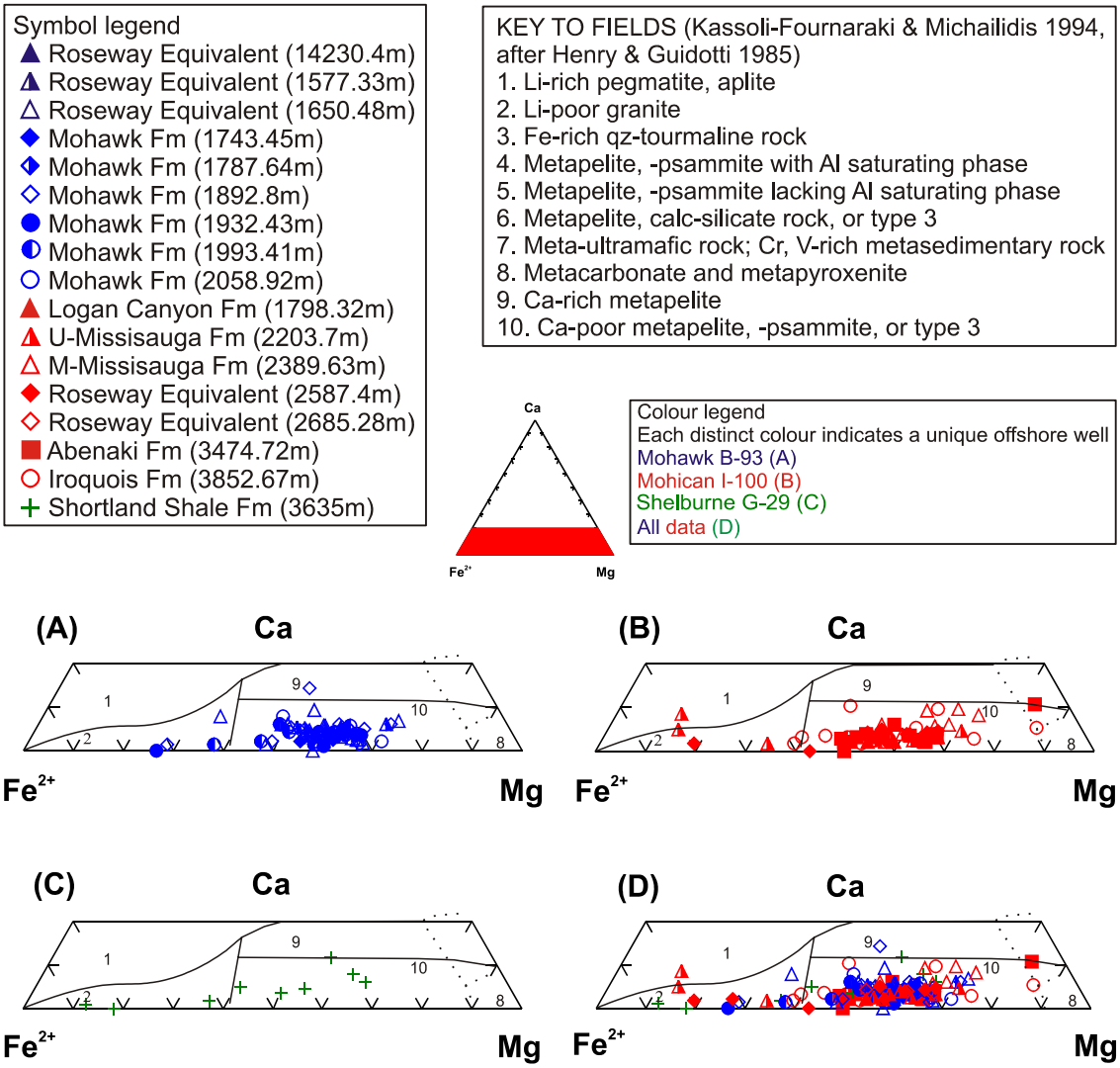

Fig.4.22: Chemical variations in tourmaline based on Ca - Mg - Fe^{2+}.

Chinampas O-37

No detrital tourmaline has been identified in the samples from this well.

Mohawk B-93

Only 2 of the 4 types interpreted by Pe-Piper et al. (2009) have been distinguished in samples from Mohawk B-93, which are type 1 and type 4 (Fig.4.23 A). The overall dominant tourmaline type is 4 and its presence can be observed in samples collected

from Roseway Equivalent Formation, with 32 grains counted in Lower Cretaceous, as well as in samples from Mohawk Formation with 38 grains in Upper Jurassic and 35 grains in Middle Jurassic. On the other hand type 1 is restricted, with only 1 sample (1650.48m in depth) (out of 3 samples in total) from Roseway Equivalent Formation that has 2 grains in Lower Cretaceous, 3 samples (out of 6 samples in total) from Mohawk Formation, where 1 sample (1892.8m in depth) has 2 grains in the Upper Jurassic and 2 separate samples have 2 grains (1932.43m in depth) and 1 grain (1993.41m in depth) in the Middle Jurassic.

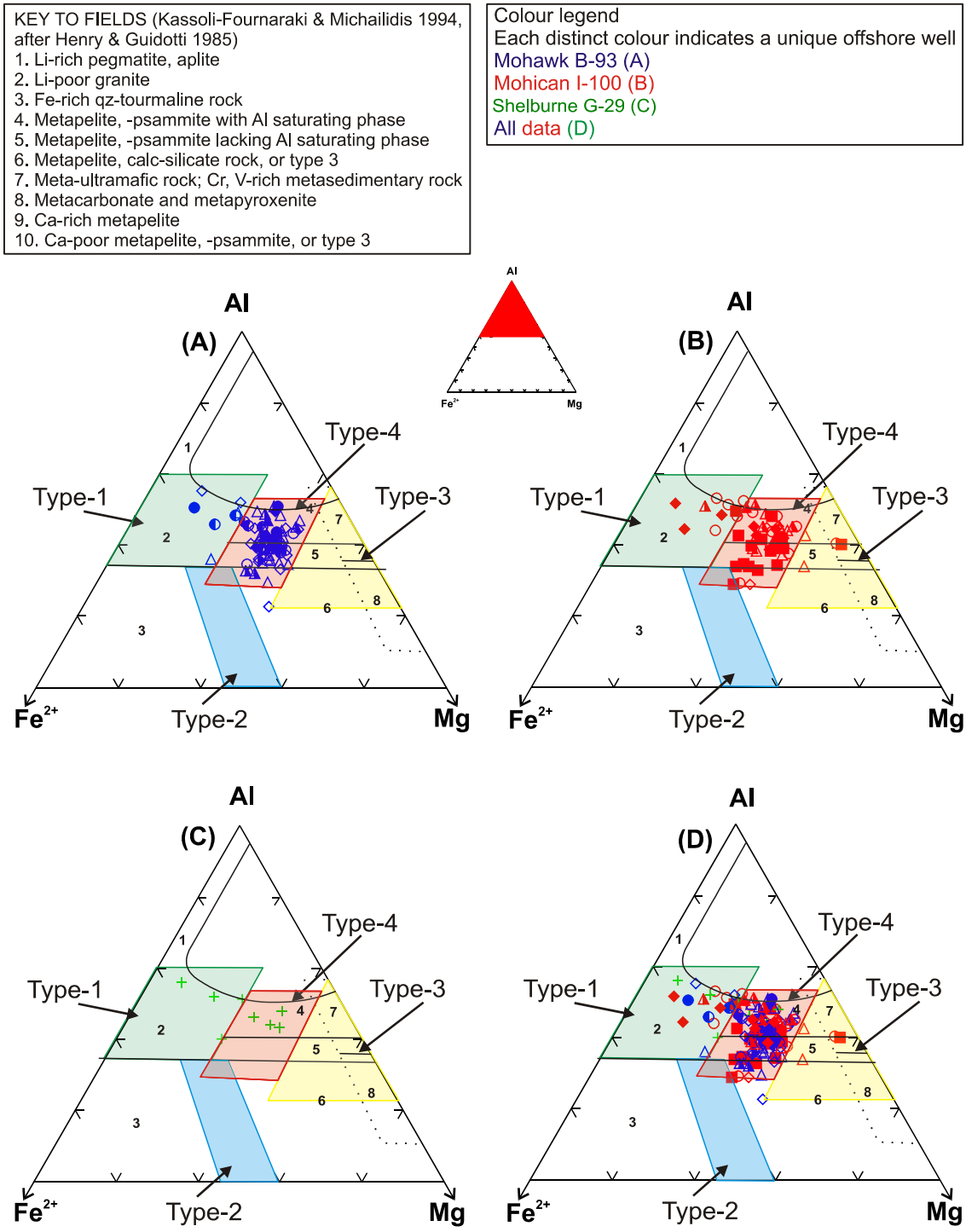

Fig.4.23: Chemical variations in tourmaline based on Al - Mg - Fe^{+2} showing discrimination of different types of tourmaline. For symbols representing different formations within same well and sample depths see Fig.4.22. The type numbers are from Pe-Piper et al. 2009.

Mohican I-100

Only 3 types of tourmaline have been identified in Mohican I-100, type 1, type 3 and type 4 (Fig.4.23 B). Type 4 is the most abundant type and is found in all formations sampled, 3 grains in Logan Canyon, 7 grains in Upper Missisauga Formation (Lower Cretaceous), 6 grains in Middle Missisauga Formation (Lower Cretaceous), 15 grains in Roseway Equivalent Formation (Upper Jurassic-Lower Cretaceous), 14 grains in Abenaki Formation (Middle Jurassic) and 32 grains in Iroquois Formation (Middle Jurassic). Type 1 is sub-ordinate to type 4 with a total of 10 grains counted from 4 formations: 1 grain is from Upper Missisauga, 3 grains are from Roseway Equivalent, 1 grain from Abenaki Formation (Middle Jurassic) and 5 grains from Iroquois Formation (Middle Jurassic). Type 3 is restricted and represented only by 4 grains, 2 from Middle Missisauga, 1 from Abenaki and 1 from Iroquois.

Shelburne G-29

Shortland Shale (Lower Cretaceous) is the only formation sampled in Shelburne G-29 for detrital heavy mineral separation. Although the total number of detrital heavy grains identified, 75, is low, tourmaline is abundant with 12 grains. Two types of tourmaline have been identified, type 4 and type 1, each represented by 4 grains, (Fig.4.23 C). Type 4 and type 1 show a linear correlation with chemical variation in Fe^{+2} and Mg.

Summary

1. Tourmaline is the second most common detrital heavy mineral identified, after

ilmenite

2. A total of 209 tourmaline grains were counted, 112 in Mohawk B-93, 89 in Mohican I-100, 8 in Shelburne G-29

3. Type 4 tourmaline is a main component when found in formations sampled, type 1 is common in all three wells, whereas type 3 is rare and restricted only in Mohican I-100 (Middle Missisauga, Abenaki and Iroquois formations)

4.3.2.2 Intermediate stability group detrital minerals

4.3.2.2.1 Garnet

Together with tourmaline, garnet represents one of the most used detrital minerals in assessing potential sources for sediments because is relatively insensitive to change in the chemical composition during transportation as well as during and after deposition (Deer et al., 1982; Arai, 1992). It also has distinctive chemical composition for different varieties. Although garnet has been frequently used as provenance indicator, two disadvantages limit its effectiveness: i) because of its relative stability, garnet may be of second cycle and thus it is hard to discriminate first cycle from second cycle sources; ii) with increase in depth, different types of garnet tend to become more corroded and eventually dissolve completely.

To classify the garnets analyzed, we compared our analyses with such analyses collected from the literature from known sources in Appalachian and Grenville bedrock (Pe-Piper et al., 2009). Garnet analyses collected from the literature are available for the following potential onshore sources: Meguma Terrane granites and Meguma Supergroup metasediments, the Clark Head orthogneiss and the Avalonian plutons in

SE Cobequid Highlands of the Avalon terrane and the Grenville Province that includes the Grenville metagabbro and the Grenville anorthosite-charnockite suite (Fig.4.24a).

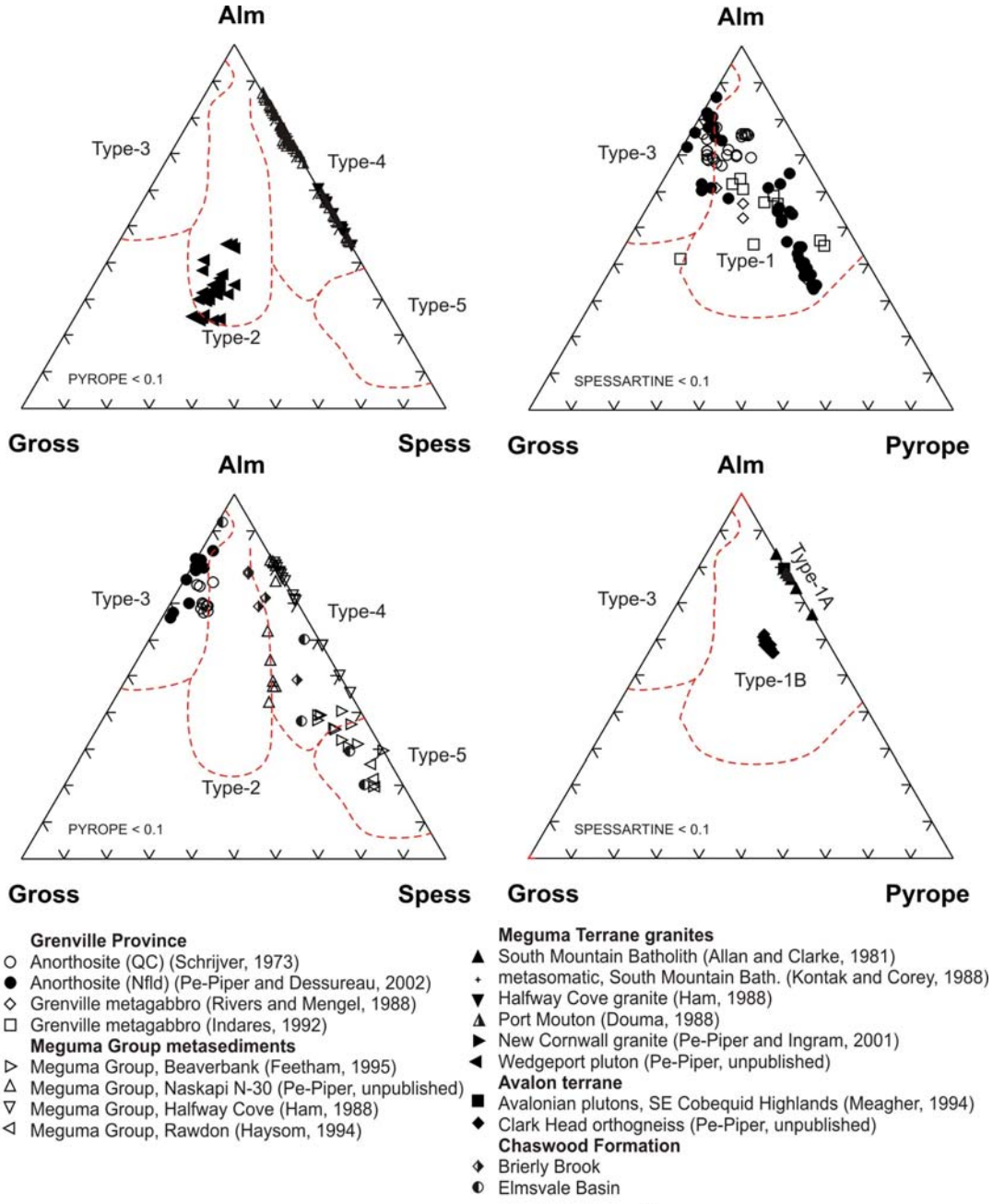

Fig.4.24a: Chemical variation in garnets from known sources in Appalachian and Grenville bedrock, modified from Pe-Piper et al. (2009). Data for Chaswood Formation from Pe-Piper et al. 2005.

Two ternary diagrams have been used for classification of garnets analyzed in this study: almandine-grossular-pyrope (with spessartine <10%) and almandine-grossular-spessartine (with pyrope <10%). Based on the chemical variations that garnet shows, 5 types have been discriminated according to Pe-Piper et al. (2009): types 1, 2, 3, 4 and 5. Depending on the conditions under which garnets in field 1 have been crystallized, such as pressure (P) and temperature (T), type 1 can be divided in two sub-categories which are type 1A and type 1B. Type 1A is characteristic of garnets that show no grossular substitution and significant almandine-pyrope substitution. On the other hand type 1B is typical of substitution between all three end-members almandine-grossular-pyrope, with significant substitution of almandine and prominent substitution of grossular and pyrope. Regarding other types, almandine with prominent spessartine and grossular substitutions are typical of type 2, almandine with prominent grossular substitutions typical of type 3, almandine with prominent spessartine substitutions typical of type 4 and spessartine with prominent almandine substitutions typical of type 5.

Chinampas O-37

Only one cutting sample from Scots Bay Formation (Lower Jurassic) has been obtained for heavy mineral separation. Garnet is one of the few detrital minerals found in this well along with biotite and chlorite. However, data are limited with two grains to have been identified from the total of 3763 grains analyzed and counted; one grain was plotted as 100% pyrope onto the almandine-grossular-pyrope ternary diagram (Fig.4.24b C), and the other represents garnet of type 5 projected on the almandine-grossular-spessartine diagram (Fig.4.24c C). Type 5 garnet from this well shows similar

chemical composition to type 5 garnet from the Meguma Supergroup metasediments (Beaverbank).

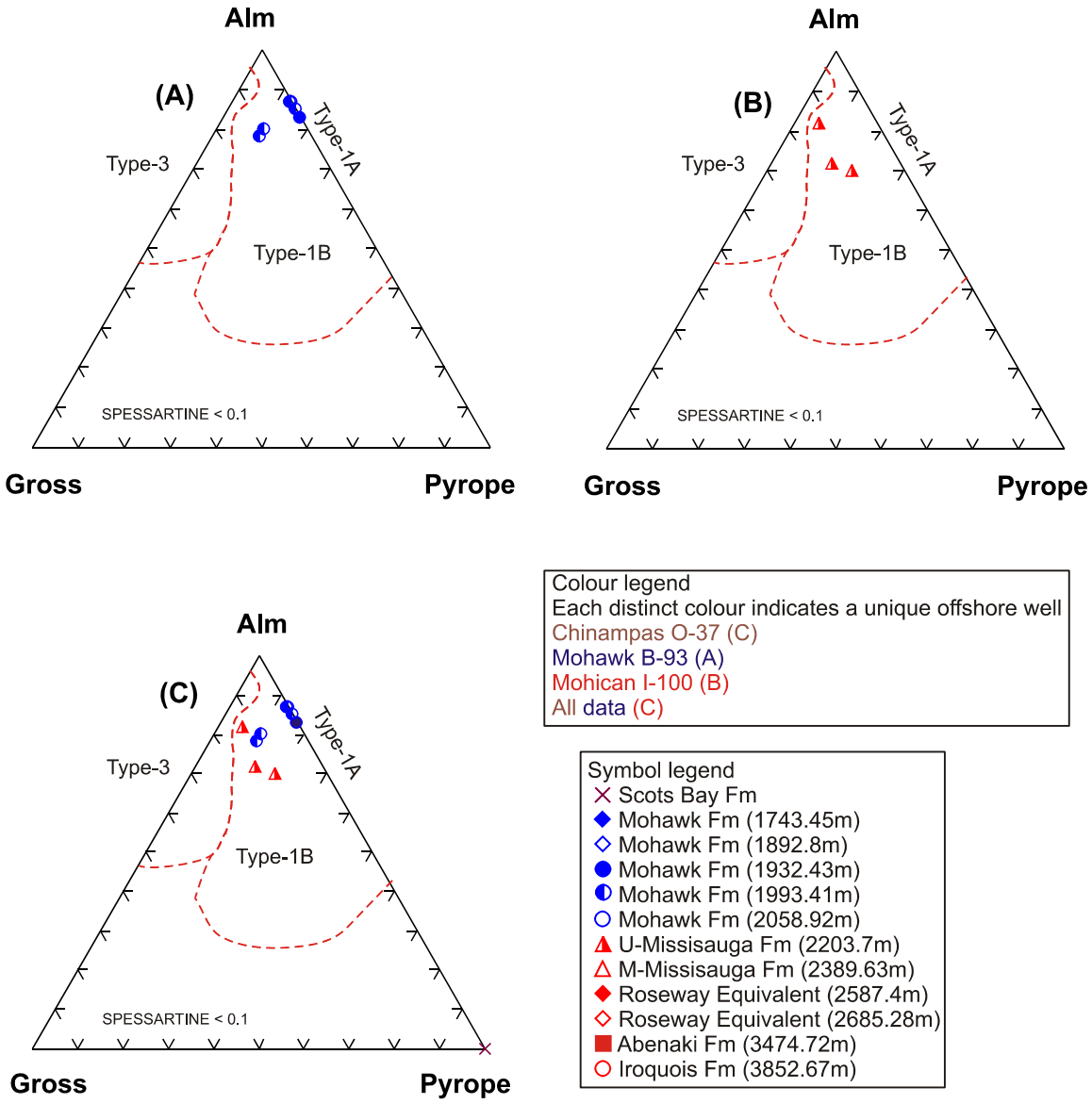

Fig.4.24b: Chemical variation in garnet projected onto Almandine - Grossular - Pyrope ternary plane, for garnet with <10% Spessartine.

Mohawk B-93

Garnet is the fourth most abundant detrital heavy mineral in this well after ilmenite, tourmaline and zircon. Both Roseway Equivalent Formation (Upper Jurassic-Lower Cretaceous) and Mohawk Formation (Upper and Middle Jurassic) sandstones have been studied for chemical variations in garnet. Garnet has been identified in both formations, but one sample from Upper Jurassic strata in Mohawk Formation at a depth of 1787.64 m lacks garnet. The absence of garnet can not be related to dissolution with increase in depth because samples obtained from greater depths contain garnet. In addition, the modal abundance of garnet shows an increase with depth.

From the total number of analyzed garnets (19 grains) in the whole well, only 6 grains, from same formation (Mohawk) with same age (Middle Jurassic), have the criteria to be plotted onto the almandine-grossular-spessartine ternary diagram as type 1A (4 grains) and type 1B (2 grains) (Fig.4.24b A). The remaining 13 grains were plotted onto the almandine-grossular-spessartine diagram as type 2, type 4 and type 5 (Fig.4.24c A). Type 4 is the most abundant type with 8 grains in total; 2 grains from Upper Missisauga Formation (Lower Cretaceous), 2 grains from Mohawk Formation (Upper Jurassic) and 4 grains from Mohawk Formation (Middle Jurassic). Two grains from Mohawk Formation (Upper Jurassic) and 1 grain from Mohawk Formation (Middle Jurassic) represent type 5. Two grains from Middle Jurassic sample (1993.41 m in depth) in Mohawk Formation are of type 2.

The Lower Cretaceous succession (Roseway Equivalent) has type 4 garnets with chemical composition that is similar to those analyzed from Naskapi N-30 offshore well (Upper Missisauga Lower Cretaceous) and Halfway Cove of the Meguma

Supergroup metasediments. Garnets in Upper Jurassic Mohawk Formation are typical of type 4 and 5 and similar to those from the Meguma Supergroup metasediments (Halfway Cove). Middle Jurassic Mohawk Formation comprises all 5 types of garnet identified in this well, type 1A, type 1B, type 2, type 4 and type 5 with chemical composition similar to those from the Meguma Terrane (Meguma Terrane granites and Meguma Supergroup metasediments) and the Grenville Province.

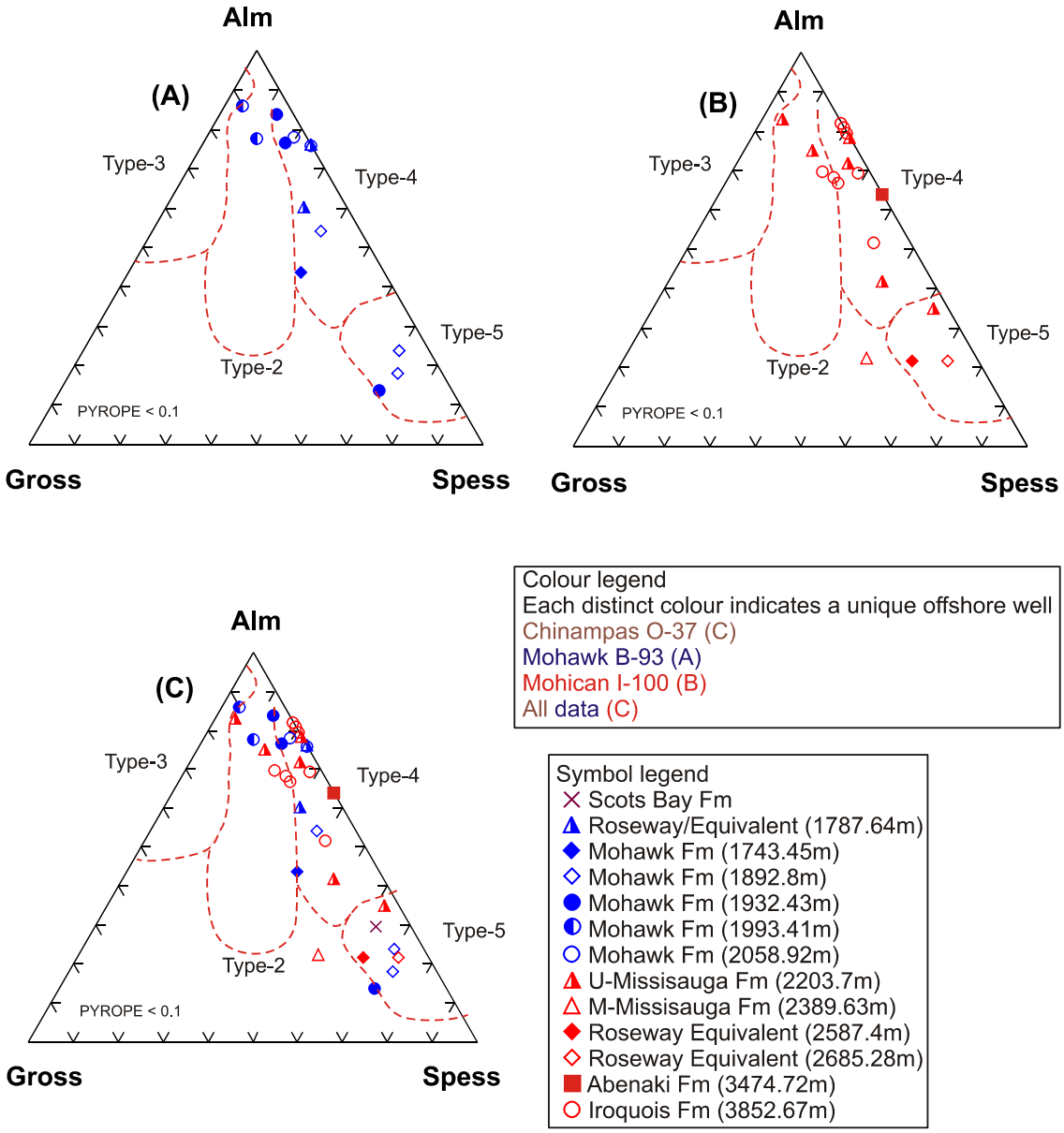

Fig.4.24c: Chemical variation in garnet projected onto Almandine - Grossular - Spessartine ternary plane, for garnet with <10% Pyrope.

Mohican I-100

All Lower Cretaceous formations, that include Logan Canyon, Upper Missisauga and Middle Missisauga, Upper Jurassic-Lower Cretaceous Formation Roseway Equivalent and Middle Jurassic formations, Abenaki and Iroquois, have been sampled and studied for detrital heavy minerals used in assessing potential sources for sediments. Garnet is a common detrital heavy mineral in samples obtained from this well with 21 grains counted in total. Upper Missisauga and Iroquois formations have the highest number of garnet, with 9 and 8 grains respectively. On the other hand Roseway Equivalent Formation is restricted to only 2 grains, whereas both Abenaki and Middle Missisauga formations have just 1.

Upper Missisauga Formation, when compared to other formations sampled in this well, is the only one with garnet analyses that plot onto the discrimination diagram in figure 4.24b, representing garnet with spessartine< 10% in its chemical composition. Three grains from Lower Cretaceous Upper Missisauga Formation are typical of type 1B (Fig.4.24b B). The remaining 6 plot onto the discrimination diagram that represents garnet with <10% pyrope as type 4 (3 grains), type 2 (2 grains) and type 5 (1 grain). Middle Jurassic Iroquois Formation is abundant in garnet of type 4 with 7 grains and rare in type 2 with only 1 grain present. Garnet analyses (2 in total) from Roseway Equivalent Formation (Upper Jurassic-Lower Cretaceous) are exclusively of type 5 (Fig.4.24c B).In contrast, Middle Jurassic Abenaki Formation is depleted in garnet with 1 grain that plots as type 4.

Compared with analyses collected from the literature (Fig.4.24a), Lower Cretaceous Upper Missisauga Formation has similar garnets as those from both the

Meguma Supergroup metasediments (Beaverbank and Naskapi N-30) and the Grenville Province. The Upper Jurassic-Lower Cretaceous Roseway Equivalent Formation, when compared to Lower Cretaceous formations, has garnets similar only to those from the Meguma Supergroup metasediments (Beaverbank and Rawdon), as is the case for Middle Jurassic Abenaki and Iroquois formations.

Shelburne G-29

No detrital garnet has been found in this well. The lack of garnet can be assessed to the fact that the sample collected was obtained from a depth of 3635 m; hence most of the garnet might have been completely dissolved as a result of garnet dissolution.

Summary

1. Garnet is an abundant detrital mineral in Mohawk B-93 (23 grains in total), Mohican I-100 (21 grains in total), rare in Chinampas O-37 (2 grains in total) and absent from Shelburne G-29
2. Ten garnet grains (6 from Mohawk B-93, 3 from Mohican I-100 and 1 from Chinampas O-37) from total 46 have chemical composition with spessartine< 10%
3. The most abundant type present is type 4 (almandine with prominent spessartine substitution) (11 grains); type 1A (almandine with almost no grossular substitution) and type1B (almandine with significant grossular and pyrope substitution) are rare (4 grains and 5 grains), type 2 (almandine with prominent spessartine and grossular substitutions) and type 5 (spessartine with prominent almandine substitution) are almost absent and share the same number of grains (3)

4. Type 1A is restricted only in Mohawk B-93 (Mohawk Formation/Middle Jurassic)

5. Type 1B is present only in Mohawk B-93 (Mohawk Formation/Middle Jurassic) and Mohican I-100 (Middle Missisauga Formation)

6. Type 4 and 5 garnet have similar chemical composition to garnets from Meguma Supergroup metasediments and Meguma Terrane granites

7. Type 1A garnet resembles most that at Meguma Terrane granites whereas type 1B and type 2 are similar to those from the Grenville Province

4.3.2.3 Light group detrital minerals (S.G. < 2.9 g/cm^3)

4.3.2.3.1 Feldspar

Feldspar is a common detrital mineral in the heavy mineral separates for the studied wells regardless its specific gravity ~2.6g/cm^3. The abundance in detrital feldspar in Mohican I-100 well is confirmed in the conventional cores analyzed. Petrographic analyses showed that after quartz, feldspar is the most common detrital mineral present in polished thin sections of conventional cores.

Feldspars provide important information in terms of petrology and geochemistry of the potential source rocks. Alkali feldspars, for example, commonly exhibit optical or sub-optical intergrowths of albite and K-feldspar (perthite), which have morphologies and crystallographic characteristics that are distinctive of the igneous or metamorphic environment in which they grew. Beyond chemical composition, microtextures can also be used as a provenance indicator for clastic sediments. However, the effectiveness of the detrital feldspars as source indicators may be limited by their sensitivity to chemical and mechanical changes during both transport and burial. Previous research has shown

that the amount of detrital feldspar tends to decrease systematically with burial depth (Wilkinson and Haszeldine, 1996; Wilkinson et al., 1997, Pe-Piper and Yang, 2014).

Due to lack of organized data from the literature regarding chemistry of feldspar from known rock sources no comparison diagrams were made. For classification of feldspar we used ternary plots showing chemical variations based on K-Na-Ca composition.

Chinampas O-37

Only 3 grains, from Scots Bay Formation (Lower Jurassic) were identified from the total of 3763 grains analyzed. All 3 grains identified are K-feldspar (Fig.4.25).

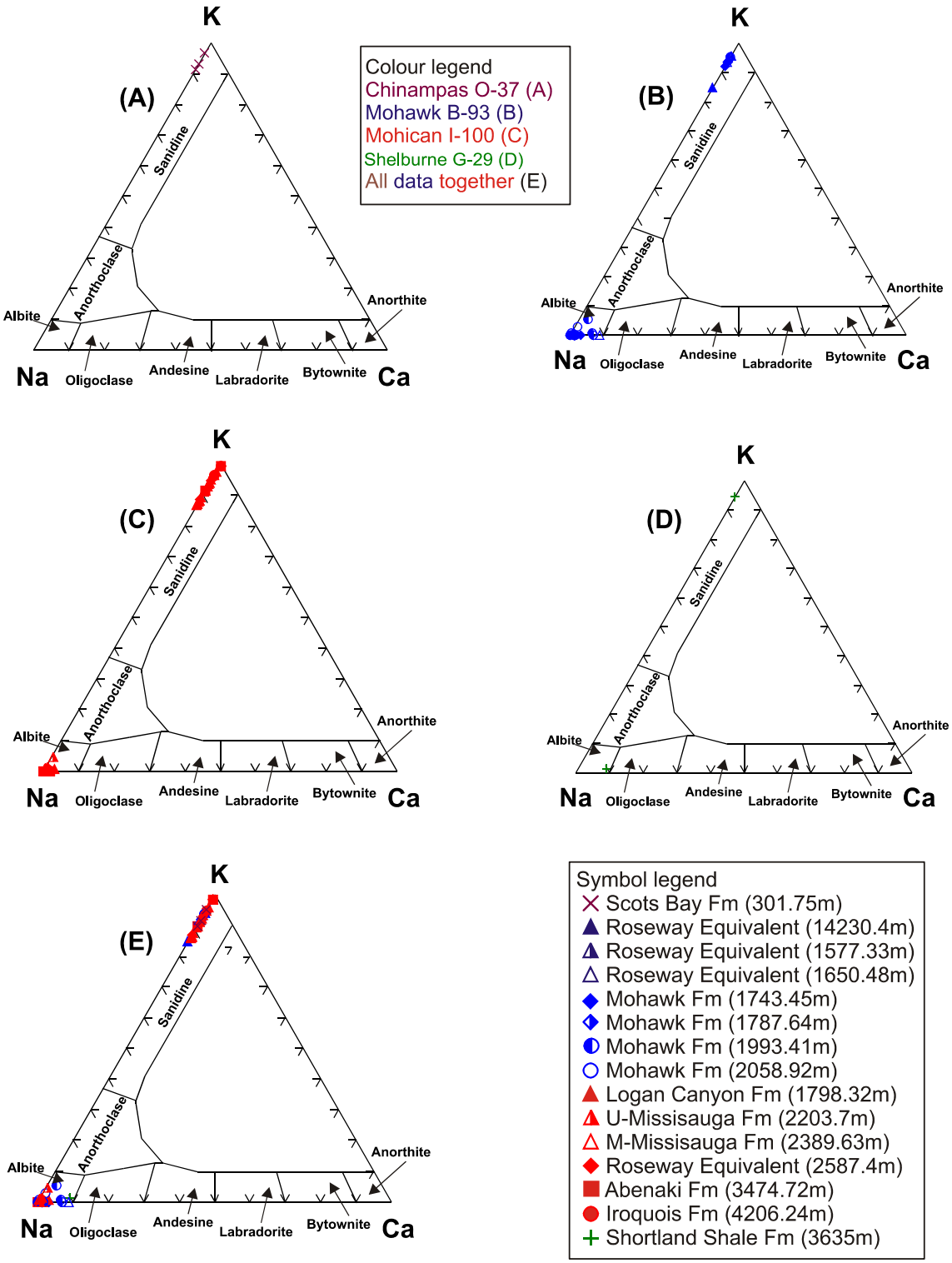

Fig.4.25: Ternary plots showing chemical variations of feldspars based on K-Na-Ca composition.

Mohawk B-93

A total of 26 grains of detrital feldspars were counted in the Middle Jurassic to Lower Cretaceous samples. Five samples were from the Roseway Equivalent Formation and 21 from Mohawk Formation. Seven grains, 2 from Roseway Equivalent Formation, 4 from Upper Jurassic strata and 1 from Middle Jurassic strata in Mohawk Formation, are K-feldspar and have chemical composition with K>90% (Fig.4.25). Exception is only 1 grain from Roseway Equivalent Formation, with K~85%. The remaining 14 grains, 2 from Roseway Equivalent Formation, 8 from Upper Jurassic strata in Mohawk Formation and 8 from Middle Jurassic strata in Mohawk Formation are 100% albite.

Mohican I-100

K-feldspar and albite are the only feldspars identified in cutting samples from Mohican I-100 (Logan Canyon, Upper and Middle Missisauga, Roseway-Equivalent, Abenaki and Iroquois formations). Both K-feldspar and albite are common in this well, present within almost each formation sampled. Exceptions are 1 sample from Roseway-Equivalent Formation at 2685.28 m depth and 1 sample from Iroquois Formation at 3852.67 m depth where no feldspar was identified.

Polished thin sections of rock slabs from conventional cores have shown that K-feldspar and albite (counted together) are the second most abundant detrital minerals, after quartz, in sedimentary rocks, especially in Middle Jurassic strata. In addition, compared to cutting samples, perthite was identified and is sub-ordinate to K-feldspar and albite.

A total of 42 feldspar grains were counted in heavy mineral separates: 24 from Lower Cretaceous sandstones (18 grains in Logan Canyon Formation, 4 grains in Upper Missisauga Formation and 2 grains in Middle Missisauga Formation), 6 grains from Upper Jurassic-Lower Cretaceous sandstones (Roseway Equivalent Formation) and 12 grains from Middle Jurassic sandstones (5 grains in Abenaki Formation and 7 grains in Iroquois Formation). From the total number of feldspar counted in this well, 23 grains from Lower Cretaceous sandstones (16 from Logan Canyon Formation, 1 from Upper Missisauga Formation and 6 from Middle Missisauga Formation), 2 grains from Upper Jurassic sandstones (Roseway Equivalent Formation) and 6 grains from Middle Jurassic sandstones (Abenaki Formation and Iroquois Formation) are K-feldspar (Fig.4.25). On the other hand the remaining 11 grains, 7 from Lower Cretaceous formations (2 from Logan Canyon, 4 from Upper and 1 from Middle Missisauga), 3 from Upper Jurassic-Lower Cretaceous Formation (Roseway Equivalent) and 1 from Middle Jurassic formations (Iroquois) are albite.

Shelburne G-29

Only two grains, one K-feldspar and one albite have been identified in Lower Cretaceous Shortland Shale Formation in Shelburne G-29 (Fig.4.25).

Summary

Important observations from figure 5.4, on feldspars from heavy mineral separates together with interpretations made on polished thin sections of conventional cores are summarized as follows:

1. K-feldspar and albite are the only end-members from the feldspar mineral group identified in mineral separates; perthite was identified only in polished thin sections of conventional cores

2. End-members of the feldspar mineral group are common in heavy mineral separates in Mohawk B-93 (26 grains in total), Mohican I-100 (42 grains) and almost absent from Chinampas O-37 (3 grains) and Shelburne G-29 (2 grains)

3. Polished thin sections of conventional cores from Mohican I-100 show and confirm that feldspar is common

4. K-feldspar is more abundant (45 grains) compared to albite (28 grains) in cutting samples

5. Lower Cretaceous Logan Canyon Formation (Mohican I-100) has the highest number of feldspar counted in mineral separates with a total of 18 grains (16 are K-feldspar and 2 are albite) whereas Shortland Shale Formation (Mohican I-100) has only two

4.3.2.3.2 Muscovite

Muscovite is absent from the polished thin sections of the heavy mineral fraction of Chinampas O-37, Mohican I-100 and Shelburne G-29. Muscovite analyses were obtained only from grains analyzed in Mohawk B-93; thus the number of detrital muscovite grains analyzed from the wells studied is low (only 10 in total). The paucity of muscovite can be related to two facts: i) during diagenetic alteration it changes into hydromuscovite, illite and/or kaolinite which usually develop along its cleavage planes making it thus difficult to obtain good quality chemical analyses, ii) is considered a

light detrital mineral and as a result is has been removed from cutting samples during heavy mineral separation. Due to limited data obtained during chemical analysis of muscovite from heavy mineral separates, chemical analyses of detrital muscovite from polished thin section of conventional cores at Mohican I-100 and Moheida P-15 have been used.

For interpretation of data collected during EDS analyses we used analyses from known sources in the literature such as the Lower Cretaceous Chaswood Formation at Vinegar Hill (New Brunswick) and Elmsvale Basin (Nova Scotia), the Lower Cretaceous formations (Logan Canyon, Upper and Middle Missisauga) at Naskapi N-30 and Venture field (Lower Missisauga Formation) as well as the Meguma Supergroup metasedimentary rocks and the Meguma Terrane granites (Fig.4.26).

The purpose was first to distinguish igneous from metamorphic muscovite and second to assess potential sources for the studied sediments based on variations in muscovite chemical composition.The total Al and total K (expressed as atomic formula units [a.f.u.] calculated on the basis of Si= 8) can be used to distinguish metamorphic from igneous muscovite (Fig.4.26). The field for metamorphic muscovite has a range in K [a.f.u] from 1.1 to 1.6, whereas K [a.f.u.] for igneous muscovite has a range from 1.6 to 2.0 (Reynolds et al., 2010).

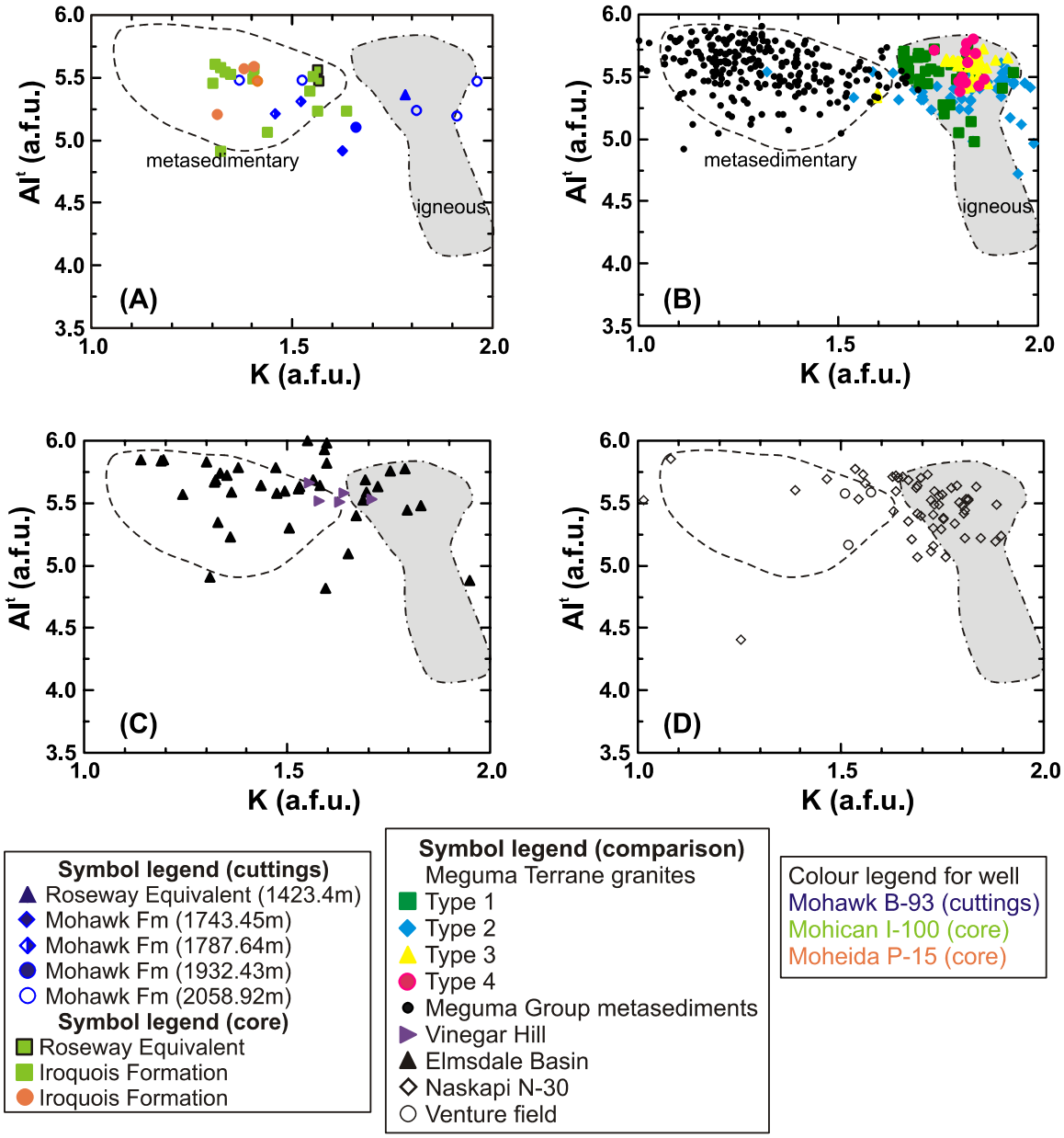

Fig.4.26: Potential source rock for muscovite from studied wells (A). (B) Meguma Terrane granites (igneous rocks), which comprise, type 1=South Mountain Batholith, type 2=Port Mouton, type 3=Eastern Meguma plutons (primary muscovite), type 4=Eastern Meguma plutons (secondary plutons) and Meguma Supergroup metasedimentary rocks. The igneous and metasedimentary fields for the Meguma terrane rocks (igneous and metamorphic) are from Reynolds et al. (2010) C) Lower Cretaceous Formation at Vinegar Hill and Elmsvale Basin (data taken from Pe-Piper et al. 2004a; 2004b; Pe-Piper and Piper, 2007) D) Previous dated offshore Cretaceous muscovites Naskapi N-30, Venture field (data taken from Reynolds et al. (2009).

Chinampas O-37

No muscovite was found in samples from this well.

Mohawk B-93

From the total of 10 detrital muscovite analyses obtained from heavy mineral separates, 4 plotted in the metamorphic field, 4 in the igneous field and 2 do not belong to either category. Mohawk B-93 has muscovite in both formations that were studied and sampled, Roseway Equivalent (Lower Cretaceous) and Mohawk (Upper Jurassic and Middle Jurassic). Muscovite in Roseway Equivalent Formation is 100% igneous and is represented by only 1 grain. On the other hand Mohawk Formation has both metamorphic (2 grains in Upper Jurassic and 2 grains in Middle Jurassic) and igneous muscovite (3 grains in Middle Jurassic).

Consideration of observations made from the discrimination diagram in figure 4.26, shows that 1 muscovite from Roseway Equivalent Formation (Lower Cretaceous) and 3 from Mohawk Formation (Middle Jurassic) have a similar composition as muscovite from both the Meguma Terrane granites (South Mountain Batholith) and the Lower Cretaceous formations at Naskapi N-30. Al^{t}-Fe^{2+}-Mg ternary plot (Fig.4.27) shows that muscovite from Mohawk Formation (Upper Jurassic and Middle Jurassic) tend to be depleted in Mg and enriched in Fe^{2+}.

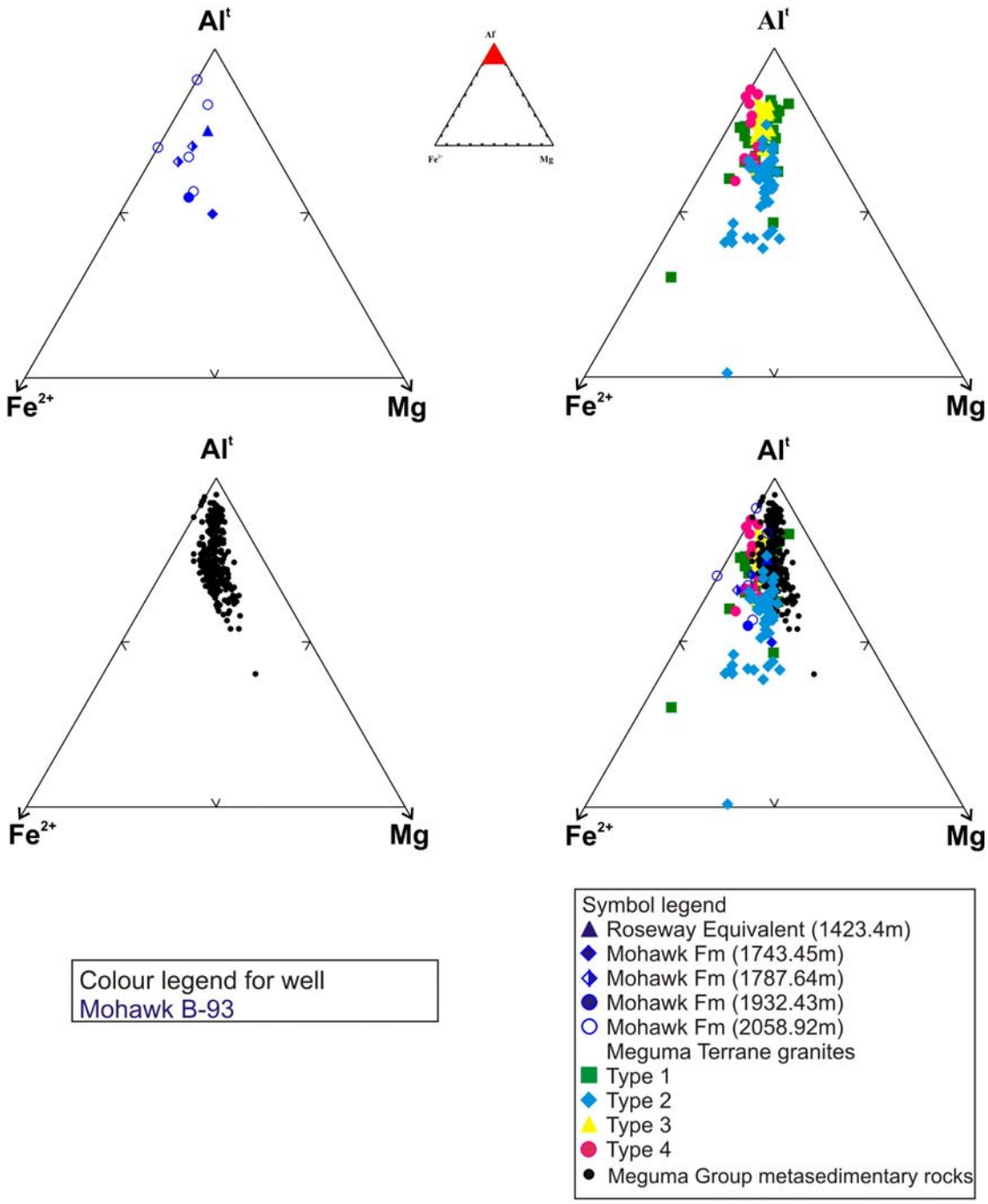

Fig.4.27: Al^t-Fe_t-Mg ternary plot of muscovite from studied wells in comparison with muscovite from Meguma terrane. A) Mohawk B-93 offshore well, B) Meguma Terrane granites (igneous rocks), which comprise type 1=South Mountain Batholith, type 2=Port Mouton, type 3=Eastern Meguma plutons (primary muscovite), type 4=Eastern Meguma plutons (secondary plutons), C) Meguma Group metasedimentary rocks, D) comparison of data from Mohawk B-93 with data from Meguma terrane rocks.

Mohican I-100

Polished thin sections at Mohican I-100 were made from core slabs representing the Roseway Equivalent, the Mohican and the Iroquois ormations. Muscovite analyses are available only for Roseway Equivalent and Iroquois formations. Almost all analyses (15) plot in the field that represents metamorphic muscovite as is the case for metasedimentary rocks of the Meguma terrane and the sedimentary rocks at Elmsvale Basin and Venture field (Fig.4.26). Exceptions are 2 analyses that plot outside the boundaries of the field.

All muscovite chemical analyses for this well were obtained from framework grains that are principal components of sedimentary rocks. However, detrital muscovite was also identified as inclusions in both detrital quartz and detrital ilmenite. The accurate chemical composition for muscovite inclusions was not determined, because contamination occurred during EDS analyses as a result of their small size.

Moheida P-15

Three formations, Roseway Equivalent, Abenaki and Iroquois were sampled for polished thin sections. Iroquois is the only formation to have chemical analyses of detrital muscovite. In total 4 grains were identified as muscovite. All analyses (4) plot in the field that represents muscovite of metamorphic origin (Fig.4.26).

Shelburne G-29

No muscovite was found in samples from this well.

Summary

1. Detrital muscovite in mineral separates from Mohawk B-93 is almost absent; muscovite analyses are abundant in polished thin sections of rock slabs at Mohican I-100 and rare at Moheida P-15

2. Analyses from Mohican I-100 and Moheida P-15 represent only metamorphic muscovite

3. Muscovite at Mohawk B-93 is both metamorphic and igneous

4. Chemical analyses of muscovite from polished thin sections are similar to those from the Meguma Supergroup metasediments and those at Venture field and Chaswood Formation at Elmsvale Basin

5. Chemical analyses of muscovite from heavy mineral separates are similar to those from both the Meguma Supergroup metasediments and Meguma Terrane granites

4.3.2.3.3 Biotite

Available organized data in the literature regarding biotite chemistry from potential rock sources around the Scotian Basin are restricted. Biotite data in this study were compared with analyses from one onshore potential source, the Port Mouton Pluton of the Meguma Terrane granites as well as with biotite analyses from Lower Cretaceous formations at Naskapi N-30 (Fig.4.28). The interpretation was made in terms of chemical variations in biotite based on TiO_2 vs Al_2O_3 and A^{IIV} vs Fe/(Fe+Mg) discrimination diagram (Fig.4.29). Data in figure 4.30E from Fleet (2003) was used for interpretation of chemical variations in biotite regarding potential rock type sources (metamorphic, igneous and peraluminous igneous rocks). For further discrimination of

igneous biotite, the MgO-FeO-Al_2O_3 ternary plot was used showing potential rock sources such as alkali, calcalkali and peraluminous igneous rocks (Fig.4.31).

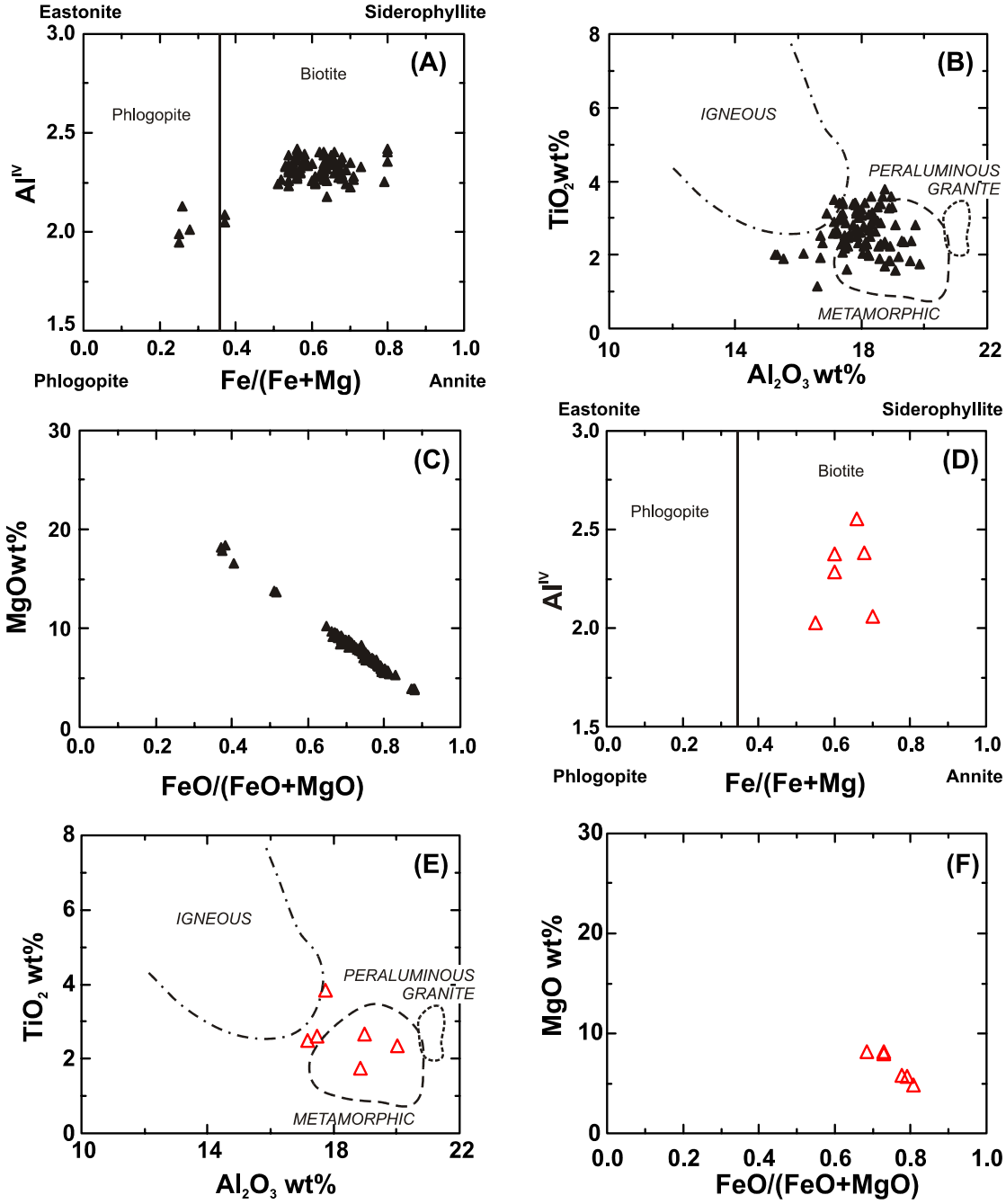

Fig.4.28: Biotite analyses from the Port Mouton Pluton (A,B,C) (Douma, 1988) and Naskapi N-30 (D,E,F) (Pe-Piper et al., 2009), A)&D) Chemical variations in biotite and phlogopite based on Al^{IV} vs Fe/(Fe+Mg), nomenclature from Deer et al. (1992), B)&E) Chemical variations in biotite showing potential rock type sources for biotite, the data for the distinctive fields (igneous, metamorphic and peraluminous) are from Fleet (2003), C)&F) Chemical variations in biotite based on MgO wt% vs FeO/(FeO+MgO).

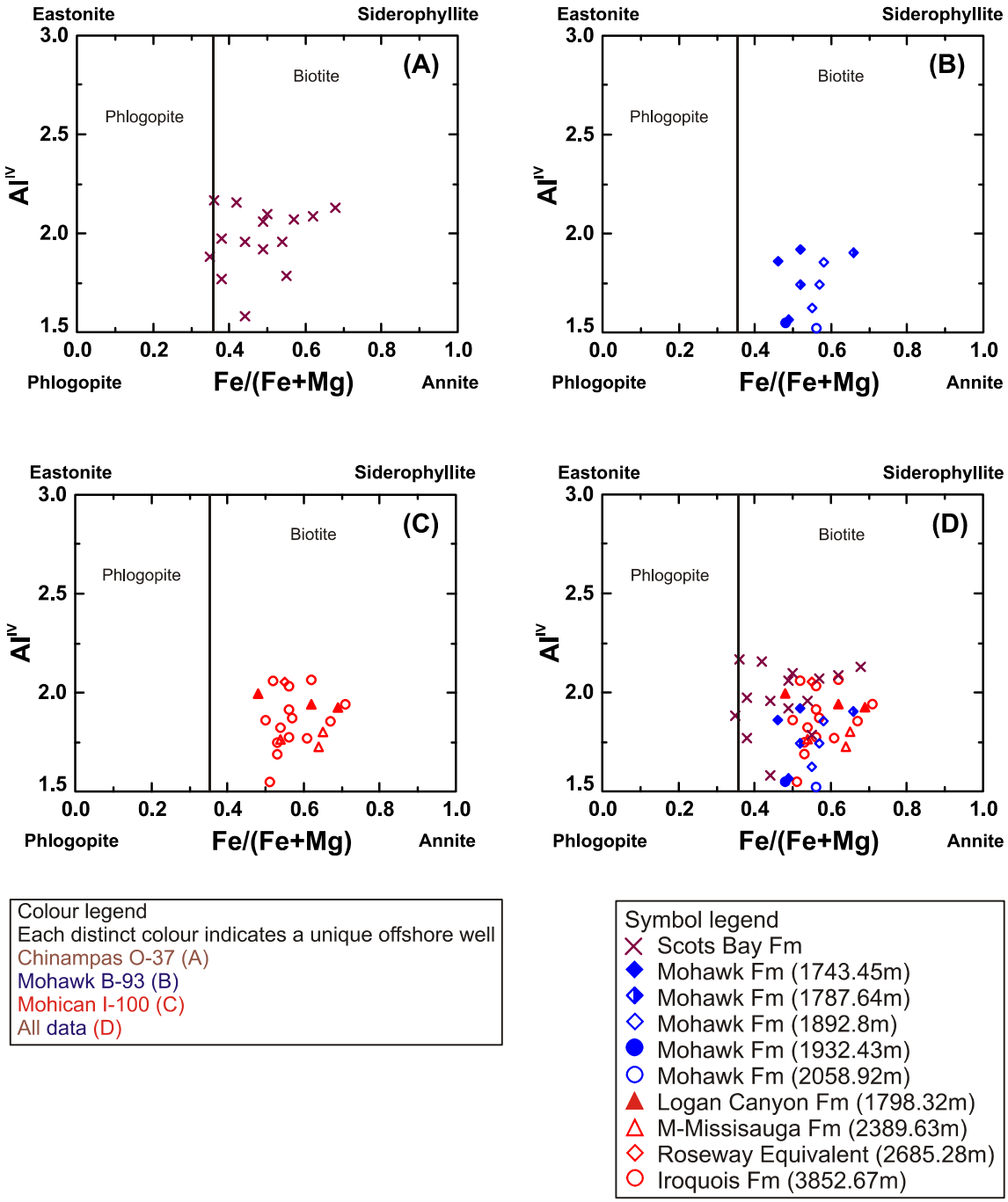

Fig.4.29: Chemical variations in biotite and phlogopite based on Al^{IV} vs Fe/(Fe+Mg). Nomenclature from Deer et al. (1992).

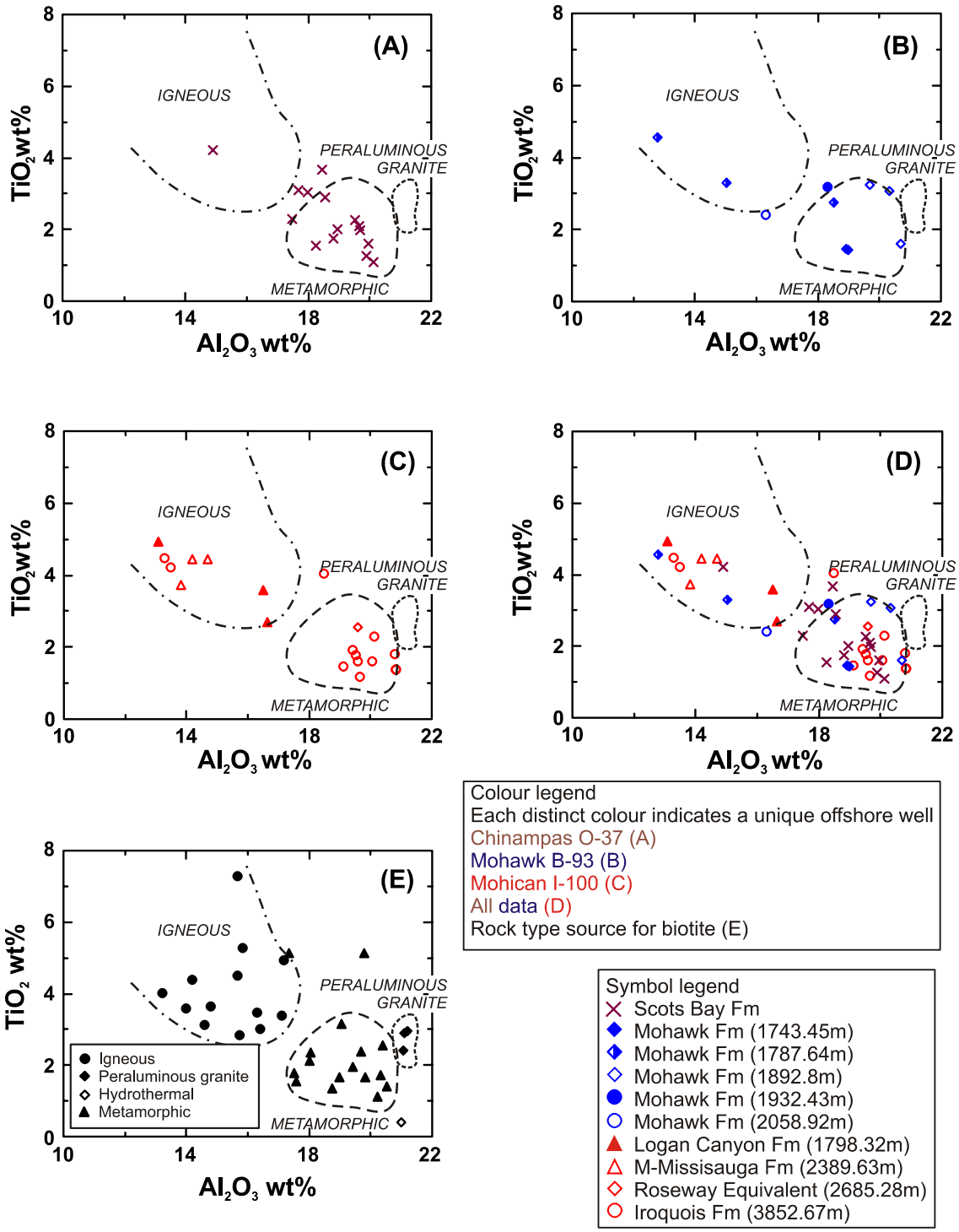

Fig.4.30: Chemical variations in biotite showing potential rock type sources for biotite. The data in E are from Fleet (2003) and fields based on this data are shown in A, B, C and D.

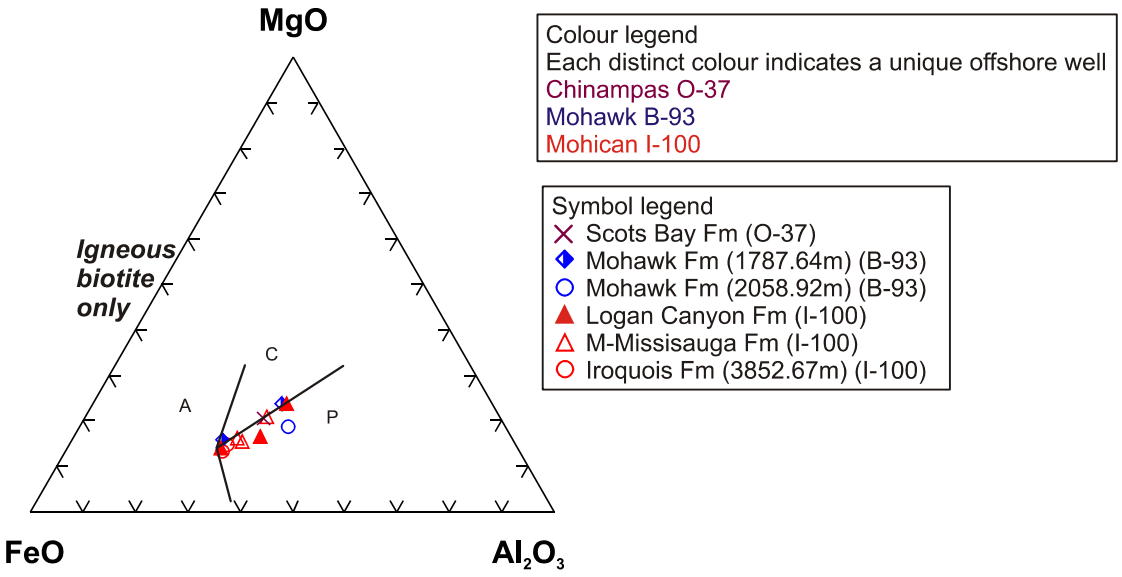

Fig.4.31: Fields showing chemical discrimination of igneous biotite based on data taken from Abdel Rahmen (1994); A=alkali, C=calcalkali, P=peraluminous.

Chinampas O-37

Most of the analyses from Scots Bay Formation are biotite and only two analyses have chemical composition biotite/phlogopite (Fig.4.29 A). Biotite from Chinampas O-37 is mostly of metamorphic origin (13 grains from 18 in total) and only 1 grain is of igneous origin (Fig.4.30 A). Four grains were plotted in the gap between the fields that represent igneous and metamorphic biotite. The igneous biotite plots on the boundary between calcalkali and peraluminous sources (Fig.4.31). The analyzed biotites show a linear correlation between MgO and FeO/(FeO+MgO) (Fig.4.32). Biotite at both Port Mouton Pluton and Naskapi N-30 has different chemical composition to biotite from this well (Fig.4.28).

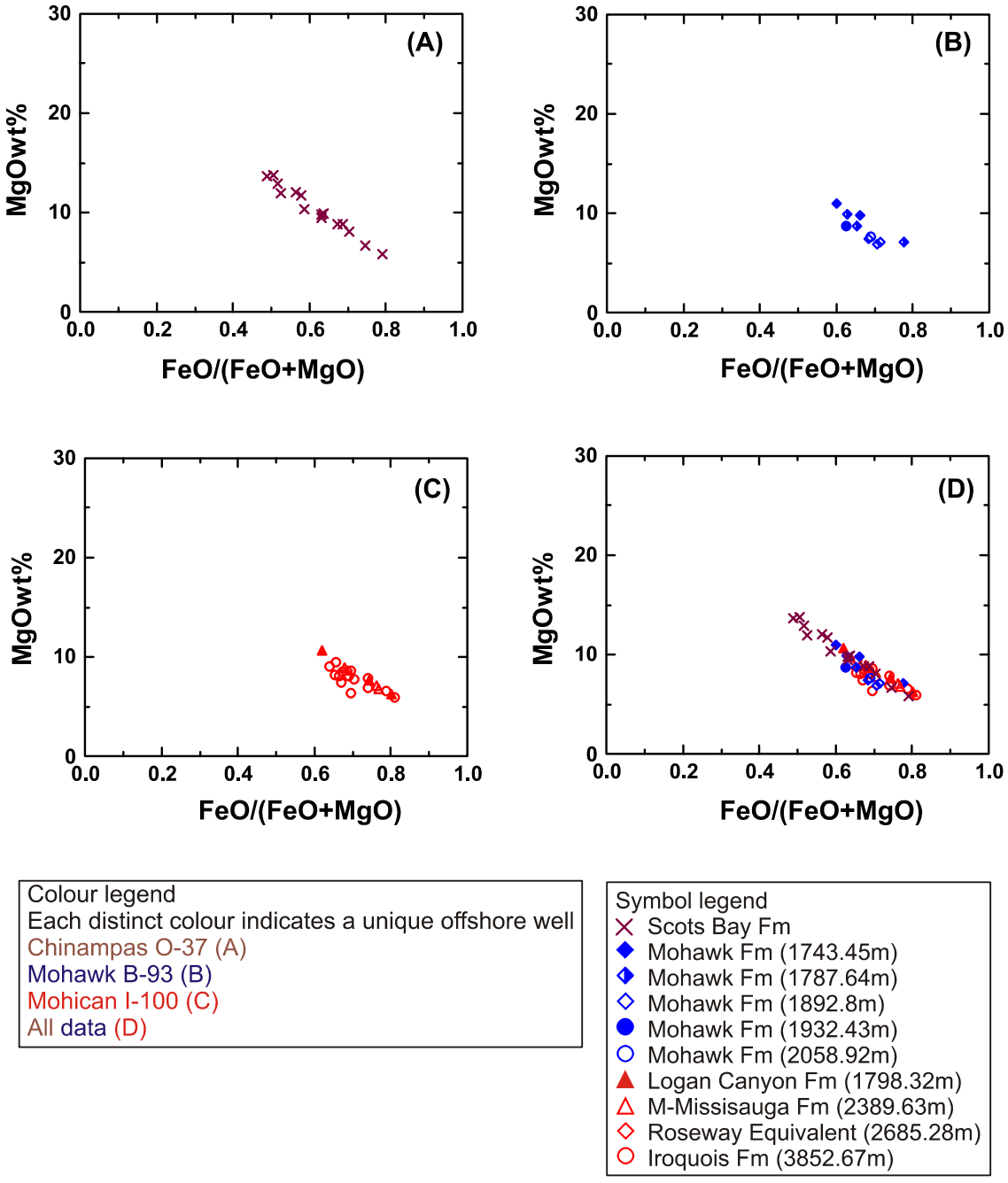

Fig.4.32: Chemical variations in biotite based on MgO wt% vs FeO/(FeO+MgO).

Mohawk B-93

Two formations, Roseway Equivalent and Mohawk, have been sampled and analyzed for detrital biotite. No detrital biotite has been identified in any of the samples collected from Roseway Equivalent Formation. On the other hand, detrital biotite was

found in samples from Mohawk Formation at different depths representing different ages. The majority of biotite (8 grains from 10) is from the Upper Jurassic samples of Mohawk Formation and it is of metamorphic origin (6 of 8) (Fig.4.30 B). The remaining two grains are of igneous origin. Two biotite grains have also been identified in Middle Jurassic sandstones (Mohawk Formation) and plot in the space between the igneous and metamorphic fields. From the igneous biotite of the Mohawk Formation (Upper Jurassic), one analysis plots onto the boundary between calcalkali and peraluminous rock discrimination diagram and one plot onto the field that represents 100% biotite from peraluminous rocks (Fig.4.31). Biotite at Port Mouton Pluton and Naskapi N-30 show different chemical differentiation composition to biotite from this well (Fig.4.28).

Mohican I-100

No biotite was identified in samples from Upper Missisauga and Abenaki formations. Biotite is abundant in Iroquois Formation, 11 grains from the total of 19 analyzed in the well. Logan Canyon and Middle Missisauga formations share the same number of grains, 3, whereas Roseway Equivalent Formation has only 1 grain. One grain from Iroquois Formation does not belong to any of the biotite fields created in figure 4.30 for biotite discrimination.

From the binary discrimination plot in figure 4.30 C, it can be observed that biotite in the Iroquois Formation has an origin from both metamorphic (9 grains) and igneous rocks (2 grains). Biotite from Lower Cretaceous sandstones is 100% of igneous origin with 3 grains in each of the Logan Canyon and Middle Missisauga formations. The

igneous biotite in Mohican I-100 can be alkali, calcalkali and peraluminous (Fig.4.31). No correlation was made between biotite at Mohican and that from Naskapi N-30 and Port Mouton Pluton.

Shelburne G-29

No biotite was identified in Shelburne G-29 well.

Summary

1. Biotite has been identified in 3 of the 4 wells studied: 2 of the wells are from the SW Scotian Basin (Mohawk B-93 and Mohican I-100) and 1 from Fundy Basin (Chinampas O-37); no biotite was identified in Shelburne G-29 (SW Scotian Basin)
2. Overall in all the wells studied the most abundant biotite type is of metamorphic origin
3. Biotite of igneous origin is present in Mohawk B-93, 2 grains in Mohawk Formation (Upper Jurassic) and Mohican I-100, 6 grains in Lower Cretaceous strata (3 in Logan Canyon Formation and 3 grains in Middle Missisauga Formation) and 2 grains in Middle Jurassic sandstones (Iroquois Formation)
4. Both the Port Mouton Pluton and the Naskapi N-30 offshore well have biotite with different chemical composition compared to biotite found in the studied wells

4.3.2.3.4 Chlorite

The chemistry of chlorite from Chinampas O-37, Mohawk B-93, Mohican I-100 and Shelburne G-29 offshore wells, has been studied using EDS analyses. Chlorite is a

mineral that can form under a wide range of pressure and temperature; hence it is difficult to distinguish detrital from diagenetic chlorite. The purpose of determining chemical composition of chlorite was to try to discriminate chemically detrital from diagenetic chlorite. Detrital chlorite occurs in metamorphic rocks and hydrothermal rocks. Diagenetic chlorite may originate through alteration of mafic minerals (pyroxene, amphibole, biotite etc.) in igneous rocks or through diagenesis in sedimentary rocks. Data from studied wells was compiled using only good chlorite analyses (those not containing more than 1 wt% of CaO, TiO_2, K_2O or Na_2O). For the discrimination between diagenetic and detrital chlorite we used a series of suitable diagrams as demonstrated by Pe-Piper and Weir-Murphy (2008) and Sedge (2015).

Data from the literature regarding chlorite analyses from onshore potential sources is restricted. Chlorite chemistry from the wells studied were compared only with chlorite from the Meguma Supergroup metasediments (personal communication with Dr. Chris White) and from the Venture field of the Scotian Basin (Gould, 2007). A total of four distinctive chlorite types have been discriminated by Gould (2007) which are: type 1= chlorite rims, type 2= from expanded mica, type 3= pore filling and type 4= grain replacement. The MgO vs. SiO_2 (Fig.4.33) and the FeO^t/Mg vs SiO_2 (Fig.4.34) were used first for discrimination of metamorphic and diagenetic chlorite based on weight percent of SiO_2 in the chemical composition. Chlorite with chemical composition >30 wt% SiO_2 is characterized as diagenetic, whereas chlorite with <30% SiO_2 is considered detrital (Sedge, 2015). The FeO^t/MgO vs. MgO (Fig.4.35) diagram was used to show differences between diagenetic and detrital chlorite regarding chemical differentiation of Mg and Fe. In addition, the FeO^t/MgO vs. SiO_2/Al_2O_3

discrimination diagram by Pe-Piper and Weir-Murphy (2008) (Fig.4.36a, b) was plotted with fields for diagenetic, metamorphic (detrital), and igneous (detrital) types of chlorite. To improve the diagram, which used chlorite analyses from Cretaceous rocks from the Orpheus Graben (Weir-Murphy, 2004), we added a new field that represents diagenetic chlorite based on chemical analyses obtained from diagenetic chlorite from sandstone samples of the Venture field (Fig.4.36a, b). In this work chlorite nomenclature is after Hey (1954) (Fig.4.37a, b).

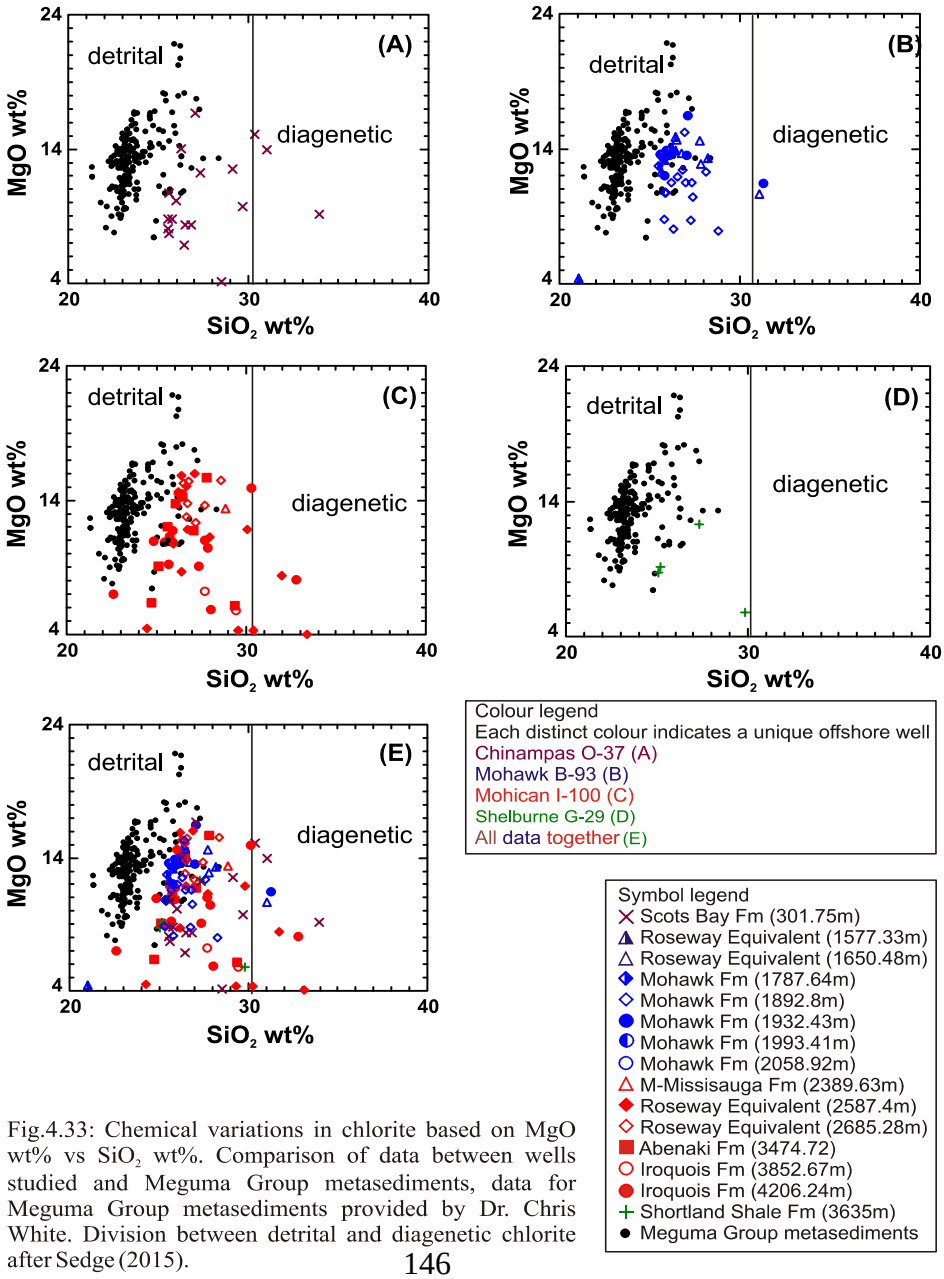

Fig.4.33: Chemical variations in chlorite based on MgO wt% vs SiO_2 wt%. Comparison of data between wells studied and Meguma Group metasediments, data for Meguma Group metasediments provided by Dr. Chris White. Division between detrital and diagenetic chlorite after Sedge (2015).

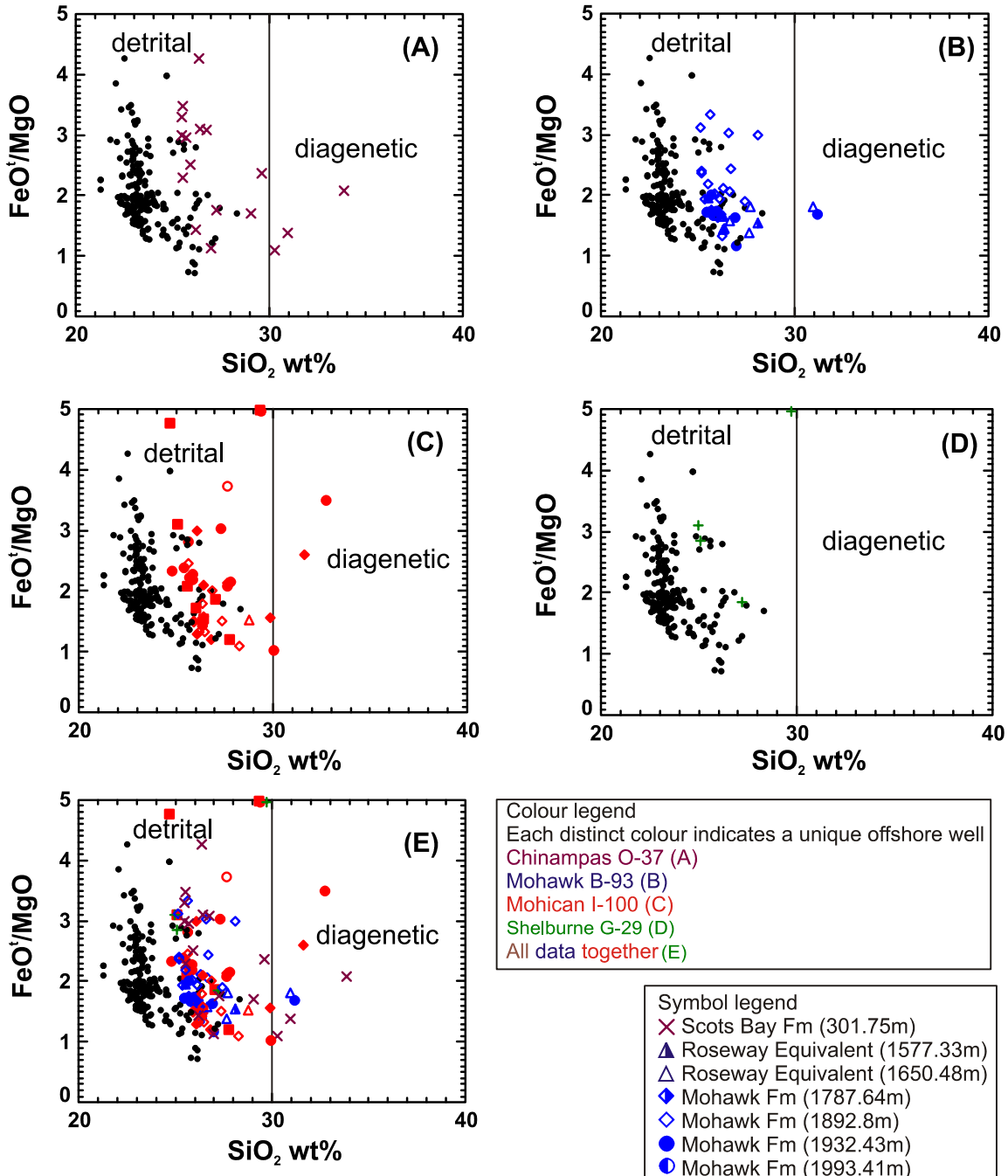

Fig.4.34: Chemical variations in chlorite based on FeOt/MgO wt% vs SiO_2 wt%. Comparison of data between wells studied and Meguma Group metasediments, data for Meguma Group metasediments provided by Dr. Chris White.Division between detrital and diagenetic chlorite after Sedge (2015).

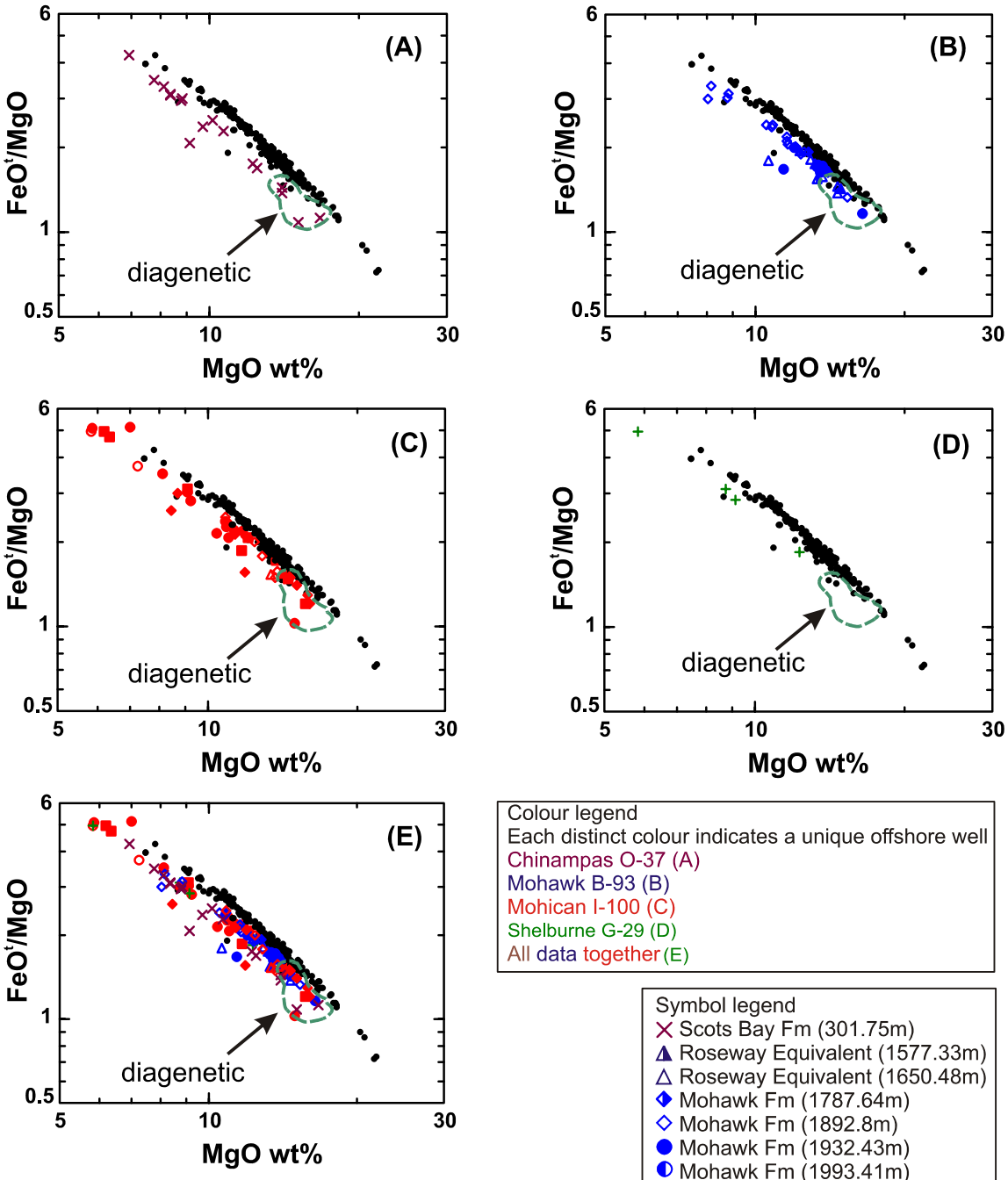

Fig.4.35: Chemical variations in chlorite based on FeO^t/MgO vs MgO wt%. Comparison of data between wells studied and Meguma Group metasediments, data for Meguma Group metasediments provided by Dr. Chris White. Diagenetic chlorite field after Sedge (2015).

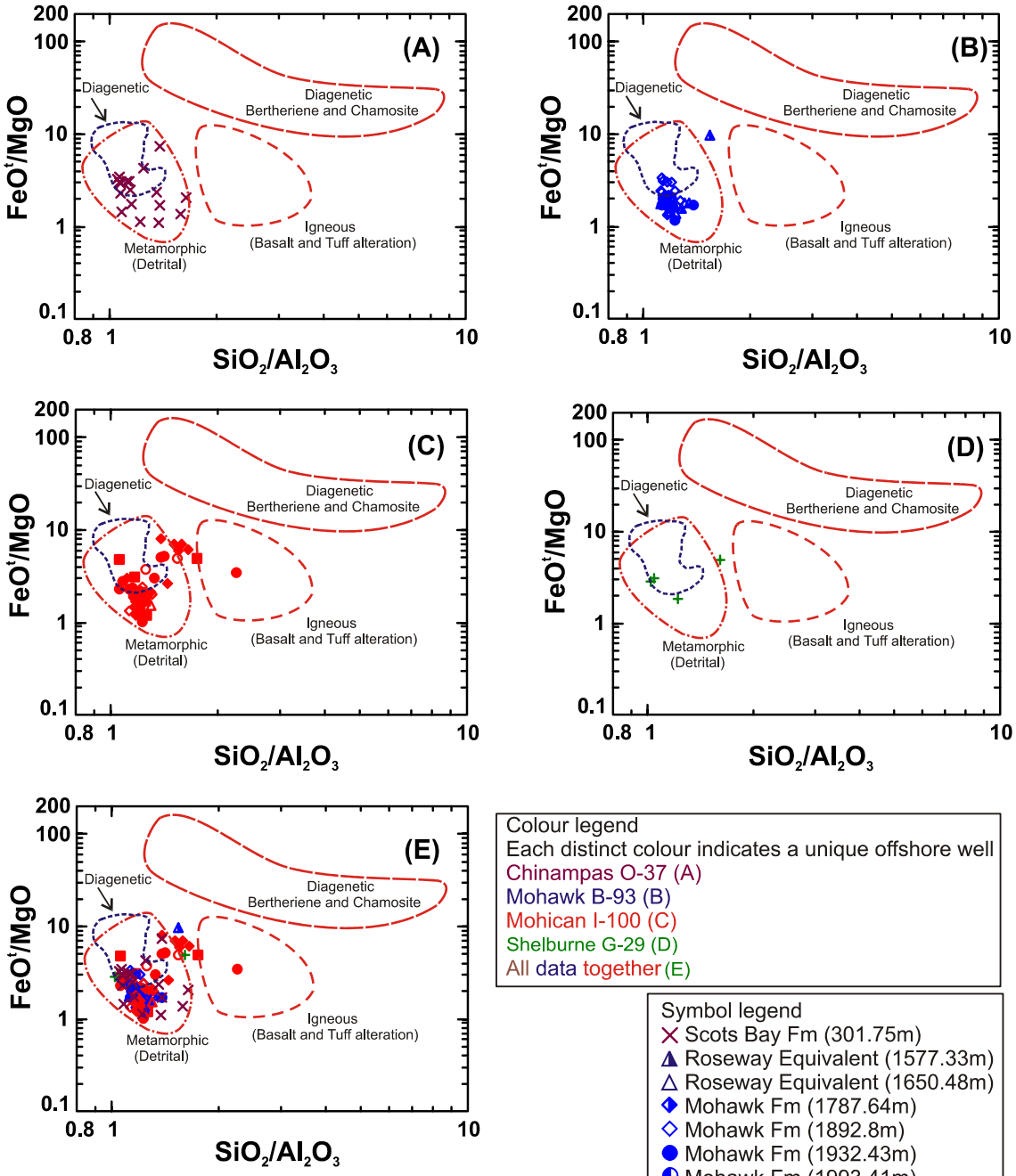

Fig.4.36a: FeO^t/MgO vs SiO_2/Al_2O_3 discrimination diagram of chlorite from studied wells. FeO^t/MgO vs SiO_2/Al_2O_3 discrimination diagram of chlorite from Weir-Murphy (2004). The discrimination fields have been plotted using chlorite analyses from the Cretaceous rocks from Orpheus Graben (Pe-Piper & Weir-Murphy, 2008). Diagenetic chlorite field after Sedge (2015).

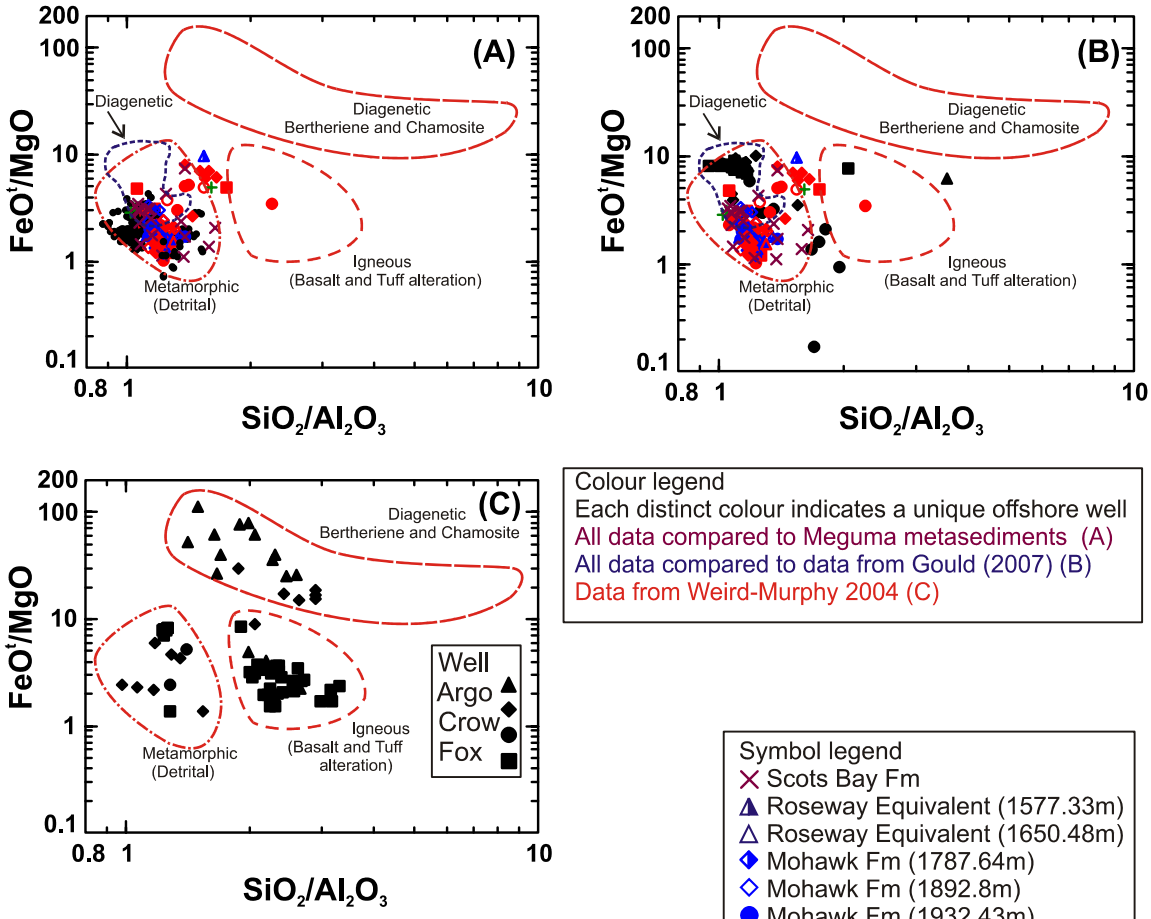

Fig.4.36b: A) FeO^t/MgO vs SiO_2/Al_2O_3 chlorite discrimination diagram for wells studied and Meguma Group metasediments. B) FeO^t/MgO vs SiO_2/Al_2O_3 chlorite discrimination diagram for wells studied and different types of chlorite as mentioned by Gould (2007) : type 1=chlorite rims, type 2=expanded mica, type 3=pore filling and type 4=grain replacement. C) FeO^t/MgO vs SiO_2/Al_2O_3 discrimination diagram of chlorite from Weir-Murphy (2004). The discrimination fields have been plotted using chlorite analyses from the Cretaceous rocks from Orpheus Graben (Pe-Piper & Weir-Murphy, 2008).

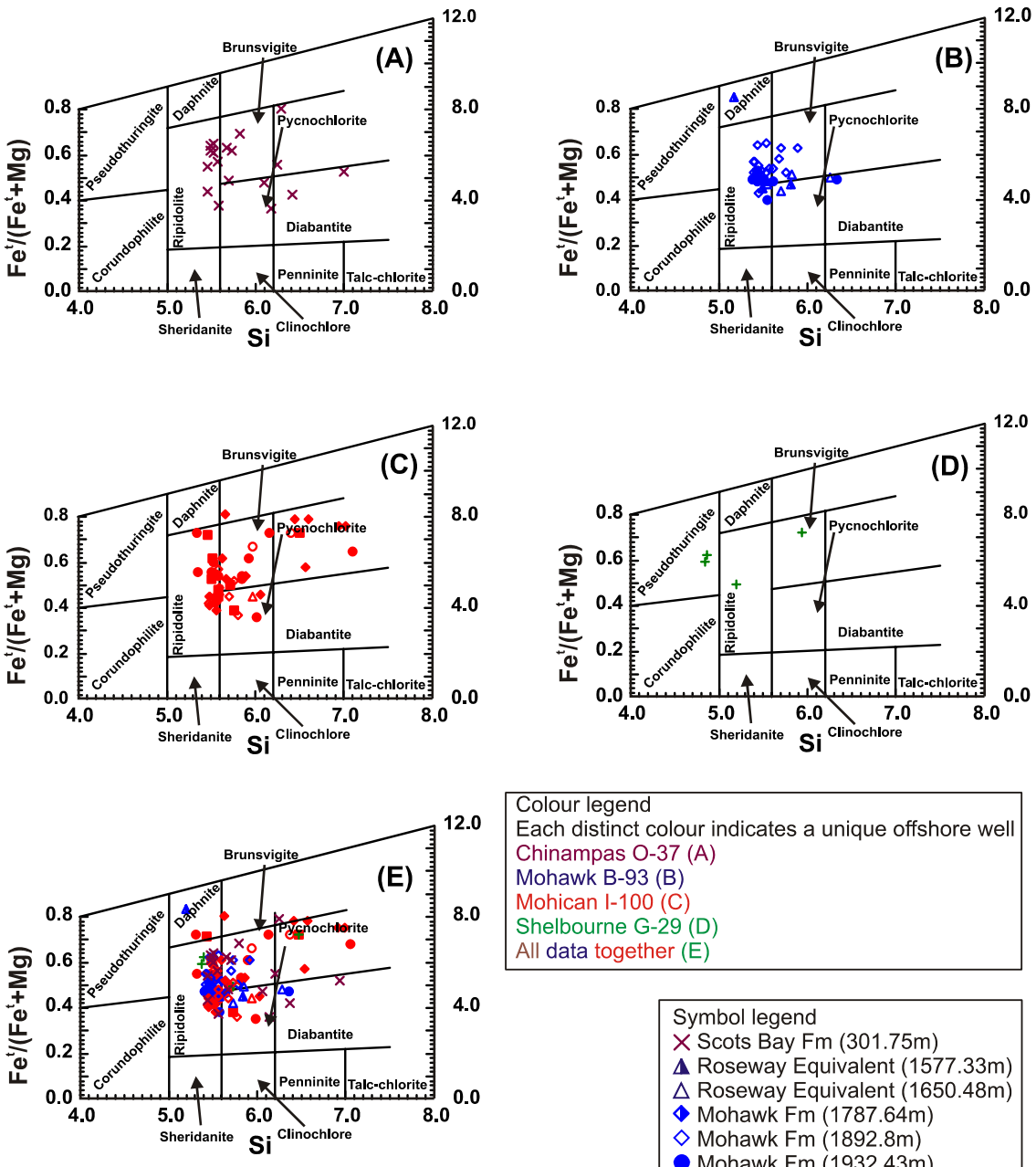

Fig.4.37a: Chlorite nomenclature diagrams for wells studied based on the system of Hey (1954).

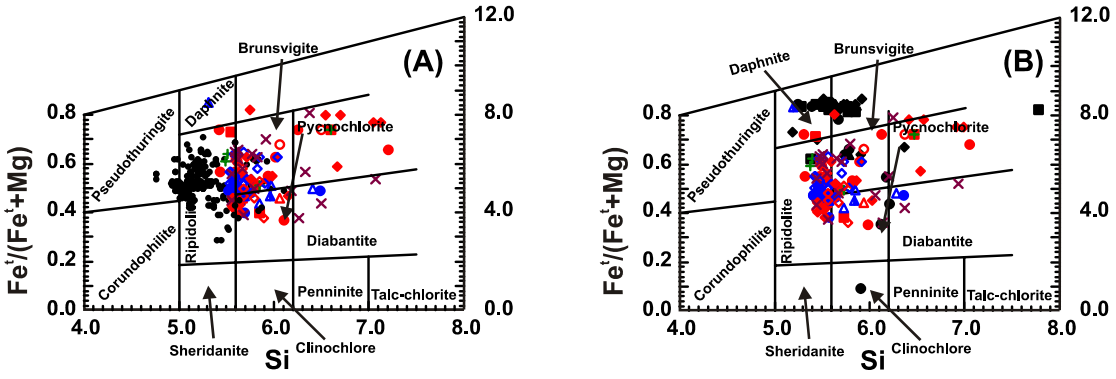

Symbol legend
- Scots Bay Fm
- Roseway Equivalent (1577.33m)
- Roseway Equivalent (1650.48m)
- Mohawk Fm (1787.64m)
- Mohawk Fm (1892.8m)
- Mohawk Fm (1932.43m)
- Mohawk Fm (1993.41m)
- Mohawk Fm (2058.92m)
- M-Missisauga Fm (2389.63m)
- Roseway Equivalent (2587.4m)
- Roseway Equivalent (2685.28m)
- Abenaki Fm (3474.72m)
- Iroquois Fm (3852.67m)
- Iroquois Fm (4206.24m)
- Shortland Shale Fm (3635m)

Meguma Terrane (Metamorphic rocks)
- Meguma Group metasediments

Meguma Terrane (Igneous rocks)
Gould, 2007
- Type 1
- Type 2
- Type 3
- Type 4

Colour legend
Each distinct colour indicates a unique offshore well
All data compared to Meguma metasediments (A)
All data compared to data from Gould (2007) (B)

Fig.4.37b: Chlorite nomenclature diagrams for wells studied based on the system of Hey (1954), with comparison to Meguma Group metasediments (A) and Gould (2007) (B), where Type 1=chlorite rims, Type 2=expanded mica, Type 3=pore filling, and Type 4=grain replacement.

Chinampas O-37

The only formation sampled for detrital chlorite in this well is Scots Bay (Lower Jurassic). Chlorite is a common mineral in Chinampas O-37. Three analyses from the total of 18 plot as diagenetic chlorite and the rest plot as detrital (Figs.4.33, 4.34). Based on discrimination diagram by Pe-Piper and Weir-Murphy (2008) most of the analyses obtained plot onto the field with the lowest ratio between FeO^t/MgO and SiO_2/Al_2O_3 (Fig.4.36a A), which represents detrital metamorphic chlorite. However,

almost half (7 of 18 grains) of the chlorite analyses plot in the new field that represents what we consider chlorite of diagenetic origin.

At least three different types of chlorite have been distinguished based on their chemical composition. The most abundant type of chlorite is ripidolite (8 grains from the total of 18) (Fig.4.37a A). Four grains were identified as brunsvigite, whereas pycnochlorite and diabanite are represented by 2 grains each. Two analyses do not belong to any of the chlorite types, based on the system suggested by Hey (1954) (Fig.4.37a A).

Compared to chlorite analyses from Meguma Supergroup metasedimentary rocks, diagenetic chlorite from Chinampas O-37 generally has higher percentage of SiO_2 (Figs.4.33 A, 4.34A) and almost the same percentage of MgO (Fig.4.35 A).

Mohawk B-93

The chemistry of chlorite from both the Roseway Equivalent Formation (Lower Cretaceous) and Mohawk Formation (Upper Jurassic and Middle Jurassic) have been studied. Chlorite is abundant with a total of 37 grains analyzed.

All chlorite grains, except 2, plot as detrital in the diagrams from figures 4.33 B and 4.34 B. In addition, almost all analyses plot in the metamorphic (detrital) field produced by Pe-Piper and Weir-Murphy (2008). Exception are 7 grains, all from Mohawk Formation (Upper Jurassic) that plot in the new field created by us representing diagenetic chlorite (Fig.4.35a B).

Chlorite in Mohawk B-93 is represented by different types which are based on chemical composition ripidolite, brunsvigite, daphnite, diabanite and pycnochlorite

(Fig.4.37a B). Ripidolite is the most abundant chlorite type (23 grains from 37) and it is found in both Roseway Equivalent (Lower Cretaceous) and Mohawk (Upper Jurassic and Middle Jurassic) Formation. Brunsvigite is the second most abundant chlorite type with 5 grains restricted to the Mohawk Formation (Upper Jurassic). Pycnochlorite (Roseway Equivalent) and diabanite (Roseway Equivalent and Mohawk-Middle Jurassic) are represented by 2 grains each and 1 grain is daphnite (Roseway Equivalent).

Compared to chlorite analyses from Meguma Supergroup metasediments, diagenetic chlorite from Mohawk B-93 has a higher percentage of SiO_2 (Figs.4.33 B, 4.34 B) and almost the same percentage of MgO (Fig.4.35 B).

Mohican I-100

Chlorite is abundant in Mohican I-100 and can be observed in Lower Cretaceous to Middle Jurassic formations (Logan Canyon, Upper and Middle Missisauga, Roseway Equivalent, Abenaki, Iroquois).

Based on MgO vs SiO_2 and FeO/MgO vs SiO_2 diagrams, only 3 grains from the total of 48 are diagenetic (Figs.4.33 C, 4.34 C). The majority of chlorite grains analyzed plot as metamorphic (detrital) in the field of Pe-Piper and Weir-Murphy (2008) with exception one grain that was plotted in the field that represents igneous chlorite (Fig.4.35a C). Eleven chlorite analyses plot in the new field for diagenetic chlorite. Lower Cretaceous chlorites are concentrated only in the metamorphic (detrital) field. On the other hand chlorite from Upper Jurassic and Middle Jurassic sandstones tends to concentrate in both the detrital field (created with data from Orpheus Graben chlorites)

and the new diagenetic field (produced after chlorites from the Venture field).

The chlorites analyzed classify as ripidolite, pycnochlorite and brunsvigite (Fig.4.37a C). The most abundant chlorite type identified is ripidolite (25 grains from a total of 48) with analyses from all the Mesozoic formations. Brunsvigite and pycnochlorite are common chlorite types in Mohican I-100 with 10 and 6 grains respectively, present from Lower Cretaceous to Middle Jurrasic.

In general, chlorites from Mohican I-100 have higher percentage of SiO_2 and lower or similar MgO as the chlorites from Meguma Supergroup metasediments (Figs.4.33 C, 4.34 C).

Shelburne G-29

Chlorite is almost absent from Shelburne G-29, with only 4 analyses available. Three grains are detrital according to diagrams in figures, 4.33 D, 4.34 D, 4.35a D and 1 analysis plotted outside the discrimination fields.

Three distinctive types of chlorite have been identified, pseudothuringite, ripidolite and brunsvigite (Fig.4.37a D). Two grains are pseudothuringite, 1 grain is ripidolite and 1 grain is brunsvigite.

Summary

1. Chlorite in present in all the wells studied in the SW Scotian Basin
2. 6 different types of chlorite have been identified based on their chemical composition: ripidolite, brunsvigite, daphnite, pseudothuringite, pycnochlorite and diabanite

3. Ripidolite is the most abundant chlorite type found in the SW Scotian Basin and it is present in Lower Cretaceous, Upper Jurassic and Middle Jurassic sandstones from Chinampas O-37, Mohawk B-93, Mohican I-100 and Shelburne G-29

4. Most of the chlorite grains analyzed are metamorphic (detrital); diagenetic chlorite is rare in each of the wells studied: Chinampas O-37 (8 grains from 17), Mohawk B-93 (7 from 35) Mohican I-100 (11 from 45) and Shelburne G-29 (1 grain from 4)

5. All chlorite analyses show a higher percentage of SiO_2 and lower or equal percentage of MgO compared to chlorite analyses from Meguma Supergroup metasediments

4.3.2.4 Rare high stability group detrital minerals

4.3.2.4.1 Spinel/Chromite

Spinel/chromite is a common detrital mineral in Lower Cretaceous sandstones from the Scotian Basin, specifically in the central part (Pe-Piper et al., 2009). Although spinels/chromites have not been widely used in work related to sedimentary provenance, they can provide significant information due to their advantages which are the same as for garnet: i) relatively stable during diagenetic processes ii) wide chemical compositional range that can be correlated to particular rock lithologies and tectonic environments. However, there is one distinctive characteristic that make spinels/chromites more useful in assesing potential sources for sediments when compared to garnets: spinels/chromites do not dissolve nor disappear with increase in depth as is the case for specific types of garnet. On the other hand because

spinels/chromites are insensitive to weathering and to diagenetic factors that influence sediments during transportation, deposition and after burial, there is a lack of evidence of surface corrosion, they are better preserved, and therefore are more likely to be polycyclic.

The elements used for chromite discrimination are: Cr, Al, Fe^{3+}. Combinations between these parameters have led previous researchers to produce several discrimination diagrams for spinels/chromites. For work that is related to provenance of sediments, we used 2 discrimination diagrams: one for classification of spinels/chromites based on variations in their chemical composition, after Stevens (1944) and one for potential sources after Pearce et al. (2000).

Chinampas O-37

No detrital spinels/chromites have been identified in cutting samples from this well.

Mohawk B-93

Two formations from this well, Roseway Equivalent (Lower Cretaceous) and Mohawk (Upper Jurassic and Middle Jurassic) were sampled for detrital heavy minerals. Only Middle Jurassic Mohawk samples contain detrital spinels/chromites at a depth of 1932.43 m. One grain has been identified as spinel/chromite from the total of 271 detrital heavy mineral grains, and based on the classification diagram proposed by Stevens (1944) plots as Cr-spinel (Fig.4.38 A). Regarding sedimentary provenance and origin of the tectonic environment, the spinel/chromite grain plots in the field that represents mid-ocean ridge basalt (MORB) (Fig.4.39 A).

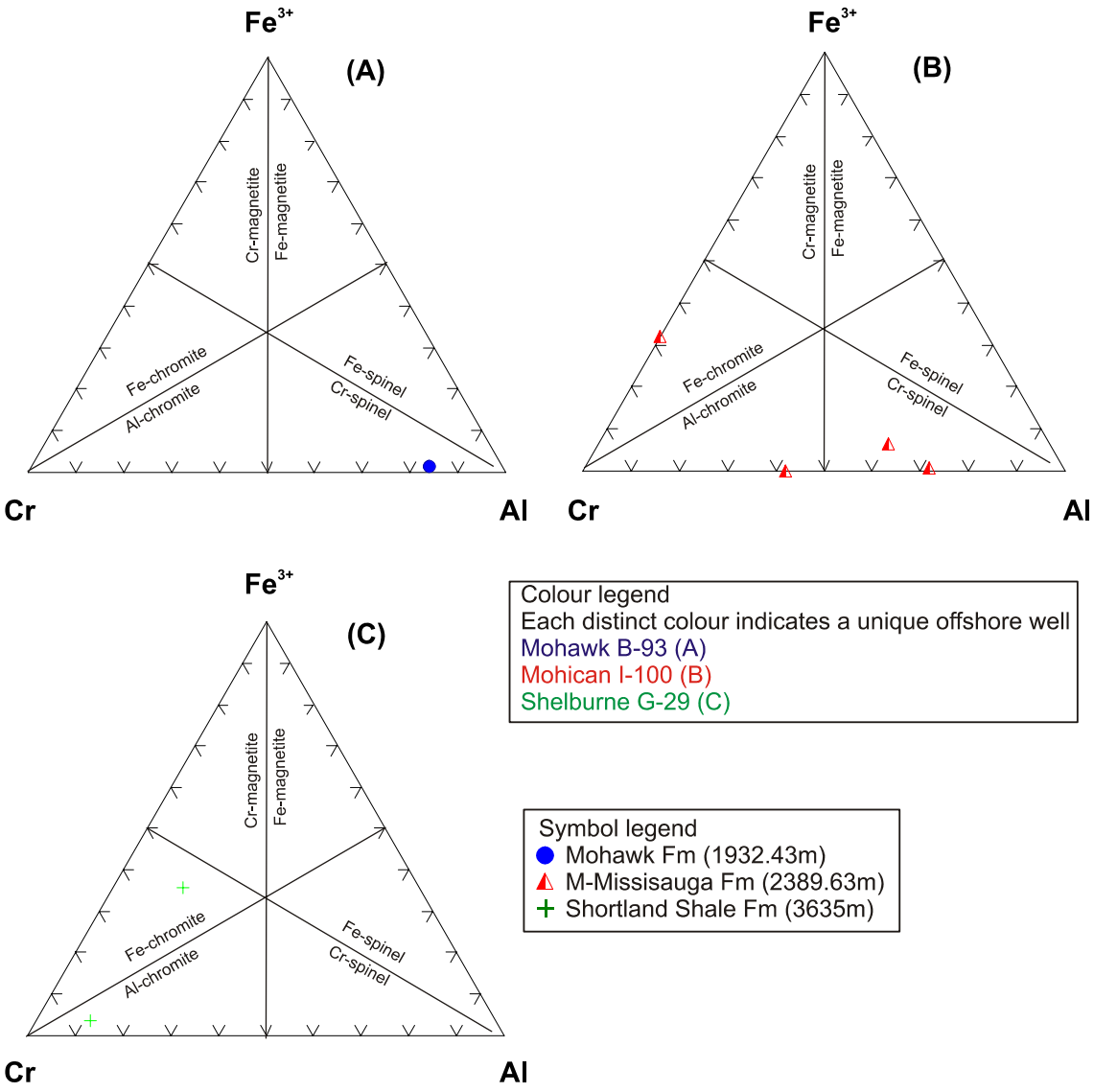

Fig.4.38: Chemical variation in spinel/chromite. The fields are after Stevens (1944)

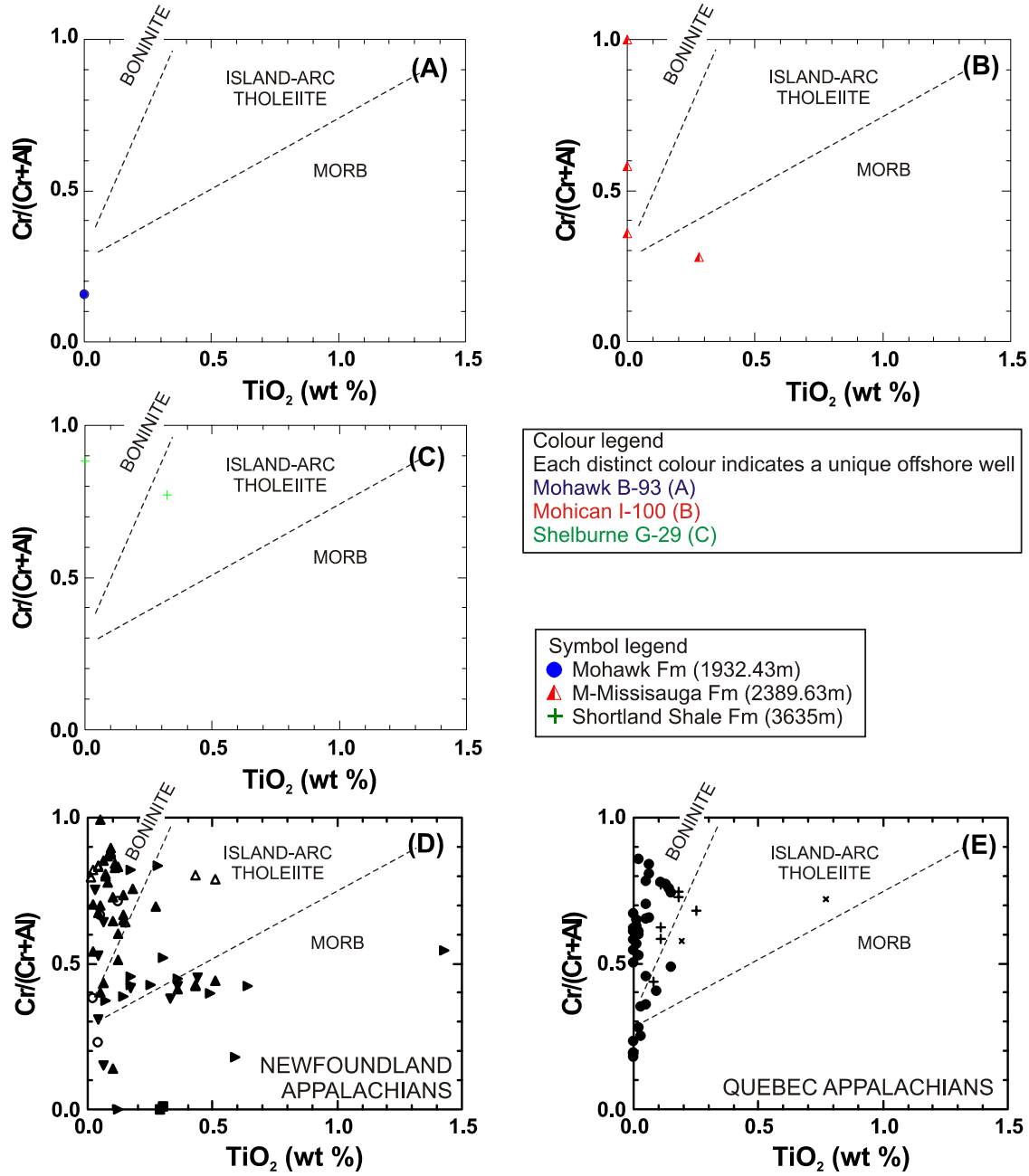

POTENTIAL SOURCE AREAS

Newfoundland Appalachians

- ■ Newfoundland Anorthosite (Pe-Piper and Dessureau, 2002)
- △ Betts Cove Ophiolite (Coish, 1989)
- ▲ Bay of Islands Ophiolite (Malpas and Strong, 1975)
- ◀ Bay of Islands Ophiolite (Suhr and Robinson, 1994)
- ▶ Bay of Islands Ophiolite (Bédard and Hébert, 1998)
- ○ Bay of Islands Ophiolite (Varfalvy and Hébert, 1997)

Quebec Appalachians

- + Thetford Mines Ophiolite (Laurent and Kacira, 1987)
- × Quebec Appalachian Ophiolites (Hébert and Laurent, 1989)
- ● Thetford Mines Ophiolite (Pagé et al., 2008)

Fig.4.39: Chemical variation in spinel/chromite in wells of the SW Scotian Basin (above) and for potential source rocks (below). Fields after Pearce et al. (2000).

Mohican I-100

This well has the highest number of detrital spinel/chromite grains (4 in total) identified compared to the other wells studied. All 4 grains are found in the Lower Cretaceous Upper Missisauga Formation. Only 3 distinctive spinel/chromite types (6 in total) have been identified which are: Cr-spinel (2 grains), Al-chromite (1 grain) and Fe-chromite (1 grain) (Fig.4.38 B).

The TiO_2 depleted Cr-spinel, the Al-chromite, and the Fe-chromite have boninites as host rocks suggesting a fore-arc basin as tectonic environment, whereas the other Cr-spinel have MORB as host rock, suggesting thus a mid-ocean ridge environment (Fig.4.39 D).

Shelburne G-29

Two grains from Lower Cretaceous Shortland Shale Formation are spinels/chromites. Both grains have been identified as chromites. One grain has almost no Fe in its chemical composition and plots as Al-chromite, whereas the other is enriched in Fe and plots as Fe-chromite (Fig.4.39 C).

Summary

1. Spinels/chromites are not common detrital heavy minerals in sediment samples from the SW Scotian Basin
2. Only 3 of the total 6 types of spinels/chromites have been identified in the wells studied which are: Cr-spinel, Al-chromite and Fe-chromite
3. The most abundant type identified is the Cr-spinel with a total of 3 grains, 2 from

Lower Cretaceous Upper Missisauga Formation (Mohican I-100) and 1 from Middle Jurassic Mohawk Formation (Mohawk B-93); Al-chromites and Fe-chromites are subordinate with 2 grains for each type from Shortland Shale (Shelburne G-29) and Upper Missisauga (Mohican I-100) formations

4. Most of the spinels/chromites (4 grains) were derived from boninite originating in fore-arc basin representing a subduction zone; 2 grains were derived from mid-ocean ridge basalts, whereas one grain had as a host rock island arc tholeiites

4.3.2.4.2 Rutile

Detrital rutile, one of the 3 titania (TiO_2) polymorphs, is rare within Mesozoic sandstone formations in the Scotian Basin. After tourmaline, rutile is the second detrital heavy mineral from the high stability group used for identification of potential onshore rock sources for sediments in our study. Although rutile is an ultra-resistant heavy mineral, its usage in sedimentary provenance is restricted mostly because it usually tends to concentrate in polycyclic and mature sandstones, where most of the diagnostic detrital heavy minerals are destroyed by weathering and diagenetic processes (Zack et al., 2002; 2004). However, past researchers have created discrimination diagrams for rutile (Zack et al., 2002; 2004; Ledger, 2013) based on its chemical composition, particularly in abundance of trace elements (Zr, Nb, V), useful in tracing the source of this detrital mineral.

For this research we used 3 diagrams related to potential onshore sources. One was produced by Zack et al. (2002) that represents only the Cr vs Nb discrimination and was improved by Ledger (2013) by adding new fields for potential onshore sources

(Fig.4.40). The other 2 discrimination diagrams are taken from Ledger (2013) and represent chemical differentiations between two groups of trace elements Zr vs V and Zr vs Nb (Figs.4.41, 4.42). To classify the rutile analyzed we compared our analyses with those from known sources presented by Ledger (2013).

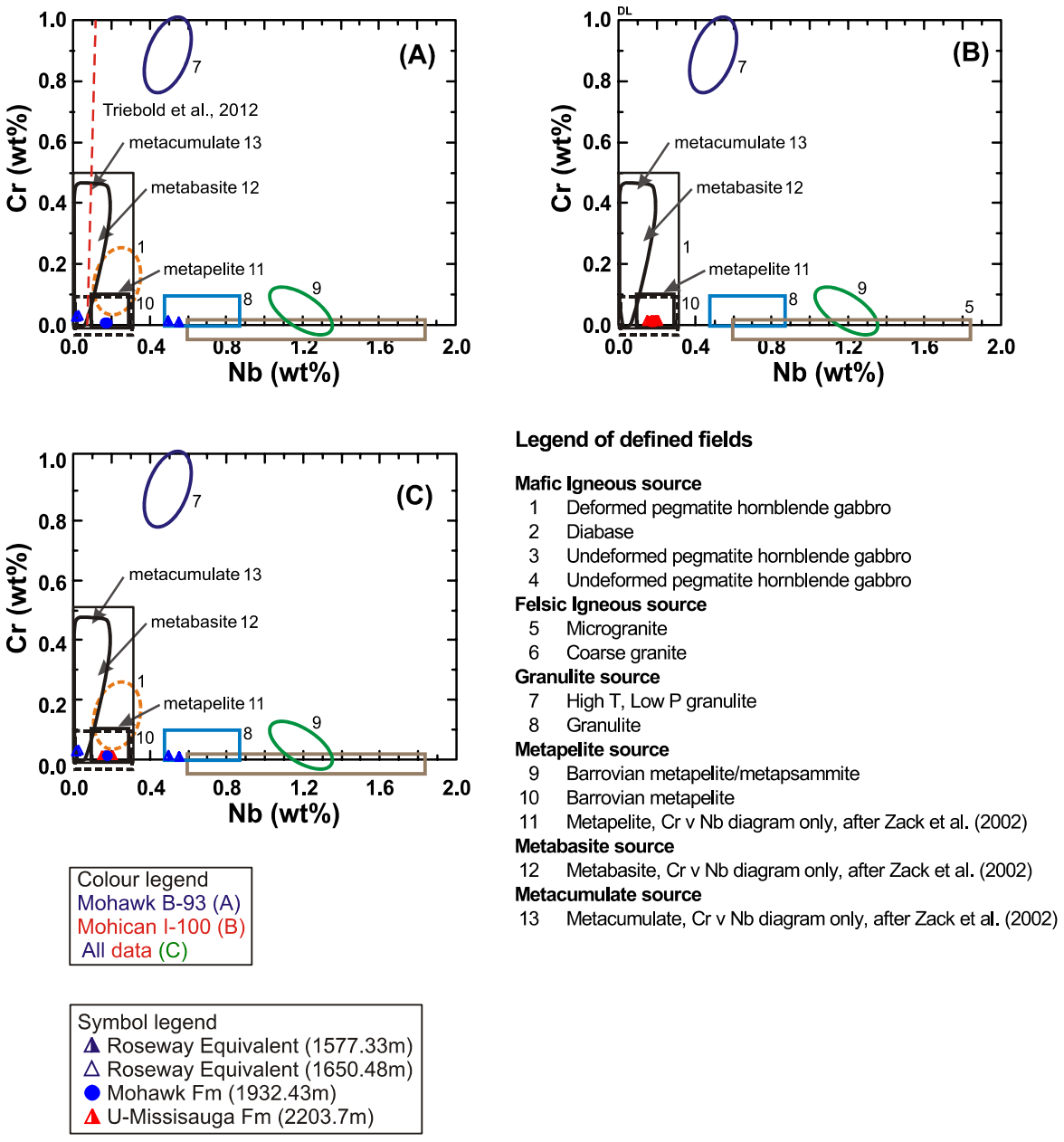

Fig.4.40: Cr vs. Nb chemical variation diagrams that show the best discrimination of some potential source rocks, fields taken from Zack et al. 2002.

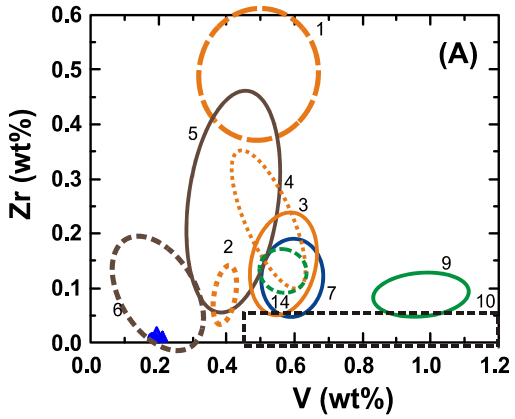

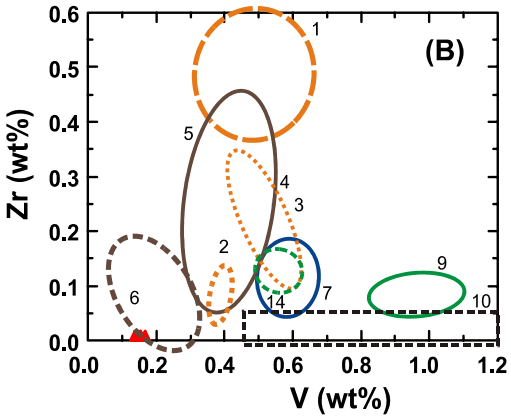

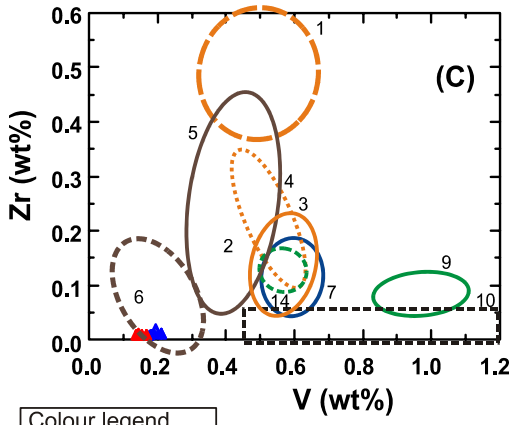

Colour legend
Mohawk B-93 (A)
Mohican I-100 (B)
All data (C)

Symbol legend
▲ Roseway Equivalent (1577.33m)
△ Roseway Equivalent (1650.48m)
● Mohawk Fm (1932.43m)
▲ U-Missisauga Fm (2203.7m)

Legend of defined fields

Mafic Igneous source
1 Deformed pegmatite hornblende gabbro
2 Diabase
3 Undeformed pegmatite hornblende gabbro
4 Undeformed pegmatite hornblende gabbro

Felsic Igneous source
5 Microgranite
6 Coarse granite

Granulite source
7 High T, Low P granulite
8 Granulite

Metapelite source
9 Barrovian metapelite/metapsammite
10 Barrovian metapelite
11 Metapelite, Cr v Nb diagram only, after Zack et al. (2002)

Metabasite source
12 Metabasite, Cr v Nb diagram only, after Zack et al. (2002)

Metacumulate source
13 Metacumulate, Cr v Nb diagram only, after Zack et al. (2002)

Fig.4.41: Zr vs V chemical variation diagrams that show the best discrimination of some potential source rocks, fields after Ledger (2013).

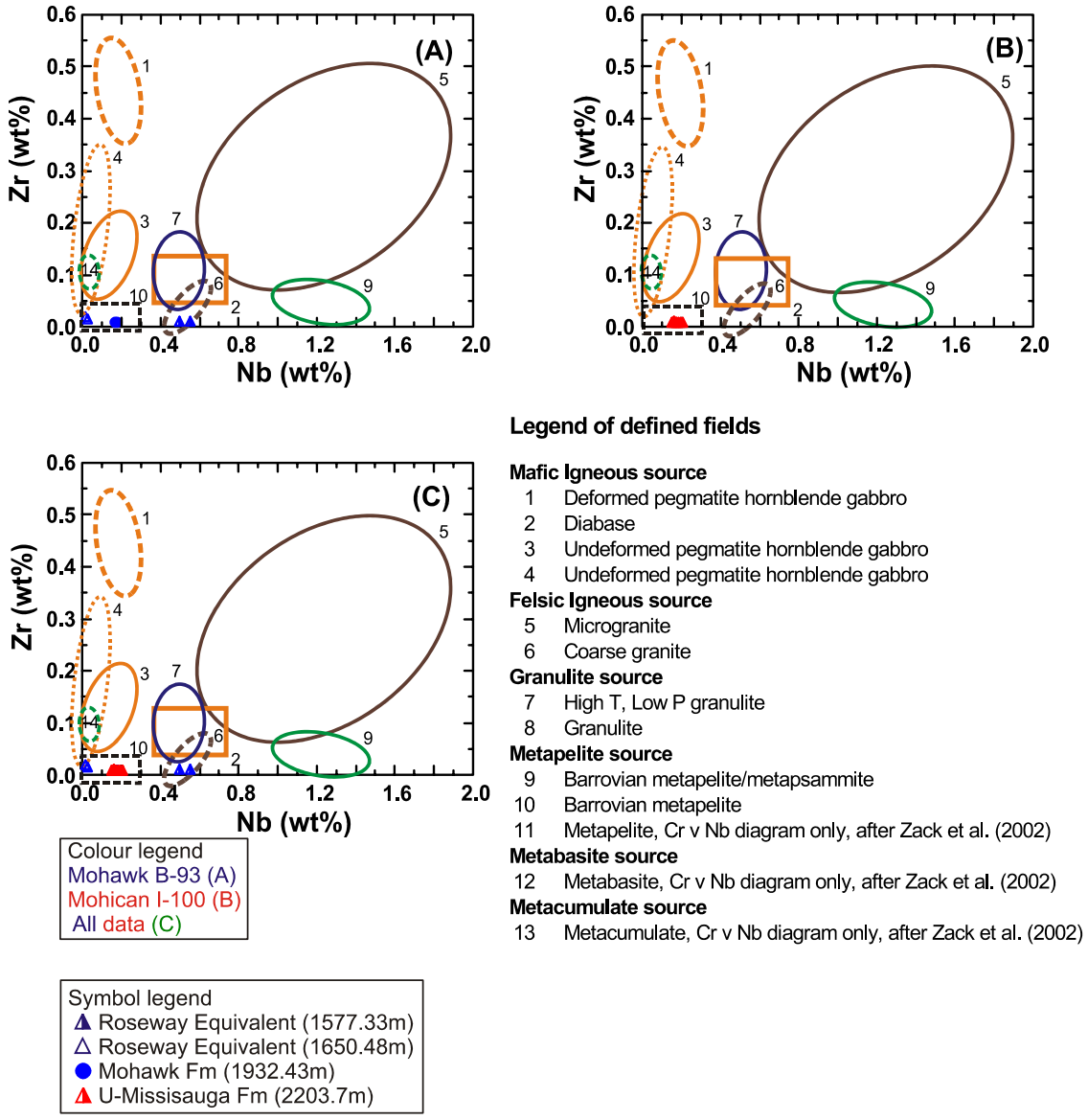

Fig.4.42: Zr vs Nb chemical variation diagrams that show the best discrimination of some potential source rocks, fields after Ledger (2013).

Chinampas O-37

No detrital rutile has been identified in cutting samples from this well.

Mohawk B-93

Three samples, from the total of 9 collected from sandstones in this well, contain detrital rutile, 2 from Roseway Equivalent Formation (Lower Cretaceous) and 1 from Mohawk Formation (Middle Jurassic). Two samples from 1577.33 m and 1650.48 m (Roseway Equivalent) each contain 2 detrital rutile grains, as does the sample from Mohawk Formation (1932.43 m).

The discrimination diagram proposed by Zack et al. (2002), Cr vs Nb (Fig.4.40 A), when compared to that proposed by Ledger (2013), for Zr vs Nb, (Fig.4.42 A) shows similarity regarding weight percentage participation of Cr and Zr within the samples collected, with variation in Nb. The grains from 1650.48 m in Roseway Equivalent Formation have higher percentage in Cr compared to samples from Mohawk Formation and from Roseway Equivalent Formation (1577.33m). Figure 4.41 A shows that all samples collected have similar weight percentageof V and Zr.

Two known types of onshore bedrock have rutile with chemical composition similar to those from this well (Figs.4.40, 4.41, 4.42): 1 is the granulite or the coarse granite, for sediments that comprise the Roseway Equivalent Formation at a depth of 1650.48 m and the other is metapelite for sediments that comprise Mohawk Formation at a depth of 1932.43 m and Roseway Equivalent Formation at a depth of 1577.33 m.

Mohican I-100

All samples with detrital rutile are from the Lower Cretaceous Upper Missisauga Formation. All 6 rutile chemical analyses from these samples plot in the same field regardless of the discrimination diagram, suggesting similar participation of two groups of trace elements, niobium/vanadium and zirconium/chromium (Figs.4.40 B, 4.42 B) in the samples collected from this well. Rutile analyses in this well are similar to rutile from known crystalline bedrock such as metapelite and coarse granite.

Shelburne G-29

No detrital rutile has been identified in cutting samples from this well.

Summary

1. Rutile is almost absent from sandstone formations sampled, with 6 detrital grains identified in each of the Mohican I-100 and Mohawk B-93

2. Lower Cretaceous formations are the only ones to have detrital rutile in Mohican I-100, 6 grains in Upper Missisauga; 4 grains were identified in Roseway Equivalent and 2 grains in Mohawk Formation from Mohawk B-93

3. Discrimination diagrams proposed by Zack et al. (2002) and Ledger (2003) suggest that rutile analyses in the SW Scotian Basin are similar to those from metapelites and somewhat resemble those from granulites or coarse granites

4.3.2.5 Other diagnostic detrital minerals

4.3.2.5.1 Ilmenite

Ilmenite is an important component of sedimentary rocks originating in the central and eastern part of the Scotian Basin. In the SW Scotian Basin, ilmenite is the most abundant detrital heavy mineral identified in cutting samples, making up 40 to 80% of the heavy mineral fraction. Although ilmenite is a common detrital mineral in sedimentary rocks, its usage as provenance indicator for clastic sediments is restricted because of two factors: i) ilmenite alters during transport and diagenesis with progressive loss of Fe (Teufer and Temple, 1966; Force, 1991; Schroeder et al., 2002) and ii) it has a simple chemical composition, $FeTiO_3$, with only minor chemical variation between grains from different sources. It is well known from the literature that ilmenite alters first to pseudorutile (a mineral with a well defined structure), then to leucoxene (a fine-scale mix of pseudorutile and rutile) and finally to either anatase or rutile (Pe-Piper et al., 2005).

Previous studies of the chemical composition of detrital ilmenite in Holocene and Pleistocene sands (Darby, 1984; Darby and Tsang, 1987; Basu and Molinaroli, 1989) have been successful in identifying source rock variability. However, as Darby and Tsang (1987) pointed out, a more comprehensive analysis of detrital ilmenite from specific source rocks would allow to one match rock types with individual ilmenite grains.

Mathison (1975) and Haggerty (1976a) have showed that the enrichment and narrow range in TiO_2 content of detrital ilmenite from mafic sources is consistent with studies of ilmenite in mafic igneous rocks. On the other hand, the enrichment in MnO

content of detrital ilmenite from felsic sources is also consistent with studies of ilmenite in felsic igneous rocks (Haggerty, 1976b; Whalen and Chappell, 1988). However, strict adherence to presence and percentage of these oxides in the chemical composition of detrital ilmenite can lead to error in provenance interpretation. Nonetheless, a full understanding of the chemical complexities of detrital ilmenite is still lacking. To avoid sedimentary provenance interpretation based on ilmenite chemistry we used other characteristics such as texture and mineral inclusions. Interpretation of characteristic textures and inclusions were made using back-scattered electron images of ilmenite from polished thin sections of both heavy mineral separates and conventional cores. For identification of ilmenite and determination of the chemical composition of mineral inclusions, EDS chemical analyses were obtained.

Chinampas O-37

From a total of 11 grains identified as detrital minerals in this well, only one is ilmenite. The surface of the crystal is covered in places with black round patches interpreted as quartz inclusions. The crystal form is lathlike, narrow in the central part and elongated towards the edges, as well as anhedral with well curved crystal outlines that have embayments as a result of erosion during transportation.

Mohawk B-93

Ilmenite is the most abundant detrital heavy mineral this well making a total of 72% of the heavy mineral separates. Upper Jurassic Mohawk Formation has the highest average in ilmenite, ~80%, when compared to Lower Cretaceous Roseway Equivalent

Formation (~53%) and Middle Jurassic Mohawk Formation (~74%). Mineral inclusions in ilmenite from this well are characterized by unoriented round low back-scattered minerals representing detrital quartz. Rarely, muscovite and/or feldspar inclusions with prismatic form are present. The crystal form of detrital ilmenite varies a lot between grains with shapes from ellipsoid to annular. Ilmenite is commonly anhedral; however some subhedral ilmenite is also present. Back-scattered electron images show a wide range of textures, which are most likely inherited and preserved from the original ilmenite. Almost all detrital ilmenite are fresh having homogenous intensity in back-scattered electron images. Alteration is almost absent with only few exceptions. Few grains present alteration characterized by dark, dusty areas, probably due to the creation of pores as the development of pseudorutile begins.

Mohican I-100

Sixty percent of the heavy mineral separates in Mohican I-100 are made up ilmenite, the second highest percentage in the Scotian Basin. Lower Cretaceous formations are represented by 60% of ilmenite, Upper Jurassic Formation by 53% and Middle Jurassic by 73%. Most of the ilmenite grains have a large number of unoriented quartz inclusions. In some cases other detrital minerals such as muscovite and feldspar are present. Ilmenite in polished thin sections from this well appears with two different types of textures: 1) as detrital minerals with quartz, muscovite and feldspar inclusions and 2) as part of mineral aggregates that form the lithic clasts, lacking mineral inclusions. Ilmenite exhibiting type 1 texture is presented in more detail in the paragraph regarding the lithic clasts (see below). Round quartz inclusions come into

direct contact with the host ilmenite and persist without any change throughout the alteration processes.

Shelburne G-29

No detrital ilmenite has been identified in cutting samples from this well.

Summary

1. Ilmenite is the most abundant mineral in heavy mineral separates from the SW Scotian Basin
2. Mohican I-100 and Mohawk B-93 are abundant in ilmenite; Chinampas O-37 has only one grain, whereas Shelburne G-29 lacks ilmenite
3. Most of the ilmenite is characterized by abundance of quartz inclusions with minor presence of muscovite and feldspar inclusions
4. Alteration of ilmenite is rare in polished thin sections of both heavy mineral separates and conventional cores

4.3.2.5.2 Lithic clasts

Only polished thin sections of conventional cores from Mohican I-100 and Moheida P-15 were used due to lack of lithic clasts in heavy mineral separates. From a total of 11 polished thin sections (7 in Mohican I-100 and 4 in Moheida P-15) only 4 have lithic clasts (3 in Mohican I-100 and 1 in Moheida P-15). Two of the thin sections in Mohican I-100 that have lithic clasts are from the Lower Cretaceous Roseway Equivalent Formation, whereas the third one is from the Middle Jurassic Mohican

Formation. In Moheida P-15 lithic clasts were found in a polished thin section of the Middle Jurassic Iroquois Formation.

Lithic clasts are common in the Lower Cretaceous Roseway Equivalent in Mohican I-100, with abundant polycrystalline quartz (metapsammite) and some greenschist metamorphic rocks (chlorite schist) with a foliation. Abundant chlorite and polycrystalline quartz and lesser muscovite point to metamorphic rocks.

Lithic clasts are abundant in polished thin sections of Middle Jurassic conventional cores in both Mohican I-100 and Moheida P-15. Most lithic clasts are metapsammites and metapelites with characteristic mineralogical composition: a) ilmenite, chlorite, muscovite and quartz, b) muscovite, chlorite and ilmenite with inclusions of quartz and muscovite. In addition, rare lithic clasts of polycrystalline quartz are present. Based on mineral composition, lithic clasts in Middle Jurassic strata at both Mohican I-100 and Moheida P-15 tend to be from metapsammites and metapelites. Based on textures lithic clasts in Middle Jurassic strata at both Mohican I-100 and Moheida P-15 have high content in ilmenite. Many lithic clasts in Mohican I-100 lack foliation.

4.4 Diagenesis

The data presented for diagenesis in this section is based on analytical methods outlined in chapter 3. Mineral analyses from the both the SEM and the EMP, along with accompanying back-scattered electron images, were collected and interpreted (see appendices 9 and 10). Informative detrital and diagenetic minerals, clasts, textures and relative relationships from samples at Mohican I-100 and Moheida P-15 were studied and documented with microphotos and chemical analyses. All these describe the

petrography of cores from these wells. Chemical analyses obtained from SEM and EMP were utilized, using appropriate diagrams, to determine the secondary chemical mineralogy developed during diagenesis of these wells.

Calcite is a common diagenetic mineral in most of the sedimentary rocks. Based on chemical composition, calcite in this study was discriminated in four types regarding their content in CaO, MgO and FeO (table 4.2). The relative ages of these four types of calcite have been established using their textural relationship in back-scattered electron images. The four types are described below and representative chemical analyses for each calcite type are presented in table 4.2.

Calcite: CaO>54%, MgO<1% and FeO<1%

Mg-calcite: CaO=51-53%, MgO=1-3% and FeO<1%

Fe-calcite: CaO=52-53%, MgO<1% and FeO=1-2%

Mg-Fe-calcite: CaO=52-53%, MgO=1-2% and FeO=1-2%

Table. 4.2: Representative EDS chemical analyses for calcite types

Sample	Depth (m)	Site	Position	Mineral	SiO_2	TiO_2	Al_2O_3	FeO^t	MgO	CaO	Na_2O	K_2O	P_2O_5	SO_3	Recalculated Total	Actual Total
I-100 2526.53	2526.53	2	6	Mg-Cal					3.15	52.25				0.60	56	61
I-100 2526.53	2526.53	2	7	Mg-Cal	0.38			0.55	2.23	52.33				0.50	56	61
I-100 2526.53	2526.53	3	5	Mg-Cal	0.53				1.10	54.48					56	76
I-100 2526.53	2526.53	3	9	Mg-Cal				0.78	1.79	55.44					56	57
I-100 2526.53	2526.53	5	8	Cal	0.55			0.60	0.95	53.92					56	63
I-100 2526.53	2526.53	5	9	Mg-Cal	0.43			0.69	1.75	53.12					56	62
I-100 2526.53	2526.53	5	10	Mg-Cal	0.40			0.32	2.69	51.90				0.70	56	62
I-100 2526.53	2526.53	5	11	Cal	0.45			0.88	0.81	53.86					56	62
I-100 2526.53	2526.53	5	13	Mg-Cal				0.52	2.00	52.64				0.85	56	62
I-100 2526.53	2526.53	5	15	Cal	0.44				0.96	54.59					56	69
I-100 2526.53	2526.53	6	6	Mg-Cal					3.09	52.50					56	42
I-100 2526.53	2526.53	6	7	Cal				0.74	0.66	53.86				0.50	56	42
I-100 2526.53	2526.53	6	8	Fe-Cal	0.46			1.22	0.95	53.37					56	56
I-100 2526.53	2526.53	6	9	Cal	0.61			0.37		55.02					56	61
I-100 2526.53	2526.53	6	10	Cal	0.55			0.37	0.40	54.68					56	62
I-100 2526.53	2526.53	6	11	Mg-Fe-Cal	0.59			1.08	1.10	53.25					56	62
I-100 2526.53	2526.53	6	12	Mg-Cal	0.43			0.72	1.11	53.74					56	62
I-100 2526.53	2526.53	6	13	Mg-Cal					3.84	51.75					56	61
I-100 2526.53	2526.53	6	17	Mg-Cal	0.55				3.05	52.15					56	61
I-100 2526.53	2526.53	7	2	Cal				0.50		55.50					56	43
I-100 2526.53	2526.53	7	8	Cal				0.76	0.40	54.84					56	61
I-100 2526.53	2526.53	7	9	Mg-Cal	0.41				2.95	52.50					56	55
I-100 2526.53	2526.53	7	11	Mg-Cal					1.43	53.92				0.64	56	56
I-100 2526.53	2526.53	7	12	Cal	0.52			0.36		55.12					56	55
I-100 2526.53	2526.53	7	15	Mg-Cal	0.71				3.07	51.42				0.81	56	58
I-100 2529.62	2529.62	1	5	Cal				0.56		55.43					56	112
I-100 2529.62	2529.62	1	8	Mg-Cal	0.67			0.85	1.65	52.82					56	116
I-100 2529.62	2529.62	1	11	Mg-Cal	0.59			0.58	1.69	52.90					56	50
I-100 2529.62	2529.62	1	12	Cal	0.88		0.39	0.88	0.61	53.23					56	50

Table. 4.2: Representative EDS chemical analyses for calcite types (continued)

Sample	Depth (m)	Site	Position	Mineral	SiO_2	TiO_2	Al_2O_3	FeO^t	MgO	CaO	Na_2O	K_2O	P_2O_5	SO_3	Recalculated Total	Actual Total
I-100 2529.62	2529.62	1	13	Mg-Fe-Cal	0.85			1.41	1.25	52.49					56	52
I-100 2529.62	2529.62	1	15	Mg-Cal	0.34			0.49	1.37	53.82					56	51
I-100 2529.62	2529.62	1	16	Mg-Fe-Cal	0.68			1.32	1.01	52.99					56	50
I-100 2529.62	2529.62	2	4	Mg-Cal				0.63	1.11	53.74				0.52	56	111
I-100 2529.62	2529.62	2	5	Fe-Cal	0.67			1.40	0.86	52.54		0.17			56	112
I-100 2529.62	2529.62	2	10	Cal	0.44			0.66	0.58	54.33					56	51
I-100 2529.62	2529.62	2	11	Fe-Cal	0.52			1.00	0.86	53.64					56	50
I-100 2529.62	2529.62	2	16	Mg-Cal				0.43	1.78	52.88				0.90	56	51
I-100 2529.62	2529.62	2	17	Cal	0.88			0.80		54.33					56	50
I-100 2529.62	2529.62	3	9	Mg-Fe-Cal	0.54			1.04	1.13	53.30					56	51
I-100 2529.62	2529.62	3	10	Mg-Fe-Cal	0.69			1.41	1.09	52.81					56	51
I-100 2529.62	2529.62	3	12	Mg-Cal					3.10	52.11				0.80	56	51
I-100 2529.62	2529.62	3	13	Mg-Cal	0.49				2.92	51.64				0.95	56	52
I-100 2529.62	2529.62	3	14	Mg-Cal	0.42				3.81	50.86				0.91	56	52
I-100 2529.62	2529.62	3	15	Fe-Cal	0.84		0.40	1.33	0.86	52.57					56	51
I-100 2529.62	2529.62	3	16	Mg-Cal	0.40			0.63	1.40	52.65				0.92	56	52
I-100 2529.62	2529.62	4	7	Fe-Cal				1.03	0.96	54.00					56	116
I-100 2529.62	2529.62	4	9	Mg-Cal	0.55			0.78	1.48	52.53				0.67	56	51
I-100 2529.62	2529.62	4	11	Fe-Cal	0.52			1.26	0.92	53.31					56	50
I-100 2529.62	2529.62	4	12	Cal	0.76			0.73	0.51	54.01					56	50
I-100 2529.62	2529.62	4	14	Mg-Cal	0.37			0.63	1.27	53.10				0.40	56	49
I-100 2529.62	2529.62	4	15	Mg-Fe-Cal	0.44			1.10	1.06	53.41					56	50
I-100 2529.62	2529.62	6	2	Mg-Cal				0.55	2.47	52.13				0.85	56	114
I-100 2529.62	2529.62	6	3	Cal	0.58			0.91	0.99	53.52					56	134
I-100 2538.84	2538.84	1	6	Mg-Cal	0.92		0.52		1.88	52.68					56	125
I-100 2538.84	2538.84	2	6	Cal				0.94	0.89	54.17					56	129
I-100 2538.84	2538.84	3	3	Cal				0.56		55.43					56	127
I-100 2538.84	2538.84	3	4	Cal				0.44		55.56					56	122

4.4.1 Mohican I-100 well

Diagenetic minerals and paragenetic sequence of Lower Cretaceous Roseway Equivalent sandstones and oolitic limestone

Sample I-100 2526.53 (Roseway Equivalent Formation, 2526.53 m) fine grained carbonate-cement sandstone (Appendix 9-1)

Description

Diagenetic minerals present in this sample are calcite, chlorite, quartz overgrowths, dolomite, kaolinite, illite, pyrite, TiO_2 mineral and F-apatite. Some illite and TiO_2 mineral are part of both the matrix and the cement. Calcite invades (Fig.4.8 A) or engulfs (Figs.4.8 C, D) Mg-calcite. In addition, calcite fills secondary porosity and embayments in detrital quartz (Fig.4.8 C). Mg-calcite seems to be cross-cut by Mg-Fe-calcite (Fig.4.8 H). Secondary porosity in Mg-calcite is filled by framboidal pyrite (Fig.4.8 C). Fe-calcite shows straight crystal outlines and tends to invade Mg-calcite (Fig.4.8 H). Fe-calcite in a bioclast is partly replaced by pyrite (Fig.4.8 F). Some diagenetic chlorite is fibrous and fills secondary porosity in Mg-calcite (Fig.4.8 A) and embayments in detrital quartz (Figs.4.8 B, D). Some other diagenetic chlorite is part of the cement together with illite (Fig.4.8 G) and cross-cuts late fractures (Fig.4.8 E). Quartz overgrowths have straight outlines and invade Mg-calcite suggesting that they are later (Fig.4.8 B). Rarely, at the contact between quartz grains, one grain has undergone dissolution leading to the penetration of one grain by another, thus creating concavo-convex contacts (c-c) (Fig.4.8 C). The dolomite rhombohedrons show replacive texture against diagenetic chlorite in the cement (Fig.4.8 A). Kaolinite booklets fill primary porosity and in places tend to fill

embayment in Mg-calcite (Fig.4.8 B) and detrital quartz (Fig.4.8 C). In addition, kaolinite fills open space between diagenetic chlorite and detrital zircon (Fig.4.8 A) and embayment in Mg-calcite (Fig.4.8 C). Rarely diagenetic TiO_2 minerals show replacive texture against detrital quartz grains (Fig.4.8 D). Framboidal pyrite is associated with all the diagenetic minerals mentioned above filling secondary porosity. Late fractures lack diagenetic minerals.

Paragenetic sequence: Mg-calcite and calcite predate Mg-Fe-calcite and Fe-calcite. Kaolinite postdates Fe-calcite and predates quartz overgrowths. Chlorite together with illite, pyrite and TiO_2 mineral predate the quartz overgrowths. Dolomite seems to be the last diagenetic minerals to have crystallized.

Sample I-100 2529.62 (Roseway Equivalent Formation, 2529.62 m) fine grained carbonate-cement sandstone (Appendix 9-2)

Description

The diagenetic minerals present in this sample are calcite, chlorite, pyrite, illite and quartz overgrowths. Calcite seems to be homogenous in back-scattered electron images and engulfs, invades or fills secondary porosity in Mg-calcite (Figs.4.9 A, F). Based on texture there seem to be two generations of Mg-Fe-calcite: one that shows high secondary porosity and is filled with chlorite and one that shows low secondary porosity and is partly replaced by illite (Fig.4.9 B). The Mg-Fe-calcite seems to invade Mg-calcite and engulf Mg-Fe-calcite (Fig.4.9 B). In general Mg-calcite tends to show dissolution voids that lack diagenetic minerals. Rarely quartz overgrowths

form around detrital quartz and invade Mg-calcite (Figs.4.9 A, B), Mg-Fe-calcite and Fe-calcite (Figs.4.9 C, D). Diagenetic divergent fibrous chlorite fills embayments in corroded quartz and calcite and/or occupies intragranular space between framework grains and cement (Figs.4.9 A, E). Moreover, diagenetic chlorite fills secondary porosity in Mg-calcite and open space between Mg-calcite and detrital quartz (Figs.4.9 B, C). Illite can be compact with characteristic secondary fractures that are often filled by framboidal pyrite (Fig.4.9 A) or can be part of the cement in form of fibres (Fig.4.9 C). Framboidal pyrite fills secondary porosity in Mg-calcite (Fig.4.9 C). Mg-calcite tends to invade fibrous illite (Fig.4.9 C). Crystal boundaries between detrital quartz grains are hard to distinguish in places where the cement is SiO_2 (Fig.4.9). Rarely, at the contact between quartz grains, one grain has undergone dissolution leading to the penetration of one grain by another, thus creating a concavo-convex contact (Fig.4.9 D). Unknown calcite type, illite and other diagenetic minerals fill secondary porosity in detrital quartz. Late fractures and often secondary porosity lack diagenetic minerals, they are barren (Fig.4.9 E).

Paragenetic sequence: Mg-calcite predates Fe-calcite, calcite and Mg-Fe-calcite which in turn predate chlorite, illite and TiO_2 mineral. Quartz overgrowths postdate all the previous diagenetic minerals.

Sample I-100 2530.47 (Roseway Equivalent Formation, 2530.47 m) oolitic bioclastic limestone (Appendix 9-3)

Description

Diagenetic minerals identified in this sample are calcite, ankerite, TiO_2 mineral,

chlorite, quartz overgrowths and illite. The Fe-calcite represents the main supporting cement for the framework grains in the sample. In places, the cement is very fine made up of chlorite, calcite and pyrite or rarely it can be represented by ankerite (Fig.4.10 A). Rarely, diagenetic chlorite tends to fill secondary porosity in Fe-calcite (Figs.4.10 A, B). TiO_2 mineral together with illite fill secondary porosity in detrital quartz (Fig.4.10 D). Often, quartz overgrowths form around detrital quartz and replace Fe-calcite cement (Figs.4.10 A, D). Ankerite engulfs Fe-calcite and invades chlorite and pyrite (Fig.4.10 B).

Paragenetic sequence: Fe-calcite predates quartz overgrowth, chlorite and pyrite. Ankerite postdates all the previous diagenetic minerals.

Sample I-100 2538.84 (Roseway Equivalent Formation, 2538.84 m) fine grained carbonate-cement sandstone (Appendix 9-4)

Description

Diagenetic minerals in this sample are calcite, TiO_2, pyrite, F-apatite, chlorite and quartz overgrowths. The calcite and the Mg-Fe-calcite were identified in this sample filling primary porosity. The calcite tends to show homogenous light grey color, whereas the Mg-Fe-calcite often shows brittle fracturing (Fig.4.11 B). Calcite of unknown type replaces detrital chlorite along its cleavage planes. Calcite fills secondary porosity in detrital quartz together with other diagenetic minerals, which is referred as carbonate cement (Fig.4.11 B). The cement can be calcite, Mg-Fe-calcite or calcite plus other diagenetic minerals. Rarely, diagenetic F-apatite showing straight crystal outlines fills secondary porosity in the carbonate cement (Fig.4.11 C).

Diagenetic chlorite fills embayment in detrital quartz grain (Fig.4.11 B). TiO_2 mineral and pyrite show replacive texture against the carbonate cement (Fig.4.11 C). Quartz overgrowths are rare, form around detrital quartz grains and tend to invade calcite (Figs.4.11 B, C). Secondary porosity often lacks diagenetic minerals.

Paragenetic sequence: Mg-Fe-cal predates calcite which predates pyrite, F-apatite, TiO_2 mineral and quartz overgrowths.

Diagenetic minerals and paragenetic sequence of Middle Jurassic Mohican sandstone

Sample I-100 3692.41 (Mohican Formation, 3692.41 m) coarse grained sulphate-cement sandstone (Appendix 9-5)

Description

Diagenetic minerals in this sample are anhydrite, quartz overgrowths and albite. Anhydrite is the main cement composed of aggregate of anhydrite grains with visible cleavage planes and shows high porosity around grain boundaries. Anhydrite cement fills primary porosity between framework grains. Detrital K-feldspar at depths > 3 km is partly replaced with diagenetic albite (albitization of detrital K-feldspar). Albitized K-feldspar is partly replaced by anhydrite (Figs.4.12 A, D). Anhydrite is a mobile mineral, thus remobilization of anhydrite replacing albitized K-feldspar can be from late anhydrite cement or from early anhydrite, in form of nodules, through veins, as noted by Sedge (2015). Secondary porosity in the cement and the matrix (Fig.4.12 E) lacks diagenetic minerals. Quartz overgrowths form around detrital quartz grains and

invade anhydrite cement (Fig.4.12 B). At the contact between quartz grains, one quartz grain has undergone dissolution leading to the penetration of one grain by another, thus creating concavo-convex contacts (c-c) (Fig.4.12 C). Rarely, TiO_2 mineral fills primary porosity in the matrix (Fig.4.12 D).

Paragenetic sequence: Anhydrite cement predates albitization of detrital K-feldspar and quartz overgrowths. Albitized K-feldspar predates remobilized anhydrite.

Diagenetic minerals and paragenetic sequence of Middle Jurassic Iroquois sandstone and limestone

Sample I-100 3964.6A (Iroquois Formation, 3964.6m) fine grained sulphate-cement sandstone (Appendix 9-6)

Description

Diagenetic minerals in this sample are anhydrite, pyrite, quartz overgrowths, pure calcite and TiO_2 mineral. The sample has very low primary porosity that is filled by anhydrite (Fig.4.13 B). Anhydrite partly replaces detrital K-feldspar and albite and engulfs biotite and muscovite (Fig.4.13 B). Quartz overgrowths form around detrital quartz grains and seem to invade anhydrite cement (Fig.4.13 B). Framboidal pyrite shows replacive texture against the matrix (Fig.4.13 A) and TiO_2 show replacive texture against detrital quartz, micas and anhydrite (Fig.4.13 C). Rarely, calcite tends to partly replace albite and/or fill intragranular space (Fig.4.13 C).

Paragenetic sequence: Anhydrite predates quartz overgrowths, calcite and TiO_2 mineral.

Sample I-100 4098.08 (Iroquois Formation, 4098.08m) sandy limestone (Appendix 9-7)

Description

Diagenetic minerals are anhydrite, calcite, chlorite, quartz overgrowth, pyrite and TiO_2. Micritic calcite is the main cement that replaced anhydrite cement (Fig.4.14). Rare quartz overgrowths form around detrital quartz grains. Pyrite and TiO_2 mineral show replacive textures against the detrital quartz grains and the micritic carbonate cement. In general, diagenetic chlorite, pyrite and TiO_2 mineral appear to nucleate on cement and framework grains boundaries, and often they are replacing pre-extisting detrital minerals.

Paragenetic sequence: The data obtained for this sample are not enough to determine the precise paragenetic sequence. However, based on the textural relationships between diagenetic minerals it seems that anhydrite or calcite predate TiO_2 mineral and pyrite.

4.4.2 Moheida P-15 well

Diagenetic minerals and paragenetic sequence of Lower Cretaceous Roseway Equivalent oolitic ironstone

Sample P-15 2563.67 (Roseway Equivalent Formation, 2563.67 m) oolitic ironstone (Appendix 10-1A)

Description

The intragranular space in this sample is filed with a mixture of ankerite, siderite and chlorite (Figs.4.15 B, C). Mg-Fe-calcite is partly replaced by late siderite

(Fig.4.15 C). Based on textural relationship there seems to be two generations of ankerite, early and late and two generations of siderite, early and late (Figs.4.15 B, C). Early ankerite has subrounded crystal outlines and seems to be invaded by early siderite (Fig.4.15 B). Early siderite and early ankerite are surrounded and partly replaced by late siderite (Figs.4.15 B, C). Late ankerite tends to cross-cut both early and late siderite as well as diagenetic chlorite (Fig.4.15 C). Fe-Mg-calcite fills primary porosity and is replaced by late siderite (Fig.4.15 A). Diagenetic chlorite is rare, fibrous and when present tends to be associated with calcite or fills secondary porosity in the cement (Fig.4.15 C). Bioclast is entirely replaced by Mg-calcite (Fig.4.15 A).

Diagenetic paragenesis: Fe-Mg-calcite and Mg-calcite predate predate Fe-calcite, early ankerite and early siderite. Late siderite postdates Fe-cal and early ankerite and predates chlorite which in turn predates late ankerite.

Diagenetic minerals and paragenetic sequence of Upper Jurassic Abenaki oolitic limestone

Sample P-15 3306.03 (Abenaki Formation, 3306.03 m) oolitic limestone (Appendix 10-2)

Description

The supporting material is a mixture of silt size dolomite, diagenetic chlorite, pyrite, muscovite, Fe-calcite and detrital quartz (Fig.4.16 B). Quartz overgrowths form around detrital quartz and tend to replace Fe-calcite (Fig.4.16 B). Fe-calcite is the main cement replacing dolomite. Pyrite is diagenetic and shows replacive texture against dolomite and e-calcite cement (Fig.4.16 B). Secondary porosity in the cement

lacks diagenetic minerals (Fig.4.16 A).

Paragenetic sequence: Dolomite predates Fe-calcite and pyrite.

Diagenetic minerals and paragenetic sequence of Middle Jurassic Iroquois sandstone and dolostone

Sample P-15 3744.92 (Iroquois Formation, 3744.92 m) fine grained sulphate-cement sandstone (Appendix 10-3)

Description

Diagenetic minerals identified are anhydrite, pyrite, quartz overgrowths, illite, kaolinite and TiO_2 mineral. Anhydrite fills primary porosity and engulfs biotite (Fig.4.17 A) and muscovite (Fig.4.17 C). Kaolinite and illite fill embayments in detrital quartz (Fig.4.17). In places illite forms in the space between detrital quartz and anhydrite cement (Fig.4.17 A). Quartz overgrowths form around detrital quartz grains and tend to invade anhydrite cement (Fig.4.17 A). Framboidal pyrite shows replacive texture against the anhydrite (Fig.4.17 C) and TiO_2 mineral show replacive texture against biotite (Fig.4.17 B) and anhydrite (Fig.4.17 C). Both TiO_2 mineral and pyrite seem to cross-cut all the other minerals (Fig.4.17 C).

Paragenetic sequence: Anhydrite predates TiO_2 which in turn predates kaolinite and illite. Quartz overgrowths predate all the previous diagenetic minerals.

Sample P-15 3750.94 (Iroquois Formation, 3750.94 m) dolostone (Appendix 10-4)

Description

Secondary porosity is filled by anhydrite (Fig.4.18).

5. Discussion

5.1 Provenance

The main objective of this chapter is to use the results presented in chapter 4 to interpret the provenance of Mid Jurassic to Early Cretaceous sediments deposited in the SW Scotian Basin and Early Jurassic sediments in the Fundy Basin.

The chemical composition and the relative abundance of detrital heavy minerals such as tourmaline, garnet, spinel/chromite, rutile, of detrital light minerals like muscovite, biotite, chlorite, feldspar and mineralogical composition of lithic clasts from Mid Jurassic to Early Cretaceous sandstones in the SW Scotian Basin are compared with the mineralogical composition of local onshore potential rock sources such as the Meguma terrane (Nova Scotia) and more distant onshore rock sources from both more inboard Appalachian terranes, like Avalon and Gander (New Brunswick) and outboard parts of the Canadian Shield such as the Grenville Province (Labrador). In addition, the chemistry and the relative abundance of these minerals is compared with elsewhere in the Scotian Basin, particularly in the central part (Sable sub-basin and Abenaki sub-basin) and the western part (Naskapi N-30 well) and with the Chaswood Formation on land (Nova Scotia and New Brunswick).

5.1.1 Sources for Lower Cretaceous sandstones in the SW Scotian Basin

5.1.1.1 Tourmaline

Tourmaline is common in the Lower Cretaceous in Mohican I-100, with same chemical characteristics as in Naskapi N-30: type 4 abundant, type 1 subordinate to 4 and type 3 rare. However, it is different from the tourmaline in the Abenaki sub-basin,

at Dauntless D-35, the Sable sub-basin at Musquodoboit E-23, Alma K-85, Chebucto K-90 and the Laurentian sub-basin, at Emerillon C-56 and Hermine E-94 (Fig.5.1). The only exceptions in the Sable sub-basin are wells in the Thebaud, Glenelg and Venture fields (Pe-Piper et al., 2009), which have similar tourmaline as Mohican I-100 and Naskapi N-30.

Type 4 from Mohican I-100, derived from metapelitic/metapsammitic rocks, shows the similar chemical variation as type 4 tourmaline in Naskapi N-30 but has a wider range of Al content. The Al content is also more variable compared to tourmaline from Lower Cretaceous formations in wells from other parts of the Scotian Basin, such as those at the Thebaud field, Alma K-85 and Chebucto K-90 in the Sable sub-basin and Emerillon C-56 and Hermine E-94 in the Laurentian sub-basin. Type 1 from igneous rocks, and type 3 from meta-ultramafic and meta-carbonate rocks, are similar only to those in Naskapi N-30.

Tourmaline of type 1 and type 4 at Mohawk B-93 and Shelburne G-29 wells has similar abundance and chemical composition to tourmaline from Lower Cretaceous formations at Mohican I-100 and Naskapi N-30. However type 3 is absent in both wells. Sediment samples at Vinegar Hill have the same tourmaline types (1, 3 and 4) as those found in Mohican I-100 and Naskapi N-30, in part of metapelitic/metapsammitic origin and in part of granitic origin, where the latter is likely to be derived from the Silurian peraluminous tourmaline granites of central New Brunswick, including the Pokiok batholith (Piper et al., 2007). Tourmaline of type 1 at Vinegar Hill is almost as abundant as type 4 and not subordinate to the latter, which is the case for wells originating in the SW Scotian Basin (Mohican I-100 and Mohawk B-93). In addition,

tourmaline types 1 and 4 have a narrow chemical range enriched in Al, whereas tourmaline in wells on La Have Platform (Mohican I-100 and Mohawk B-93) and the Scotian Slope (Shelburne G-29) show a wide range of Al content within same type, as well from one type to another. Chemical mineralogy and abundance of tourmaline in the SW Scotian Basin suggests that during Early Cretaceous the clastic sediments were derived mostly from metamorphic rocks of the Meguma terrane, rather than igneous rocks.

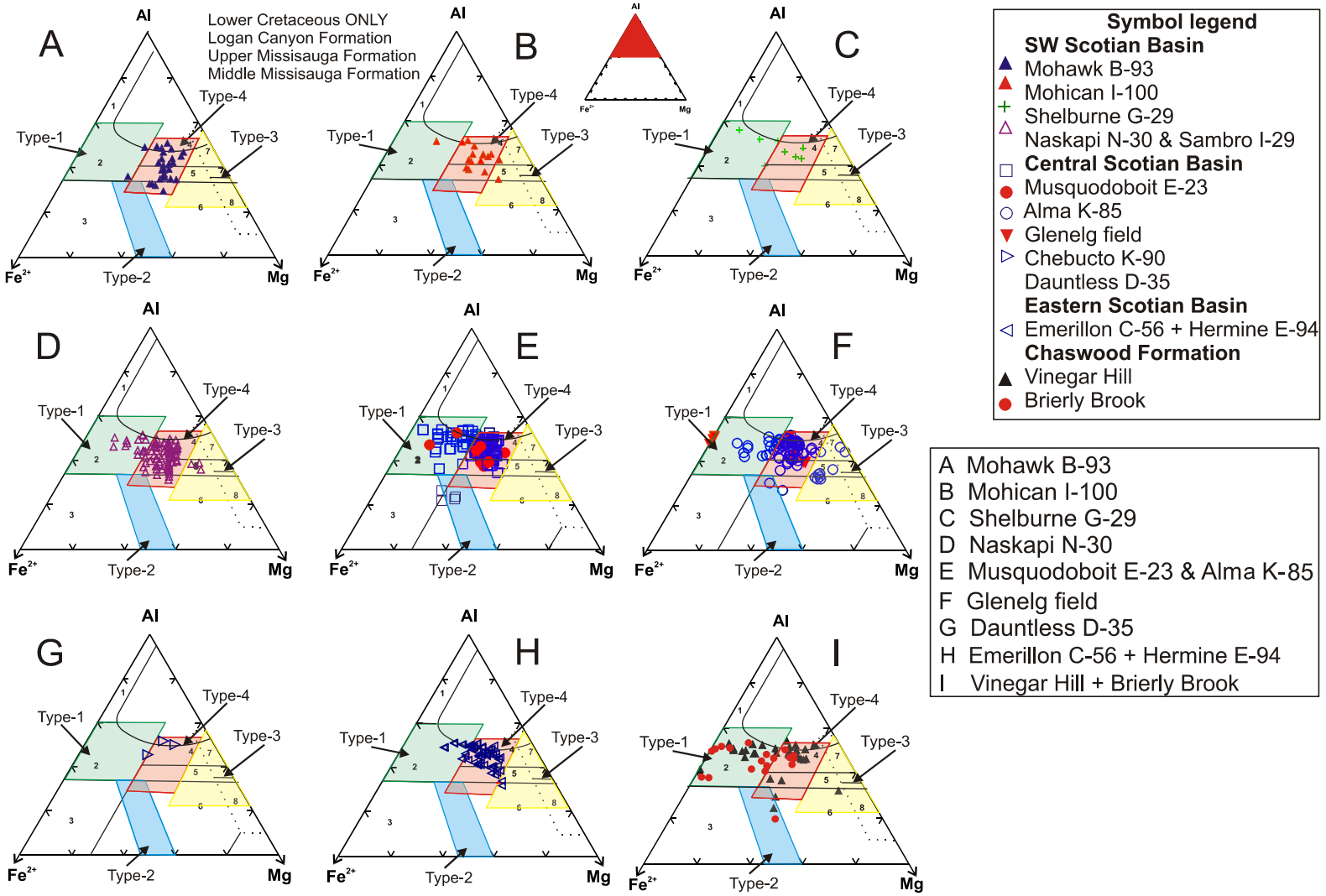

Fig.5.1: Chemical variation in tourmaline based on Al - Mg - Fe showing definition of types from wells studied and wells-formations used for comparison. Fields and data for wells not included in this study are taken from Pe-Piper et al. (2009).

5.1.1.2 Garnet

Wells from the central (Musquodoboit E-23 and Dauntless D-35) and the eastern part (Hermine E-94 and EmerillonC-56) of the Scotian Basin and the Orpheus graben (Argo F-38 and Jason C-20) show differences in the chemical composition and the relative abundance of garnet when compared to the four types identified in the SW Scotian Basin for Lower Cretaceous formations (Fig.5.2). Specifically types 1A and 1B are the most abundant types identified in the central and eastern Scotian Basin and the Orpheus graben, followed by type 2 or type 3. In addition, types 4 and 5 are absent from all the wells. Only 2 grains were identified as spessartine and grossular in samples from Vinegar Hill.

Naskapi N-30 and Alma K-85 are the only wells in the Scotian Basin to have some garnets with similar chemical composition and relative abundance of specific types as those in Mohican I-100 and Mohawk B-93. Types 4 and 5 garnets at Naskapi N-30 and Alma K-85 are similar to those from Mohawk B-93 and Mohican I-100. These types 4 and 5 garnets also resemble types 4 and 5 garnets from the Meguma Supergroup metasedimentary rocks (Pe-Piper et al., 2009). Type 1B and type 2 are absent from Naskapi N-30, but present in Mohican I-100 well.

The garnets at Mohican I-100 chemically are types 1B, 2, 4, and 5 (Fig.5.2). Such garnets are characteristic of anorthosites from the Grenville Province (type 1B and 2) and metamorphic rocks of the Meguma terrane (type 4 and 5) (Pe-Piper et al., 2009). Types 4 and 5 are abundant, type 1B subordinate and type 2 rare. Type 4 garnet from the Roseway Equivalent Formation in Mohawk B-93 is the only type identified, rare with most likely sources in the Meguma Supergroup metasediments. Shelburne G-29 is

lacking garnet, most likely due to dissolution with increase in depth as the sample studied was obtained from 3635 m depth.

The chemical composition and relative abundance of garnet at Mohawk B-93 and Mohican I-100, for Lower Cretaceous strata, point to a dominant sediment supply from the Meguma terrane, similar to that for Naskapi N-30 and Alma K-85, which most likely are the Meguma Supergroup metasediments and the Meguma terrane granites (Fig.5.2). The presence of type 1B and type 2 garnet in Mohican I-100 similar to type 1B and type 2 in Alma K-85 suggests a minor derivation of sediments from meta-ultramafic rocks.

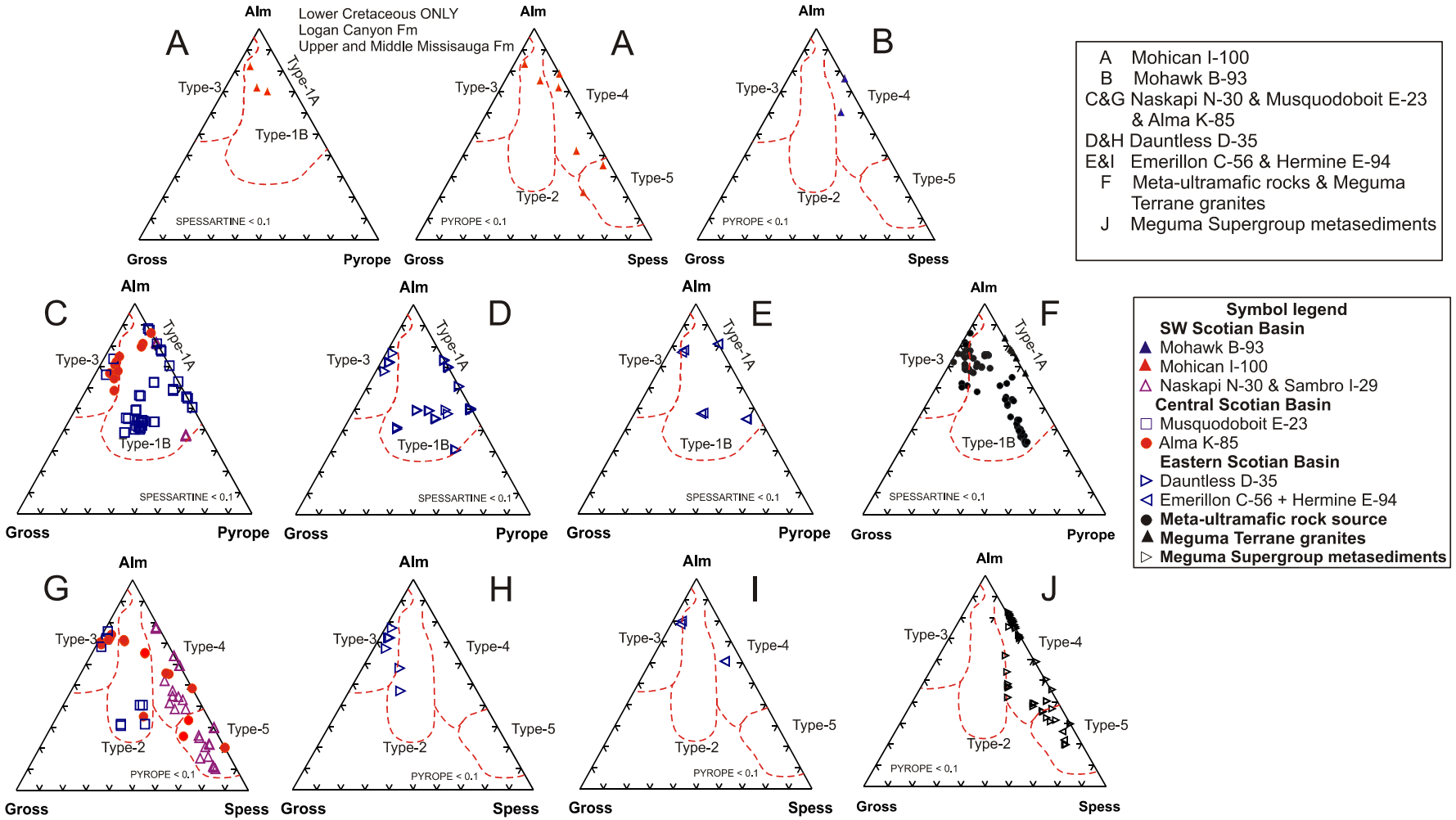

Fig.5.2: Chemical variation in garnet projected onto the Almandine - Grossular - Pyrope plane, for garnets with < 10% Spessartine and onto the Almandine - Grossular -Spessartine plane, for garnets with < 10% Pyrope for Lower Cretaceous Formations from the studied wells and wells used for comparison as well as for onshore known potential rock sources. Fields and data for wells not included in this study are taken from Pe-Piper et al. (2009).

5.1.1.3 Spinel/chromite

A few spinel/chromite grains have been analyzed from Lower Cretaceous formations in the SW Scotian Basin (Middle Missisauga in Mohican I-100 and Shortland Shale in Shelburne G-29). Spinel/chromite is absent from Mohawk B-93 well. Chemically the spinel/chromites in Mohican I-100 resemble those from boninites and this is the most abundant type followed by MORB and island-arc tholeiite derived spinel/chromite type (Fig.5.3). The same mineral assemblage is found in Shelburne G-29 with sub equal boninite and MORB types (Fig.5.3). The absence of spinel/chromite in Chaswood Formation at Vinegar Hill and in Naskapi N-30 suggests that the spinel/chromite is not derived from the Meguma terrane rock lithologies, or from the more inboard terranes of New Brunswick. The lack of supply with sediments from central and northern New Brunswick at the Naskapi N-30 can be confirmed as well from the absence of Early Paleozoic monazite from the same area (Reynolds et al., 2009).

Similar assemblage of spinel/chromite to that in the SW Scotian Basin has also been found in Lower Cretaceous formations in the central and eastern part of the basin, where it is more abundant (e.g. in Musquodoboit E-23, Alma K-85, Thebaud and Glenelg fields of the Sable sub-basin and Dauntless D-35 and Peskowesk A-99 in the Abenaki sub-basin) (Fig.5.3) and where the spinel/chromite to zircon ratio is high. The relative proportion of the three types in the SW Scotian Basin is similar to proportions in Sable sub-basin (Fig.5.4). However, the difference in the overall abundance of spinel/chromite supports the suggestion that Lower Cretaceous formations in offshore wells in the SW Scotian Basin (Mohican I-100 and Shelburne G-29) have different

potential sources from equivalent formations in wells in the central and eastern part. Spinel/chromite of MORB, IAT and boninitic affinity in the central and eastern Scotian Basin strongly suggests an ultimate source in ophiolites and/or reworking of Paleozoic sandstones. During Lower Cretaceous the central and eastern Scotian Basin were influenced with sediments transported by Sable River. As a result, most likely, at times, a distribution of the Sable River extended southwestward to the Mohican I-100 well. The periodic distribution of sediments from an ancestral Sable River in Mohican I-100 is also implied from presence of type 3 tourmaline and type 1B and type 2 garnet with sources in meta-ultramafic rocks.

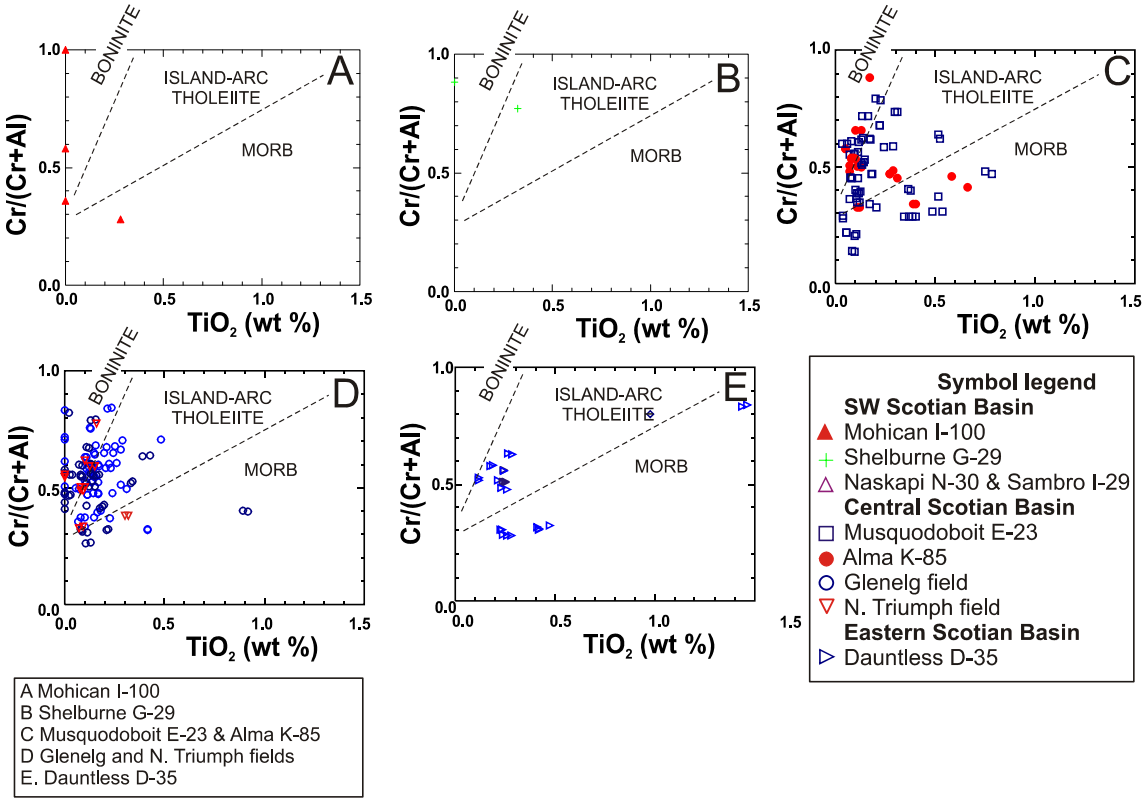

Fig.5.3: Chemical variation in spinel/chromite in wells studied and wells in the central and eastern Scotian Basin used for comparison. Fields after Pearce et al. (2000).

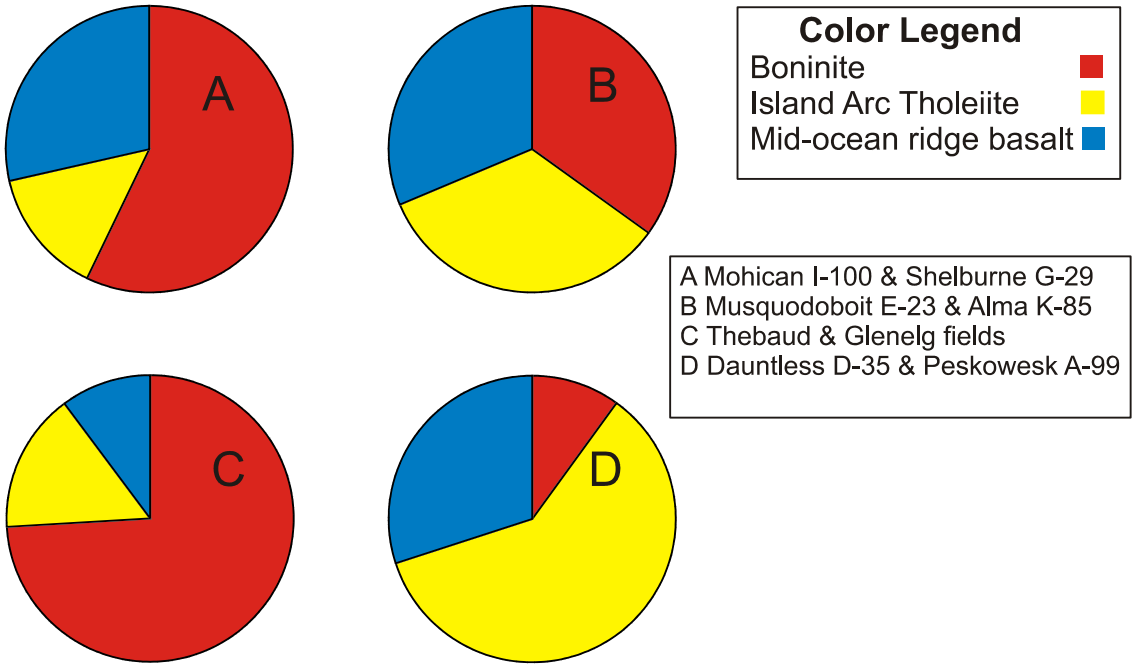

Fig.5.4: Relative proportion of the three types of spinel/chromite in the SW Scotian Basin and in the Sable and Abenaki sub-basins.

5.1.1.4 Rutile

Most of the rutile analyses from Lower Cretaceous formations in Mohican I-100 and Mohawk B-93 plot in the field that represents metapelite on a Cr vs. Nb diagram (Zack et al., 2002). Nevertheless, a Zr vs Nb discrimination diagram (Ledger, 2013) shows potential sources similar to those as shown by tourmaline (type 1 and 4) and garnet (type 4 and 5), discussed in the preceding text, either directly from an igneous (granite) or a metamorphic protolith (metapelite/metapsammite).

5.1.1.5 Micas and chlorite

Rather few muscovite analyses from heavy mineral separates in cutting samples only from Mohawk B-93 are available for Lower Cretaceous formations in SW Scotian

Basin, which have chemical composition that point to igneous rock sources (granitoids), presumably the South Mountain Batholith of the Meguma terrane. The chemical composition of muscovite in polished thin sections of conventional cores in Mohican I-100, suggest a metamorphic origin similar to muscovite from metamorphic rocks of the Meguma terrane. However, the presence of muscovite as mineral inclusions in detrital quartz indicates that some of the muscovite was derived from peraluminous igneous rocks (Fig.5.5) as well.

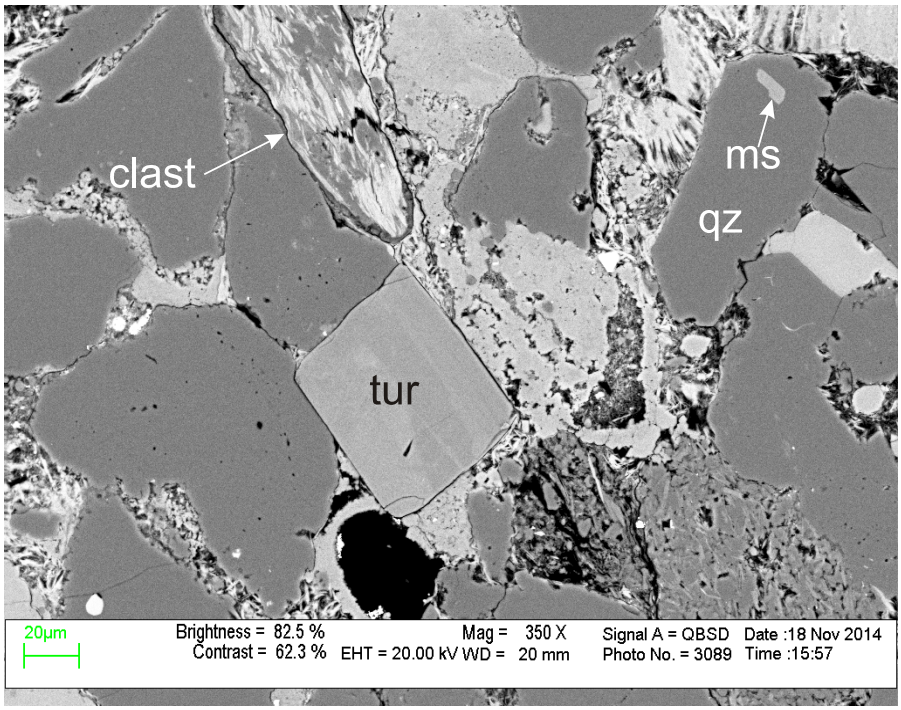

Fig.5.5: SEM back-scattered electron image of Lower Cretaceous sedimentary rock from Mohican I-100 well showing inclusion of muscovite in detrital quartz.

Muscovite ages for rock samples collected from one conventional core, at Naskapi N-30, taken from near the top of the Missisauga Formation, show derivation from the South Mountain Batholith of the Meguma terrane (Reynolds et al., 2009). On the other hand, muscovite chemistry indicates a dominant supply from metamorphic rocks and minor supply from the igneous rocks of the Meguma terrane similar to muscovite from

the SW Scotian Basin. Horton Group clastic rocks in Nova Scotia comprise muscovite with ages that reflect a late stage of exhumation of the South Mountain Batholith or ages older than the metamorphic rocks of the Meguma terrane (Reynolds et al., 2010). Only few muscovite ages from rock samples in the Horton Group are similar to those from the South Mountain Batholith. As a result, metamorphic muscovite in the SW Scotian Basin (Moheida P-15, Mohican I-100 and Mohawk B-93) was derived directly from the metamorphic rocks of the Meguma terrane, whereas igneous muscovite was sourced either from igneous rocks of the Meguma terrane or from reworking of previously deposited Horton Group clastic rocks in Nova Scotia.

Biotite chemistry from Mohican I-100 resembles some of that at Naskapi N-30, enriched in Al_2O_3 and depleted in TiO_2, representing biotite of igneous origin from peraluminous granites.

Detrital chlorite containing <1% CaO, TiO_2, K_2O and Na_2O seems to be abundant in Mohawk B-93 and almost absent from Mohican I-100 and Shelburne G-29. In all three wells detrital chlorite has higher SiO_2 and lower MgO compared to most of the detrital chlorite from the Meguma terrane (Fig.5.6). All detrital chlorite analyses in the SW Scotian Basin have < 30 wt% SiO_2, which represents the boundary between diagenetic and detrital chlorite (Sedge, 2015).

Pe-Piper and Weir-Murphy (2008) used texture, morphology mode of occurrence and grain size to classify the chlorites of the Lower Cretaceous sandstones from the Orpheus Graben into diagenetic and detrital. They further subdivided the detrital chlorites into metamorphic (sourced from metamorphic rocks) and igneous (sourced from alteration of magmatic minerals in igneous rocks, mostly basaltic cuttings). These

groups of chlorite were used to subdivide a discrimination diagram: FeO/MgO vs SiO_2/Al_2O_3. This same discrimination diagram was used in Sedge (2015) to plot the data of Gould (2007) who studied chlorite rims (diagenetic) from the Venture field of the Scotian Basin. The chlorite data of Gould (2007) defines a small field representing diagenetic minerals within the "metamorphic field" of Pe-Piper and Weir-Murphy (2008). Detrital chlorite analyses from Mohawk B-93, Mohican I-100 and Shelburne G-29 plot in the "metamorphic" field of Pe-Piper and Weir-Murphy (2008) but outside of the diagenetic field of Gould (2007).

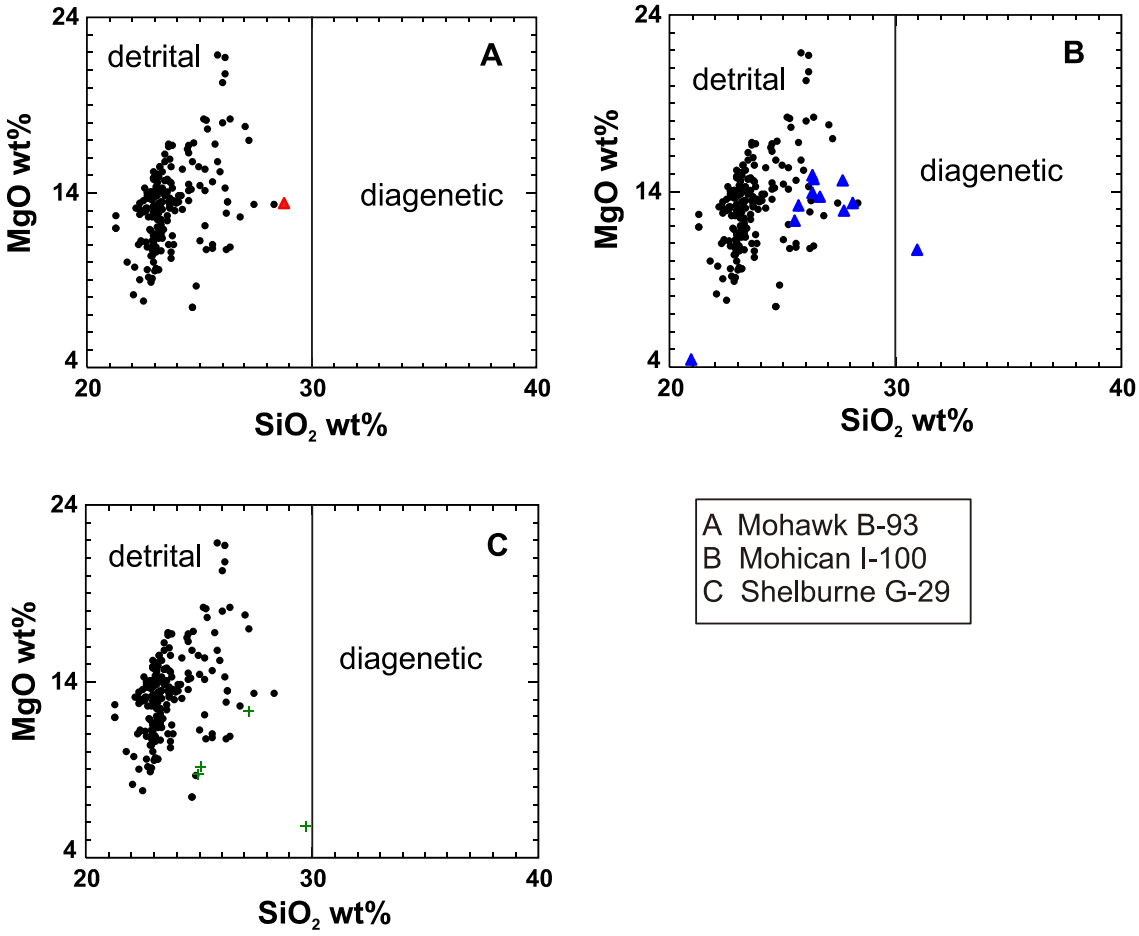

Fig.5.6: Chemical variations in chlorite based on MgO wt% vs SiO2 wt% for studied wells (colored symbols). Comparison of data between wells studied and Meguma Group metasediments, data for Meguma Group metasediments (black dots) taken from Dr. Chris White. Fields taken after Pe-Piper et al. (2009).

5.1.1.6 Other heavy minerals

Staurolite and some ilmenite from cutting samples collected at Mohican I-100 and Mohawk B-93, show similar low composition in MnO (<0.5 wt% for staurolite and <1.5 wt% for ilmenite), as does most of staurolite and ilmenite from Vinegar Hill, southern New Brunswick (Piper et al., 2007). However, the chemistry of a mineral is not always characteristic of a single source and thus both minerals could have been derived from the Meguma terrane.

Ilmenite with low abundance in Mn at Vinegar Hill, with likely provenance from igneous rocks (Basu and Molinaroli, 1989), when compared to those from northern Nova Scotia (Pe-Piper et al., 2005*b*), suggest that rivers depositing sediments at Vinegar Hill did not extend to Nova Scotia (Piper et al., 2007). Therefore, it is more likely that Vinegar Hill River and other rivers might have passed through low lands in the Fundy Basin, entered and finally deposited some sediments to the Shelburne delta (Wade and MacLean, 1990).

5.1.1.7 Feldspar and lithic clasts

Feldspar is a very abundant detrital mineral in polished thin section of conventional cores from Mohican I-100. Specifically, orthoclase and perthite are the most common feldspars identified (Fig.5.7). The presence of potassic feldspar together with intimate intergrowth of sodic and potassic feldspar (perthite) suggests derivation from felsic igneous rocks like granite, syenite and granodiorite. The high abundance in potassic rich feldspars is also observed from the feldspar classification diagram where most of the analyses plot as orthoclase.

Lithic clasts are common in Mohican I-100, with abundant polycrystalline quartz (metapsammite) and some greenschist facies metamorphic rocks (chlorite schist) with a foliation. The characteristic mineralogical assemblage of lithic clasts that point to metamorphic rock sources is abundant chlorite and polycrystalline quartz and lesser muscovite (Fig.5.8) Based on mineralogical composition and texture and their similarity to lithic clasts from Naskapi N-30, most likely rock sources for these lithic clasts are slates and metasandstones of the Meguma Supergroup.

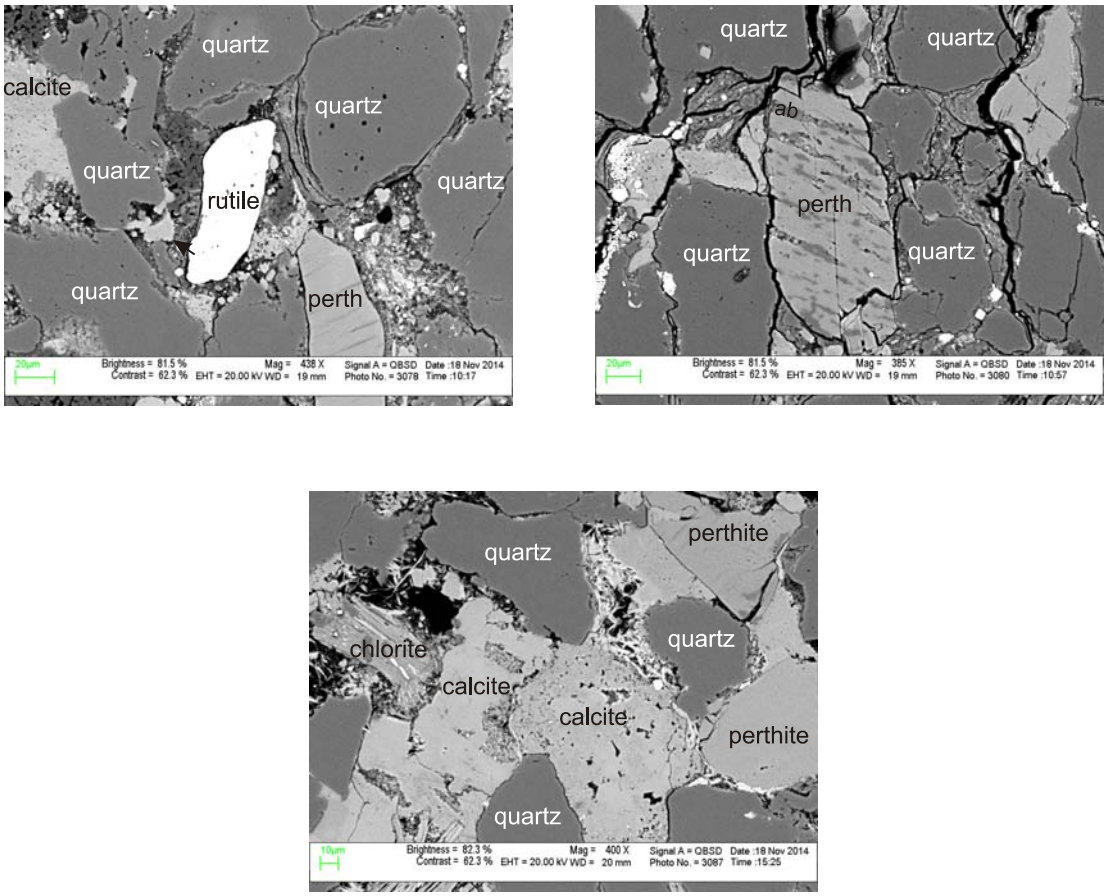

Fig.5.7: SEM back-scattered electron images of Lower Cretaceous sedimentary rocks from samples studied at Mohican I-100 showing abundance in detrital K-feldspar and perthite.

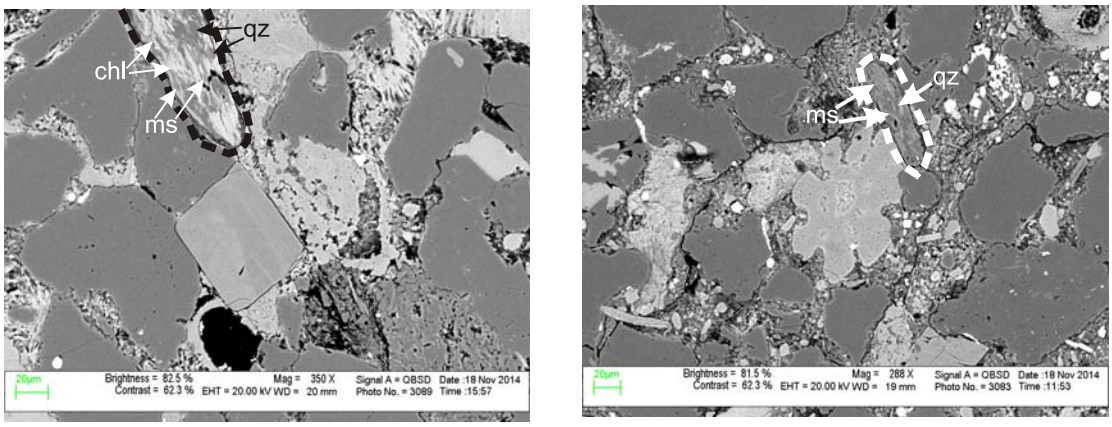

Fig.5.8: SEM back-scattered electron images of Lower Cretaceous sedimentary rocks from samples studied at Mohican I-100 showing mineralogical composition in lithic clasts.

5.1.1.8. Stratigraphic trends in modal abundance of heavy minerals-Lower Cretaceous

The different sources for sediments in the SW Scotian Basin, when compared to central Scotian Basin, can also be revealed from modal abundance of detrital heavy minerals. The dominant detrital minerals at Mohawk B-93, Mohican I-100 and Shelburne G-29 are in decreasing order ilmenite, tourmaline, zircon, garnet, rutile and spinel/chromite (Fig.5.9). In contrast, in the central Scotian Basin, zircon is the most abundant; spinel/chromite is subordinate followed by tourmaline, and garnet, which are rare.

Based on modal mineral abundance, the Lower Cretaceous rock sources for sediments in the SW Scotian Basin are also different from sources for the Chaswood Formation in Nova Scotia and New Brunswick (Fig.5.9). The fluvial Chaswood Formation was mostly supplied with sediments from central New Brunswick at Vinegar Hill (southern New Brunswick) and from northern New Brunswick at Elmsvale (central Nova Scotia) and Brierly Brook (eastern Nova Scotia), based on monazite geochronology (Pe-Piper and MacKay, 2006). Staurolite and andalusite are the most

abundant minerals at Vinegar Hill, most likely derived from a metapelitic rock source (Piper et al., 2007). Ilmenite, tourmaline and staurolite are the most abundant at Elmsvale Basin and Brierly Brook probably sourced from more inboard Appalachians with a minor influence from rocks of the Meguma terrane (Piper et al., 2008).

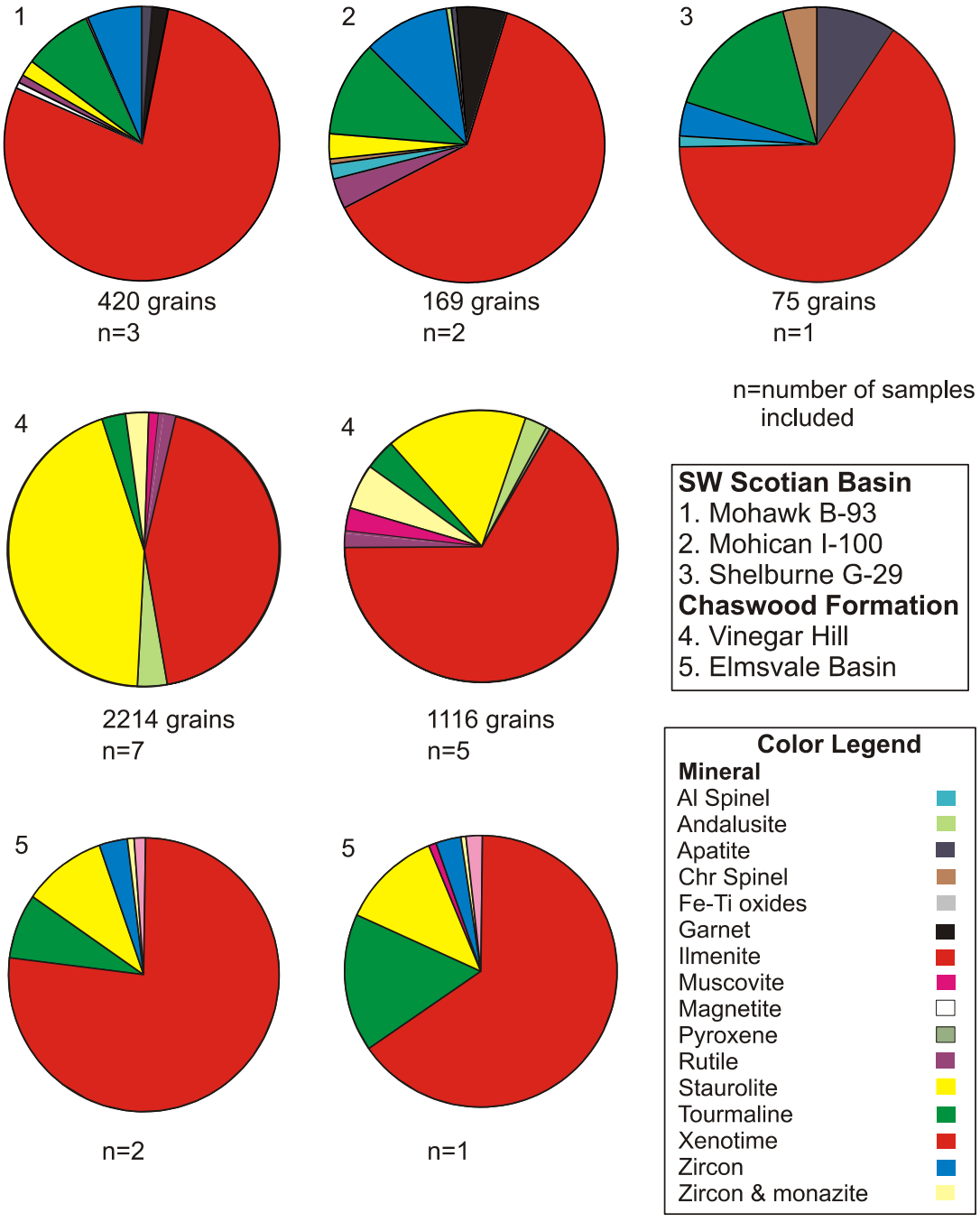

Fig.5.9: Pie chart diagrams showing differences in the modal abundance of detrital heavy minerals in cutting samples for Lower Cretaceous Formations in the studied wells and samples from the Lower Cretaceous Chaswood Formation. Data for the Vinegar Hill is taken from Piper et al. (2007), whereas data for the Elmsvale Basin is taken from Pe-Piper et al. (2004) and Piper et al. (2008).

The Horton Group in Nova Scotia has same modal abundance in detrital heavy minerals as Lower Cretaceous formations in the SW Scotian Basin (Tsikouras et al., 2011). However, the chemical composition and the relative abundance of different types of tourmaline and garnet in the Horton Group do not resemble entirely garnet and tourmaline from the SW Scotian Basin. From the four types identified in the Horton Group only three, types 1, 2 and 3 are present in the SW Scotian Basin. Although types 1, 3 and 4 in the SW Scotian Basin have same relative abundance as types 1, 3 and 4 tourmaline in the Horton Group, type 2 is absent. Garnet from the Horton Group is typically grossularite, which is abundant, followed by Mn-almandine, Ca- Mg-almandine and rare andradite. SW Scotian Basin is abundant in spessartine and Mn-rich almandine garnet. Differences in modal abundance of detrital heavy minerals are also observed between Mohawk B-93, Mohican I-100 and Shelburne G-29. These differences include mostly the abundance of ilmenite, tourmaline, garnet, staurolite, zircon and rutile. In Mohawk B-93 ilmenite is the most dominant mineral. Zircon and tourmaline are equal in abundance and subordinate, with rare but equal abundance in staurolite and garnet. Although zircon represents an important component in the heavy mineral separates, its percentage decreases significantly with increase in depth, compared to ilmenite which shows high increase and tourmaline which shows low increase with depth (Fig.5.10). The decrease in proportion of ultra-stable zircon to ilmenite and the absence in ilmenite alteration products may indicate less supply from polycyclic sources and more supply from crystalline bedrock abundant in ilmenite and tourmaline. The abundance of metamorphic over igneous tourmaline in the modal composition indicates strong input from metamorphic rock sources.

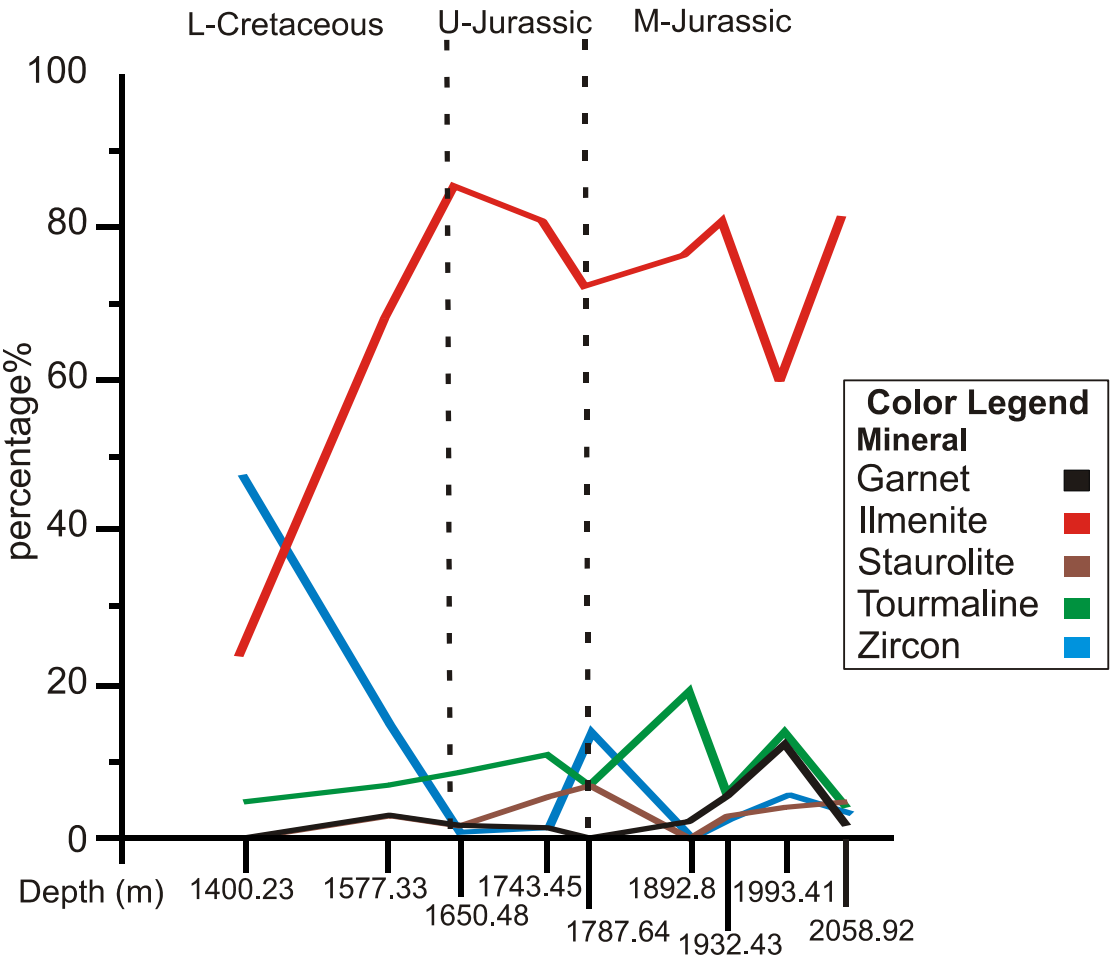

Fig.5.10: Scatter plot showing variations in abundance of the 5 most abundant detrital minerals found at Mohawk B-93.

In Mohican I-100 ilmenite is the most abundant detrital heavy mineral identified, followed by tourmaline and garnet (almandine, spessartine), whereas zircon and staurolite are rare. Tourmaline at Mohican I-100 is inversely proportional to ilmenite, which decreases in abundance with increasing depth (Fig.5.11). The increase in tourmaline at different depths, might suggest that the rivers supplying were draining crystalline rocks with different amounts of tourmaline. Specifically, the high presence of tourmaline with a metapelitic/metapsammitic origin, when compared to those with an igneous and a meta-ultramafic origin, together with abundance in types 4 an 5 garnet suggest that the rivers were probably draining large areas of metamorphic rocks. The

decrease in ilmenite might be a result of its loss through alteration, which implies polycyclic origin e.g. with reworking of Carboniferous sandstones of the Horton Group and/or Jurassic sandstones in the proximal part of the Scotian Basin. However, specific evidence for this process is lacking in Mohican I-100 as ilmenite alteration products (TiO_2 minerals) are almost absent in all samples. Detrital rutile is present only in one stratigraphic level from Lower Cretaceous Upper Mississauga Formation.

Different types and relative abundance of garnet were identified in sandstones from Mohawk B-93 and Mohican I-100. Almandine with prominent substitution of spessartine, pyrope and grossular is abundant whereas spessartine with prominent almandine substitution is rare. According to Morton (1987) garnet compositions become less diverse due to preferential dissolution of the more calcium-rich garnets, especially below about 2 km. In this study, Shelburne G-29 is a deep well (4000m total depth), the sample studied was obtained from 3635m and Ca-garnet dissolution may be the reason why garnet is lacking.

Modal abundance at Shelburne G-29 is represented by abundant ilmenite with less presence of tourmaline and rare apatite, spinel/chromite and zircon.

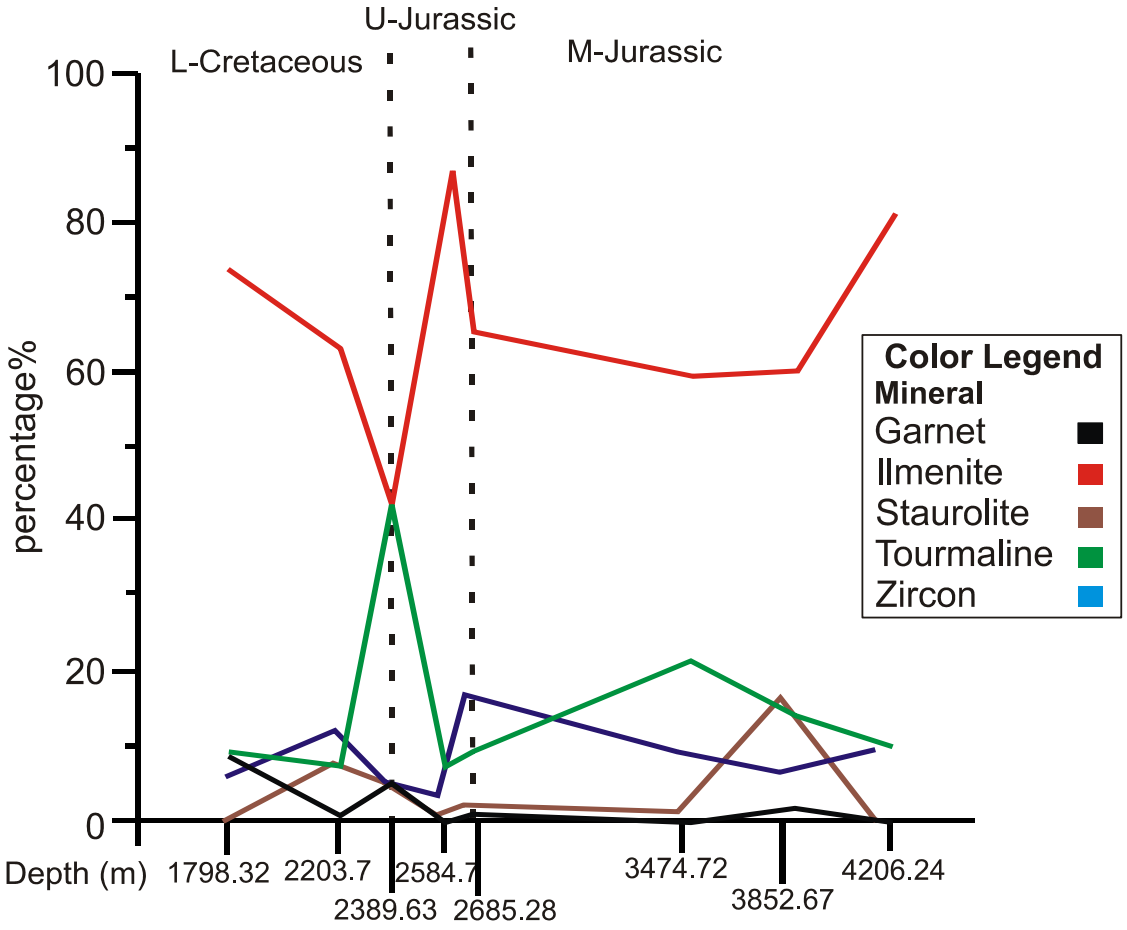

Fig.5.11: Scatter plot showing variations in abundance of the 5 most abundant detrital minerals found at Mohican I-100.

5.1.1.9 Polycyclic sources to the SW Scotian Basin-Lower Cretaceous

Magnetite is the dominant mineral in clastic deposits in the Fundy Basin with rare apatite, tourmaline, garnet, tremolite, richerite and anthophyllite. The absence of ultra-stable detrital minerals, such as zircon and rutile, indicative of polycyclic sources, suggests that the sediments are first cycle and probably were sourced from crystalline rocks enriched in magnetite, such as basalts. On the other hand Lower Cretaceous clastic deposits in southernw New Brunswick are enriched in staurolite and andalusite, followed by ilmenite and its alteration products, with rare tourmaline, zircon and rutile.

In general, the mineralogical composition of clastic deposits in the Fundy Basin and in southern New Brunswick suggests that the sediments tend to be first cycle from crystalline rocks.

Specifically, the Scots Bay Formation at Chinampas O-37 in the Fundy Basin has different mineral composition compared to sediments in the SW Scotian Basin at Mohawk B-93, as well as different modal abundances of detrital heavy minerals in cuttings samples (Fig.5.12).

Although it is believed that the Vinegar Hill River deposited in southern New Brunswick might have passed through the Fundy Basin, there is no evidence that it deposited in the SW Scotian Basin as far east as Mohawk B-93. For example heavy mineral separates in Mohawk B-93 are enriched in ilmenite, tourmaline and zircon, whereas the Scots Bay Formation is abundant in magnetite. This fact implies that there was no influence from reworking of Early Jurassic rocks from the Fundy Basin in the SW Scotian Basin during Early Cretaceous.

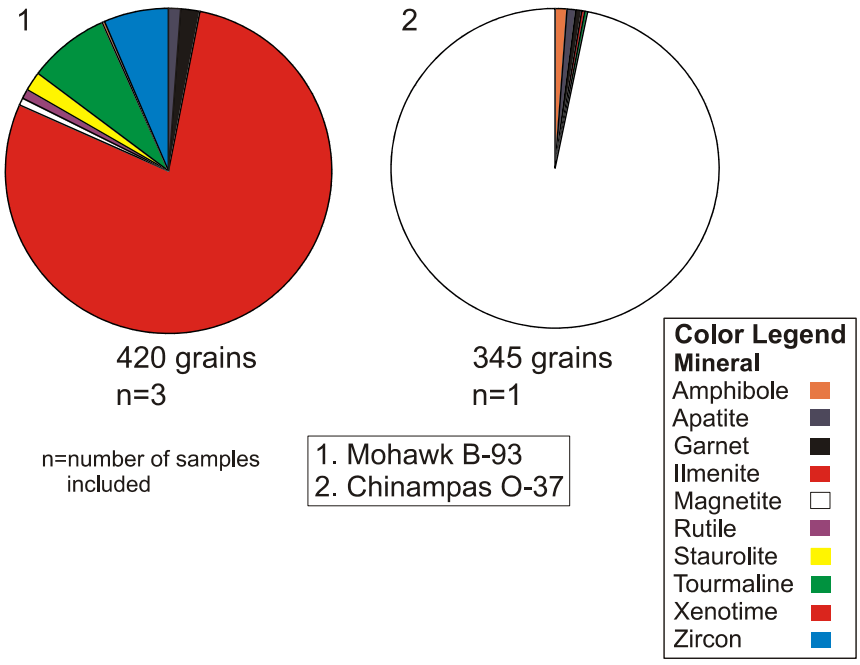

Fig.5.12: Pie chart diagrams showing differences in the modal abundance of detrital heavy minerals in cutting samples for Lower Cretaceous Formations at Mohawk B-93 and samples from the Scots Bay Formation at Chinampas O-37 in the Fundy Basin.

5.1.1.10 Summary

The heavy and light mineral analysis has been proved to be a valuable tool for discrimination of sources for Lower Cretaceous sediments in the Scotian Basin. Tourmaline, garnet, rutile, muscovite and biotite chemistry, together with mineral abundance, all indicate different sources to the SW compared to the central and eastern Scotian Basin. For example, the SW Scotian Basin was supplied by a source almost lacking spinel/chromite, in comparison with the central and eastern Scotian Basin, which shows sources abundant in zircon and spinel/chromite through reworking of Paleozoic sandstones. Chemical composition and modal abundance of detrital minerals in Mohican I-100, Mohawk B-93 and Shelburne G-29 do not reflect any influence from polycyclic sources through reworking of sedimentary rocks older than Mesozoic. Monazite and zircon geochronology in the central Scotian Basin suggests derivation of sediments through a river draining local areas of the Meguma terrane. Monazite is absent from the SW part of the basin. In addition, garnet and tourmaline in the SW Scotian Basin have different chemical composition and thus different types when compared to garnet and tourmaline from the central and eastern part of the basin.

Ilmenite, tourmaline, garnet, rutile, muscovite, chlorite and biotite chemistry all indicate that the predominant source area comprises mostly metapelites/metapsammites and granites. Abundant Mn-rich ilmenite is known from the Meguma Supergroup metasediments. Tourmaline is almost exclusively from metapelites/metapsammites (low grade metamorphic rocks) with small amount from granites. Garnet, rutile and chlorite are mostly all from metamorphic rock sources. Muscovite as tourmaline is both of metamorphic and igneous origin. Muscovite and tourmaline inclusions in detrital

quartz indicate peraluminous granites. Orthoclase is a major component in felsic rocks such as granite. Lithic clasts in the studied rocks have characteristic mineralogical composition typical of low-grade metamorphic rocks, as is the case for metasedimentary rocks of the Meguma terrane. The only such source area in Atlantic Canada that is characterized by rocks of low grade greenschist metamorphism, abundant in ilmenite/tourmaline, and peraluminous granites is the Meguma terrane of the southern Nova Scotia.

In addition to the main source from the Meguma terrane, several lines of evidence suggest a small influence from one or more rivers draining one or more distant sources occurred during Lower Cretaceous, particularly in Mohican I-100. The evidence includes the presence of unusual type 1B and type 2 garnets (almandine with significant grossular substitution), with chemical composition similar to those from anorthosite, possibly from anorthositic bedrock of the Grenville Province, from a small presence of spinel/chromite with sources from meta-ultramafic rocks and from the presence of type 3 tourmaline. This evidence suggests that in Mohican I-100, because of its location, mixing of sediments from rivers with different sources was possible. At times, an ancestral Sable River depositing sediments in the Sable sub-basin (Zhang et al., 2014) might have transported sediments from Labrador westwards in Mohican I-100 well. This fact is confirmed from comparison of types and chemical composition only of garnet and spinel/chromite at Alma K-85, which was predominantly supplied by Sable River, with minor Meguma terrane input.

Similar types and abundances of spinel/chromite and garnet are found at Alma K-85 compared to spinel/chromite and garnet at Mohican I-100. A total of six garnet types

were identified (1A, 1B, 2, 3, 4 and 5) at Alma K-85, whereas at Mohican I-100 only four types are present (1B, 2, 4 and 5). Types 2 and 3 at Alma K-85 are similar to type 2 from Mohican I-100 with sources from the Grenville Province. In both wells the common types 1B, 2, 4 and 5 have similar abundances. Although type 1A is absent from Mohican I-100, at Alma K-85 only one garnet is type 1A.

Spinel/chromite is the most representative mineral showing transportation of sediments by the Sable River in the central (e.g. Alma K-85) and eastern Scotian Basin (e.g. Peskowesk A-99). Spinel/chromites at both Mohican I-100 and Alma K-85 have two types with similar chemical composition, one enriched in Al and one enriched in Fe.

Although garnet and spinel/chromite at Mohican I-100 when compared to similar minerals at Alma K-85 have same characteristics there are differences in the modal abundance for each of the mineral species in both wells. Garnet and spinel/chromite are abundant at Alma K-85 whereas at Mohican I-100 are rare. However, abundance differences are expected as ~80% of the sediments at Alma K-85 were transported by an ancestral Sable River with sources from the Grenville Province and Labrador (Zhang et al., 2014) and ~20% were transported by local rivers draining areas of the Meguma terrane. On the other hand at Mohican I-100 ~90% of the sediments were transported by rivers draining areas of the Meguma terrane and only ~10% seem to have been transported by an ancestral Sable River.

At Alma K-85 tourmaline of type 4 is abundant with the remainder type 1 subordinate; type 3 is absent. However, only 7 analyses have been reported (Pe-Piper et al., 2009). Type 4 tourmaline at Mohican I-100 is as abundant as in Alma K-85, type 1

is still subordinate and type 3 is rare. Type 3 tourmaline was interpreted by Pe-Piper et al (2009), based on Kassoli-Fournaraki and Michailidis (1994), in the central and eastern Scotian Basin as sourced from meta-ultramafic rocks, meta-carbonate rocks or Cr-V-rich metasedimentary rock. Tsikouras et al. (2011) found type 3 tourmaline in the Horton Group and in sand from the Debert River in northern Nova Scotia. This observation implies that some sources for type 3 tourmaline exist in the Meguma and Avalon terranes. The type 3 tourmaline at Mohican I-100 thus might have been sourced either from the Grenville Province meta-carbonate rocks of the Meguma or Avalon terranes.

Tourmaline of type 3, spinel/chromite and garnet of type 1B and 2 are absent from all the samples at Mohawk B-93, suggesting that the most SW part of the Scotian Basin did not receive sediment dispersed southwestward from the Sable River during Lower Cretaceous. Spinel/chromite is present at Shelburne G-29, which suggests a possible Sable River source.

5.1.2 Sources for the Upper Jurassic sandstones in the SW Scotian Basin

5.1.2.1 Tourmaline

The chemical composition and the modal abundance of detrital heavy minerals, such as tourmaline, garnet and detrital light minerals such as muscovite, biotite and chlorite, from Upper Jurassic formations, are compared to chemical composition and modal abundance of similar minerals from Lower Cretaceous strata in the SW Scotian Basin and Upper Jurassic strata in the Sable sub-basin.

Tourmaline from Upper Jurassic strata in Mohican I-100 (Roseway Equivalent

Formation) and Mohawk B-93 (Mohawk Formation) has similar chemical composition and abundance in types 4 and 1 as Lower Cretaceous tourmaline in same wells. A lack of type 3 tourmaline in Upper Jurassic strata in both wells indicates no influence from a meta-ultramafic or a meta-carbonate rock source (Fig.5.13). As argued previously for Lower Cretaceous strata, the presence of type 4 and type 1 tourmaline suggests sediments with sources from metamorphic and igneous rocks of the Meguma terrane, respectively.

Tourmaline from the lower member of Missisauga Formation at the Thebaud and Venture fields in the Sable sub-basin has types 4 and 1 similar in abundance as tourmaline from Upper Jurassic strata. However, differences in the chemical composition suggest different sources (Fig.5.13). Type 4 tourmaline in Mohican I-100 and Mohawk B-93 tend to show a wide range of Al and small range in Mg and Fe, whereas tourmaline from the Venture and Thebaud fields show consistent Al composition and important differentiation in Mg and Fe. Moreover type 3 present at both the Venture and Thebaud fields is absent from both Mohawk B-93 and Mohican I-100.

In general Upper Jurassic tourmaline shows less variability regarding chemical composition in both Mohawk B-93 and Mohican I-100 compared to Lower Cretaceous tourmaline, with depletion in Fe and enrichment in Mg.

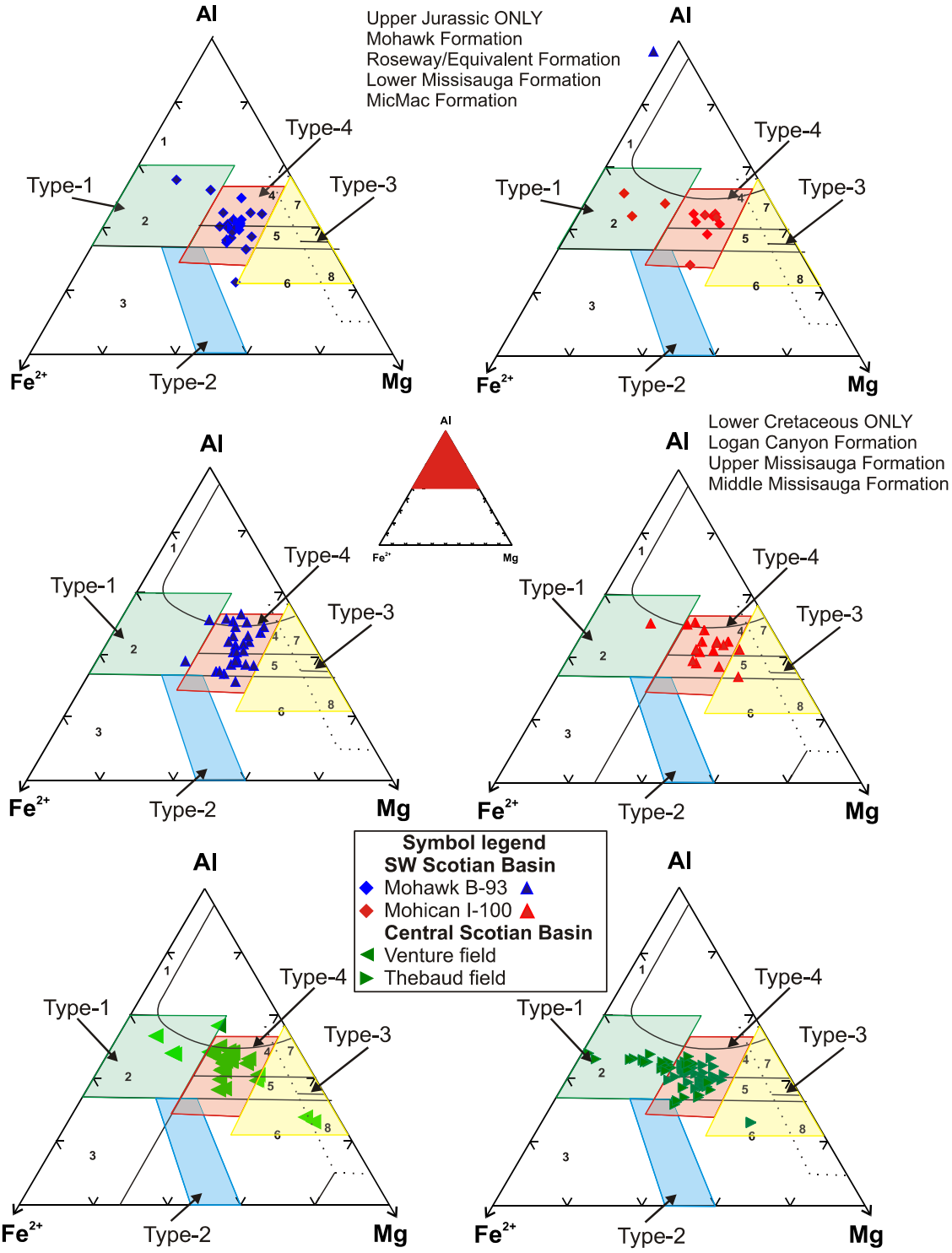

Fig.5.13: Chemical variation in tourmaline based on Al - Mg - Fe showing differences and similarities in types between Lower Cretaceous and Upper Jurassic. Fields after Pe-Piper et al. (2009).

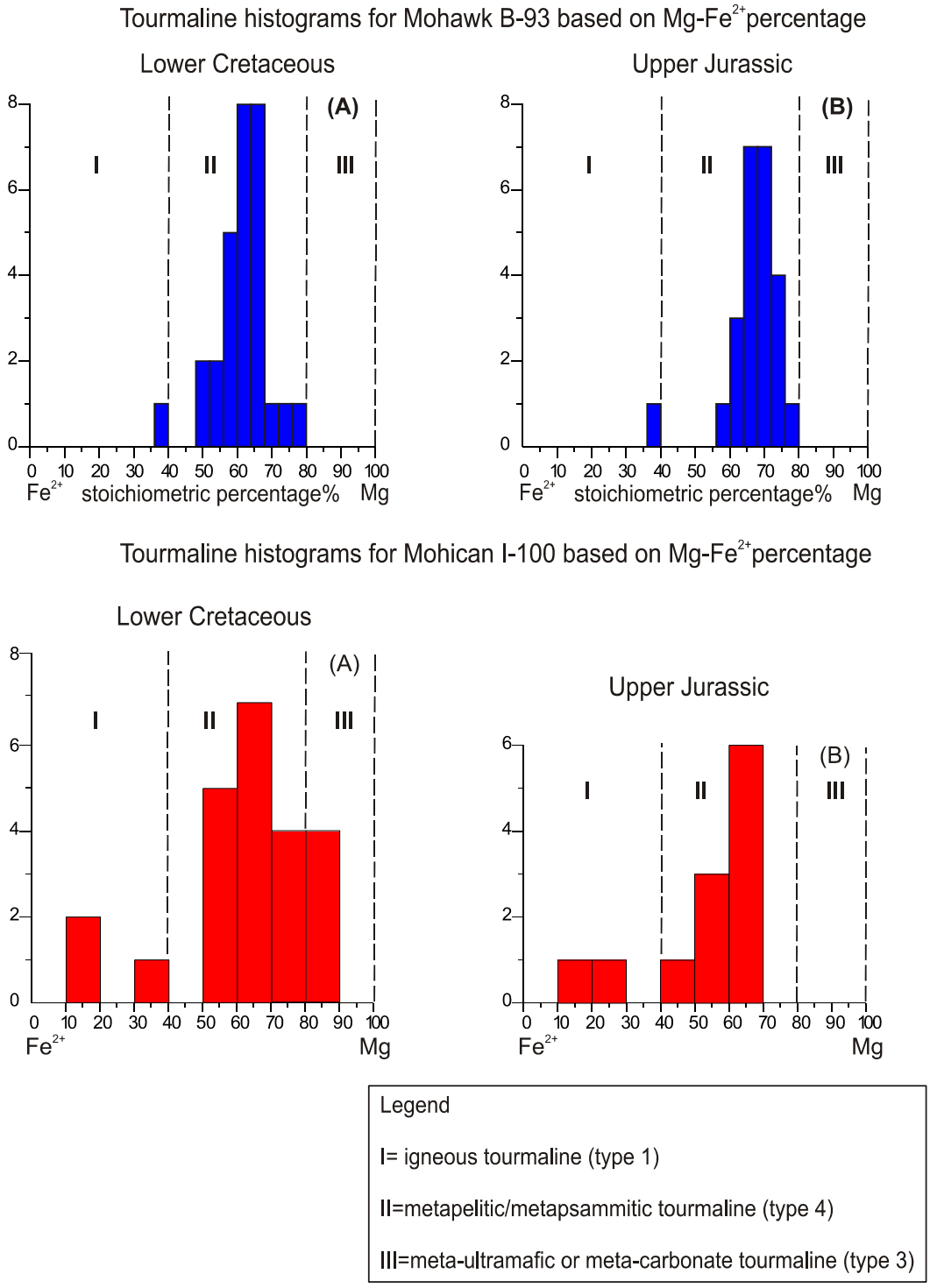

Fig.5.14: Histrograms of detrital tourmaline from the studied wells showing chemical differentiation in Fe^{2+} and Mg and thus different potential rock sources.

5.1.2.2 Garnet

Type 5 garnet is the only type found in the Upper Jurassic Formation in Mohican I-100. In Mohawk B-93 two types, 4 and 5 were identified in Upper Jurassic formations. Types 4 and 5 in both wells have chemical composition similar to those of the Meguma Supergroup metasediments from Beaverbank (Feetham, 1995) and Rawdon (Haysom, 1994). Similar chemical composition to types 4 and 5 garnet from Upper Jurassic strata have also been seen in Lower Cretaceous formations at Mohawk B-93 and Mohican I-100 (Fig.5.15). Garnet from Upper Jurassic strata in the central and eastern Scotian Basin is known only from the lower member of the Missisauga Formation in the Thebaud field. Its chemical composition represents types 1A and 4. Type 4 is enriched in Fe when compared to type 4 in Mohawk B-93, which is enriched in Mn.

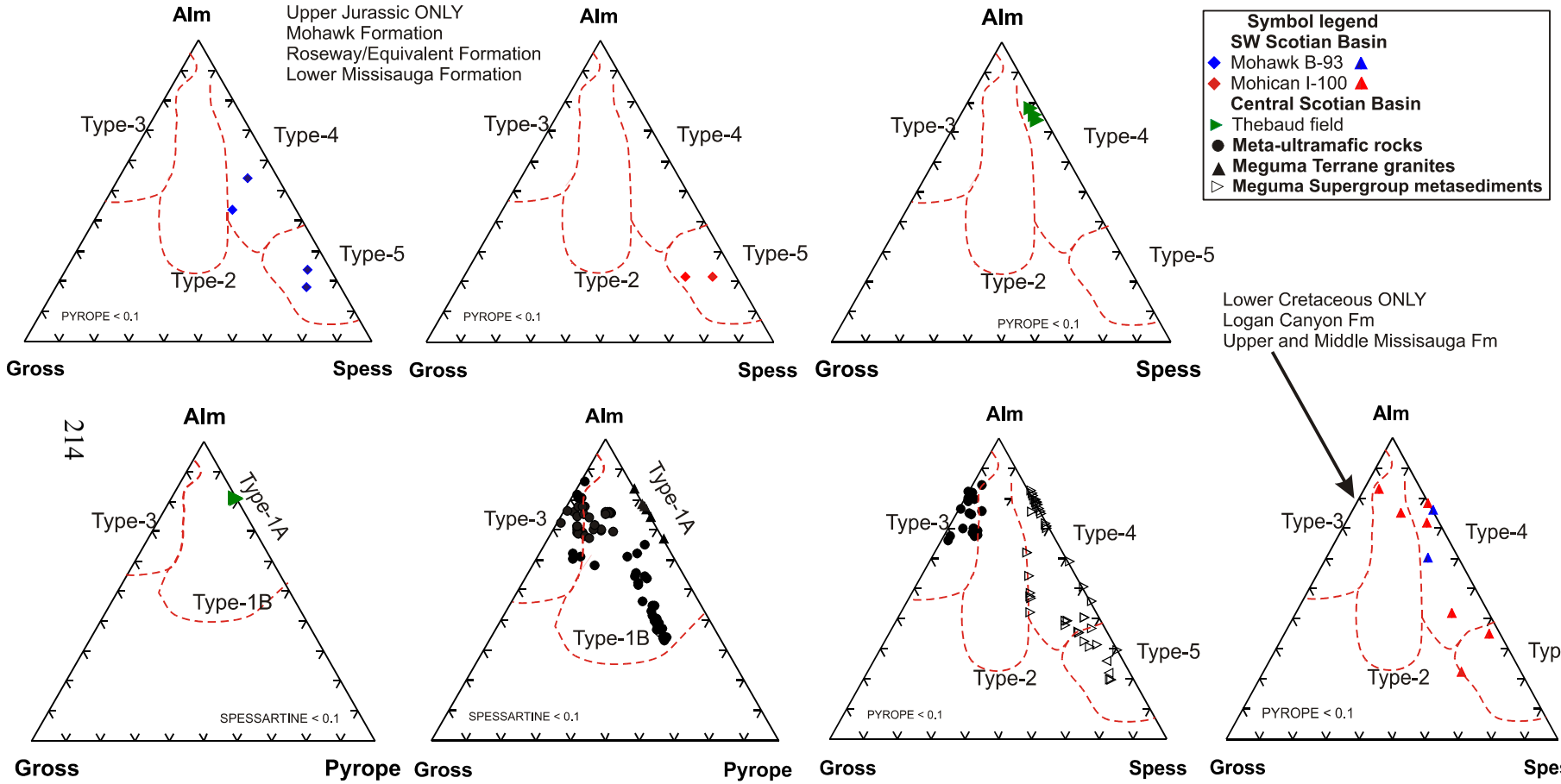

Fig.5.15: Chemical variation in garnet projected onto the Almandine - Grossular - Pyrope plane, for garnets with < 10% Spessartine and onto the Almandine - Grossular -Spessartine plane, for garnets with < 10% Pyrope for Lower Cretaceous-Upper Jurassic strata from the studied wells, Upper Jurassic strata for wells used for comparison as well as for onshore known potential rock sources. Fields after Pe-Piper et al. (2009).

5.1.2.3 Muscovite

Muscovite chemistry is restricted, indicating derivation from metamorphic rocks, which Reynolds et al. (2009) showed for Naskapi N-30 was from rocks metamorphosed in the Acadian and Alleghanian orogenies (Pe-Piper and Jansa, 1999). This observation implies some erosion of the Meguma terrane on the inner Scotian Shelf. Muscovite in the Venture and Thebaud fields is similar to Upper Jurassic muscovite in the SW Scotian Basin.

5.1.2.4 Biotite

Biotite is absent at Naskapi N-30 and the Thebaud and Venture fields, whereas in Mohican I-100 and Mohawk B-93 is dominant, depleted in Al_2O_3 and enriched in TiO_2. Biotite enriched in TiO_2 and depleted in Al_2O_3 is characteristic of amphibolite (intermediate) grade metamorphic rocks, with only minor amounts at greenschist (low) grade. Its appearance is characteristic of upper greenschist grade but it becomes more abundant at amphibolite grade.

5.1.2.5 Chlorite

Detrital chlorite in Mohican I-100 and Mohawk B-93 has similar composition in SiO_2 and MgO as most of the detrital chlorites from both Lower Cretaceous strata and metamorphic rocks of the Meguma terrane. All detrital chlorite analyses plot in the "metamorphic" field based on detrital chlorite analyses from Pe-Piper and Weir-Murphy (2008) but outside of the diagenetic field based on diagenetic chlorite analyses from Gould (2007).

5.1.2.6 Ilmenite

Ilmenite at Mohican I-100 and Mohawk B-93 shows similar low content of MnO (<1.5 wt%) as does most of ilmenite from Lower Cretaceous strata in the same wells and Vinegar Hill. The chemistry of a single mineral species is not always characteristic of a single source and thus ilmenite could have been derived from the Meguma terrane or from other sources that provided sediments to Vinegar Hill. However, because the chemistry of other detrital minerals such as tourmaline and types 4 and 5 garnet in the SW Scotian Basin tend to show a local supply from the Meguma terrane, it is most likely that same source has provided ilmenite.

5.1.2.7 Stratigraphic trends in modal abundance-Upper Jurassic

Modal abundance of detrital minerals in Upper Jurassic strata shows less diversity in detrital heavy minerals, compared to modal abundance for Lower Cretaceous strata in the same wells (Fig.5.16). The only detrital heavy minerals identified are ilmenite, tourmaline, zircon, staurolite and garnet; rutile and spinel/chromite are absent.

Ilmenite is still the most abundant detrital mineral identified in Upper Jurassic sandstones at both Mohawk B-93 and Mohican I-100, as it is for Lower Cretaceous formations in the same wells. However, ilmenite from the Upper Jurassic at Mohawk B-93 decreases with depth. In contrast ilmenite from the Upper Jurassic at Mohican I-100 increases with depth. This implies that although both wells are located in the SW Scotian Basin, at different different rock sources were eroded: at Mohican I-100 a source enriched in ilmenite, whereas at Mohawk B-93 a source depleted in ilmenite. Alternatively this difference may be due to different weathering of the transported

detritus and/or increase of ilmenite dissolution as the burial depth increases and/or hydraulic sorting.

Tourmaline is the second most abundant detrital heavy mineral in Mohawk B-93, with higher percentage than tourmaline from the Lower Cretaceous in the same well. In addition, tourmaline tends to increase with depth, suggesting an increasingly more tourmaline dominant source (see Fig.5.10). A small change in tourmaline abundance is observed towards the base of the Late Jurassic in Mohawk B-93 suggesting less contribution from rocks rich in tourmaline. Tourmaline in Mohican I-100 decreases with depth compared to Lower Cretaceous tourmaline (see Fig.5.11). All these changes probably are due to local variations in tourmaline in the source rocks.

Garnet decreases in Upper Jurassic strata in Mohican I-100, continuing a trend shown by the Lower Cretaceous in the same well (see Fig.5.10). Regarding Mohawk B-93, garnet shows a small increase with depth compared to Lower Cretaceous strata (see Fig.5.11). The increase is represented by presence of type 5 garnet, which is absent from Lower Cretaceous strata.

Zircon decreases from the Cretaceous to the Upper Jurassic and is subordinate to tourmaline in Mohawk B-93 (see Fig.5.10). The exception is in the lower Upper Jurassic where a sudden increase in zircon is observed. On the other hand zircon abundance in Mohican I-100 tends to be constant and have the same abundance as Lower Cretaceous zircon (see Fig.5.11).

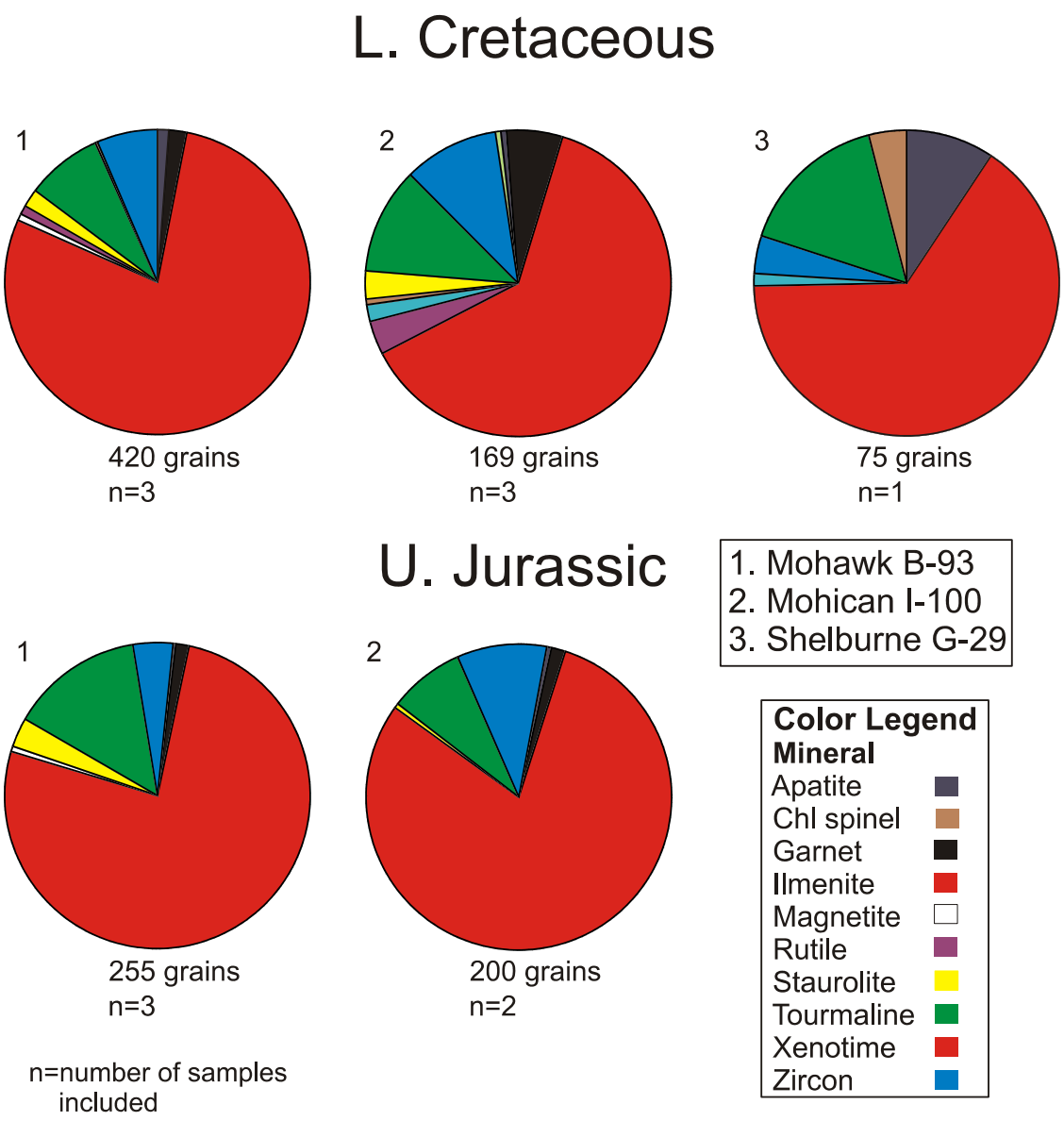

Fig.5.16: Pie chart diagrams showing differences in the modal abundance of detrital heavy minerals in cutting samples between Lower Cretaceous and Upper Jurassic strata in the studied wells.

5.1.2.8 Summary

Garnet, muscovite and chlorite chemistry all show derivation only from the metamorphic rocks of the Meguma terrane. Tourmaline is sourced from both metamorphic and igneous rocks, presumably of the Meguma terrane, as implied from

similar chemistry of Lower Cretaceous tourmaline. Biotite is mostly metamorphic with a small presence of biotite of igneous origin. Abundant Mn-rich ilmenite is known from the Meguma Supergroup metasedimentary rocks. Thus the main source for sediments for Upper Jurassic strata is the Meguma terrane, with a major influence from metamorphic rocks and a minor influence from igneous rocks. Although the main source for sediments in both Lower Cretaceous and Upper Jurassic strata in the SW Scotian Basin is the same, the local distribution of metamorphic and igneous source lithologies is different in Mohican I-100 and Mohawk B-93. Sediments during Early Cretaceous in Mohican I-100 were eroded from areas of the Meguma terrane enriched in tourmaline, whereas during Late Jurassic areas enriched in ilmenite were eroded. The opposite is the case for Mohawk B-93 where ilmenite-rich rocks were eroded during Early Cretaceous and tourmaline rich rocks were eroded during Late Jurassic. The fact that the distribution with sediments is different for Mohican I-100 and Mohawk B-93 implies that probably more than one river drained different areas of the Meguma terrane and thus depositing sediments with different character off SW Nova Scotia.

Apart from a major contribution of sediments from the Meguma terrane, during the Late Jurassic, a small influence from rocks rich in ultra-stable minerals was detected in samples from Mohawk B-93, as implied by the small increase in modal abundance of zircon. The increase in zircon abundance can be a result of reworking of sedimentary rocks or derivation with sediments from a source hosting zircons, as for example granites. There is no evidence of any contribution from the Sable River or the Vinegar Hill River to Mohican I-100 or the wells around it.

5.1.3 Sources for the Middle Jurassic sandstones in the SW Scotian Basin

5.1.3.1 Tourmaline

The detrital heavy minerals from Middle Jurassic strata were also compared to Lower Cretaceous and Upper Jurassic detrital minerals from Mohawk B-93 and Mohican I-100. Middle Jurassic Mohican and Iroquois formations in Mohican I-100 have tourmaline with similar types and chemical composition as Lower Cretaceous tourmaline in the same well (Fig.5.17). Three types of tourmaline were identified, type 1, 3 and 4; type 4 is abundant type 1 sub-ordinate to type 4 and type 3 rare. Type 4 is sourced from metamorphic and type 1 from igneous rocks of the Meguma Terrane. The presence of Mg-rich tourmaline (type 3) suggests a contribution from most likely meta-ultramafic or meta-carbonate rocks.

Middle Jurassic Mohawk Formation in Mohawk B-93 has the same tourmaline types and chemistry as Lower Cretaceous and Upper Jurassic tourmaline from same well (Fig.5.17). The same chemical compositions and types are also found in Upper Jurassic sandstones at Mohican I-100. Types 1 and 4 were identified with type 4 abundant and type 1 rare. Types 4 and 1 tourmaline in the SW Scotian Basin as already mentioned suggest derivation from metamorphic and igneous rocks of the Meguma terrane, respectively.

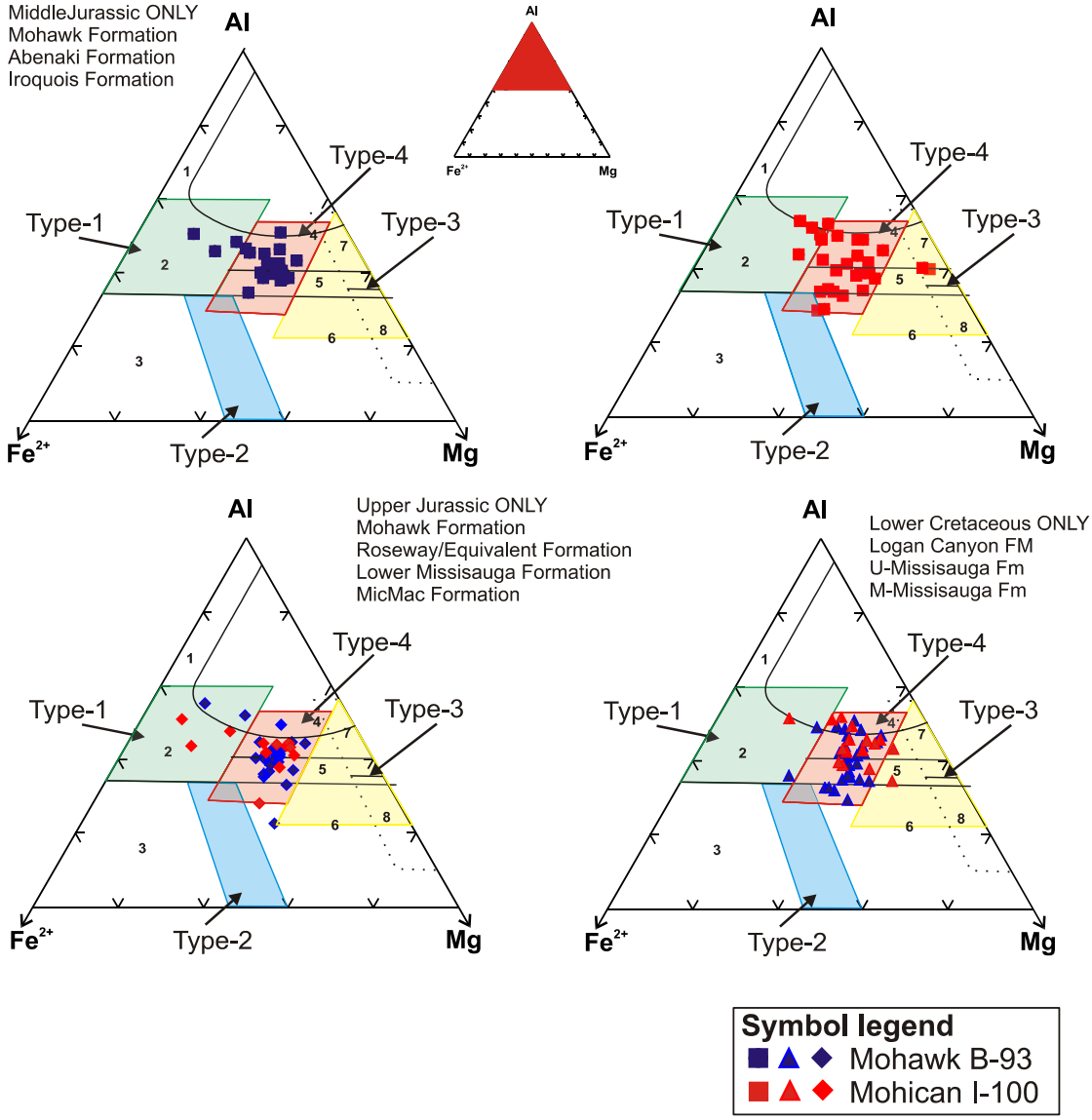

Fig.5.17: Chemical variation in tourmaline based on Al - Mg - Fe showing differentiation and similarity in types between Lower Cretaceous, Upper Jurassic and Middle Jurassic samples from wells studied. Fields after Pe-Piper et al. (2009).

5.1.3.2 Spinel/chromite

One spinel/chromite grain was identified in the Mohawk Formation in Mohawk B-93. Based on chemical composition is an Al-rich spinel/chromite. Similar spinel/chromite was identified in Lower Cretaceous formations at Alma K-85 (Sable sub-basin) and Mohican I-100 (Shelburne sub-basin).

5.1.3.3 Garnet

Middle Jurassic garnet in Mohican I-100 almost entirely resembles Lower Cretaceous garnet in the SW Scotian Basin, with type 4 abundant and type 2 rare; however, type 1B and type 5 are absent (Fig.5.18). Middle Jurassic type 4 has similar chemical composition to garnet from metasedimentary rocks of the Meguma terrane, whereas type 2, as mentioned for Lower Cretaceous, has chemistry similar to garnets from anorthositic rocks of the Grenville Province.

Unusual types of garnet are present in Mohawk B-93. Types 1A, 1B and 2, 4 and 5 are all representative of distinctive sources. These types are different compared to Lower Cretaceous and Upper Jurassic garnet where only two of the types, 4 and 5, were found to represent metamorphic rocks of the Meguma Terrane (Fig.5.18). Type 1A was not identified in other samples from the SW Scotia Basin with potential source in igneous rocks of the Meguma terrane. Types 1B and 2 are representative of anorthositic rocks from the Grenville Province, whereas types 4 and 5 are similar to garnet from metamorphic rocks of the Meguma terrane.

The presence of small amounts of type 1B garnet in Mohawk B-93 and type 2 garnet in both Mohican I-100 and Mohawk B-93 is unusual as this type of garnet tend to occur in meta-ultramafic rocks. During the Mid Jurassic, the presence of other representative mineral indices of meta-ultramafic rocks at Mohawk B-93, such as spinel/chromite, suggests that an equivalent river to the Lower Cretaceous Sable River at Alma K-85 has contributed sediments from the Labrador and the Grenville Province. The contribution with sediments from a distant source can be confirmed from the fact that same types of garnet (1A, 1B, 2, 4 and 5) and spinel/chromite (Al-spinel) are found

in both Mohawk B-93 and Alma K-85.

Spinel/chromite or other minerals indicative of a meta-ultramafic rocks source are absent in Middle Jurassic formations at Mohican I-100. The absence of minerals indicative of meta-ultramafic source implies that a type of rock source different from that at Mohawk B-93 may have been eroded. Data regarding garnet chemistry from meta-ultramafic rocks in the Appalachians is absent. The only data regarding garnet from meta-ultramafic rocks is available from the Grenville Province (Schrijver, 1973; Rivers and Mengel, 1988; Indares, 1992; Pe-Piper and Dessureau, 2002). As a result, other potential sources for type 2 garnet at Mohican I-100 can be as a second cycle origin from Carboniferous sandstones covering areas of the Meguma Terrane or an unusual metamorphic origin of rocks associated with the Meguma Terrane gabbros (Tate and Clarke, 1995).

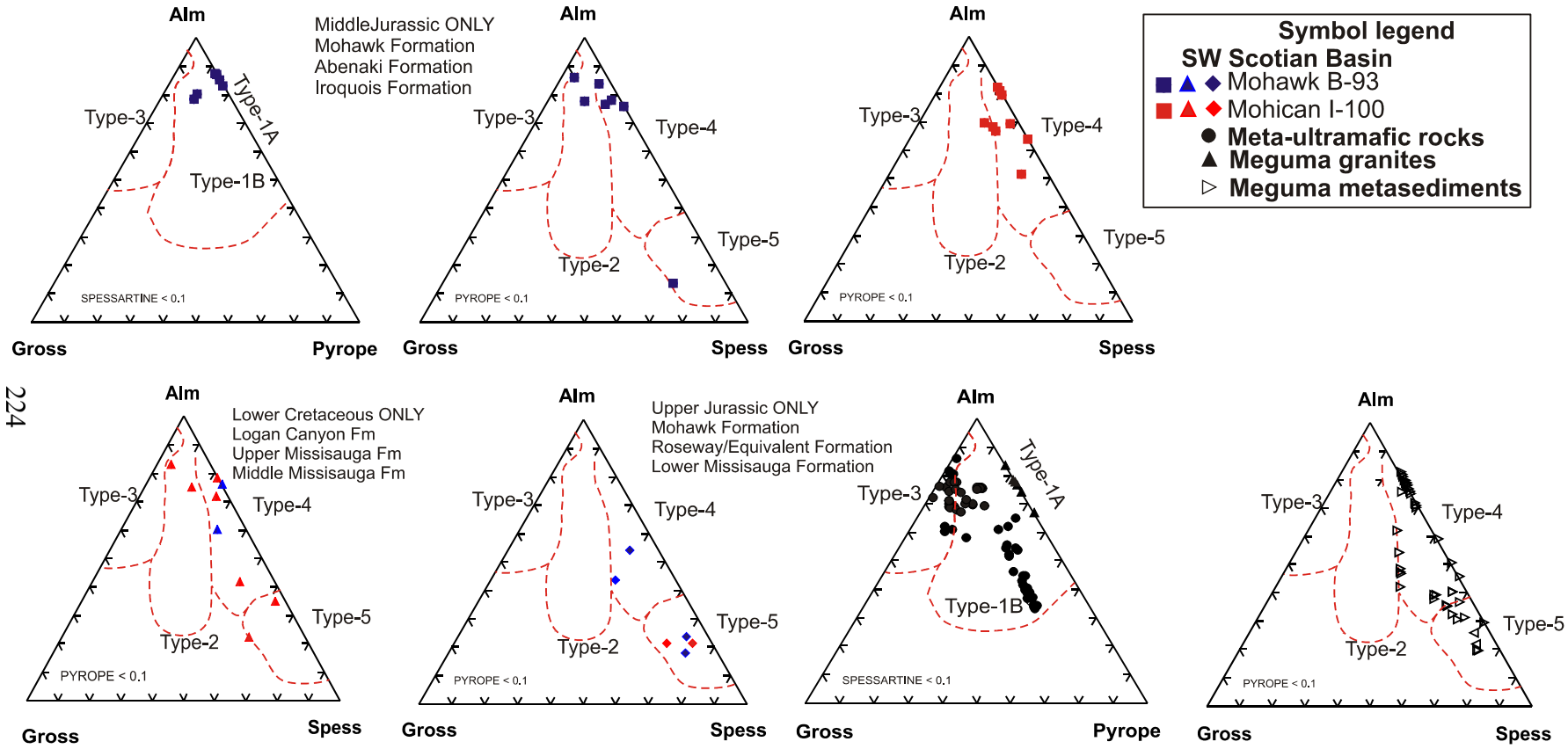

Fig.5.18: Chemical variation in garnet projected onto the Almandine - Grossular - Pyrope plane, for garnets with < 10% Spessartine and onto the Almandine - Grossular -Spessartine plane, for garnets with < 10% Pyrope for Lower Cretaceous, Upper Jurassic and Middle Jurassic strata from the studied wells as well as for onshore known potential rock sources. Data used for comparison between different types. Fields after Pe-Piper et al. 2009).

5.1.3.4 Micas and chlorite

Rare muscovite analyses in Mohawk B-93 are of both metamorphic and igneous origin. The metamorphic muscovite resembles the muscovite from the metamorphic rocks of the Meguma Terrane, whereas igneous muscovite resembles muscovite from the deformed East Kemptville leucogranite that experienced sodium metasomatism and Alleghanian resetting (Kontak et al., 1995). Muscovite analyses from core samples in Mohican I-100 and Moheida P-15 show derivation only from the metamorphic rocks of the Meguma terrane. The metamorphic origin of muscovite is also confirmed from some muscovite of similar chemical composition in Lower Cretaceous strata in Naskapi N-30, which Reynolds et al. (2009) suggested is presumably from the Meguma Supergroup metasediments (Fig.5.19).

Biotite from Middle Jurassic strata in Mohican I-100 is different from Lower Cretaceous biotite, predominantly metamorphic with minor presence of grains of igneous origin. In contrast, biotite in Mohawk B-93 is almost absent with potential source only in metamorphic rocks.

Detrital chlorite in Mohawk B-93 and Mohican I-100 is similar in composition to detrital chlorite from Lower Cretaceous and Upper Jurassic strata as well as from Meguma terrane (Fig.5.20). All detrital chlorite analyses plot in the “metamorphic” field produced by Pe-Piper and Weir-Murphy (2008) but outside of the diagenetic field produced by Sedge (2015).

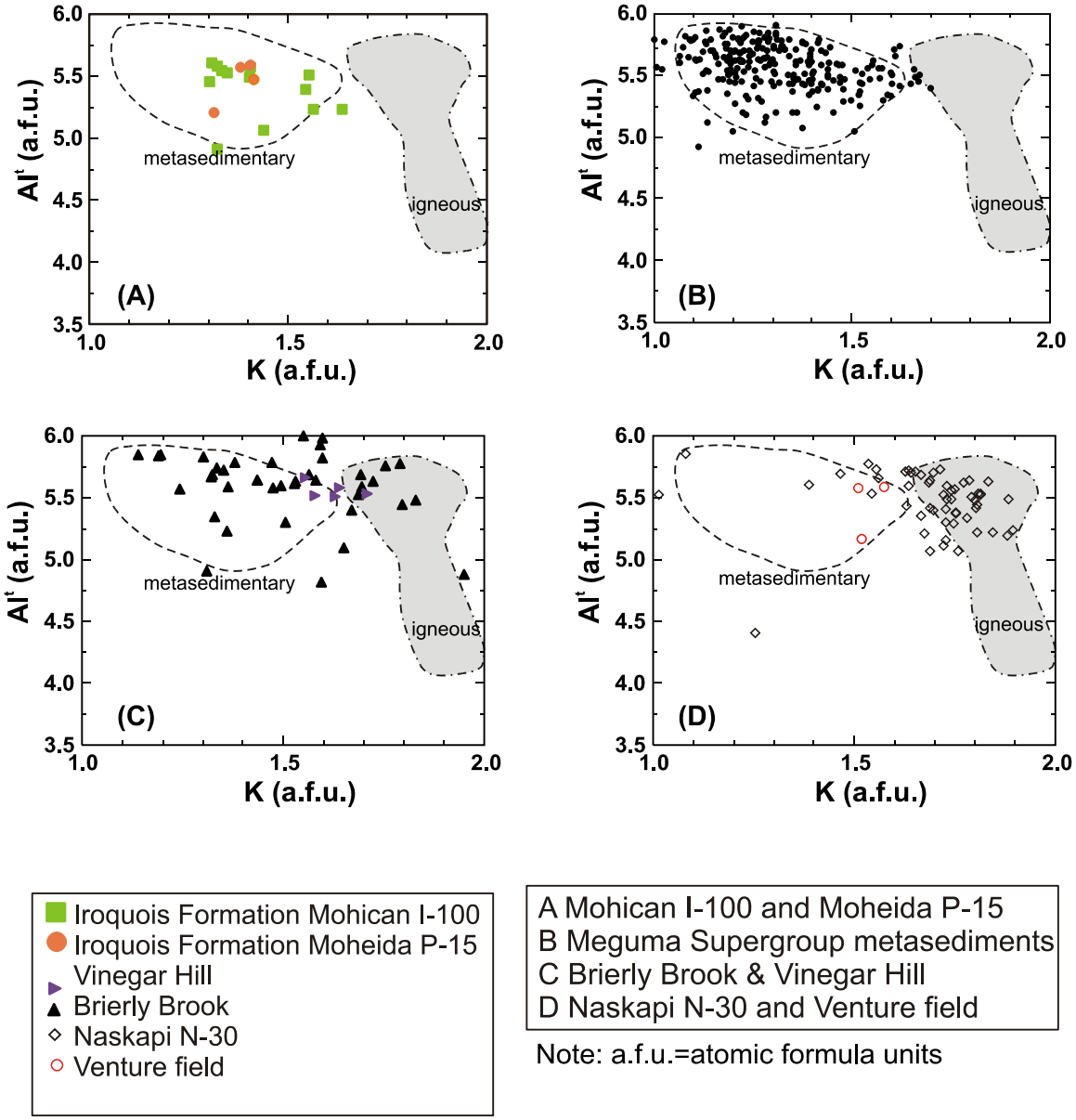

Fig.5.19: Potential source rock for muscovite from studied wells (A). (B) Meguma Supergroup metasediments. The metasedimentary fields for the Meguma terrane rocks are from Reynolds et al. (2010). C) Lower Cretaceous Formation at Vinegar Hill and Elmsvale Basin (data taken from Pe-Piper et al. 2004; Piper et al., 2007). D) Previous dated offshore Cretaceous muscovites Naskapi N-30, Venture field (data taken from Reynolds et al., 2009).

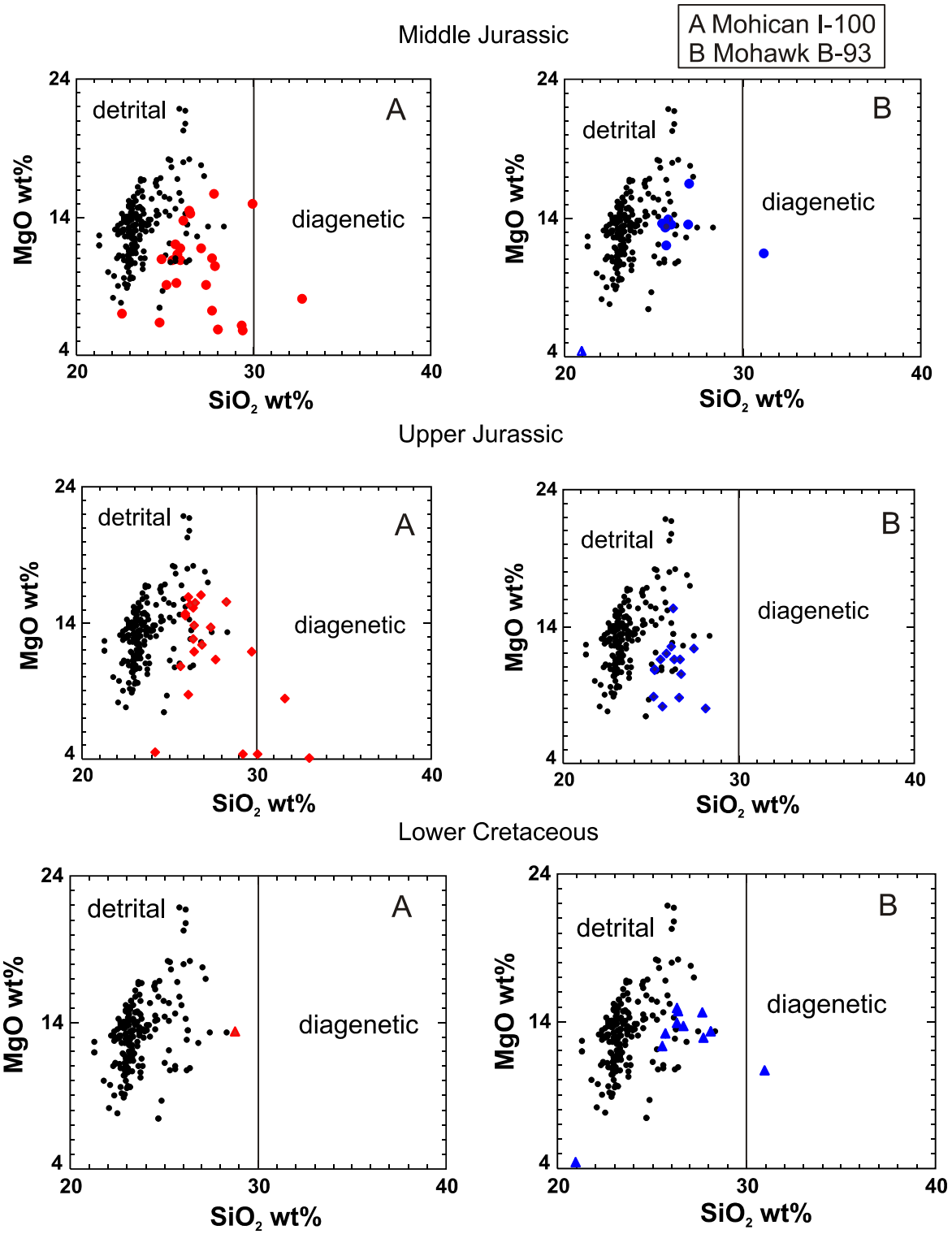

Fig.5.20: Chemical variations in MgO wt% and SiO2 wt% for Lower Cretaceous,Upper Jurassic and Middle Jurassic strata for the studied wells. Comparison of data between wells studied and Meguma Group metasediments, data for Meguma Group metasedimentary rocks provided by Dr. Chris White.

5.1.3.5 Feldspar and lithic clasts at Mohican I-100 and Moheida P-15

Sandstones from the Iroquois Formation at Mohican I-100 and Moheida P-15 contains abundant feldspars. Orthoclase is the most common potassium feldspar, representing the majority of detrital minerals other than quartz found in the SW Scotian Basin (Fig.5.21). Potassium feldspars suggest felsic igneous rocks, especially granites as source rocks.

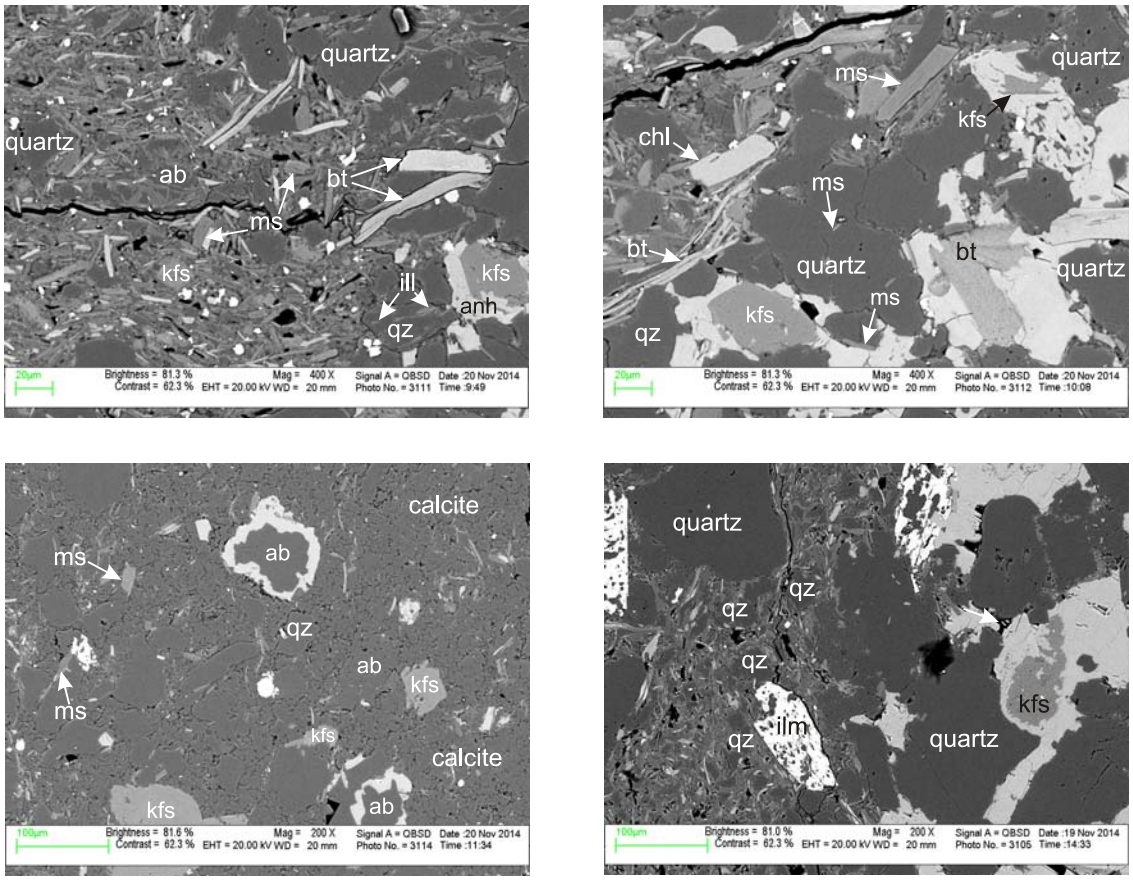

Fig.5.21: SEM back-scattered electron images of Middle Jurassic sedimentary rocks from samples studied at Mohican I-100 showing abundance in detrital K-feldspar.

Lithic clasts are abundant in polished thin sections of conventional cores in both Mohican I-100 and Moheida P-15. The abundance of lithic clasts in Middle Jurassic strata at Mohican I-100 and Moheida P-15, as well as Lower Cretaceous Formation, is in contrast to the lack of clasts in Upper Jurassic formations. Most lithic clasts are

metapsammites and metapelites with characteristic mineralogical composition: a) ilmenite, chlorite, muscovite and quartz, b) muscovite, chlorite and ilmenite with inclusions of quartz and muscovite. In addition, rare lithic clasts of polycrystalline quartz are present. Based on mineral composition lithic clasts from metapsammites and metapelites in Middle Jurassic strata at both Mohican I-100 and Moheida P-15 are similar to those from Lower Cretaceous. However, based on abundance lithic clasts in Middle Jurassic sandstones at Mohican I-100 are more common than lithic clasts in Lower Cretaceous sandstones in same well. Examples of other differences are the high presence of ilmenite in Middle Jurassic lithic clasts, compared to low presence in Lower Cretaceous clasts as well as lack of both foliation and lithic clasts of polycrystalline quartz. The absence of foliation in lithic clasts from Middle Jurassic formations at Mohican I-100 suggests that the sediments were sourced from rocks that experienced lower grade metamorphism (metapsammites) than the Lower Cretaceous lithic clasts (slates) that are indicative of higher grade metamorphism. In conclusion Middle Jurassic lithic clasts at Mohican I-100 are sourced from the Meguma Supergroup metasediments however from different areas than Lower Cretaceous lithic clasts. Lithic clasts in Moheida P-15 show foliation and are similar to those from Lower Cretaceous sandstones in Mohican I-100 suggesting similar sources from high grade metamorphic rocks (Fig.5.22). Although lithic clasts in Middle Jurassic and Lower Cretaceous strata seem to have been eroded from different areas of the Meguma Supergroup metasediments, no difference in grain size was observed.

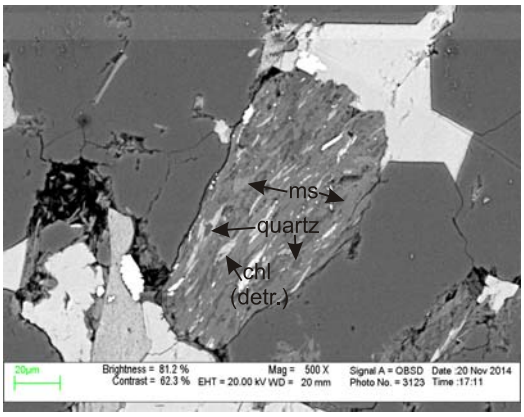

Middle Jurassic Moheida P-15

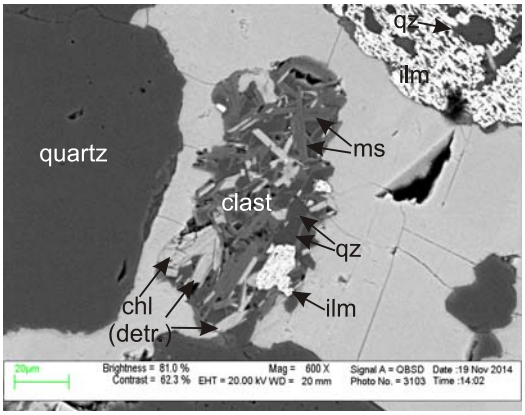

Middle Jurassic Mohican I-100

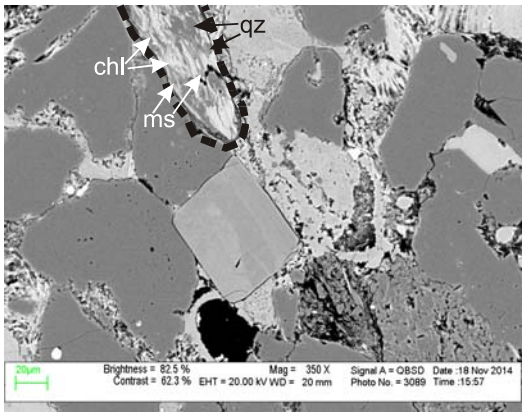

Lower Cretaceous Mohican I-100

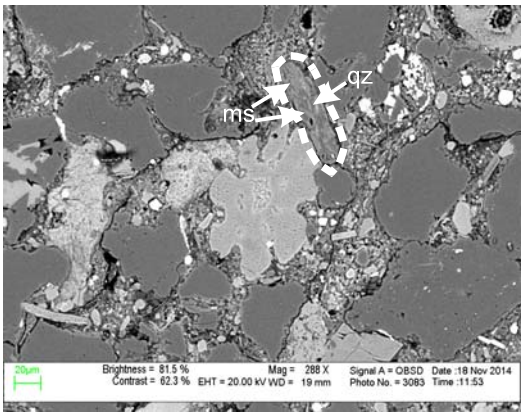

Lower Cretaceous Mohican I-100

Fig.5.22: SEM back-scattered electron images of sedimentary rocks showing textural and compositional differences between Lower Cretaceous and Middle Jurassic lithic clasts found in the wells studied.

5.1.3.6. Stratigraphic trends in modal abundance-Middle Jurassic

The modal abundance of heavy minerals in Middle Jurassic strata shows the same diversity in detrital heavy mineral species as Lower Cretaceous strata (Fig.5.23). Small differences in diversity of mineral species are observed in Mohican I-100, compared to Upper Jurassic strata in same well, with rutile and spinel/chromite to be absent. Mohawk B-93 has the same diversity in mineral species as Upper Jurassic strata in the same well.

In Mohican I-100 ilmenite abundance tends to be constant with depth in the mid

and late part of the Mid Jurassic. In Mohawk B-93 ilmenite percentages vary with depth, with notable increases in Early and Mid Jurassic strata in both wells.

Tourmaline in Mohican I-100 and Mohawk B-93 is the second most abundant detrital heavy mineral with a small increase with depth. In general Middle Jurassic tourmaline shows higher percentage, compared to Lower Cretaceous and Upper Jurassic tourmaline.

Middle Jurassic zircon in Mohican I-100 has a higher percentage compared to Lower Cretaceous and Upper Jurassic zircon. In general the modal abundance of zircon is constant with a small decrease in depth. The exception is the Middle Jurassic where an increase has been observed.

Garnet (almandine and spessartine) and staurolite are almost absent in Mohican I-100, except towards the early Middle Jurassic, where an important influence with garnet is identified. In Mohawk B-93 the same minerals show variation.

The consistency in abundance of tourmaline, zircon, garnet and staurolite in Mohican I-100 in Mid Jurassic strata, suggests that the sediments were derived from rock sources that did not show high differences in mineralogical composition. The increase in ilmenite, garnet and zircon towards the beginning of Mid Jurassic implies sources enriched in these minerals. The small increase in zircon might suggest a contribution with sediments from a second cycle source.

On the other hand, variation in modal abundance for same minerals in Mohawk B-93 suggests that one source was enriched in tourmaline, zircon, garnet and staurolite and another was enriched in ilmenite.

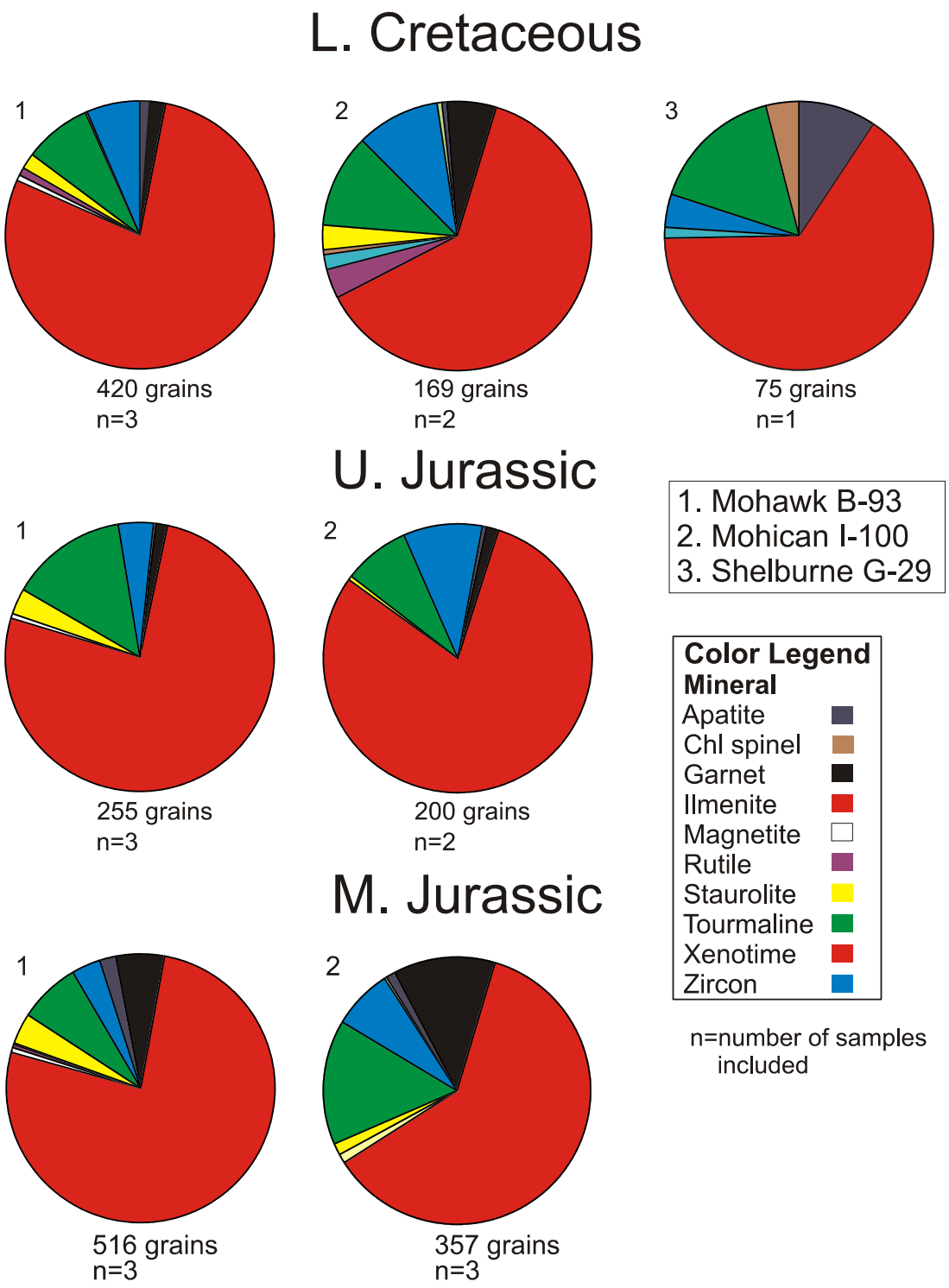

Fig.5.23: Pie chart diagrams showing differences in the modal abundance of detrital heavy minerals in cutting samples for Lower Cretaceous, Upper Jurassic and Middle Jurassic Formations in the studied wells.

5.1.3.7 Summary

Middle Jurassic ilmenite has similar potential sources as Lower Cretaceous and Upper Jurassic ilmenite from metamorphic rocks of the Meguma terrane. Muscovite and chlorite resemble metamorphic muscovite and chlorite in the Meguma Supergroup metasediments. Lithic clasts are sourced from metapelites and metapsammites. Garnet from Middle Jurassic formations in Mohawk B-93 is almost similar to garnet from Lower Cretaceous formations at Alma K-85 sourced from rocks of the Meguma terrane and meta-ultramafic rocks. Lithic clasts seem to have been derived exclusively from the Meguma Supergroup metasediments. In conclusion the main source for Middle Jurassic strata in the SW Scotian Basin is from the Meguma terrane with probably a small contribution of sediments derived from Labrador and the Grenville Province. This latter statement is based on types 1B and 2 garent with chemical composition to garnet from the Grenville Province and spinel/chromite with similar chemistry as spinel/chromite found in Alma K-85 interpreted as derived mainly from Humber terrane lower Paleozoic ophiolites, perhaps second cycle via Paleozoic sandstones.

By the Middle Jurassic, sufficient subsidence of the rift shoulder had taken place so that clastics of the Iroquois and Mohican formation were deposited. The high abundance of lithic clasts in Middle Jurassic strata derived from a metamorphic protolith, reflects rapid unroofing of the Meguma Terrane. This evidence supports the idea that during Middle Jurassic the Meguma Terrane experienced significant erosion, under the influence of tectonic setting of the hinterland that led to concentration of sedimentation in the developing central Atlantic rift (Li et al., 2012) and/or the development of a proto river system draining different areas of the Meguma terrane.

5.1.4 Lower Jurassic strata, Fundy Basin

In the Lower Jurassic Scots Bay Formation at the Chinampas O-37 well in the Fundy Basin, only the chemistry of the detrital garnet and biotite were used for provenance. Although one grain was identified as tourmaline, the chemical analysis was not pure enough to be plot onto discrimination diagrams. Other heavy and light detrital minerals identified based on their chemical composition are ilmenite, apatite and amphibole. Based on chemical composition, the 4 amphiboles identified belong to 3 different groups, Mg-Fe-Mn-Li, calcic and sodic-calcic (Na-Ca) (Fig.5.24A), considering the amphibole classification proposed by Leake et al. (1997). Chemically the two calcic amphiboles are tremolite, however in the discrimination diagram for calcic amphiboles (Fig.5.24B) only one plots in the tremolite field. The sodic-calcic amphibole is probably winchite or richterite, whereas the Mg-Fe-Mn-Li amphibole is probably anthophyllite or ferro-anthophyllite. The classification of these amphiboles was done only chemically as none of them could be plot on the diagrams used by Leake et al. (1997) for classification of these amphiboles.

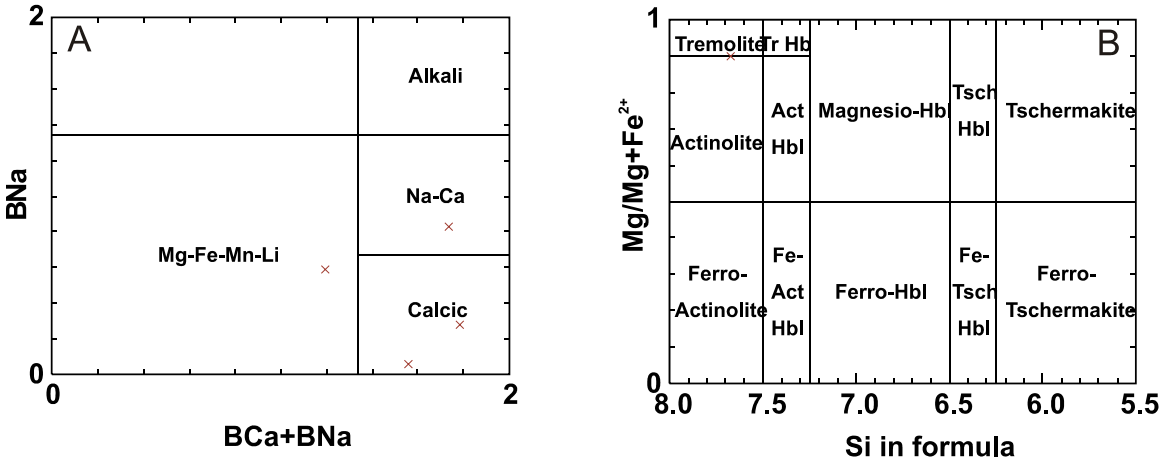

Fig.5.24: A) Nomenclature of amphiboles and B) calcic amphibole group based on the classification system of Leake et al. (1997).

The garnet from this well is type 5 Mn-rich garnet (spessartine) and has chemical composition similar to spessartine-rich garnet present in some Mn-rich Meguma Supergroup metasedimentary rocks (Pe-Piper et al. 2009; Tsikouras et al. 2011) (Fig.5.25). Mg-rich garnet (pyrope) plots as 100% pyrope and this type of garnet is an indicator for high pressure rocks, most commonly derived from the mantle, sourced from mafic/ultramafic rocks and/or from high grade metamorphic rocks such as eclogites.

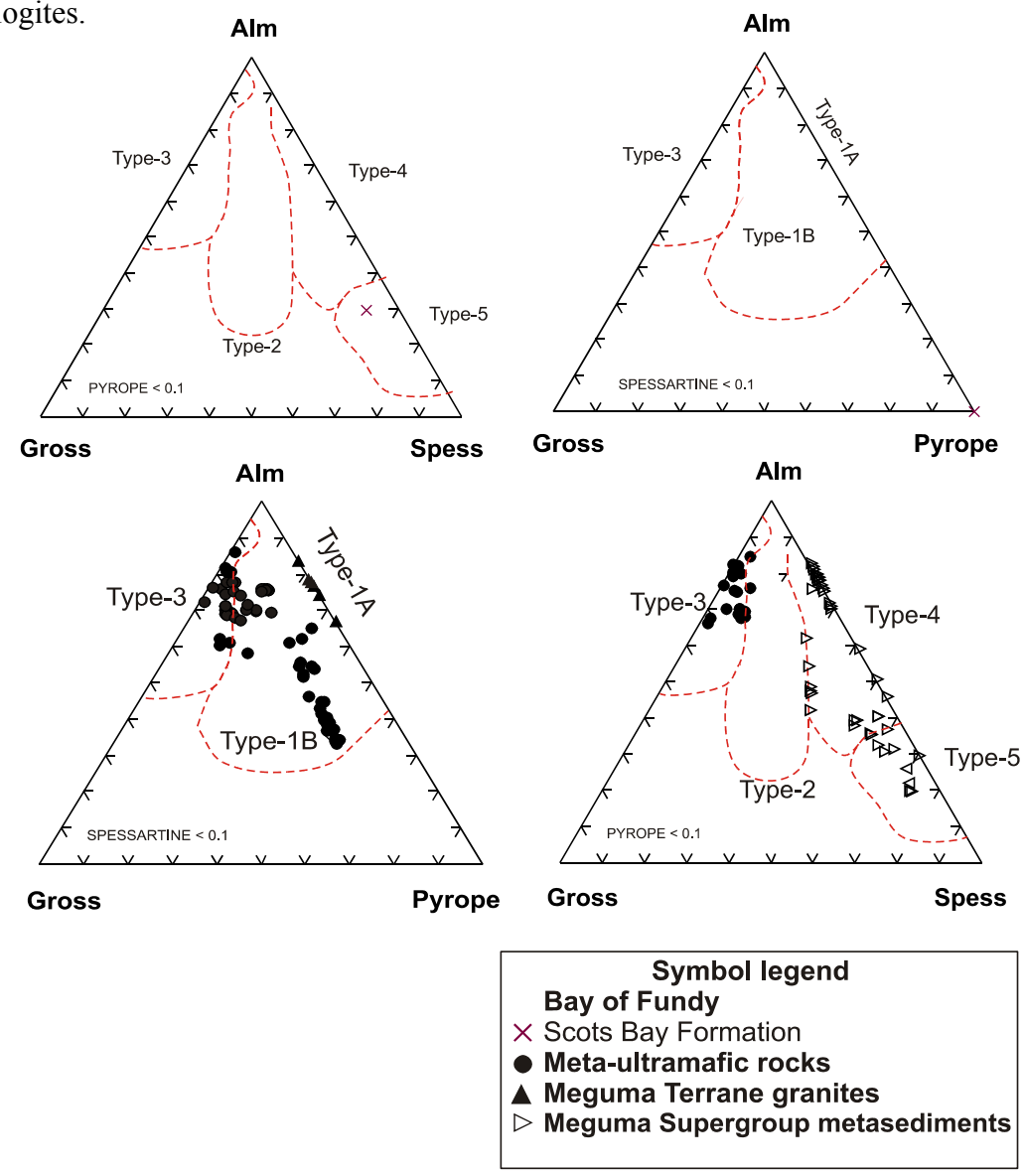

Fig.5.25:Chemical variation in garnet projected onto the Almandine - Grossular - Pyrope plane, for garnets with < 10% Spessartine and onto the Almandine - Grossular - Spessartine plane, for garnets with < 10% Pyrope for Lower Cretaceous Jurassic Scots Bay Formation from Chinampas O-37 and onshore known potential rock sources. Fields after Pe-Piper et al. (2009).

Most biotite from Chinampas O-37 is of metamorphic origin and the rest of igneous origin. Some biotite resembles that of Mohican I-100 and some that of Naskapi N-30 suggesting that its source could be from the metamorphic rocks of the Meguma terrane.

Fe-oxides are the most abundant detrital grains found in Chinampas O-37. Three hypotheses have been considered regarding the high levels of Fe-oxides: i) unreported weighting material from drilling the well, ii) episodic laterite weathering of mafic and ultra-mafic rocks e.g. basalt, peridotite and iii) a detrital origin from a local Fe-oxide hydrothermal deposit. Each of the hypotheses is discussed below.

i) During the process of drilling oil and natural gas wells or even simple boreholes, such as water wells, drilling mud is used. The main functions of drilling mud include providing hydrostatic pressure to prevent formation fluids from entering into the well bore, keeping the drill bit cool and clean during drilling, carrying out drill cuttings, and suspending the drill cuttings while drilling is paused and when the drilling assembly is brought in and out of the hole. The well history report of Chinampas O-37 in the Fundy Basin includes an incomplete list of materials with distinct chemical composition used as drilling mud. None of the drilling mud reported materials that include any FeO in its chemical composition.

ii) The second hypothesis is related to the fact that Fe-oxides can be a product of a prolonged process of chemical weathering called laterization. Fe-oxides occur in mafic igneous rocks and other iron-rich rocks. The Chaswood Formation at Vinegar Hill sourced from central New Brunswick, is abundant in Fe-Ti oxides, whereas modal abundance in Scots Bay Formation is enriched in Fe-oxides. This suggests that the sediments deposited in the Fundy Basin during Early Jurassic do not have same sources

as sediments at Vinegar Hill and that there are no deposits in New Brunswick enriched in meta-ultra mafic minerals. The absence of minerals indicators of meta-ultramafic rocks together with a lack of remnants or detrital minerals altered into Fe-oxides suggests that their origin is not from laterites.

iii) The third hypothesis was tested using three different microscopes, optical, scanning electron microscope and electron microprobe. The Fe-oxides are opaque under the optical microscope when polarized light is used. In contrast, when reflected light is used the Fe-oxides have a characteristic grey color with brownish tint. Fractures are common in most of the grains which tend to have a cubic to prismatic shape.

Electron dispersion spectroscopy geochemical analyses of Fe-oxides show FeO with concentrations ranging from 97 to 99 wt % and an actual total of 85%. On the other hand, wavelength-dispersive spectroscopy (WDS) geochemical analyses of same Fe-oxides show similar FeO concentrations (~ 98 wt %) but higher actual total (~ 98%). The only FeO rich mineral that crystallizes in the isometric system, is isotropic with transmitted light, has a grey color under reflected light and has more than 89% wt FeO in its chemical composition is magnetite. In conclusion most likely the Fe-oxides are sourced from a magnetite parental rock, likely the North Mountain Basalt that outcrops in the north-west Nova Scotia around the Fundy Basin.

Based on interpretation of chemical analyses from detrital minerals (heavy and light) and modal abundance it can be summarized that the main source from the Scots Bay Formation is probably in part from the Meguma terrane, presumably from the Meguma Supergroup metasediments. Other minerals, such as pyrope, tremolite, richterite and winchite are not normally found in the Meguma terrane. However,

tremolite is known from the Musquodoboit E-23 well, apparently derived from the Meguma terrane (Pe-Piper et al., 2009). Sodic amphiboles are also known from the Avalon terrane of Northern Nova Scotia (Papoutsa and Pe-Piper, 2013), and are likely present in similar rocks in New Brunswick. Their low abundance at Vinegar Hill may be due to the intense diagenesis or weathering in those deposits.

5.2 Diagenesis

To determine the paragenetic sequence, textural relationships between diagenetic and detrital minerals were used. Quartz overgrowths provide a useful marker for distinguishing between early cement, where intergranular pores are filled by other diagenetic minerals and thus predate the overgrowths, and later cements, which are synchronous with or engulf the overgrowths and thus postdate quartz cementation. For a better discrimination we separate the diagenetic minerals in this study based on chemical composition in three groups which are: the carbonate cements, the silicate cements and the other diagenetic mineral cements. The carbonate cement group includes diagenetic minerals such as calcite, Mg-calcite, Mg-Fe-calcite, Fe-calcite, ankerite, dolomite and siderite. The quartz overgrowths, albite, kaolinite, chlorite and illite all together represent the silicate cement group. The third cement group includes pyrite, TiO_2 minerals, F-apatite and anhydrite. The coated grains, the oolites and the peloids, which represent sea-floor diagenesis, are discussed separately.

5.2.1 Mineral assemblages

5.2.1.1 Mohican I-100

Lower Cretaceous Roseway Equivalent sandstones and oolitic limestone

Carbonate cements

The most abundant carbonate cement recognized is Mg-calcite. Generally, Mg-calcite tends to fill primary porosity prior to compaction or to replace bioclasts. Back-scattered electron images have shown that Mg-calcite appears to have a dark grey color. Often, the Mg-calcite cement in back-scattered electron images shows numerous

dissolution voids. Both calcite and Fe-calcite fill intragranular space or replace bioclasts and have homogenous light grey color in back-scattered electron images. Fe-calcite is in form of individual euhedral grains that tend to resemble rhombohedrons. Very often, calcite fills secondary porosity and embayments in detrital quartz and Mg-calcite, and thus postdates Mg-calcite. Mg-Fe-calcite is rare and when present tends to show a mixture between Mg-calcite and Fe-calcite rather than a homogenous composition. All calcite cements come in direct contact with detrital grains and predate quartz overgrowths. Ankerite cement having euhedral rhombohedrons was recognized only in sample I-100 2530.37 replacing Fe-calcite cement. A few dolomite euhedral rhombohedrons seem to show replacive texture against diagenetic chlorite. Secondary porosity within the cement at lower depths is mostly associated only with dissolution voids that tend to be replaced by diagenetic minerals. With increase in depth the dissolution voids are replaced by brittle fracturing of the cement, thus showing an increase in secondary porosity which suggests possible overpressure conditions.

Silicate cements

Kaolinite booklets are abundant and fill large intragranular pores between detrital grains only in sample I-100 2526.53. Kaolinite commonly fills embayments in detrital quartz, thus predating quartz overgrowths. With increased depth kaolinite seems to be replaced by illite and chlorite. Illite has been recognized having two textures: i) one that is massive filling primary porosity, with late fractures that lack diagenetic minerals and ii) one that is fibrous, mostly filling secondary porosity in the Mg-calcite and the Mg-Fe-calcite. When present, the fibrous illite is usually associated with fibrous chlorite.

Moreover, fibrous chlorite tends to replace kaolinite booklets or to fill open space between Mg-calcite and detrital quartz. Quartz cement forms around detrital quartz grains in places where the carbonate cement starts to dissolve and occurs as euhedral overgrowths.

Other cements

Diagenetic minerals identified from this group are F-apatite, TiO_2 and pyrite. F-apatite filling secondary porosity in calcite was identified only in sample I-100 2538.84. On the other hand, pyrite and TiO_2 minerals are recognized in all the samples. Pyrite is framboidal and is associated mostly with Mg-calcite filling dissolution voids, whereas TiO_2 is associated with all the digenetic minerals.

Middle Jurassic Mohican and Iroquois sandstones and limestone

Carbonate cements

Calcite is the only diagenetic mineral identified from this group. However, it is absent in sample I-100 3692.41 from Mohican I-100 well in the Mid Jurassic Mohican Formation. With increase in depth, and thus age, calcite appears replacing detrital minerals such as albite as well as anhydrite cement. Calcite becomes the main supporting material for framework grains in Mid Jurassic samples in the Iroquois Formation.

Silicate cements

Quartz overgrowths and albite are the only diagenetic minerals recognized from this group. Quartz overgrowths are common and form around detrital quartz grains in

open space within the anhydrite cement. Albite is recognized as dark grey patches on the surface of detrital K-feldspars having irregular shape. Although some grains show chemical composition similar to that of illite, the chemical analyses contain contaminants and thus it is hard to recognize if the grains are diagenetic illite, muscovite clasts or altered muscovite.

Other cements

Anhydrite is the main cement filling large intragranular space between framework grains in sample I-100 3692.41 from the Mohican Formation (Late Bathonian to Callovian). In samples I-100 3964.6A and I-100 4098.08 from Iroquois Formation with age from Bajocian to Late Bathonian, anhydrite has a local character filling small intragranular space and partly replacing detrital K-feldspar. The TiO_2 mineral and pyrite tend to be present in all the Mid Jurassic samples filling secondary porosity in other diagenetic minerals or in the matrix. An exception is the sample from Mohican Formation which lacks pyrite.

5.2.1.2 Moheida P-15

Lower Cretaceous Roseway Equivalent oolitic ironstone

Carbonate cements

The carbonate diagenetic minerals identified in sample P-15 2563.67 are calcite, siderite and ankerite. All diagenetic minerals are part of the cement filling large intragranular space. Based on chemical composition calcite can be Mg-calcite, Fe-calcite or Mg-Fe-calcite. Based on textural relationship ankerite and siderite can be

both early and late. Both early siderite and ankerite have subhedral crystal grains. On the other hand, late ankerite shows euhedral rhombohedral grains. Late siderite looks amorphous in back-scattered electron images.

Silicate cements

Chlorite is the only diagenetic mineral identified from this group. Texturally, chlorite is in form of needles and seems to fill secondary porosity in the cement or to replace Mg-Fe-calcite.

Upper Jurassic Abenaki oolitic limestone

Carbonate cements

Dolomite and calcite are the only diagenetic minerals recognized from this group representing the main cement in sample P-15 3306.03. Dolomite grains are euhedral rhombohedrons and are scattered through the entire sample. Calcite varies in composition from Fe-calcite to pure calcite (FeO<1% and MgO<1%). Generally, calcite grains have amorphous shape and are smaller in size compared to the dolomite grains.

Silicate cements

Quartz overgrowths and chlorite are the silicate cement identified in sample P-15 3306.03. Quartz overgrowths form around detrital quartz grains, whereas chlorite can be found scattered in places, having local character. In general, both the quartz overgrowths and the chlorite are rare.

Other diagenetic cements

Pyrite is rare, with cubic grains that have local character.

Middle Jurassic sandstone and dolostone

Carbonate cements

Carbonate cements were not identified in any of the samples. However, sample P-15 3750.49 is entirely made up of dolomite, thus is a dolostone.

Silicate cements

Quartz overgrowths, kaolinite and illite are diagenetic minerals recognized from this group. Quartz overgrowths are common and form around detrital quartz grains in open space where the anhydrite cement is dissolved. Illite and kaolinite tend to have needle like shape and fill embayments in detrital quartz. Rarely, illite and kaolinite fill open space between detrital quartz and anhydrite cement.

Other diagenetic cements

In general, anhydrite is the main cement filling large intragranular space between framework grains. Only in sample P-15 3750.94 anhydrite fills secondary porosity within dolomite. The TiO_2 mineral and pyrite both show replacive texture against detrital minerals (e.g. biotite) and fill secondary porosity in the cement.

5.2.2 Coated grains, ooids and peloids

Only two samples (from 11 studied), I-100 2530.47 from Lower Cretaceous

Roseway Equivalent Formation in Mohican I-100 well and P-15 2563.67 from same formation in Moheida P-15 well, have coated grains as framework grains. Coated grains in Mohican I-100 have spherical to oval shape and have a nucleus of peloids coated by micritic calcite, chlorite and pyrite. Chemically the nucleus is made up of Mg-calcite, Fe-Mg-calcite and pyrite. Coated grains in Moheida P-15 show concentric layers that are made up mostly of siderite with minor chlorite, kaolinite and pyrite. Rarely, the coated grains have a nucleus of an intraclast made up of Fe-calcite, kaolinite and siderite. Often, calcite is between siderite-rich concentric layers and has been recrystallized to sparry Fe-Mg-calcite. We compared the coated grains in this study with those identified by Okwese et al. (2012). Type A coated grains are Fe-rich, with the outermost layer comprising siderite, glauconite, chlorite or francolite. Inner concentric layers include the same minerals, in addition to Fe-calcite, illite, kaolinite, and Fe-chlorite. Intergranular cements include Fe-calcite, calcite, siderite, minor pyrite and chlorite. Type B coated grains have alternating layers of Fe-calcite and chlorite. Type C coated grains consist of calcite or Fe-calcite and pyrite, and may include a cortex of clay minerals, probably of detrital origin. The outer rim of some coated grains includes small crystals of pyrite and Fe-calcite. Type D coated grains have an outer layer of Mg-calcite, and commonly an inner layer of ankerite, with Fe-calcite, pyrite, and clay minerals present in lesser amounts. The nucleus is commonly either chlorite or Fe-calcite. There are small differences between coated grains in this study compared to those identified by Okwese et al. (2012). The Mohican sample although it has pyrite and clay minerals (chlorite), instead of calcite or Fe-calcite which is in type C and Mg-calcite and ankerite which are in type D, has Mg-Fe-calcite.

The Moheida P-15 sample has concentric layers made up mostly of siderite and kaolinite instead of Fe-calcite and chlorite which is the case for type B coated grains. Based on chemistry and texture in back-scattered electron images, the coated grains from Mohican well are most likely similar to type D coated grains from the Mid Jurassic MicMac Formation in the Peskowesk A-99 well, whereas coated grains from the Moheida P-15 well are most likely type B coated grains from the Lower Cretaceous Lower Member of the Missisauga Formation in the Thebaud C-74 well.

Sample I-100 2530.47 together with coated grains contains peloids as framework grains. Sample P-15 3306.03 from Upper Jurassic Abenaki Formation in Moheida P-15 also contains peloids. In both samples the peloids tend to have same brightness and irregular shape in back-scattered electron images. Peloids in Mohican I-100 are made up of a mixture of calcite, Mg-calcite, Mg-Fe-calcite, Fe-calcite, silt size detrital quartz and pyrite. Peloids in Moheida P-15 have similar chemical composition as peloids in Mohican I-100 with the difference that Fe-calcite is absent. Although, the peloids in both samples are similar regarding texture and chemistry there is a difference in grain size. Peloids in Mohican I-100 have a grain size around 30 μm whereas the same grains in Moheida P-15 are around 200 μm in size. In addition, detrital quartz in peloids from Moheida P-15 varies in size from of 20 μm to 100 μm, whereas in Mohican I-100 detrital quartz is ~10 μm. Ooids were recognized only in sample P-15 3306.03 from Moheida P-15 well having oval shape and lacking internal structure (i.e. nucleus, concentric layers). Compared to the peloids in the same sample, the ooids tend to be homogenous in composition made up of Mg-calcite.

5.2.3 Dissolution events

5.2.3.1 Mid Jurassic

The Mid Jurassic sandstone samples from Mohican I-100 and Moheida P-15 wells seem to be affected by at least three dissolution events. However, the information regarding the dissolution voids is not enough to determine the exact order in which these events took place. One dissolution event is related to the presence of dissolution voids in the inner part of detrital grains, such as quartz, lithic clasts and K-feldspars (Figs.4.12 A, C) as well as in the matrix (Fig.4.12 D). Anhydrite cement in Mid Jurassic sandstones shows secondary porosity as a result of volume reduction from a gypsum precursor. This dissolution event is distinct from the previous event as the secondary porosity occurs at anhydrite grain boundaries that fill primary porosity (Fig.4.12 B). Other types of cement from Mid Jurassic sandstones that show secondary porosity which lacks diagenetic minerals (Figs.4.16 A, B) are considered to have been influenced by a different event compared to the other two events mentioned above.

5.2.3.2 Upper Jurassic and Lower Cretaceous

Four dissolution events have been recognized in Upper Jurassic-Lower Cretaceous sandstones from Mohican I-100 and Moheida P-15. One dissolution event is related to the presence of open space between detrital grains, especially quartz, and carbonate cements, especially Mg-calcite, which often is partly filled with diagenetic chlorite, favourable for precipitation of quartz overgrowths (Fig.4.9 C). Another dissolution event is related to the presence of embayments in the quartz overgrowths. These embayments are result of dissolution caused by corrosive fluids, which are filled by

diagenetic chlorite (Figs.4.8 D, 4.9 C, position E), suggesting that this event postdates the previous event. A distinct dissolution event is related to both bioclasts and detrital grains. Bioclasts that are made up of Mg-calcite together with detrital minerals (quartz, perthite, and rutile) tend to show dissolution voids (Figs.4.8 B, E, G, 4.9 C), which do not seem to have any relationship with the carbonate cements that fill primary porosity. Often, the carbonate cements that fill primary porosity are characterized by dissolution voids visible on their surface, mostly in the Mg-calcite cement, which are filled by late diagenetic minerals (Figs.4.8 A, C, 4.9 C). This dissolution event is considered to be distinct from the previous events. Another dissolution event is recognized from the presence of open space around detrital crystal boundaries that lack diagenetic minerals (Figs.4.8 C, 4.9 C).

5.2.4 Paragenetic sequence

5.2.4.1 Early Cretaceous and Late Jurassic paragenetic sequence

Sea-floor diagenesis during Late Jurassic-Early Cretaceous in Abenaki and Roseway Equivalent formations is represented by coated grains, peloids, ooids and bioclasts (Fig.5.26). Coated grains usually develop as a result of episodic burial and erosion at the sea-floor (Pufahl and Grimm, 2003). Thus, they preserve sea-floor diagenetic minerals which are informative of early diagenesis. Based on chemical composition the two types of coated grains identified, B (mostly siderite) and D (mostly calcite) were formed under different sea- floor conditions. The abundance of siderite (A) and the absence of pyrite in type B coated grains (Moheida P-15) imply no activity of sulphide ion, but high ratio of Fe^{2+} to Ca^{2+} compared to type D coated grains

(Mohican I-100). Often, between layers there is sparry Fe-Mg-calcite, suggesting recrystallization of the precursor calcite. The preservation of discrete concentric layers of mostly siderite (A) suggests that probably there was no replacement of the carbonate mineral by another during mesodiagenesis, but isochemical replacement cannot be excluded (Okwese et al., 2012). The chemical assemblage of Mg-calcite (A), Mg-Fe-calcite (A) and pyrite (A) in type D coated grains in this study implies activity of sulphide ion and high ratio of Ca^{2+} to Fe^{2+}. The presence of calcite (A) and pyrite (A) in the outer rim of some of the type D coated grains suggest that the calcite precipitated in the sulphidic zone by the time the coated grain was buried (Okwese et al., 2012). In addition chlorite (A) in the outer rim of type D coated grains is inferred to have replaced Fe-rich clays and berthierine precursors during mesodiagenesis (Aagaard et al., 2000). Similar replacement is observed in the proximal part of the eastern Scotian Basin, where the coated grains are buried and preserved at a depth less than 600 m (Pe-Piper and Weir-Murphy, 2008). Previous studied have shown that the transformation of berthierine to chlorite occurs at temperatures between 70-100º C (e.g. Aagaard et al., 2000; Worden and Morad, 2003). Although there is no evidence in the studied samples, it is likely that the berthierine was the precursor of the chlorite. The nucleus in both types of coated grains is made up mostly of Fe-calcite (A) suggesting that the primary conditions were uniform at the time they began to form.

Ooids in the Moheida P-15 well are made up mostly of Mg-calcite (B) suggesting that at the time they were formed the sea-floor conditions were uniform. Peloid chemistry is almost similar to that of type D coated grains, with the difference that silt size detrital quartz is present. The absence of internal structure together with the texture

implies that most likely they are product of biomineralization in the zone of physical reworking.

The bioclasts in both wells are mostly made up of Mg-calcite (C) which represents the original Mg-calcite skeleton. Rarely, together with Mg-calcite, some calcite (B) (MgO<1% and FeO<1%) can be identified in some bioclasts (Figs.4.8 F, 4.10B). The fact that the calcite is part of bioclasts, which probably are gastropods, implies that it might have occurred from recrystallization of the original aragonite. However, replacement of the Mg-calcite with calcite can not be ruled out. If calcite formed through replacement then most likely it was isochemical and took place during early diagenesis.

Kaolinite (A) tends to fill only intragranular space between framework grains (Fig.4.8 A). The fact that kaolinite is present only in one sample (I-100 2526.53) suggests influence of meteoric water, which is required for kaolinite precipitation (Rossi et al., 2001), only at specific stratigraphic layers. Samples lacking kaolinite suggest that most likely rapid burial with sufficient subsidence took place so that important flux of meteoric water did not occur.

Mg-calcite (D), calcite (C), Mg-Fe-calcite (B), Fe-calcite (B) in Mohican I-100 well and ankerite (A), siderite (B) and dolomite (A) in Moheida P-15 well are usually the main cement in uncompacted sandstone filling primary porosity (Figs.4.8 D, 4.11 B, 4.8 H, 4.10 A, 4.15 C, 4.16 B) indicating precipitation of cement under early diagenetic conditions. Mg-calcite is considered a mobile mineral and the fact that it is one of the most abundant cements, and the main component in bioclasts which are abundant in most of the sandstones, suggests that the later is probably the source for Mg-calcite.

Iron in Fe-calcite (B) is most likely ultimately detrital from alteration of ilmenite or diagenetic from remobilization of Fe^{2+} present in Mg-Fe-calcite. In Moheida P-15, ankerite (A) is thought to fill primary porosity during early diagenesis and most likely precipitated before quartz overgrowths (Fig.4.15 C). Dolomite was identified in Moheida P-15 filling primary porosity, and at greater depths is partly replaced by Fe-calcite (C) (Fig.4.16 B).

Compact illlite (A) filling intragranular space in sandstones from Lower Cretaceous Roseway Equivalent Formation (Mohican I-100) (Fig.4.9 A) most likely formed due to dissolution of perthite and K-feldspar, which are abundant in these rocks, and could be a source of K for illite.

Fe-calcite (B) cement filling primary porosity in rocks from Mohican I-100 (Fig.4.10 B) is partly replaced by ankerite (B). On the other hand, ankerite (A) and siderite (B) in Moheida P-15 are partly replaced by siderite (C) (Fig.4.15 C), which means the later postdates the previous two carbonate cements.

Mesogenetic fibrous chlorite (B) fills secondary porosity in Mg-calcite (C), Fe-Mg-calcite (B), ankerite (A) and siderite (A,B) cements (Figs.4.8 A, 4.9 B, 4.15 C) , and pores between Mg-calcite cement and detrital quartz (Fig.4.9 C). Fibrous chlorite also tends to replace kaolinite (A) that fills primary porosity and fills embayments in places where detrital quartz is corroded (Fig.4.8 D). The presence of fibrous chlorite in detrital quartz embayments suggests that most likely the corrosive fluid that produced the embayments is the same that led to chlorite formation.

Pyrite (B), illite (B), TiO_2 minerals, F-apatite and calcite (D) all fill secondary porosity in the carbonate cement or show replacive texture against other detrital or

diagenetic minerals (Figs.4.8 C, 4.9 B, 4.8 D, 4.11 A, 4.9 A). In places, pyrite fills secondary porosity in both the carbonate cement and the quartz overgrowths (Fig.4.8 D) and thus postdates them. The possible source for Ti for TiO_2 mineral and Fe for pyrite and illite is probably detrital ilmenite, which is the most abundant detrital heavy mineral in all the samples as shown from provenance work done in this study, but also elsewhere in the Scotian Basin as discussed by Pe-Piper et al. (2005). Although Ti may be mobile during diagenesis, that mobility usually is local (Pe-Piper et al., 2011).

Diagenetic dolomite (B) occurs as euhedral rhombohedrons at shallow depths in the Roseway Equivalent Formation (Mohican I-100 well) showing replacive texture against mesogenetic fibrous chlorite (B) (Fig.4.8 A). Quartz overgrowths invade Mg-calcite (D), Fe-Mg-calcite (B) and Fe-calcite (B) (Figs.4.8 D, 4.9 C, 4.10 B), and thus they are later.

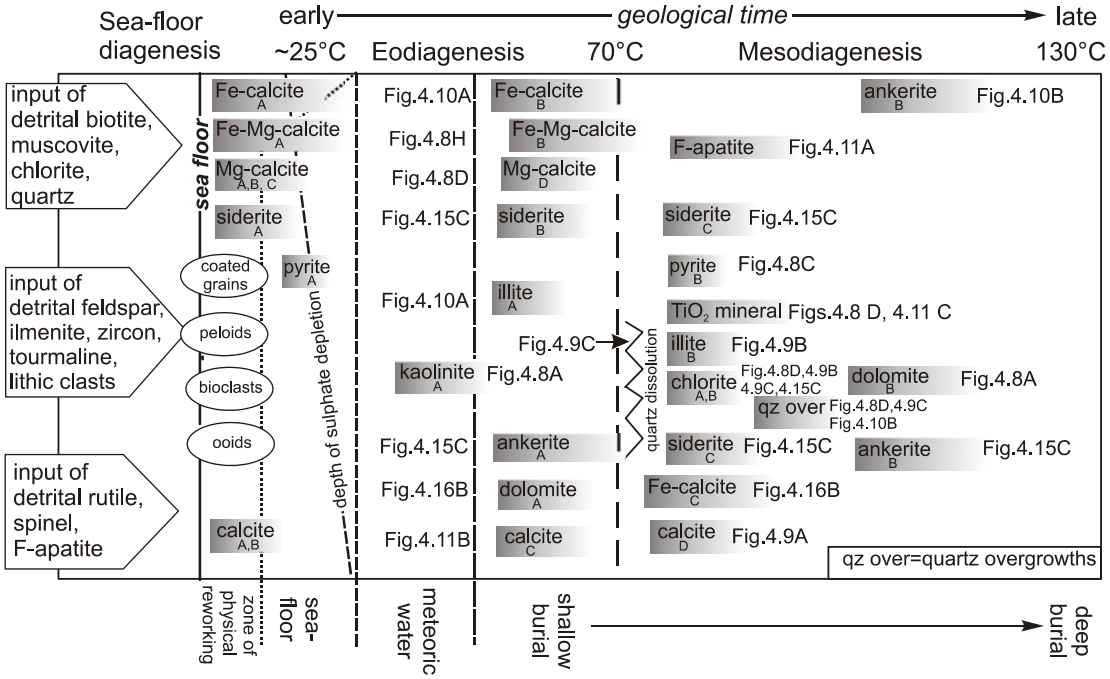

Figure 5.26: Paragenetic sequence deduced from mutual textural relationship in Late Jurassic and Early Cretaceous sandstones from Mohican I-100 and Moheida P-15 well. The boundary between eodiagenesis and mesodiagenesis is according Morad et al. (2000) and El-Ghali et al. (2006b).

5.2.4.2 Comparison to paragenetic sequences in Early Cretaceous rocks from the Sable sub-basin

Sea floor-diagenetic processes recorded and preserved in coated grains, during Late Jurassic-Early Cretaceous in the Mohican Graben located in the eastern part of the SW Scotian Basin (Mohican I-100 and Moheida P-15 wells) seem to be different from those in the Sable sub-basin during same time period. Specifically, the Sable sub-basin at Thebaud C-74 well has types A and B coated grains (Okwese et al., 2012), compared to the SW Scotian basin where types B and D coated grains were identified (see 5.2.3).

The presence of type A coated grains in the Sable sub-basin with nucleus of detrital quartz and outer rim of mostly siderite and Fe-chlorite indicates precipitation in the ferruginous diagenetic zone. On the other hand, type D coated grains in the Mohican Graben (SW Scotian Basin) have inner zones of pyrite and Fe-calcite and outer zones composed of calcite, chlorite and pyrite. These inner zones resemble type C coated grains that appear to have been reworked and transported (Okwese et al., 2012) into areas with different chemical conditions as implied from the composition of the outer zones. The presence of small pyrite grains in the outer zone may imply that the calcite precipitated in the sulphidic zone.

Although type B coated grains occur in both the Sable sub-basin and the Mohican Graben, the diagenetic minerals forming this type of coated grains differ from one sub-basin to another, suggesting different sea-floor diagenetic evolution. Type B coated grains in the Mohican Graben have concentric layers mostly of siderite with minor kaolinite whereas the same type in the Sable sub-basin has alternating layers of Fe-calcite and chlorite (Okwese et al., 2012). This change in mineral composition within

same type implies a higher ratio of Fe^{2+} to Ca^{2+} in the Mohican Graben compared to the Sable sub-basin where a higher ratio of Ca^{2+} is observed. The lower ratio of Fe^{2+} to Ca^{2+} in the Sable sub-basin is also confirmed from the Fe-calcite rich coated grains identified in the Glenelg, Thebaud and Kegeshook fields, as noted by Karim et al. (2010). The change in types of coated grains, and chemical composition within same type of coated grains from one sub-basin to another, suggests that during that time period the sea-floor conditions in the Mohican Graben in the eastern SW Scotian Basin were different from those in the Sable sub-basin.

The difference in sea-floor conditions from one sub-basin to another is also observed in the chemical composition of bioclasts identified. For instance, in the Sable sub-basin the original Mg-calcite skeleton in bioclasts has been replaced by Fe-calcite, whereas bioclasts in the Mohican Graben have kept their original Mg-calcite skeleton composition. The fact that bioclasts in the Mohican Graben maintained their primary composition suggests that the input of Fe^{2+} was used entirely for the formation of Fe-rich type B coated grains or that the sea-floor conditions did not favour replacement of Mg-calcite by Fe-calcite. Nevertheless, the high input of Fe^{2+} in both basins suggests availability from breakdown of detrital ilmenite with release of reactive Fe (Pe-Piper et al., 2005).

Eodiagenesis in the Mohican Graben is represented mostly by Mg-calcite, with minor Fe-calcite, Fe-Mg-calcite, kaolinite, illite, siderite, dolomite and ankerite. On the other hand, mostly siderite, with minor kaolinite, calcite, pyrite, Fe-calcite and Mg-calcite are early diagenetic minerals identified in the Sable sub-basin. The main cement in the Mohican Graben is Mg-calcite compared to the Sable sub-basin where siderite is

one of the most abundant diagenetic minerals showing variation in Mg^{2+} and Ca^{2+} (Karim et al., 2010). The abundance of Mg-calcite cement in the Mohican Graben suggests full marine conditions during Late Jurassic-Early Cretaceous and less fluvial influence compared to the Sable sub-basin where the variation in Mg^{2+} and Ca^{2+} in siderite from the Sable sub-basin is interpreted to result from fluctuating salinity of seawater in the sea-floor diagenetic system from input of fresh meteoric water from rivers (Karim et al., 2010).

Eogenetic siderite and ankerite in the Mohican Graben were identified only as supporting cement between type B, Fe-rich coated grains. On the other hand, siderite cement in the Sable sub-basin not only is found with type B, but also as cement in uncompacted sandstones. Slight corrosion of the siderite cement and pyrite in the Sable sub-basin may be caused by input of meteoric water that led to the creation of secondary porosity as well as precipitation of kaolinite (Rossi et al., 2001). Kaolinite in the Mohican Graben is engulfed by Mg-calcite cements, and thus predates them. The fact that kaolinite in the Sable sub-basin postdates siderite implies that the fully marine conditions experienced some flux of meteoric water (Karim et al., 2010). On the other hand, the Mohican Graben in the eastern SW Scotian Basin was influenced first by fresh meteoric water with precipitation of kaolinite, before fully marine conditions seem to have occurred. The influence with fresh meteoric water from rivers in both basins suggests that the subsidence rates were not sufficient to avoid the input with fresh water in the sea-floor diagenetic systems.

Mesodiagenesis in the Mohican Graben is represented by diagenetic minerals that fill secondary porosity or show replacive textures against detrital or other diagenetic

minerals. Examples of such mesodiagenetic minerals are F-apatite, siderite, pyrite, ankerite, TiO_2, illite, chlorite, Fe-calcite, calcite, quartz overgrowths and dolomite. Chlorite, illite, quartz overgrowths, ankerite, Fe-calcite, albite, and siderite represent the mesodiagenetic minerals identified in the Sable sub-basin (Karim et al., 2010).

Pyrite, chlorite and siderite in the Sable sub-basin are the first mesodiagenetic minerals to form synchronous with quartz overgrowths (Karim et al., 2010). Although there is no clear evidence of which mesodiagenetic minerals were formed first and which formed last in the Mohican Graben in the eastern SW Scotian Basin, most likely chlorite, calcite and pyrite are the first to have precipitated, probably at the same time. This assumption is made based on the fact that all three previous mesodiagenetic minerals are identified, sometimes, together filling secondary porosity in Mg-calcite which is considered an early eodiagenetic phase. The synchronous precipitation of both siderite and calcite with pyrite suggests that the conditions in both basins were indicative of sulfate reduction. Although both basins have same early mesodiagenetic minerals there is a slight difference, the Mohican Graben has calcite instead of siderite identified in the Sable sub-basin. This difference can be related to the fact the Sable sub-basin has abundance in shales, which are made up mostly of illite, but they do contain chlorite and very fine-grained iron hydroxides. In addition, these shales contain siderite which is considered a common eodiagenetic mineral forming pre-compaction concretions. As a result shales in the Scotian Basin comprise a variety of diagenetic minerals which contain Fe^{2+}, which is necessary for the precipitation of late siderite. On the other hand, the Mohican Graben is mostly limestone, and thus the calcite precipitation.

Two types of mesodiagenetic chlorite were identified in the Sable sub-basin: one as chlorite rims overlying Fe-rich clays and forming around detrital grains, and one as fibrous chlorite filling secondary porosity (Karim et al., 2010). In the Mohican Graben, eastern SW Scotian Basin, only the fibrous chlorite was identified. Although the fibrous chlorite type was identified in both sub-basins it seems to show different preference from sub-basin to sub-basin. In the Sable sub-basin this chlorite type fills intragranular pores and predates widespread carbonate cementation (Karim et al., 2010), whereas in the Mohican Graben the same chlorite type tends to fill secondary porosity in the carbonate cements (e.g. Fig.4.8 A).

Detrital K-feldspar in the Sable sub-basin is partly replaced by albite whereas the same mineral in the Mohican Graben is still fresh. The absence of albitized K-feldspar in the SW Scotian Basin is at depths < 2.4 km and so do not reach depths that favour K-feldspar dissolution, > 2.2 km in the Sable sub-basin (Pe-Piper, 2012).

The latest diagenetic phases in the Mohican Graben are ankerite and dolomite whereas in the Sable sub-basin, ankerite, Fe-calcite and calcite are the last mesodiagenetic minerals to have formed. Again, this slightly difference is the result of abundance in sedimentary rocks in each of the sub-basins as mentioned earlier.

In conclusion, the Late Jurassic-Early Cretaceous sandstones in the Sable sub-basin are grain supported and cemented mostly by Fe-rich diagenetic minerals, whereas in the Mohican Graben of the eastern SW Scotian Basin similar rocks seem to be cemented by Mg-rich diagenetic minerals. Taking in consideration that the Fe^{2+} is mostly detrital from ilmenite breakdown and probably as Fe-hydroxides in clay flocs derived from river erosion of soils, the influence with meteoric water from rivers appears to have

been higher in the Sable sub-basin compared to the eastern SW Scotian Basin where mostly full marine conditions occur.

5.2.4.3 Mid Jurassic

Early eodiagenesis in the Mohican Formation, in both the Mohican I-100 and Moheida P-15 well (Fig.5.27), is consistent with a sabkha depositional environment (Sedge, 2015). When the seawater evaporates on tidal flats, gypsum crystals precipitate at the top of the water table. During burial diagenesis, gypsum then converts to anhydrite cement. Cement-supported sandstone implies that the anhydrite cement (A) (Fig.4.12 A, B) precursor was an early cement or concretion. It seems that the anhydrite precursor was gypsum, which undergoes a reduction of ~20% of the volume when it converts to anhydrite (Fig.4.12 F). Volume reduction creates porosity, probably around grain boundaries, enabling formation of quartz overgrowth around detrital quartz, that postdate anhydrite cement (A) (Fig.4.12 F).

Kaolinite together with illite (A) fill primary porosity and seem to be engulfed by anhydrite cement, thus they predate both quartz overgrowths and anhydrite cement (Figs.4.17 B, C). Possible sources for K required for kaolinite and illite are detrital K-feldspars which after a depth > 2 km tend to dissolve, as seen in Mohican I-100 well. Although K-feldspar is considered to be a high K source, it is most likely that illite in this case occured from alteration of detrital muscovite.

Mesodiagenesis starts at depths >3 km, where most of the detrital K-feldspars are replaced by albite (A) (Figs.4.12 A, D). This results in small albite crystal patches nucleating on the K-feldspar surface together with dissolution voids lacking diagenetic

minerals. The presence of incomplete filling of the available dissolved surface by diagenetic albite suggests that K-feldspar dissolution was more intense than the precipitation of albite supposed to maintain the replacement (Pe-Piper and Yang, 2014). According to Saigal et al. (1988) and Aagaard et al. (1990) such replacement of K-feldspar occurs at around 60-80 º C. Possible sources for the Na required for albite precipitation are detrital plagioclase precursors enriched in Na. Provenance work has shown that all the sandstones are abundant in plagioclase, specifically albite and oligoclase.

Anhydrite is a mobile mineral, and can be seen in more than one generation in the sedimentary sequences (Sedge, 2015). Partial replacement of detrital K-feldspar by remobilized anhydrite (B) postdates albitization, as albite patches in the albitized K-feldspar are engulfed by remobilized anhydrite (B) (Fig.4.12 A, D). The source for anhydrite can be either remobilization of anhydrite from the anhydrite cement or possibly remobilization through veins from early anhydrite nodules, as mentioned by Sedge (2015). Secondary porosity at crystal boundaries favours the formation of quartz overgrowths around detrital quartz grains (Figs.4.12 F, 4.17 B). With increase in depth the anhydrite cement (A) is replaced by calcite (A) (Figs.4.13 C, 4.14), which becomes the main supporting cement filling primary porosity in sandstones or secondary porosity in dolostone. TiO_2 minerals and pyrite fill secondary porosity or show replacive texture against the anhydrite cement (Figs.4.13B, C).

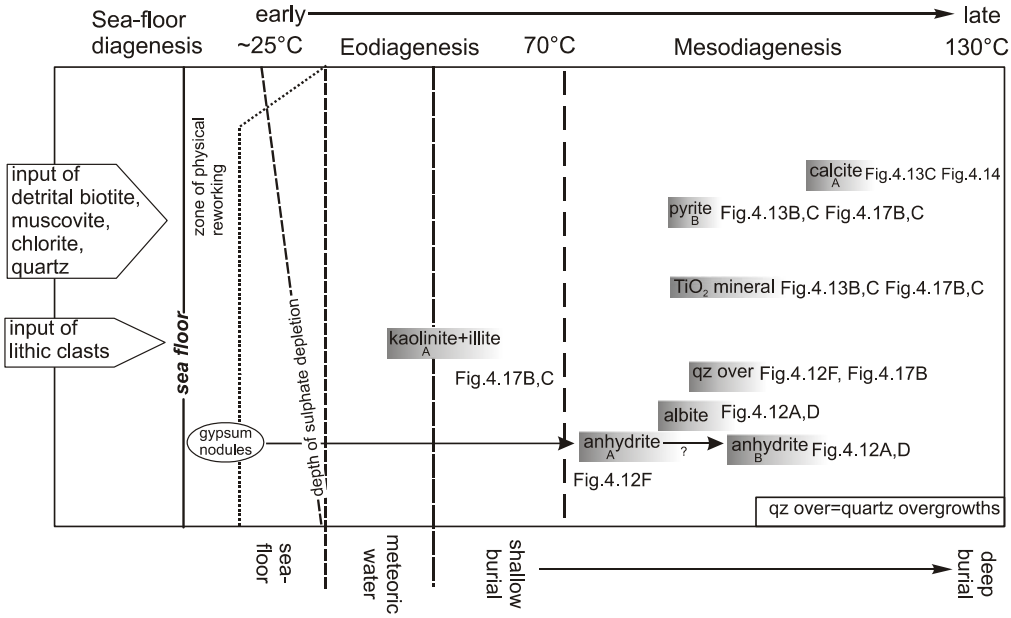

Figure 5.27: Paragenetic sequence deduced from mutual textural relationship in Mid Jurassic sandstones from Mohican I-100 and Moheida P-15 well. The boundary between eodiagenesis and mesodiagenesis is according Morad et al. (2000) and El-Ghali et al. (2006b).

5.3 Overall Summary

5.3.1 Provenance and tectonic implication of the Early Jurassic to Early Cretaceous sediments

During the Early Jurassic provenance and sediment dispersion are poorly understood in the Fundy Basin. In the Scotian Basin there is no evidence regarding sediment conditions, as there are no definite rocks of that age. The absence of sediment on the Scotian Shelf in the Scotian Basin at this time suggests uplift of the rift shoulder on what is now the Scotian Shelf.

Based on seismic interpretation and estimates of unroofing almost 2 km of principally shales from the top of the thick terrestrial Scots Bay Formation, thought to have been as young as Aalenian, were removed due to erosion in the Fundy Basin (Wade et al., 1996). The oldest, preserved, part of the formation is of Pliensbachian

age. During that time, abundant magnetite with minor Mn-rich spessartine, igneous and metamorphic biotite, ilmenite and amphibole (tremolite, richterite and winchite) were deposited. Garnet, biotite and ilmenite chemistry all indicate derivation from the Meguma terrane, with influence mostly from metamorphic rocks, rather than igneous. The only magnetite parental rock around the Fundy Basin is the North Mountain Basalt. Tremolite at Musquodoboit E-23 well is thought to be derived from the Meguma terrane (Pe-Piper et al., 2009). Sodic amphiboles are known from the Avalon terrane of northern Nova Scotia (Papoutsa and Pe-Piper, 2013). The fact that the mineral chemistry of the magnetite shows influence mostly from magmatic sources suggests that soon after cooling, the North Mountain Basalt was exposed to extensive erosion. Exposure of the North Mountain Basalt to surface conditions probably occurred from minor uplift of western Nova Scotia. However, an uplift of the area north of the Cobequid-Chedabucto fault zone in northern Nova Scotia and erosion of rocks of the North Mountain Basalt that covered the area at that time can not be excluded. The second assumption is related to the fact that from the seismic profile (Fig.16) of the Scots Bay Formation in Wade et al. (1996) it seems that both the North Mountain Basalt and the Scot Bay Formation were synchronously folded. However, towards the edges of the basin onlap of the Scots Bay Formation onto the North Mountain Basalt can be observed. This local uplift does not seem to have influenced the structural character of the Fundy Basin as sediments of the Scots Bay Formation continued to be deposited at least until Aalenian (Wade et al., 1996). Other minerals such as pyrope, richterite and winchite are not normally found in the Meguma terrane and may indicate a source from the north. However, the Lower Cretaceous Chaswood Formation at

Vinegar Hill in southern New Brunswick, with sources from the Gander terrane in central and northern New Brunswick, does not contain any garnet or amphibole (Piper et al., 2007). The absence of amphibole may be due to intense diagenesis or alteration of those deposits. The local character of sediments in the Fundy Basin, with abundance of magnetite, is characteristic of arid rift systems where the main sources are considered local. The low contribution with sediments from rocks of the Meguma terrane implies that any uplift in Nova Scotia during the Lower Jurassic was minor.

By the Mid Jurassic, subsidence and peneplanation of the uplifted rift shoulder began, as sediments of the Iroquois and Mohican formations were deposited in rift basins on the Scotian Shelf. The detrital mineral data in this study together with the abundance of metamorphic lithic clasts show that the Mid Jurassic sediments on the Scotian Shelf were derived exclusively from the metamorphic rocks of the Meguma terrane. Few igneous lithic clasts imply minor contribution with sediments from igneous rocks of the Meguma terrane exposed at that time. The derivation with sediments from crystalline rocks, rather than reworking of older sedimentary rocks, is confirmed by the higher proportion of ilmenite and tourmaline to ultrastable zircon. The abundance of lithic clasts suggests tectonic uplifting of the Meguma terrane with rapid unroofing. The presence of type 1A garnet in Mohawk B-93 well with chemistry similar to that from the South Mountain Batholith suggests that the Late Devonian igneous rocks of the Meguma terrane were exposed to erosion by that time. Small amounts of spinel/chromite and types 1B and 2 garnet at Mohawk B-93 are similar to those from Lower Cretaceous Upper and Middle Members of the Missisauga Formation at Alma K-85 (Pe-Piper et al., 2009) that indicate a distant source from the ophiolites of

the inboard Appalachians and mafic intrusions of the Grenville Province. The current absence of clastic sediments at Bonnet P-23 implies that the Fundy Basin most likely did not experience uplift, followed by deformation and erosion until after Middle Jurassic and that the outer shelf did not receive sediments. However, from the presence of clastic sediments at Mohawk B-93, to the NE of Bonnet P-23, suggests that possible uplift, predating rocks penetrated at the base of Bonnet, can not be ruled out. What is clear is that there is no evidence of supply of sediments from the North Mountain Basalt at that time, except the abundant magnetite in the Mic-Mac H-86 well (Li et al., 2012).

Late Jurassic at Mohican I-100 and Moheida P-15 is considered a period with low transportation and deposition of sediments to the outer shelf as the carbonate banks of the Abenaki Formation with shale interbedding were deposited. Similar carbonate sediments to those at Mohican I-100 and Moheida P-15 are present at Bonnet P-23 well. Northward of Mohican I-100, at Sambro I-29 well, and northward of Bonnet P-23, at Mohawk B-93, the status is different as the thick clastic sands of the Mohawk Formation were deposited. The deposition of sediments mostly on the inner shelf suggests that the influence from tectonics was insignificant compared to that from sea level rise as indicated from the maximum flood event (TMFS) that took place in the latest Jurassic. However, in periods of low sea level sand might have reached the shelf edge and get deposited locally, as indicated by the presence of small sandy intervals in between maximum flood surfaces in the stratigraphic column.

Chemically, garnet, muscovite, chlorite and the majority of tourmaline and biotite in both Mohican I-100 and Mohawk B-93 wells show supply from metamorphic rocks

of the Meguma terrane. There is no evidence of influence with sediments from Labrador as is the case in the Venture and Thebaud fields inferred from monazite and zircon geochronology for the former and abundance in spinel/chromite for the latter (Pe-Piper et al, 2009). The absence of sands at Bonnet P-23, but presence of shales in the Abenaki Formation at Mohican I-100 and Moheida P-15 and their absence from the Mohawk Formation at Mohawk B-93 suggests that fine grained sediments were transported from Mohawk B-93 well eastwards and deposited at Mohican I-100. Another explanation could be that clastic sediments were not deposited at all at Mohawk B-93 during the Late Jurassic, whereas the presence of shales at Mohican I-100 implies small changes in the sea level at times. The structural inversion of the Fundy Basin may be the result of dextral strike slip movement (Pe-Piper and Piper, 2004) on the Cobequid-Chedabucto fault zone that occurred during the extension of the proto-North Atlantic between Grand Banks and Labrador. In this case, the inversion may have been initiated in the Kimmeridgian. During the same period of time the inner Scotian Shelf in the eastern part of the Scotian Basin was exposed to erosion as indicated from the presence of Alleghanian muscovite in the Venture B-93 well. Erosion is also clearly imaged on seismic reflection profiles (e.g. Deptuck et al., 2014). Probably, by Late Tithonian the Fundy Basin was uplifted and the sediments of the Scots Bay Formation started to erode. This evidence can be confirmed by the presence of an unconformity in the Bonnet P-23 well most likely caused by rivers transporting sediments from the Fundy Basin southwards, presumably across the bank edge into deep water, during low sea level stands.

During the Early Cretaceous thick sand successions, several km in thickness, of

the Missisauga and Logan Canyon formations were deposited on the Scotian Shelf at Mohican I-100 and Moheida P-15 wells. Detrital mineral chemistry implies direct supply of sediments from the metamorphic and igneous rocks of the Meguma terrane. The influence from igneous rocks, as shown from detrital mineral chemistry, seems to be higher compared to Mid and Upper Jurassic strata where the sediments showed mostly a metamorphic source. This supports the idea that by the Early Cretaceous, much of the Meguma metamorphic rocks were already eroded, unroofing igneous intrusive rocks, exposing them to Early Cretaceous erosion. Metamorphic clasts in Early Cretaceous strata tend to show higher metamorphic grade with foliation, compared to Mid Jurassic metamorphic clasts that lack foliation, derived from inboard crystalline rocks of the Meguma terrane. The oldest known age in the Chaswood Formation basins on land is Valanginian (Falcon-Lang et al., 2007). These facts may indicate intensification of the structural inversion in the Fundy Basin and uplift of the inner Meguma terrane and the inner Scotian Shelf, during Early Cretaceous, that led to erosion and transportation of Alleghanian metamorphic lithic clasts to the Scotian Basin. Few grains of type 1B garnet and spinel/ chromite in Mohican I-100 are similar in composition with those at Alma K-85 well, supplied by ancestral Sable River draining areas of the Labrador and the Grenville Province (Pe-Piper et al., 2009). This could be a result of occasional progradation of delta distributary, or marine reworking of the Sable delta deposits to the west with mixing of sediments. The abundance of ultrastable zircon at one stratigraphic level (1423.4 m) of Hauterivian age in Roseway Equivalent Formation at Mohawk B-93 well indicates possible reworking of older sedimentary rocks. Those rocks might be from erosion of Jurassic rocks in the Fundy

Basin as can be observed at Bonnet P-23 where there is significant reworking of Jurassic palynomorphs and nannofossils in an interval (1822-2065 m) that yielded Valanginian to Hauterivian ages within the Roseway Equivalent Formation. If significant intensification of the structural inversion of the Fundy Basin took place at that time with erosion, most likely the sediments were transported south in the Shelburne sub-basin. The decrease in abundance of high stability detrital zircon to ilmenite and tourmaline from younger to older strata in Mohawk B-93, suggests greater derivation of sediments from crystalline rocks in the older part of the section rather than reworking of older sedimentary rocks.

5.3.2 River patterns and paleogeography

Paleocurrent studies in the Fundy Basin suggest that Triassic sediments were transported by rivers draining local areas of the Meguma terrane (Leuleu and Hartley, 2010). The chemistry of detrital minerals from the Lower Jurassic Scots Bay Formation in this study confirms the local character of sediments. Most likely the rivers supplying sediments ran along the Cobequid-Chedabucto fault zone westwards and deposited in the Fundy Basin (Fig.5.28). We suggest this river pathway as the Meguma terrane supplied sediments to another river running along the Cobequid-Chedabucto fault zone to the Orpheus graben (Tanner and Brown, 1999). However, a river path directly from the Meguma terrane that did not flow along the Cobequid- Chedabucto fault zone can not be excluded. During the Early Jurassic the Fundy Basin was located 20º N of the equator, and the climate was hot and semi arid (Olsen and Et-Touhami, 2008). This suggests that the sediments were deposited mostly by small local seasonal rivers during

heavy rainfall seasons that resulted in high fluvial discharge. However, the deposition of sediments by organized river systems that involved long-distance fluvial supply, draining the Canadian Shield and the inboard terranes of the Appalachians, can not be excluded, as shown from detrital mineral chemistry.

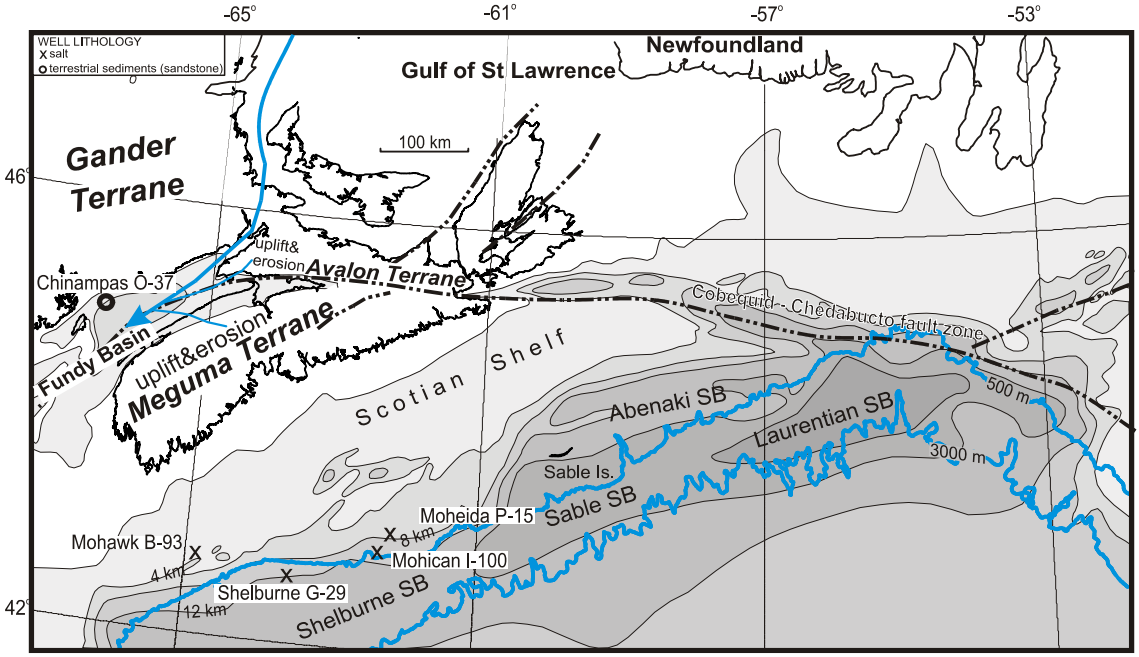

Fig.5.28: Schematic map showing potential rivers and sources for Early Jurassic sediments in the SW Scotian Basin and the Fundy Basin (this study). 2 km isopachs of offshore basins are from Williams and Grant (1998).

Detrital mineral chemistry of Mid Jurassic strata at both Mohican I-100 and Mohawk B-93 wells suggest rivers with local character draining areas of the Meguma terrane. However, sediments from the Labrador and the Grenville Province may have reached the Mohawk B-93 well through a river running along the Cobequid-Chedabucto fault zone that entered and deposited in the Fundy Basin (Fig.5.29). It is unlikely that such a river passed through the Orpheus graben before following the path to the Fundy Basin. We suggest that the river most likely entered the present Chignecto Bay to the Fundy Basin, because if it would have taken a more easterly path it would

have supplied sediments to the Wyandot E-53 and Mic Mac H-86 wells, where no distant mineral indicators are known (Li et al., 2012). Sediments deposited by this river in the Fundy Basin may have reached the Mohawk B-93 areas by coastal longshore drift, shallow water tidal currents or a separate local river. Although the sediments at both Mohican I-100 and Moheida P-15 have a local source, there is a lateral change in composition of Late Bathonian to Callovian strata with sand, shale, limestone and dolomite of the Mohican Formation and limestones of Scatarie Member and shales of the Misaine Member in the east to the coarse sandstones and shale of the Mohawk Formation to the west. At the Mohican I-100 and Moheida P-15 wells, the Mid Jurassic strata have similar composition, which means that the sediments were probably deposited by the same rivers. On the other hand, at Mohawk B-93 the Mid Jurassic coarse sandstone of the Mohawk Formation seem to have been deposited continuously by one river as the lithology tends to be consistent (coarse sandstone with small shaly intervals). Dolomite and limestones at Bonnet P-23 well and the lack of sandstone in Shelburne G-29 well suggest that the river(s) depositing at Mohawk B-93 did not deposit sediments west to the Bonnet P-23 well. Mid Jurassic sandstones at both Mohican I-100 and Moheida P-15 wells have grain-supporting anhydrite cement, most likely recrystallized from a gypsum precursor deposited in a sabkha environment. The presence of a Top Callovian Maximum Flooding Surface (TCMFS) representing a period with highstand of sea level, suggests that probably the sediments were trapped in estuaries which experienced water evaporation and precipitation of evaporite. The fact that in Moheida P-15 kaolinite filling primary porosity is engulfed by anhydrite suggests that the sediments received some fresh meteoric water through rivers entering

and depositing there. Based on the previous statements it seems that the same semiarid to arid climate, as that during Late Triassic and Early Jurassic when the Eurydice and the Argo formations were deposited, continued during Mid Jurassic.

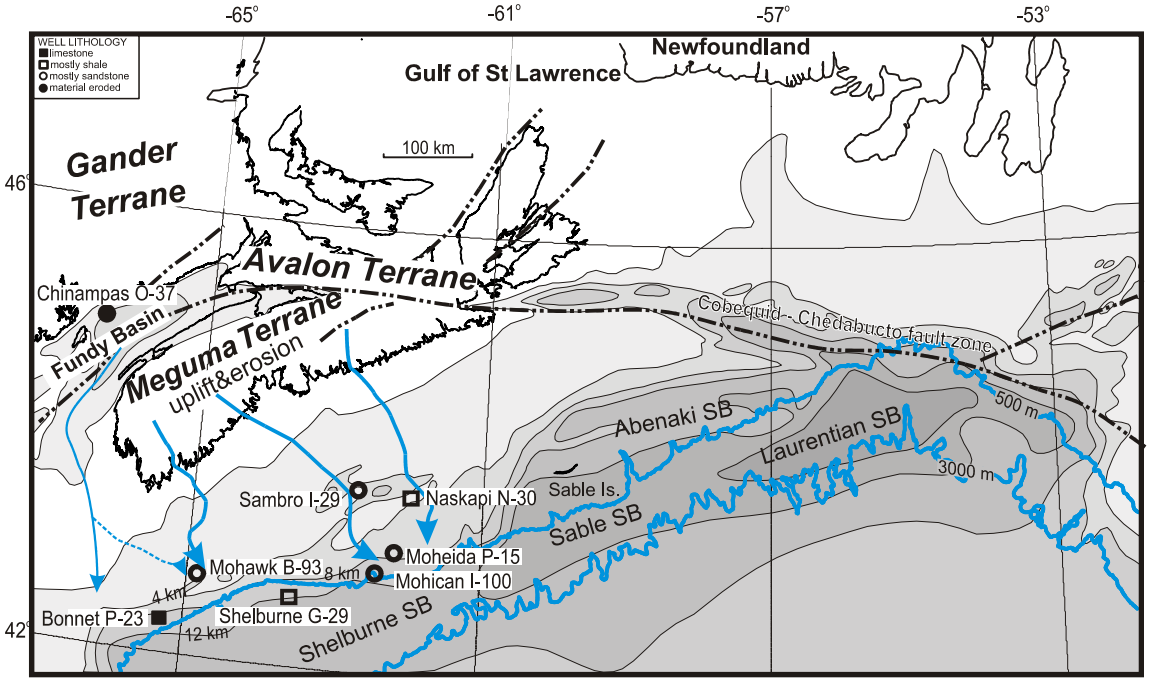

Fig.5.29: Schematic map showing potential rivers and sources for Middle Jurassic sediments in the SW Scotian Basin and the Fundy Basin (this study). 2 km isopachs of offshore basins are from Williams and Grant (1998).

Late Jurassic river supply of sediments to the SW Scotian Basin was not any different from that during Mid Jurassic, except that there is no influence with sediments from distant rivers (Fig. 5.30). The thick carbonate Abenaki Formation with interbedded shale at Mohican I-100 and Moheida P15 wells is equivalent to the sandy Mohawk Formation at Mohawk B-93 well. According to Tucker (2003), the thick carbonate sequence of Abenaki Formation with thick clastic successions of the Missisauga and Logan Canyon formations above it are representative of a lower carbonate-upper sandstone sequence stratigraphy. Based on that, most likely the limestones were initiated during a rapid sea-level rise as the entire Late Jurassic was

influenced by a highstand of sea level (top Tithonian maximum flood surface) (Weston et al., 2012). The absence of coarse clastic sediments in the Abenaki Formation suggests that sands were deposited only on the inner shelf, forming the Mohawk Formation in Sambro I-29 well north of Mohican I-100 and Moheida P-15. It is more likely that the fine grained interbeds (shales) within the Abenaki Formation were transported to the east by east-flowing currents from Mohawk B-93. The relationship between clastic sediments and limestone is a situation that is found on many low-latitude continental shelves. The mixed cycles in Mohican I-100 and Moheida P-15 may have been controlled by sea-level changes, or possibly by fault-related uplift (Tucker, 2003). The sea level rise might have been such that there was little time for reworking of the coastal plain (Tucker, 2003). However, a plentiful supply of terrigenous material is necessary to generate the upper clastic unit of the carbonate-upper sandstone sequence. The fact that the Bonnet P-23 well southwest of Mohawk B-93 comprises only carbonates, equivalent to the sandy deposits at Mohawk, suggests that most likely the river-derived sands did not pass through the carbonate banks and were not deposited in deep water basins, at least until the early Tithonian. However, the presence of clinoforms extending from the Mohawk sands in the Mohawk well to the margin hinge zone suggests that during periods of low sea level sediments were deposited in deepwater basins. Clearly there is no Sable Delta on the SW Shelf, but there were probably gaps in the carbonate banks (particularly in the lower part, above the J163) and in the Mohican equivalent section. Because of the very few data points (wells), seismic data is required. A modern analogue to the area around Mohawk B-93 well and Mohican I-100 during Late Jurassic is the Great Barrier Reef of Australia on

the outer shelf, where coral reefs are equivalent to the Abenaki Formation and landward sand deposits supplied by rivers draining eastern Australia are equivalent to the sandy Mohawk Formation. The fact that the Late Jurassic sandy deposits in Mohawk B-93 are continuous from the Mid Jurassic sandy deposits and have been attributed to the same formation (Mohawk) suggests that probably the same river that deposited during Mid Jurassic continued to deposit in the Late Jurassic.

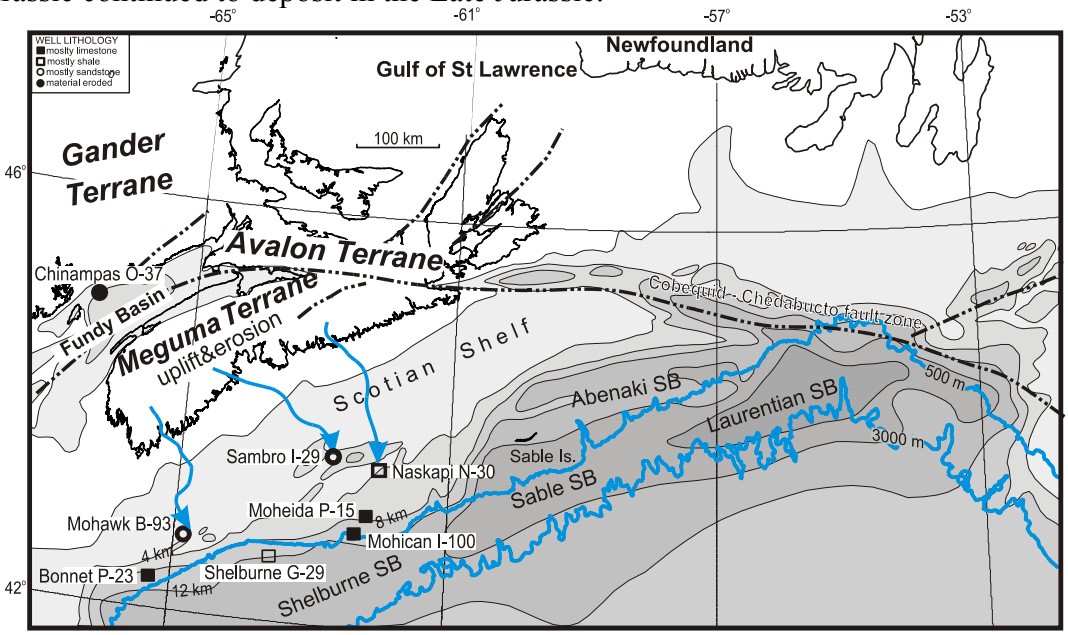

Fig.5.30: Schematic map showing potential rivers and sources for Upper Jurassic sediments in the SW Scotian Basin and the Fundy Basin (this study). 2 km isopachs of offshore basins are from Williams and Grant (1998).

Supply of terrigenous material was plentiful from Valanginian to Albian when sands and shales of the Missisauga, Logan Canyon and Shortland Shale formations were deposited on the shelf at Mohican I-100 and Moheida P-15 wells. Based on mineral chemistry, the rivers locally drained areas of the Meguma terrane and deposited sands at both wells (Fig.5.31). The accumulation of oolitic ironstones in the Lower Cretaceous Roseway Equivalent Formation at Moheida P-15 suggests that the climate was subtropical to tropical. In addition, chemistry of some garnet together with

presence of spinel/chromite implies sediments from distant rivers draining the Grenville Province and ophiolites of the inboard Appalachians were deposited at Mohican I-100. The river might have deposited directly at Mohican I-100 or it could be the result of occasional progradation of a delta distributary, or marine reworking of the Sable delta deposits to the west. The latter hypothesis is most likely the correct one as the spinel/chromite and the garnet are much less common at Mohican I-100 compared to Alma K-85 where similar minerals derived from same river are abundant. On the other hand, the presence of limestones at Bonnet P-23 well and mostly limestone with sandy intervals at Mohawk B-93 shows that there was not a big influence of river derived sediment during Early Cretaceous in that area of the basin.

In conclusion, the Mesozoic strata in the western part of the SW Scotian Basin at Mohawk B-93 and Bonnet P-23 wells seem to be different from strata in the eastern part at Mohican I-100 and Moheida P-15. For example, the western part is characterized by high clasic sediment supply during Mid and Late Jurassic, whereas the eastern part is mostly limestones. On the other hand, in the Early Cretaceous lots of clastics were deposited in the eastern part of the SW Scotian basin and limestones deposited in the western part. Mineralogical data suggest that most likely the SW Scotian Basin was supplied with sediments by more than one river systems through the entire Mesozoic and that most likely mixing between the sediments of different river systems did not occur.

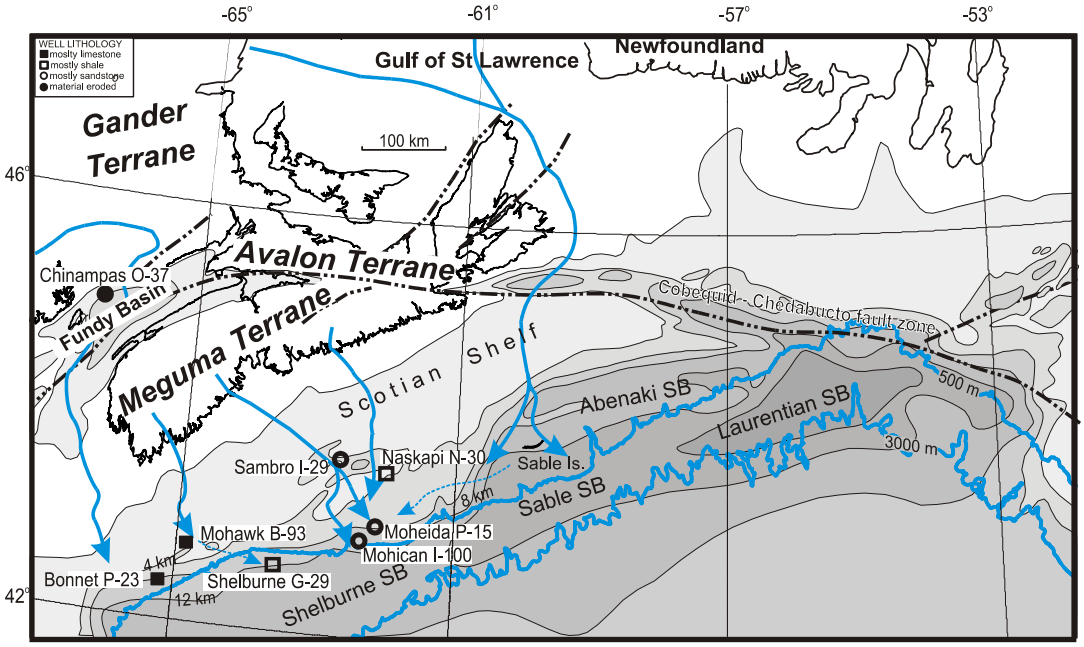

Fig.5.31: Schematic map showing potential rivers and sources for Lower Cretaceous sediments in the SW Scotian Basin and the Fundy Basin (this study). 2 km isopachs of offshore basins are from Williams and Grant (1998).

6. Conclusions

A) Provenance

- In general, detrital petrology indicates that Mid Jurassic sediments were derived mostly from the Meguma terrane; exceptions are types 1B and 2 garnet which were probably derived from meta-ultramafic rocks and spinel/chromite that was sourced from ophiolites. Both minerals were found only in the Mohawk Formation from the Mohawk B-93 well
- Upper Jurassic sediments were exclusively sourced from the Meguma terrane
- Lower Cretaceous sediments have similar sources as Mid Jurassic sediments; however the index minerals of distant sources were identified in the Upper Missisauga Formation from the Mohican I-100 well
- Rutile chemistry in this study confirms the source of sediments from Meguma terrane implying that it is an important provenance indicator; the same with light detrital minerals such as muscovite, biotite and chlorite

B) River patterns and paleogeography

- Mid Jurassic rivers draining the Grenville Province in Quebec and/or Labrador most likely ran along the Cobequid-Chedabucto fault zone and deposited in the Fundy Basin, whereas rivers draining the same areas during Early Cretaceous entered the Sable sub-basin through the Cabot Strait and deposited close to Mohican I-100 well down axis of the Mohican Graben
- Late Jurassic rivers were local; there is no evidence of sediments supply from distant rivers at that time
- During Late Jurassic the areas around Mohawk B-93 and Mohican I-100 wells

seems to have been similar to that offshore of the modern eastern Australia, where the coral barrier reefs form on the outer shelf and clastic sediments are deposited close to river mouths on the inner shelf; during periods of low sea level clastic sediments tend to overstep the carbonate edge and get deposited further away on the outer shelf or in deep water basins

C) Diagenesis-Paragenetic sequence

- The framework grains in Mid Jurassic sandstones are supported by anhydrite cement that suggests deposition of sediments in a sabkha environment; the precursor for the anhydrite cement is an early gypsum/anhydrite cement that was mobilized several times during the history of these rocks
- Kaolinite and illite fill primary porosity and are engulfed by anhydrite cement, thus they predate quartz overgrowths and sulfate cementation; at depths > 3.3 km detrital K-feldspar is no longer stable and is partly replaced with diagenetic albite, with source for Na from detrital plagioclase grains (albite and oligoclase)
- Coated grains chemistry in the Upper Jurassic and Lower Cretaceous sandstones in the SW Scotian Basin imply that the sea-floor conditions were not uniform at that time; for example coated grains in Mohican I-100 well are typical type D, enriched in calcite with inner part made up of mostly of Fe-calcite and the outer part of mixture between calcite and pyrite, whereas in Moheida P-15 coated grains are typical type B with concentric layers composed mostly of siderite
- Cements in the Upper Jurassic and Lower Cretaceous sandstones are mostly calcite, and Mg-calcite is the most common carbonate cement identified; all the carbonate cements postdate framework coated grains and in turn predate anhydrite cement

D) Diagenenetic evolution-SW Scotian Basin versus Sable Sub-basin

- Sea-floor conditions in the SW Scotian Basin are different from those in the Sable sub-basin as shown from mineral composition of coated grains; specifically coated grains in the Sable sub-basin are made up mostly of Fe-rich minerals such as chlorite and Fe-calcite with minor siderite which indicate precipitation in the ferruginous diagenetic zone, whereas coated grains in the SW Scotian Basin are made up of Fe-calcite with Mg-calcite and pyrite coating, suggesting precipitation in the sulfidic zone or mostly siderite suggesting precipitation in the ferruginous diagenetic zone
- Eodiagenesis in the SW Scotian Basin is represented mostly by Mg-calcite whereas in the Sable sub-basin siderite is the most abundant eodiagenetic mineral; the abundance in Mg-calcite in the SW Scotian Basin suggests fully marine conditions compared to the Sable sub-basin where a change in the Mg^{2+} and Ca^{2+} in siderite suggests fluctuating salinity of the sea-water from input of fresh meteoric water from rivers
- Mesodiagenesis in both the SW Scotian Basin and the Sable sub-basin is almost similar, represented by pyrite and chlorite with the difference that in the former calcite is the predominant mineral, whereas in the latter it is siderite
- The small difference in mesodiagenesis in the SW Scotian Basin and the Sable sub-basin (calcite versus siderite) is related to the mineralogical composition of rocks in each of the sub-basins; the Sable sub-basin is enriched in shales which are enriched in chlorite, thus the Fe^{2+} necessary for siderite precipitation, whereas the SW Scotian Basin is mostly carbonates which are the primary source of Ca^{2+}

REFERENCES

Aagaard, P., Egeberg, P. K., Saigal, G. C., Morad, S., and Bjorlykke, K., 1990. Diagenetic Albitization of Detrital K-Keldspars in Jurassic, Lower Cretaceous and Tertiary Clastic Reservoir Rocks from Offshore Norway, II. Formation Water Chemistry and Kinetic Considerations. Journal of sedimentary Research, 60 (4), 575-581.

Aagaard, P., Jahren, J.S., Harstad, A.O., Nilsen, O., and Ramm, M., 2000. Formation of grain-coating chlorite in sandstones. Laboratory synthesized vs. natural occurrences. Clay Minerals 35, 261-269.

Abdel-Rahmen, A.-F.M., 1994. Nature of biotites from alkaline, calc-alkaline and peraluminous magmas. Journal of Petrology, 35, 525-541.

Albertz, M., Beaumont, C., Shimeld, J. W., Ings, S. J., and Gradmann, S., 2010. An investigation of salt tectonic structural styles in the Scotian Basin, offshore Atlantic Canada: 1. Comparison of observations with geometrically simple numerical models. Tectonics, 29(4), DOI: 10.1029/2009TC002539.

Allan, B.D. and Clarke, D.B., 1981. Occurrence and origin of garnet in the South Mountain Batholith, Nova Scotia. Canadian Mineralogist, 19, 19-24.

Arai, S., 1992. Chemistry of chromian spinel in volcanic rocks as a potential guide to magma chemistry. Mineralogical Magazine, 56, 173-184.

Ascoli, P., 1988. Mesozoic-Cenozoic foraminiferal, ostracod and calpionellid zonation of the North Atlantic margin of North America: Georges Bank-Scotian basins and northeastern Grand Banks (Jeanne d'Arc, Carson and Flemish Pass basins). Biostratigraphic correlation of 51 wells. Geological Survey of Canada, Open File 1791, 41 pp.

Barss, M. S., Bujak, J., and Williams, G. L., 1979. Palynological zonation and correlation of sixty-seven wells, eastern Canada: Geol. Sur. Canada Paper, 78-24.

Basu, A., and Molinaroli, E., 1989. Provenance characteristics of detrital opaque Fe-Ti oxide minerals. Journal of Sedimentary Research, 59(6), 922–934.

Beck, M. E., and Housen, B. A., 2003. Pre-drift extension of the Atlantic margins of North America and Europe based on paths of Permo–Triassic apparent polar wander. Geophysical Journal International, 152(1), 68-78.

Bédard, J.H. and Hebert, R., 1998. Formation of chromitites by assimilation of crustal pyroxenites and gabbros into peridotitic intrusions: North Arm Mountain massif, Bay of Islands ophiolite, Newfoundland, Canada. Journal of Geophysical Research, 103, p, 5165–5184.

Berggren, W. A., 1982. Role of ocean gateways in climatic change. Climate in Earth History, 118-125.

Bhatia, M. R., 1983. Plate tectonics and geochemical composition of sandstones. The Journal of Geology, 611-627.

Bourget, J., Zaragosi, S., Ellouz-Zimmermann, S., Ducassou, E., Prins, M. A., Garlan, T., and Giraudeau, J., 2010. Highstand vs. lowstand turbidite system growth in the Makran active margin: Imprints of high-frequency external controls on sediment delivery mechanisms to deep water systems. Marine Geology, 274(1), 187-208.

Bowman, S. J., Pe-Piper, G., Piper, D. J., Fensome, R. A., and King, E. L., 2012. Early Cretaceous volcanism in the Scotian Basin. This article is one of a series of papers published in this CJES Special Issue on the theme of Mesozoic–Cenozoic geology of the Scotian Basin. Canadian Journal of Earth Sciences, 49(12), 523-1539.

Brown, D. E., 1986. The Bay of Fundy: thin-skinned tectonics and resultant early Mesozoic sedimentation. In Basins of Eastern Canada and Worldwide Analogues. Atlantic Geoscience Symposium, Halifax, Nova Scotia (pp. 13-15).

Brown, D. E., and Grantham, R. G., 1992. Fundy basin rift tectonics and sedimentation, field excursion A-3: Guidebook. Geological Association of Canada, Mineralogical Association of Canada, Atlantic Geoscience Society, Wolfville, Nova Scotia.

Coish, R.A., 1989: Boninitic lavas in Appalachian ophiolites: a review. In: Boninites and related rocks, 264-. Edited by A.J. Crawford. Unwin Hyman, London.

Clarke, D. B., Reardon, N. C., Chatterjee, A. K. and Gregorie, D. C., 1989. Tourmaline composition as a guide to mineral exploration: A reconnaissance study from Nova Scotia using discriminant function analysis. Econ. Geol. 84, 1921–1935.

Clarke, D. B., MacDonald, M. A., and Tate, M. C., 1997. Late Devonian mafic-felsic magmatism in the Meguma zone, Nova Scotia. Memoirs-Geological Society of America, 107-128.

Cummings, D.I. and Arnott, R.W.C., 2005. Shelf margin deltas: a new (but old) play type offshore Nova Scotia. Bulletin of Canadian Petroleum Geology, 53, 211-236.

Darby, D. A., 1984. Trace elements in ilmenite: a way to discriminate provenance or age in coastal sands. Geological Society of America Bulletin,95(10), 1208-1218.

Darby, D. A., and Tsang, Y. W., 1987. Variation in ilmenite element composition within and among drainage basins; implications for provenance. Journal of Sedimentary Research, 57(5), 831-838.

Davison, I., 2005. Central Atlantic margin basins of North West Africa: geology and hydrocarbon potential (Morocco to Guinea). Journal of African Earth Sciences, 43(1), 254-274.

Deer, W., Howie, R.A. and Zussman, J., 1982. Rock-forming minerals vol. 1 Orthosilicates, second ed. Longman Group Limited, England, 919 pp.

Deer, W. A., Robert, A. H. and Jack, Z., 1992. An introduction to the rock-forming minerals. Vol. 696. London: Longman.

Deptuck, M.E., 2010a. The 'slope detachment zone'on the western Scotian Slope, offshore Nova Scotia: structural style, timing, and implications for margin evolution, in Conjugate Margins II, Lisbon 2010, Metedo Directo, v. IV, p. 87-95, ISBN: 978-989-96923-1-2.

Deptuck, M. E., 2011. Proximal to distal postrift structural provinces on the western Scotian Margin, offshore Eastern Canada: Geological Context and parcel prospectivity for Call for Bids NS11-1. CNSOPB Geoscience Open File Report 2011001MF, 42 pp. Canada-Nova Scotia Offshore Petroleum Board Open-File Report 2011–001MF, 42.

Deptuck, M. E., and Campbell, D. C., 2012. Widespread erosion and mass failure from the 51 Ma Montagnais marine bolide impact off southwestern Nova Scotia, Canada 1 2 1 This article is one of a series of papers published in this CJES Special Issue on the theme of Mesozoic–Cenozoic geology of the Scotian Basin. 2 Earth Sciences Sector Contribution 20120241. Canadian Journal of Earth Sciences, 49(12), 1567-1594.

Dickie, G.B., 1986. Cretaceous deposits of Nova Scotia, Nova Scotia Department of Mines and Energy. Paper 86-1, 54p.

Dickinson, W.R., Beard, L.S., Brakenridge, G.R., Erjavec, J.L., Ferguson, R.C., Inman, K.F., Knepp, R.A., Lindberg, F.A., and Ryberg, P.T., 1983. Provenance of North American Phanerozoic sandstones in relation to tectonic setting.Geological Society of America Bulletin, 94: 222-235.

Douma, S.L.,1988.The mineralogy, petrology and geochemistry of the Port Mouton Pluton, Nova Scotia Canada [M.S.thesis]:Halifax, Nova Scotia, Dalhousie University, 324 p.

Ellouz, N., Patriat, M., Gaulier, J. M., Bouatmani, R., and Sabounji, S., 2003. From rifting to Alpine inversion: Mesozoic and Cenozoic subsidence history of some Moroccan basins. Sedimentary Geology, 156(1), 185-212.

Falcon-Lang, H. J., Fensome, R. A., Gibling, M. R., Malcolm, J., Fletcher, K. R., and Holleman, M., 2007. Karst-related outliers of the Cretaceous Chaswod Formation of Maritime Canada. Canadian Journal of Earth Sciences, 44(5), 619-642.

Faure, G., and Mensing, T. M., 2010. The Transantarctic Mountains: rocks, ice, meteorites and water. Springer Science and Business Media. DOI 10.1007/978-90-481-9390-5_9.

Feetham, M., 1995. Lithogeochemistry of the Goldenville-Halifax Transition Zone (GHT) at North Beaverbank, Nova Scotia. (B.Sc. hons. thesis, Saint Mary's University).

Fleet, M.E., 2003. Rock-forming minerals, vol. 3A, Micas, 2nd ed. The Geological Society, London, England, 758 pp.

Flugel, E., 2004. Microfacies of Carbonate Rocks: Analysis, Interpretation and Application. p.100.

Folk, R.L., 1968. Petrology of sedimentary rocks. Austin, University of Texas publication, 170p.

Force, E. R., 1991. Geology of titanium-mineral deposits. Geological Society of America, Vol. 259, p 1-112.

Fowell, S. J., and Traverse, A., 1995. Palynology and age of the upper Blomidon Formation, Fundy basin, Nova Scotia. Review of Palaeobotany and Palynology,86(3), 211-233.

Given, M. M., 1977. Mesozoic and early Cenozoic geology of offshore Nova Scotia. Bulletin of Canadian Petroleum Geology, 25(1), 63-91.

Gobeil, J. P., Pe-Piper, G., and Piper, D. J., 2006. The West Indian Road pit, central Nova Scotia: key to the Early Cretaceous Chaswood Formation.Canadian Journal of Earth Sciences, 43(3), 391-403.

Goldfinger, C., Morey, A. E., Nelson, C. H., Gutiérrez-Pastor, J., Johnson, J. E., Karabanov, E., and Party, S. S., 2007. Rupture lengths and temporal history of significant earthquakes on the offshore and north coast segments of the Northern San Andreas Fault based on turbidite stratigraphy. Earth and Planetary Science Letters, 254(1), 9-27.

Golonka, J., Ross, M. I., and Scotese, C. R., 1994, Phanerozoic paleogeographic and paleoclimatic modeling maps, in Embry, A. F., Beauchamp, B., and Glass, D. J., eds., Pangaea: Global environments and resources: Canadian Society of Petroleum Geologists Memoir 17, p. 1–47.

Gould, K.M., 2007. Chlorite diagenesis in reservoir sandstones of the Lower Missisauga formation, offshore Nova Scotia. Masters thesis, Saint Mary's University, Halifax, N.S., Canada.

Haggerty S.E., 1976a. Oxidation of opaque mineral oxides in basalts. In: Douglas Rumble (Ed.), III, Oxide Minerals. Miner. Soc. Am. (Short Course Notes), 3, chapter 4, pp.1-100.

Haggerty, S. E., 1976b. Opaque mineral oxides in terrestrial igneous rocks. In D. Rumble, III, Ed., Oxide Minerals, p.l0l-300. Mineralogical Society of America.

Hallam, A., 1984b. Continental humid and arid zones during the Jurassic and Cretaceous. Palaeogeography, Palaeoclimatology, Palaeoecology, 47(3), 195-223.

Hallam, A., and Bradshaw, M. J. 1979. Bituminous shales and oolitic ironstones as indicators of transgressions and regressions. Journal of the Geological Society, 136 (2), 157-164.

Ham, L., 1988. The mineralogy, petrology, and geochemistry of the Halfway Cove-Queensport pluton. Nova Scotia, Canada [M. Sc. thesis]: Halifax, Nova Scotia, Dalhousie University.

Haysom, S.J., 1994. The opaque mineralogy, petrology, and geochemistry of the Meguma Group metasediments, Rawdon area, Nova Scotia. Honours thesis, Saint Mary's University, Halifax, N.S., Canada.

Hebert, R., and Laurent, R.,1989: Mineral chemistry of ultramafic and mafic plutonic rocks of the Appalachian ophiolites, Quebec, Canada. Chemical Geology, 77, 265–285.

Henry, D. J., and Guidotti, C. V., 1985. Tourmaline as a petrogenetic indicator mineral: an example from the staurolite-grade metapelites of NW Maine. American Mineralogist, 70, 1-15.

Hey, M.H., 1954. A new review on the chlorites. Mineralogical Magazine, 224, 277-298.

Holser, W. T., Clement, G. P., Jansa, L. F., and Wade, J. A., 1988. Evaporite deposits of the North Atlantic rift. Triassic–Jurassic Rifting, Continental Breakup, and the Formation of the Atlantic Ocean and Passive Margins. B: Dev. Geotecton, 22(41), 525-556.

Hubert, J. F., and Mertz, K. A., 1980. Eolian dune field of Late Triassic age, Fundy Basin, Nova Scotia. Geology, 8(11), 516-519.

Hubert, J. F., and Hyde, M. G., 1982. Sheet-flow deposits of graded beds and mudstones on an alluvial sandflat-playa system: Upper Triassic Blomidon redbeds, St Mary's Bay, Nova Scotia. Sedimentology, 29(4), 457-474.

Indares, A., 1992. Eclogitized gabbros from the eastern Grenville Province: textures, metamorphic context, and implications. Canadian Journal of Earth Sciences, 30, 159-173.

Ings, S. J., and Shimeld, J. W., 2006. A new conceptual model for the structural evolution of a regional salt detachment on the northeast Scotian margin, offshore eastern Canada. AAPG Bulletin, 90(9), 1407-1423.

Irving, E., Wynne, P. J., and Globerman, B. R., 1993. Cretaceous paleolatitudes and overprints of North American craton. Evolution of the Western Interior Basin: Geological Association of Canada, Special Paper, 39, 91-96.

Jansa, L. F., and Wade, J. A., 1975. Geology of the continental margin off Nova Scotia and Newfoundland. In Offshore geology of eastern Canada. Geological Survey of Canada, Paper 74-30, pp. 51-105.

Jansa, L. F., Pe-Piper, G., Robertson, P. B., and Friedenreich, O., 1989. Montagnais: A submarine impact structure on the Scotian Shelf, eastern Canada. Geological Society of America Bulletin, 101(4), 450-463.

Karim, A., Pe-Piper, G., and Piper, D. J. W., 2010. Controls on diagenesis of Lower Cretaceous reservoir sandstones in the western Sable Subbasin, offshore Nova Scotia. Sedimentary Geology, 224(1), 65-83.

Kassoli-Fournaraki, A. and Michailidis, K., 1994. Chemical composition of tourmaline in quartz veins from Nea Roda and Thasos areas in Macedonia, Northern Greece. Canadian Mineralogist, 32, 607-615.

Kent, D. V., and Olsen, P. E., 1999. Astronomically tuned geomagnetic polarity timescale for the Late Triassic. Journal of Geophysical Research, 104(B6), 12831-12841.

Kent, D. V., and Tauxe, L., 2005. Corrected Late Triassic latitudes for continents adjacent to the North Atlantic. Science, 307(5707), 240-244.

Kent, D.V., Olsen, P.E., and Witte, W.K., 1995. Late Triassic– earliest Jurassic geomagnetic polarity sequence and paleolatitudes from drill cores in the Newark rift basin, eastern North America. J. Geophys. Res. 100, 14965–14998.

Keppie, J.D. 1983 The Minas Geofracture; Major Structural Zones and Faults of the Northern Appalachians, (ed.) P. St-Julien and J. Beland; Geological Association of Canada, Special Paper 24, p. 263-280.

Kidston, A.G, Brown, D. E., Altheim, B. and Smith, B. M., 2002. Hydrocarbon potential of the deep-water Scotian slope. Canada-Nova Scotia Offshore Petroleum Board.

Kontak, D.J. and Corey, M., 1988. Metasomatic origin of spessartine-rich garnet in the South Mountain Batholith, Nova Scotia. Canadian Mineralogist, 26, 315-334.

Kontak, D.J., Farrar, E., McBride, S.L, and Martin, R.F., 1995. Mineral chemistry and $^{40}Ar/^{39}Ar$ dating of muscovite from the East Kemptville leucogranite, southern Nova Scotia: evidence for localized resetting of $^{40}Ar/^{39}Ar$ systematics in a shear zone. Canadian Mineralogist, 33, pp. 1237– 1254.

Laurent, R., and Kacira, N., 1987: Chromite deposits in the Appalachian Ophiolites. In: Evolution of chromium ore fields, 169–193. Edited by C.W. Stowe. Van Nostrand Reinhold Co., New York.

Le Roy, P., and Piqué, A., 2001. Triassic–Liassic Western Moroccan synrift basins in relation to the Central Atlantic opening. Marine Geology, 172(3), 359-381.

Leake, B.E., Wooley, A.R., Arps, C.E.S., Birch, W.D., Gilbert, M.C., Grice, J.D., Hawthorne, F.C., Kato, A., Kisch, H.J., Krivovichev, V.G., Linthout, K., Laird, J., Mandarino, J.A., Maresch, W.V., Nickel, E.H., Rock, N.M.S., Schumacher, J.C., Smith, D.C., Stephenson, N.C.N., Ungaretti, L., Whittaker, E.J.W., and Guo, Y., 1997. Nomenclature of amphiboles: report of the subcommittee on amphiboles of the International Mineralogical Association, Commission on New Minerals and Mineral Names. American Mineralogist, 82, 1019-1032.

Ledger, S., 2013. Rutile as an indicator of provenance using texture, morphology and geochemistry and determining the source of sediments for the offshore Scotian Basin. Thesis (M.Sc. thesis), Saint Mary's University, Halifax, N.S.

Leinfelder, R.R., Schmid, D.U., Nose, M., and Werner, W., 2002. Jurassic reef patterns - The expression of a changing globe. In: Kiessling, W., Fluegel, E., Golonka, J. (Eds.), Phanerozoic Reef Patterns. SEPM Spec. Publ. 72, pp. 465-520.

Leleu, S., and Hartley, A. J., 2010. Controls on the stratigraphic development of the Triassic Fundy Basin, Nova Scotia: implications for the tectonostratigraphic evolution of Triassic Atlantic rift basins. Journal of the Geological Society,167(3), 437-454.

Li, G., Pe-Piper, G., and Piper, D.J.W., 2012. The provenance of Middle Jurassic sandstones in the Scotian Basin: petrographic evidence of passive margin tectonics. Canadian Journal of Earth Sciences, 49: 1463-1477.

MacLean, B.C., and Wade, J.A. 1993. East Coast Basin Atlas Series: seismic markers and stratigraphic picks in Scotian Basin wells. Geological Survey of Canada, Energy, Mines and Resources Canada, 276 p.

Malpas, J., and Strong, D.F., 1975. A comparison of chrome-spinels in ophiolites and mantle diapirs of Newfoundland. Geochimica et Cosmochimica Acta, 39, 1045–1060.

Manspeizer, W., 1988, Triassic-Jurassic rifting and the opening of the Atlantic: An overview, in Manspeizer, W., ed., Triassic-Jurassic rifting: Continental breakup and the origin of the Atlantic Ocean and passive margins, Part A: Developments in Geotectonics, v. 22p. 41-79.

Mathison, C. I., 1975. Magnetites and ilmenites in the Somerset Dam layered basic intrusion, southeastern Queensland. Lithos, 8, pp. 93-1 1 I.

Meagher, C., 1994. Geology of the Mount Thom complex, Cobequid Highlands, Nova Scotia. Honours thesis, Saint Francis Xavier University, Antigonish, Nova Scotia.

McIver, N. L., 1972. Cenozoic and Mesozoic stratigraphy of the Nova Scotia shelf. Canadian Journal of Earth Sciences, 9(1), 54-70.

McKee, E., D., and Gutschick, R., C., 1969. History of Redwall Limestone of Northern Arizona: Geological Society of American Memoir 11. p.726.

Morad, S., Ketzer, J.M., De Ros, L.F., 2000. Spatial and temporal distribution of diagenetic alterations in siliciclastic rocks: implications for mass transfer in sedimentary basins. Sedimentology 47, 927–942.

Morton, A. C., 1987. Influences of provenance and diagenesis on detrital garnet suites in the Paleocene Forties Sandstone, central North Sea. Journal of Sedimentary Research, 57(6).

Morton, A., and Hallsworth C.R., 1999. Processes controlling the composition of heavy mineral assemblages in sandstones. Sedimentary Geology, 124, 3-29.

Morton, A. C., and Hallsworth, C., 2007. Stability of detrital heavy minerals during burial diagenesis. Developments in Sedimentology, 58, 215-245.

Murphy, J. B., and Hamilton, M. A., 2000. Orogenesis and Basin Development: U□Pb Detrital Zircon Age Constraints on Evolution of the Late Paleozoic St. Marys Basin, Central Mainland Nova Scotia. The Journal of Geology, 108(1), 53-71.

Murphy, J. B., Waldron, J. W., Kontak, D. J., Pe-Piper, G., and Piper, D. J. W., 2011. Minas Fault Zone: Late Paleozoic history of an intra-continental orogenic transform fault in the Canadian Appalachians. Journal of Structural Geology, 33(3), 312-328.

Mutti, E., Tinterri, R., Benevelli, G., di Biase, D., and Cavanna, G., 2003. Deltaic, mixed and turbidite sedimentation of ancient foreland basins. Marine and Petroleum Geology, 20(6), 733-755.

Nadon, G. C., and Middleton, G. V., 1984. The stratigraphy and sedimentology of the Fundy Group (Triassic). of the St. Martins area, New Brunswick. Canadian Journal of Earth Sciences, 22, 1183 – 1203.

OETR (Offshore Energy Technical Research). 2011. Atlas: Play Fairway Analysis, Offshore Nova Scotia, Canada. Available from http://www.novascotiaoffshore.com/analysis#atlas (Accessed November 2011).

Okwese, A.C., Pe-Piper, G., and Piper, D.J.W. 2012. Controls on regional variability in marine pore-water diagenesis below the seafloor in Upper Jurassic-Lower Cretaceous prodeltaic sandstone and shales, Scotian Basin, Eastern Canada. Marine and Petroleum Geology, 29: 175-191.

Olsen, P. E., 1981. Comment and Reply on 'Eolian dune field of Late Triassic age, Fundy Basin, Nova Scotia' comment. Geology, 9(12), 557-559.

Olsen, P., and Et-Touhami, M., 2008. Field trip 1: Tropical to subtropical syntectonic sedimentation in the Permian to Jurassic Fundy Rift Basin, Atlantic Canada, in relation to the Moroccan Conjugate Margin. Central Atlantic Conjugate Margins Conference.

Olsen, P. E., R. W. Schlische, and P.J. W Gore, eds., 1989, Tectonic, depositional, and paleoecological history of Early Mesozoic rift basins, eastern North America: Washington, American Geophysical Union, International Geological Congress Field Trip T351, 174 p.

Olsen, P. E., Kent, D. V., Fowell, S. J., Schlische, R. W., Withjack, M. O., and LeTourneau, P. M., 2000. Implications of a comparison of the stratigraphy and depositional environments of the Argana (Morocco) and Fundy (Nova Scotia, Canada) Permian-Jurassic basins. Le Permien et le Trias du Maroc: Actes de la Premiere Reunion du Groupe Marocain du Permien et du Trias, 165-183.

Page, P., Bedard, J.H., Schroetter, J.-M and Tremblay, A., 2008. Mantle petrology and mineralogy of the Thetford Mines ophiolite complex. Lithos, 100, 255-292.

Papoutsa, A. D., and Pe-Piper, G., 2013. The relationship between REE-Y-Nb-Th minerals and the evolution of an A-type granite, Wentworth Pluton, Nova Scotia.American Mineralogist, 98(2-3), 444-462.

Pearce, J. A., Barker, P. F., Edwards, S. J., Parkinson, I. J., and Leat, P. T., 2000. Geochemistry and tectonic significance of peridotites from the South Sandwich arc–basin system, South Atlantic. Contributions to Mineralogy and Petrology, 139(1), 36-53.

Pe-Piper, G., 2012. Controls on feldspar diagenesis, as seen in the Lower Cretaceous sandstones of the Scotian Basin, Canada. Third Central & North Atlantic Conjugate Margins Conference, Trinity College Dublin, 22-24 August 2012.

Pe-Piper, G. and Ingram, S., 2001. The New Cornwall syenogranite, Nova Scotia: petrology and geochemistry. Atlantic Geology, 37, 133-151.

Pe-Piper, G. and Dessureau, G., 2002. The West Moose River anorthosites. Avalon zone, Nova Scotia.Geological Survey of Canada Open File Report 4188.

Pe-Piper, G., and Jansa, L. F., 1999. Pre-Mesozoic basement rocks offshore Nova Scotia, Canada: New constraints on the accretion history of the Meguma terrane. Geological Society of America Bulletin, 111(12), 1773-1791.

Pe-Piper, G., and Piper, D. J.W., 2004. The effects of strike-slip motion along the Cobequid-Chedabucto-southwest Grand Banks fault system on the Cretaceous-Tertiary evolution of Atlantic Canada. Canadian Journal of Earth Sciences,41(7), 799-808.

Pe-Piper, G, and Piper, D. J. W., 1997. Sedimentary petrology of the Lower Cretaceous in the Naskapi N-30 and Sambro I-29 wells, Scotian basin, offshore eastern Canada, Geological Survey of Canada, Open File 5594, 2007; 98 pages, doi:10.4095/22426.

Pe-Piper, G. and Mackay, R.M. 2006. Provenance of Lower Cretaceous sandstones onshore and offshore Nova Scotia from electron microprobe geochronology and chemical variation of detrital monazite. Bulletin of Canadian Petroleum Geology, 54, 366-379.

Pe-Piper, G., and Piper, D. J.W., 2007. Neogene backarc volcanism of the Aegean: new insights into the relationship between magmatism and tectonics.Geological Society of America Special Papers, 418, 17-31.

Pe-Piper, G., and Weir-Murphy, S., 2008. Early diagenesis of inner-shelf phosphorite and iron-silicate minerals, Lower Cretaceous of the Orpheus graben, southeastern Canada: implications for the origin of chlorite rims. American Association of Petroleum Geologists Bulletin, 92(9): 1153-1168.

Pe-Piper, G., and Piper, D. J.W., 2012. The Impact of Early Cretaceous Deformation on Deposition in the Passive-Margin Scotian Basin, Offshore Eastern Canada. Tectonics of Sedimentary Basins: Recent Advances, 270-287.

Pe-Piper, G., and Yang, X., 2014. Albitisation of detrital feldspars in the Scotian Basin: implications for the thermal evolution of the basin. Open file report 7117.

Pe-Piper, G., Jansa, L. F., and Lambert, R. St. J., 1992. Early Mesozoic magmatism on the eastern Canada margin: Petrogenetic and tectonic significance, in Puffer, J. H. and Ragland, P. C., eds., Eastern North American Mesozoic magmatism: Geological Society of America Special Paper 268, p. 13-36.

Pe-Piper, G., Dolansky, L., and Piper, D.J.W. 2004a. Petrography of the mid-Cretaceous Chaswood Formation in borehole RR-97-23, Elmsvale Basin, Nova Scotia: sedimentary environment, detrital mineralogy and diagenesis. Geological Survey of Canada Open File 4837, 231 p.

Pe-Piper, G., Stea, R.R., Ingram, S., and Piper, D.J.W., 2004b. Heavy minerals and sedimentary petrology of the Cretaceous sands from the Shubenacadie outlier, Nova Scotia. Nova Scotia Department of Natural Resources, Open File Report ME 2004-5, 78 p.

Pe-Piper, G., Piper, D.J.W., and Dolansky, L. 2005. Alteration of ilmenite in the Cretaceous sandstones of Nova Scotia, southeastern Canada. Clay and Clay Minerals, 53(5): 490-510.

Pe-Piper, G., Dolansky, L., and Piper, D.J.W., 2005b. Sedimentary environment and diagenesis of the Lower Cretaceous Chaswood Formation, southeastern Canada: The origin of kaolin-rich mudstones. Sedimentary Geology, 178: 75–97.

Pe-Piper, G., Piper, D.J.W., Hundert, T., and Stea, R.R., 2005c. Outliers of Lower Cretaceous Chaswood Formation in northern Nova Scotia: results of scientific drilling and studies of sedimentology and sedimentary petrography. Geological Survey of Canada Open File, 4845, 305 p.

Pe-Piper, G., Triantafyllidis, S., and Piper, D. J., 2008. Geochemical identification of clastic sediment provenance from known sources of similar geology: the Cretaceous Scotian Basin, Canada. Journal of Sedimentary Research, 78(9), 595-607.

Pe-Piper, G., Tsikouras, B., Piper, D.J.W., and Triantaphyllidis, S., 2009. Chemical fingerprinting of detrital minerals in the Upper Jurassic-Lower Cretaceous sandstones, Scotian Basin. Geological Survey of Canada open file 6288.

Pe-Piper, G., Karim, A., and Piper, D. J.W., 2011. Authigenesis of titania minerals and the mobility of Ti: new evidence from pro-deltaic sandstones, cretaceous scotian basin, Canada. Journal of Sedimentary Research, 81(10), 762-773.

Piper, D.J.W., Pe-Piper, G., Hundert, T. and Venugopal, D.K., 2007. The Lower Cretaceous Chaswood Formation in southern New Brunswick: provenance and tectonics. Canadian Journal of Earth Sciences, 44, 665-677.

Piper, D. J., Pe-Piper, G., and Ledger-Piercey, S., 2008. Geochemistry of the Lower Cretaceous Chaswood Formation, Nova Scotia, Canada: provenance and diagenesis. Canadian Journal of Earth Sciences, 45(10), 1083-1094.

Piper, D.J.W., and Normak, R. W., 2009. "Processes that initiate turbidity currents and their influence on turbidites: a marine geology perspective." Journal of Sedimentary Research 79.6 (2009): 347-362.

Posamentier, H. W., and Kolla, V., 2003. Seismic geomorphology and stratigraphy of depositional elements in deep-water settings. Journal of Sedimentary Research, 73(3), 367-388.

Pufahl, P.K., and Grimm, K.A., 2003. Coated phosphate grains: proxy for physical, chemical, and ecological changes in seawater. Geology 31, 801-804.

Puffer, J. H., 1992. Eastern North American flood basalts in the context of the incipient breakup of Pangea. Geological Society of America Special Papers,268, 95-118.

Rees, P. M., Ziegler, A. M., Gibbs, M. T., Kutzbach, J. E., Behling, P. J., and Rowley, D. B., 2002. Permian phytogeographic patterns and climate data/model comparisons. The Journal of Geology, 110(1), 1-31.

Reynolds, P.H., Pe-Piper, G., Piper, D.J.W. and Grist, A.M., 2009. Single-grain detrital muscovite ages from Lower Cretaceous sandstones, Scotian basin, and their implications for provenance: Bulletin of Canadian Petroleum Geology, 57: 63–80.

Reynolds, P. H., Pe-Piper, G., and Piper, D. J., 2010. Sediment sources and dispersion as revealed by single-grain 40Ar/39Ar ages of detrital muscovite from Carboniferous and Cretaceous rocks in mainland Nova Scotia. Canadian Journal of Earth Sciences, 47(7), 957-970.

Rivers, T. and Mengel, F.C., 1988. Contrasting assemblages and petrogenetic evolution of corona and non-corona gabbros in the Grenville Province of western Labrador. Canadian Journal of Earth Sciences, 25, 1629-1648.

Rossi, C., Marfil, R., Ramseyer, K., and Permanyer, A., 2001. Facies-related diagenesis and multiphase siderite cementation and dissolution in the reservoir sandstones of the Khatatba Formation, Egypt's Western Desert. Journal of Sedimentary Research 71, 459–472.

Saigal, G. C., Morad, S., Bjorlykke, K., Egeberg, P. K., and Aagaard, P., 1988. Diagenetic albitization of detrital K-feldspar in Jurassic, Lower Cretaceous, and Tertiary clastic reservoir rocks from offshore Norway, I. Textures and origin.Journal of Sedimentary Research, 58(6), p. 1003-1013.

Sawatzky, C. C., and Pe-Piper, G., 2013. Detrital quartz sources in the Scotian Basin, eastern Canada, using hot-cathode cathodoluminescence: Availability of coarse-grained sand for reservoirs. AAPG Bulletin, 97(9), 1503-1520.

Schrijver, K., 1973. Correlated changes in mineral assemblages and in rock habit and fabric across an orthopyroxene isograd, Grenville Province, Quebec. American Journal of Science, 273(2), 171-186.

Schettino, A., and Scotese, C. R., 2005. Apparent polar wander paths for the major continents (200 Ma to the present day): a palaeomagnetic reference frame for global plate tectonic reconstructions. Geophysical Journal International, 163(2), 727-759.

Schettino, A., and Turco, E., 2009. Breakup of Pangaea and plate kinematics of the central Atlantic and Atlas regions. Geophysical Journal International, 178(2), 1078-1097.

Schlische, R. W., and Olsen, P. E., 1990. Quantitative filling model for continental extensional basins with applications to early Mesozoic rifts of eastern North America. The Journal of Geology, 135-155.

Schlische, R. W., Withjack, M. O., and Eisenstadt, G., 2002. An experimental study of the secondary deformation produced by oblique-slip normal faulting.AAPG bulletin, 86(5), 885-906.

Schoene, B., Guex, J., Bartolini, A., Schaltegger, U., and Blackburn, T. J., 2010. Correlating the end-Triassic mass extinction and flood basalt volcanism at the 100 ka level. Geology, 38(5), 387-390.

Schroeder, T., John, B.E. and Frost, B.R., 2002. Geologic implications of seawater circulation through peridotite exposed at slow-spreading mid-ocean ridges, Geology 30, 367–370.

Scotese, C.R., 1997. The PALEOMAP Project: Paleogeographic atlas and plate tectonic software: Paleogeographic atlas and plate tectonic software: Austin, Texas, University of Texas, Department of Geology.

Sedge, C., 2015. Diagenesis and provenance of the Middle Jurassic sandstones and carbonates of the Mohican Formation in Mic Mac H-86, Mohican I-100, and Wyandot E-53 wells, offshore Scotian Basin. Thesis (Honours), Saint Mary's University, Halifax, N.S., 2015.

Shimeld, J., 2004. A comparison of salt tectonic subprovinces beneath the Scotian Slope and Laurentian Fan. In 24th Annual GCS-SEPM Foundation Bob F. Perkins Research Conference, Houston (pp. 291-306).

Sømme, T. O., Helland-Hansen, W., and Granjeon, D., 2009. Impact of eustatic amplitude variations on shelf morphology, sediment dispersal, and sequence stratigraphic interpretation: Icehouse versus greenhouse systems. Geology,37(7), 587-590.

Stea, R. R., Boyd, R., Fader, G. B. J., Courtney, R. C., Scott, D. B., and Pecore, S. S., 1994. Morphology and seismic stratigraphy of the inner continental shelf off Nova Scotia, Canada: Evidence for a− 65 m lowstand between 11,650 and 11,250 C 14 yr BP. Marine geology, 117(1), 135-154.

Stevens, R.E., 1944. Composition of some chromites of the western Hemisphere. American Mineralogist, 29, 1-34.

Suhr, G., and Robinson, P.T., 1994. Origin of mineral chemical stratification in the mantle section of the Table Mountain massif (Bay of Islands Ophiolite, Newfoundland, Canada). Lithos, 31, 81–102.

Tanner, L. H., and Brown, D. E., 1999. The Upper Triassic Chedabucto Formation, Guysborough County, Nova Scotia: depositional and tectonic context. Atlantic Geology, 35(2).

Tate, M. C., and Clarke, D. B., 1995. Petrogenesis and regional tectonic significance of Late Devonian mafic intrusions in the Meguma Zone, Nova Scotia. Canadian Journal of Earth Sciences, 32(11), 1883-1898.

Tauxe, L., and Kent, D. V., 2004. A simplified statistical model for the geomagnetic field and the detection of shallow bias in paleomagnetic inclinations: was the ancient magnetic field dipolar?. In: Channell, J.E.T., Kent, D., Lowrie, W., Meert, J.G. (Eds.) Timescales of the Paleomagnetic field: Geophysical Monograph, 145. AGU, Washington, DC, pp. 101–117101-115.

Telford, P. G., and Long, D. G. F., 1986. Mesozoic geology of the Hudson Platform. Canadian Inland Seas, 43-54.

Teufer, G., and Temple, A. K. ,1966. Pseudorutile—A new mineral intermediate between ilmenite and rutile in the alteration of ilmenite. Nature, 211, 179-181.

Triantaphyllidis, S., Pe-Piper, G., MacKay, R., Piper, D.J.W., and Strathdee, G., 2010. Monazite as a provenance indicator for the Lower Cretaceous reservoir sandstones, Scotian Basin. Geological Survey of Canada, Open File 6732, 452 pp.

Tsikouras B, Pe-Piper G, Piper DJW, and Schaffer M., 2011. Varietal heavy mineral analysis of sediment provenance, Lower Cretaceous Scotian Basin, eastern Canada. Sedimentary Geology 237(3-4): 150-165.

Tucker, M. E., 2003. Mixed clastic–carbonate cycles and sequences: Quaternary of Egypt and Carboniferous of England. Geologia Croatica, 56(1), 19-37.

Valdes, P.J., Sellwood, B.W., and Price, G.D., 1996. The concept of Cretaceous equability. Palaeoclim.: Data Model. 1, 139–158.

van Houten, F. B., 1985. Oolitic ironstones and contrasting Ordovician and Jurassic paleogeography. Geology, 13(10), 722-724.

van Staal, C. R., 2005. The Northern Appalachians, in Selley, R.C., Cocks, R.L.M. and Plimer, I.R.editors, Encyclopedia of Geology: Oxford, Elsevier, v. 4, p. 81–91.

Varfalvy, V. and Hebert, R., 1997. Petrology and geochemistry of pyroxenite dykes in upper mantle peridotites of the North Arm Mountain massif, Bay of Islands ophiolite, Newfoundland: implications for the genesis of boninitic and related magmas. Canadian Mineralogist, 35, 543-570.

Wade, J.A. (with contributions by Brown, D.E., Durling, P., MacLean, B.C., and Marillier, F.,) 2000. Depth to Pre-Mesozoic and Pre-Carboniferous Basements. Geological Survey of Canada Open File Report No. 3842 (1:1,250,000 map of Scotian Shelf & Adjacent Areas).

Wade, J.A. and MacLean, B.C., 1990. Aspects of the geology of the Scotian Basin from recent seismic and well data. Geology of Canada, 2, 190-238.

Wade, J. A., Williams, G. L., and MacLean, B. C., 1995. Mesozoic and Cenozoic stratigraphy, eastern Scotian Shelf: new interpretations. Canadian Journal of Earth Sciences, 32(9), 1462-1473.

Webb, G. W., 1969. Paleozoic wrench faults in Canadian Appalachians.American Association of Petroleum Geologists Memoir, 12, 754-786.

Weir-Murphy, S.L., 2004. The Cretaceous rocks of the Orpheus graben, offshore Nova Scotia. Masters thesis, Saint Mary's University, Halifax, Nova Scotia, Canada.

Weston, J.F., MacRae, R.A., Ascoli, P., Cooper, M.K.E., Fensom, R.A., Shaw, D., and Williams, G.L., 2012. A revised biostratigraphic and well-log sequence-stratigraphic framework for the Scotian Margin, offshore eastern Canada. Canadian Journal of Earth Sciences, 49: 1417-1462.

Whalen, J. B., and Chappell, B. W., 1988. Opaque mineralogy and mafic mineral chemistry of I-and S-type granites of the Lachlan fold belt, southeast Australia.American Mineralogist, 73(3-4), 281-296.

White, C. E., 2010. Stratigraphy of the Lower Paleozoic Goldenville and Halifax groups in the western part of southern Nova Scotia. Atlantic Geology, 46, 136-154.

Wilkinson, M., and Haszeldine, R. S., 1996. Aluminium loss from arkoses produces diagenetic quartzites and secondary porosity: Fulmar Formation, North Sea. Journal of the Geological Society, London, 153, 657-660.

Wilkinson, M., Darby, D., Haszeldine, R. S., and Couples, G. D., 1997. Secondary porosity generation during deep burial associated with overpressure leak-off: Fulmar Formation, United Kingdom Central Graben. AAPG Bulletin,81(5), 803-813.

Williams, H., 1978. Tectonic lithofacies map of the Appalachian orogen. Memorial University of Newfoundland.

Williams, H., 1995. Geology of the Appalachian—Caledonian Orogen in Canada and Greenland. Geological Society of America.

Williams, H., and Hatcher, R. D., 1982. Suspect terranes and accretionary history of the Appalachian orogen. Geology, 10(10), 530-536.

Williams, H. and Grant, A.C., 1998. Tectonic Assemblages Map. Atlantic Region. Canada: Geological Survey of Canada Open File 3657, scale 1:3,000.000.

Williams, G.L., Fyffe, L.R., Wardle, R.J., Colman-Saad, S.P., and Boehner, R.C., 1985. Lexicon of Canadian Stratigraphy, volume VI, Atlantic Region.Canadian Society of Petroleum Geologists, 572 p.

Withjack, M. O., Olsen, P. E., and Schlische, R. W., 1995. Tectonic evolution of the Fundy rift basin, Canada: evidence of extension and shortening during passive margin development: Tectonics, v. 14, p. 390–405.

Worden, R.H., and Morad, S., 2003. Clay minerals in sandstones: a review of the detrital and diagenetic sources and evolution during burial. In: Worden, R.H., Morad, S. (Eds.), Clay Cement in Sandstones: International Association of Sedimentologists, Special Publication, vol. 34, pp. 3–41.

Zack, T., Kronz, A., Foley, S. F., and Rivers, T., 2002. Trace element abundances in rutiles from eclogites and associated garnet mica schists.Chemical Geology, 184(1), 97-122.

Zack, T., Von Eynatten, H., and Kronz, A., 2004. Rutile geochemistry and its potential use in quantitative provenance studies. Sedimentary Geology, 171(1), 37-58.

Zhang, Y., Pe-Piper, G., and Piper, D. J., 2014. Sediment geochemistry as a provenance indicator: unravelling the cryptic signatures of polycyclic sources, climate change, tectonism and volcanism. Sedimentology, 61(2), 383-410.

Ziegler, P. A., 1989. Geodynamic model for Alpine intra-plate compressional deformation in Western and Central Europe. Geological Society, London, Special Publications, 44(1), 63-85.